



**A COLLECTION
OF
TECHNICAL PAPERS**

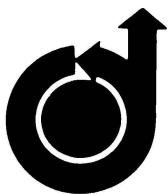
**AIAA FLIGHT SIMULATION
TECHNOLOGIES
CONFERENCE**

Arlington, Texas/Sept. 18-20, 1978

ERRATA SHEET AIAA PAPER 78-1581
PAGE 2 PARAGRAPH 4

As a result of this successful attempt of making a small holographic PANCAKE WINDOWTM* the Air Force Human Resources Laboratory (AFHRL) at Wright Patterson Air Force Base awarded Farrand a contract to develop a 17" diameter holographic PANCAKE WINDOWTM which was delivered and accepted. The Window was a mere 5/8 inch thick! Farrand is now into the next phase of the development. We have recently completed making three 21 x 24 inch holographic monochromatic PANCAKE WINDOWTM. These windows will be butted together to achieve a multiple input wide field of view. These windows are a mere 7/8 inch thick!

Just recently, AFHRL recognizing the potential of the holographic PANCAKE WINDOWTM, and again striving to advance the state-of-the-art in display technology awarded the Farrand Optical Co., Inc., a contract to develop a 32 inch full color tri-chromatic holographic PANCAKE WINDOWTM. Thus far, Farrand has successfully put together a two-color holographic PANCAKE WINDOWTM of smaller size and is currently engaged in the larger 32 inch tri-chromatic endeavor.



**A COLLECTION
OF
TECHNICAL PAPERS**

**AIAA FLIGHT SIMULATION
TECHNOLOGIES
CONFERENCE**

Arlington, Texas/Sept. 18-20, 1978

CONFERENCE COMMITTEE

General Chairman
HERBERT D. COOLES
Redifon Flight Simulation Ltd.

Technical Co-Chairmen

ARTHUR DOTY
USAF Simulator SPO

PHILIP REYNOLDS
Calspan Corp.

MOSES ARONSON
Naval Training Equipment Center

JAMES COPELAND
NASA Langley Research Center

WILLIAM HAYDEN
Vought Corp.

PATRICIA KNOOP
Air Force Human Resources Lab.

DOUGLAS LINDER
Northrop Corp.

ROGER MATHEWS
McDonnell Douglas Corp.

DALE SEAY
United Air Lines

TABLE OF CONTENTS

PAPER NO.		PAGE
78-1571	Development and Validation of Drive Concepts for an Advanced G-Cuing System - W. B. ALBERY and R. T. GILL.....	1
78-1572	Development of the Advanced G -Cuing System - G. J. KRON and J.M. KLEINWAKS....	4
78-1573	The Effect of Helmet Loader G-Cueing on Pilot's Simulator Performance - B. R. ASHWORTH and B. T. McKISSICK.....	15
78-1574	Platform Motion for Fighter Simulations -- Let's Be Realistic - R.V. PARRISH...	21
78-1575	Optimal Control Theory Applied to the Design of Cue-Shaping Filters for Motion-Base Simulators - R. L. KOSUT.....	32
78-1576	Motion: Methods and Requirements - W. T. HARRIS, J. A. PUIG, G. L. RICARD, D. G. WEINMAN.....	38
78-1577	Depth Perception and Motion Cues Via Textured Scenes - R. V. REYNOLDS, W. O. DUNGAN, JR., G. J. SUTTY.....	46
78-1578	Circles, Texture, Etc.: Alternate Approaches to CIG Scene Detail - W. M. BUNKER and CAPT. M. L. INGALLS.....	49
78-1579	COMPUTROL - A New Technique in Image Generation - R. SWALLOW, R. GOODWIN, R. DRAUDIN.....	59
78-1580	Advanced Tactical Air Combat Simulation (ATACS) - An Overview of Project 2363 - W. B. ALBERY and G. J. DICKISON.....	68
78-1583	Correlated Data Bases for the Present and Future - T. W. HOOGE.....	73
78-1584	The Application of Aircraft Motion Simulation Techniques to Land Borne Vehicles (Tank) - F. M. CARDULLO.....	79
78-1585	Accurately Reproducing Pilot's Control Forces in a Flight Simulator - B. W. McFADDEN and J. G. JOAS.....	90
78-1586	Verification of Workload - A Job for Simulation - T. C. WAY.....	99
78-1589	Computer Implemented Grading of Flight Simulator Students - F. L. COMSTOCK and H. J. J. UYTENHOVE.....	105
78-1590	Electronic Warfare Simulation for Air Force Weapon System Trainers - J. F. LETHERT.....	114
78-1591	A Unique Approach to Aerial Refueling Simulation for Training Boom Operators - J. LaRUSSA, F. G. ALBERS, S. J. ROSENGARTEN, A. J. SCHNEIDER, R.J. HEINTZMAN...	124
78-1592	Closed Loop Models for Analyzing the Effects of Simulator Characteristics - S. BARON, R. MURALIDHARAN, D. KLEINMAN.....	138
78-1593	A Model for the Pilot's Use of Motion Cues in Steady-State Roll-Axis Tracking Tasks - W. H. LEVISON and A. M. JUNKER.....	149
78-1594	Planning and Conducting Subjective Evaluations of Flight Simulators - F. A. RAGLAND and MAJOR J. A. RICHMOND.....	160
78-1595	Test Instrumentation System for Flight Simulator Handling Characteristics - W. L. CURTICE.....	164
78-1596	Time Delays in Flight Simulators: Behavioral and Engineering Analyses - G. L. RICARD and W. T. HARRIS.....	169
LATE PAPER		
78-1581	Optical Simulator With a Holographic Component - J. A. LaRUSSA and A. T. GILL..	176

DEVELOPMENT AND VALIDATION OF DRIVE CONCEPTS
FOR AN ADVANCED G-CUING SYSTEM

William B. Albery*

Richard T. Gill**

Air Force Human Resources Laboratory
Wright-Patterson AFB, Ohio 45433

I. ABSTRACT

This paper discusses the approach the Air Force Human Resources Laboratory (AFHRL) is taking to develop and validate the drive algorithms of the Advanced G-Cuing System, a second generation G-seat device developed for AFHRL by Singer-Link. The Advanced system, termed ALCOGS (Advanced Low Cost G-Cuing System), was developed as an engineering research tool to be used by AFHRL to determine the hardware and software technology required for seat cuing devices for fighter/attack aircraft such as the A-10, F-15 and F-16.

II. INTRODUCTION AND BACKGROUND

The utility of platform motion systems for fighter/attack flying training simulators has been questioned repeatedly over the past several years. In most cases, pilots have preferred no platform motion to six-post synergistic motion when training in such devices as the Advanced Simulator for Pilot Training (ASPT) and simulator for Air-to-Air Combat (SAAC). However, the G-cuing systems in these devices (the first delivered to the Air Forces) have been met with favorable comments by pilots, are generally acceptable and have demonstrated some training utility. Nevertheless, as "first generation" attempts at G-cuing devices, these research systems have been picked up by the Navy, NATO countries and are beginning to show up in Swedish and Japanese inventories. These multicelled, pneumatic systems (Fig 1) were originally developed as acceleration sustaining devices with the concept that a motion platform could provide the simulated onset acceleration and that once the platform's initial cue was "washed out" that a G-seat could provide the effect of sustaining that acceleration cue. Experimentation with the Air Force's G-seats have demonstrated that not only has the sustained acceleration concept been valid, but also acceleration onset information is provided to the pilot as the seat transitions from one acceleration magnitude to another. AFHRL recognized this motion and force cuing potential and that the first generation G-cuing hardware could not be compatible with the high performance aircraft simulation required for the A-10, F-15 and F-16.

In 1976, AFHRL awarded Singer-Link a contract for the development of the ALCOGS with the main objective to develop a flexible research tool with the engineering capability (bandwidth) to simulate the spectrum of cues available in fighter aircraft. AFHRL's objective was to use the ALCOGS in an

engineering research environment to further develop seat G-cuing hardware and drive concept technology and to develop specifications for tactical aircraft simulators, especially the F-16.

III. ALCOGS DRIVE ALGORITHM DEVELOPMENT

The ALCOGS (Fig 2) was delivered to AFHRL, Wright-Patterson AFB, Ohio in late 1977. The hardware development has been described in the literature (Refs 1, 2) and is discussed in detail in these proceedings (Ref Kron and Kleinwaks). The drive concepts of the ALCOGS are based upon those of the first generation seat as well as results of research performed on the ASPT (Ref 3). The ASPT research resulted in the recommendation for the ALCOGS approach to "moving plane and firmness bladder." In the ASPT study, the ALCOGS moving planes and firmness bladders were emulated on the first generation G-seat. Although the ASPT G-seat lacked the desired bandwidth to emulate the ALCOGS, the seats' geometry and flexible drive software afforded AFHRL and Link the opportunity to evaluate the ALCOGS approach. In short, plates were placed over the ASPT seats' metal bellows and overlaid by pneumatic firmness bladders (Fig 3). These bladders were driven by the pneumatic supply lines to the thigh panel bellows of the ASPT seat, which were deactivated during this evaluation. The

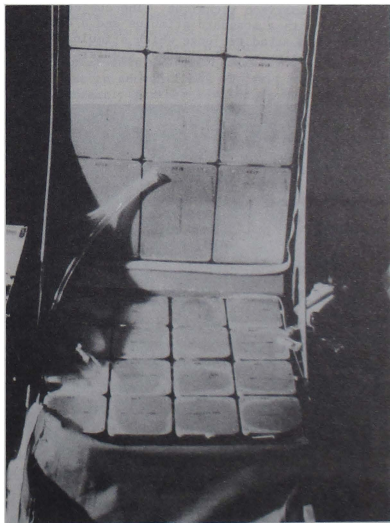


Figure 1. Front view of exposed ASPT G-seat bellows.

* Task Scientist, Motion and Force Simulation,
AIAA Member

**Electronics Engineer, Simulation Techniques Branch

Copyright 1978 by W. Albery and R. Gill, with
release to AIAA to publish in all forms.

results of the short study were very encouraging. The major finding was that the emulated ALCOGS approach gave a more unified sensation of cuing, whereas individual air bellows could be sensed sometimes on the ASPT-type seat. The concept of using the seat pan and backrest firmness bladders to provide tactile cues while driving the seat pan and backrest planes (to deliver attitude change cues) also appeared valid. The ALCOGS was delivered to AFHRL with the bladder pressure biases and drive philosophies developed during this ASPT study.

Since the acceptance of the ALCOGS in early 1978 the drive philosophy of the system has not been altered. The approach to the development and validation of the ALCOGS drive concepts has been based upon psychophysical experiments, objective data and algorithm selection.

Psychophysical Experiments

An orderly process of algorithm development for the ALCOGS was established. The first step was to determine and prioritize human sensitivities to the various seat parameters. The reason for this initial step was to determine which seat parameters the human is the most and least sensitive to. It was felt that this information was essential before initiating a program for the development and validation of drive algorithms for the ALCOGS.

Three classical psychophysical techniques were investigated to determine which method was best for algorithm development. The Method of Constant Stimuli was chosen over the Method of Limits and the Method of Adjustment. The Limits and Adjustment Methods are relatively inaccurate and lengthy to perform. The Method of Constant Stimuli is a stimulus comparison technique. The subject is presented with a standard stimulus and a comparison stimulus and asked to judge which stimulus was greater; a stimulus value judged greater 50% of

the time is defined as the point of subjective equality.

The objective of these psychophysical experiments was to determine absolute threshold (RL) and several difference thresholds (DL) for the modes of the seat and from these, determine Weber's Fraction (Eqn 1).

$$\text{Weber's Fraction} = \frac{\Delta\phi}{\phi} \quad (1)$$

ϕ = Stimulus Intensity
 $\Delta\phi$ = Difference Threshold (DL)
 at that Intensity

Absolute threshold (RL) is the point at which the subject notices a change in the position from the seats' neutral position 50% of the time. Difference threshold (DL) is the point at which the subject notices a difference in position from a standard stimulus, which can occur anywhere in the seats' operating range. The psychophysical experiments are being conducted in two phases. The objective of the first phase is to determine RL, DL, and Weber's Fraction for the seat's three primary modes of operation: hydraulic translation, hydraulic rotation and pneumatic operation. The objective of the second phase is to determine RL, DL and Weber's Fraction for specific seat parameters (e.g. backrest pitch, roll, seat pan pitch, roll). After the completion of Phase II, objective data will be collected to support the development of drive concepts.

Collection of Objective Data

The psychophysical experiments will help determine how the human perceives the operational modes of the ALCOGS G-seat. Objective data will be collected from an instrumented aircraft.

As a part of an AFHRL sponsored Gulf and Western study to be performed on the Air Force Flight Dynamics Laboratory's Total In-Flight Simulator (TIFS) aircraft, pilot seat force and

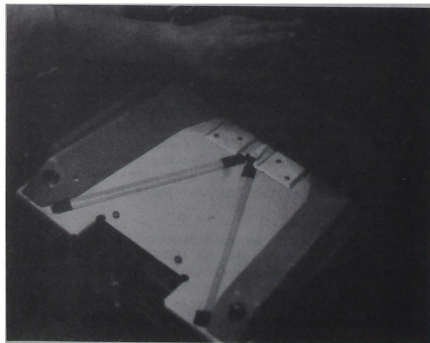


Figure 2. ALCOGS G-seat (left) and exposed seat pan (above). The ALCOGS can be operated on its test stand or in a T-38 simulator cockpit. When the upholstery and firmness bladder are removed, the thigh ramps and ischial tuberosity blocks are exposed.

and pressure data will be collected from a specially instrumented seat in the TIFS during selected maneuvers. These data will be in the form of forces measured at various locations on the pilot's seat and will be used to develop pressure contours for various acceleration levels for several axes. The objective is to use these actual data to refine the ALCOGS G-seat drive algorithms. These experiments are scheduled during late 1978.

ALCOGS ALGORITHM SELECTION

The ALCOGS has been mechanically integrated with a T-38 simulator cockpit at AFHRL, Wright-Patterson, and a three channel visual display is currently being integrated with the cockpit. It is anticipated that by late 1978 the ALCOGS will be operationally integrated with the flight and visual simulation of the T-38 simulator. Final ALCOGS algorithm selection will be based upon experimentation in the T-38 cockpit with an interactive flight program and visual display. A dual approach of using both subjective and objective measures will be employed. The subjective evaluation will be in the form of a comparative evaluation/questionnaire sheet. The objective measures will be more difficult to employ as the problem here is that the best performance may not correlate with the most realistic cues or have the best training value. This discrepancy between performance and cuing is not as serious as similar problems in the past since competing algorithms can be matched to the TIFS inflight data. One methodology may be to measure an RMS error score for a subject flying a pre-programmed maneuver. The RMS score would be computed for time and magnitude off trajectory to accent the differences between algorithms.

DETERMINATION OF G-SEAT SPECIFICATIONS

The objective of ALCOGS experimentation is to determine the engineering specifications for a G-cuing system for fighter/attack aircraft simulators. The approach to determining these specifications will be similar to the approach being taken to determine final ALCOGS drive algorithms, both subjective and objective measures will be used. The approach would involve plotting subject performance vs. the investigated parameter (e.g. seat actuator bandpass) in order to determine where the "knee" of the curve is located. The seat actuator bandpass experiment is perhaps the most important since it can help determine whether a pneumatic or hydraulic G-seat is required. Two other major parameters to be investigated include what G-seat components and how many degrees-of-freedom for each component are required, what excursion or stroke is required and what types of delays in delivering G-seat cues are acceptable. Other parameters to be analyzed include buffet with the seat shaker or through the seat pan, only, and differential lap belt drive.

CONCLUSION

A second generation seat motion and force cuing device has been developed and is currently being used in a program to further develop G-cuing technology for the Air Force's fighter/attack aircraft simulators. The advanced G-cuing

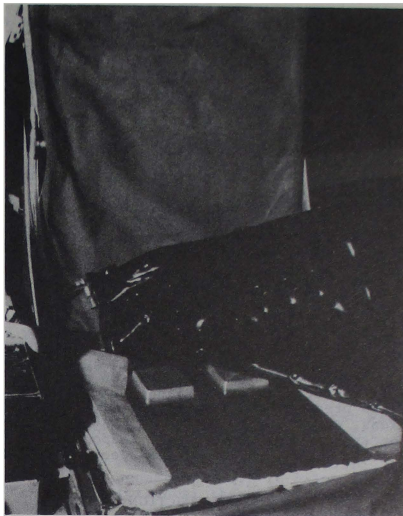


Figure 3. ALCOGS emulation on ASPT seat. Metal plates cover the metal bellows, firmness bladders overlay the plates.

system hardware has demonstrated the capability to perform in a fighter/attack aircraft simulator with its ten fold increase in actuator bandwidth and its compact seat pan and backrest packages which can fit in conventional aircraft seat frames. AFHRL is currently further developing and refining the drive concepts for this advanced system based upon psychophysical experiments, objective data, and closed-loop performance experiments using a vestigial T-38 simulator with a visual display. It is anticipated that the results from engineering experiments on the advanced G-cuing system can shape the design of G-seats and other G-cuing systems that the Air Force is developing for current and future flying training simulators.

REFERENCES

1. Kron, G., Young, L., and Alberty, W. High-G Simulation-The Tactical Aircraft Simulator Problem, NAUTRAEQUIPCEN 1N-294, Proceedings of 10th Annual Naval Training Equipment Center/Industry Conference, November 1977.
2. Kleinwaks, J. M. Advanced Low Cost G-Cuing System, Volume I, Unpublished AFHRL technical report, October 1978.
3. Alberty, W. and McGuire, D. Emulation of an Advanced G-seat on the Advanced Simulator for Pilot Training, AFHRL-TR-78-4, Advanced Systems Division, Air Force Human Resources Laboratory, Wright-Patterson AFB, April 1978.

C. J. Kron and J. M. Kleinwaks
Link Division of The Singer Company
Binghamton, New York

I. ABSTRACT

G-seats presently implemented on operational flight simulators lack the response speed necessary for research in areas of transient cuing and determination of necessary response characteristics for optimal acceleration cuing for tactical flight simulation. The Advanced G-Cuing System is a highly flexible research system with the aforementioned capabilities, along with the capability to accommodate the F-16 tilt back seat configuration and to provide closed loop servo operation. Hydraulic actuators, providing cushion surface elevation and orientation changes, and pneumatic firmness cladders, providing flesh pressure and area of contact variations, combine to form a hybrid system. The system demonstrates fast response, meeting a 30 msec. rise time specification.

II. INTRODUCTION

During maneuvering, significant somatic perceptions are available to pilots of tactical aircraft and are induced by the inertial acceleration reaction on the pilot's body and the coupling existing between body and seat. Protective devices such as G-suits are also active during predominant aircraft acceleration and contribute their own somatic sensations. Such maneuvering often carries the aircraft close to the bounds of its flight envelope and exposes the pilot to a broad range of vibratory information concerning aircraft dynamic state as well as configuration. Pilots employ these perceptions within the pilot-aircraft control loop. With such a wealth of apparently important information available to the pilot, it is not surprising that devices would evolve to provide a rendition of these cues within the simulation of tactical aircraft.

The development of these devices, G-seats, G-suit drive systems, and seat shakers or whole cockpit shakers, has proceeded to provide independent systems without emphasis on cuing interplay, shared common hardware, software, and control.

*The work reported on herein was sponsored by the Air Force Human Resources Laboratory, Wright-Patterson AFB under contract F33615-76-C-0060

The psychological utilization of the cues these systems provide is not well understood and consequently it is difficult to define and specify an optimum hardware configuration, performance capability, and drive algorithm for conventional tactical aircraft. The situation becomes more untenable with the introduction of high performance aircraft in which the strength and prevalence of somatic sensation is greater. Research is underway leading to the establishment of models describing the methods by which kinesthesia affects pilot performance. Model development and verification depend, in part, on support from experimentation with a versatile, high performance cuing system. This paper deals with the development of that system.

III. BACKGROUND

Link Division of The Singer Company developed the G-seat pictured in Figure 1 under the Advanced Simulator for Undergraduate Pilot Training (ASUPT) contract for the purpose of determining the adequacy of simulating tactile, pressure, and skeletal stature stimuli associated with flight-induced body G loading. The approach selected involved construction of seat cushions composed of mosaics of ele-

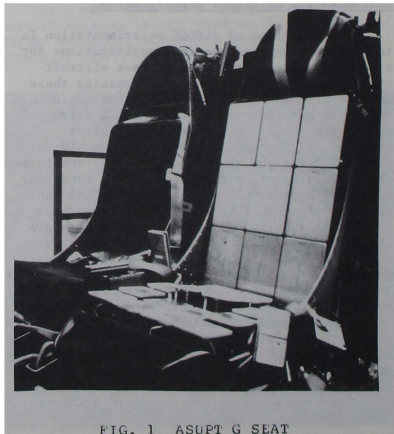


FIG. 1 ASUPT G SEAT

ments in which the elevation of each is individually controlled by the drive philosophy programmed into the simulator's computational system. It is therefore possible to change cushion attitude, elevation, and shape with the same mechanical

system. The G-seat employs a variable-tension lap belt to apply pressure stimuli in the ventral area of the pilot during negative G and/or braking conditions. The G-seat drive philosophy developed by Link primarily addresses the skeletal attitude shifts and their impact on eyepoint perspective, head/neck bobbing, and flesh scrubbing as well as localized flesh pressure changes and tactile perceived area of flesh seat contact changes associated with sustained G conditions. Experimentation with this seat indicated that not only were the sustained G stimuli presented by the seat employed positively by pilots in the control of the simulated aircraft, but in moving from one acceleration magnitude to another, a form of acceleration onset information was provided to the pilot.

The two ASUPT G-seats were Link's first domestic attempt to provide kinesthetic cues by a device designed to stimulate the somatic sensory system without dependence upon inertial acceleration effects, and its configuration became known as a "first generation" G-seat. Six of these devices are currently installed and being utilized in operational simulators, and thirty-five others are in various stages of production and due to enter the United States Air Force, Navy, NATO, Swedish and Japanese inventories.

During the above period, the value of the G-suit as a G cuing device became more widely appreciated. The G-suit cue represents an excellent example of apparent pilot G-level assessment by way of association. A predominant early perception experienced by the pilot, well before any cardiovascular effects materialize in vision, is a tactile perception associated with the pressure induced by the G-suit. The pilot appears to associate this perception with increasing G loading. Providing a similar experience within the simulation by inflating operationally issued G-suits according to the simulated flight G loading produces a very strong G loading cue for pilot utilization. Equally important is the fact that this cue is made available by a device which is present in the actual task, and, therefore, visual environmental fidelity is maintained within the simulation.

The introduction of the first generation G-seat to the tactical aircraft simulation environment demonstrated the apparent potential for inducing valuable kinesthetic stimuli via a direct approach to the somatic sensory system. However, questions arise as to whether the mechanical capabilities of the first generation G-seat optimally exercise this potential and extract a maximum benefit from this cuing source. The drive algorithm is established to provide a sense of sustained acceleration cue. However, this approach may overlook extraction of additional val-

able cues available under a transient cuing concept wherein an onset cue with subsequent washout is delivered. The bandwidth of the hardware, approximately 1 Hz, may be sufficient for sustained cuing concepts; however, it is likely too low for transient cuing concepts. The mosaic cushion approach, although certainly flexible, may not present the best method of altering pressure and area of contact stimuli. Indeed, the importance of pressure and area of contact stimuli, taken individually but in the context of a piloting task, is unknown.

The Air Force recognized that the G cuing area represents a seemingly important cue source and is likely to be pursued in operational trainer procurement. However, it is also an area wherein considerable research must be conducted to confidently establish a procurement specification which identifies the characteristics of a system providing best training yield. An advanced G cuing test bed was sought to support research leading to:

- a) A model of the role somatic sensation plays in piloting performance; thereby providing,
- b) An appreciation of piloting performance effects as a function of varying the characteristics of the delivered stimuli; which would lead to,
- c) Identifying, in specification form, the characteristics of hardware/software systems responsible for delivering somatic stimuli.

In mid 1976, the Air Force Human Resources Laboratory (AFHRL) awarded Link a contract for the development of an Advanced Low Cost G Cuing System (ALCCGS) which, in addition to preserving basic somatic capabilities of the first generation G-seat, embodies certain specific objectives:

- 1) Bring seat, suit, and shaker together as one integrated system with common control.
- 2) Improve by an order of magnitude the response characteristics of primarily the G-seat, and secondarily the G-suit, over those existing in today's operational seat/suit systems.
- 3) Provide closed-loop servo operation so that accurate means to measure system capability expended to produce a given cue can be monitored.
- 4) Investigate, develop, and embody within the final system mechanical concepts which improve the

somatic cuing quality of the G-seat over that available in the first generation G-seat approach.

- 5) Broaden the resultant hardware and software design to accommodate F-16 type tilt-back seat configurations as well as the more conventional upright seat configurations associated with the F-15 and other aircraft.
- 6) Attempt to design this system so as to lower the aggregate cost of a seat/suit/shaker system.
- 7) Build and deliver a system with the above characteristics as well as a software drive module for Air Force research.
- 8) Modify a 135 simulator cockpit such that the above G cuing system can be operated as either a free standing test bed or as part of an operational simulator.

IV. DEVELOPMENT

The research role of the device suggested, from the start, that the primary drive modalities and basic capabilities embodied in the first generation G-seat must be available in the advanced G-seat. Further, additional drive modes were sought:

- a) Differential lap belt control permitting the belt to be laterally scrubbed across the ventral area in response to simulated lateral and roll acceleration.
- b) Seat pan cushion fore/aft translation to strengthen the cues delivered in response to simulated longitudinal acceleration.
- c) Increased cushion contouring at the lower outboard regions of the backrest to strengthen tactile area of contact cues in the lower dorsal torso area. This area is more strongly simulated under reclined seat configurations than conventional upright configurations.

The mosaic approach employed in Link's first generation G-seat requires a large number of individually controlled actuators to provide flexibility in cushion surface movement. The response requirements sought in the advanced G-seat could be met only with a more sophisticated servo system. Therefore, it seemed that an approach must be generated which preserved the capabilities of the mosaic in terms of cushion surface attitude, elevation, and shape changes, but accomplished this with

fewer actuators. Secondly, we wished to produce a cushion drive system in which vibratory cuing might be generated so as to permit investigation of the suitability of eliminating the seat frame shaker system. This suggests a cushion structure more rigid than that provided by the mosaic. Lastly, if the drive system could be tightly packaged so as to fit many types of seat frames with only the design of the top surface of the cushion changed for aircraft seat type conformity, standardization of G-seat subassemblies could be more readily achieved in comparison to that permitted by the mosaic approach.

Earlier experimentation at Link employing soft plastic bellows had demonstrated their usefulness in altering either skeletal attitude and elevation or tactile pressure and area of contact. However, conflicting cues were obtained when the stroke of the soft bellows was sized to provide simulation of the 50 mm. of vertical eye point shift found to occur in positive 6G centrifuge data. That is, when the body was lowered slightly under positive G simulation, the desired affiliated cue of increased flesh pressure was missing; in fact, the seat was softer. On the other hand, a low pressure soft pliable bladder, if maintained thin enough to cause the buttocks to be poised just above a firm surface, can provide very significant flesh pressure alterations as the bladder is exhausted and the body settles on the firm surface. Localized flesh pressure concentration and changes in tactile area of contact can be scheduled by selecting a firm surface of appropriate contour.

The approach selected for the advanced G-seat employs the thin bladder discussed above and is schematically pictured in the front view of the seat pan cushion provided in Figure 2. The approach has

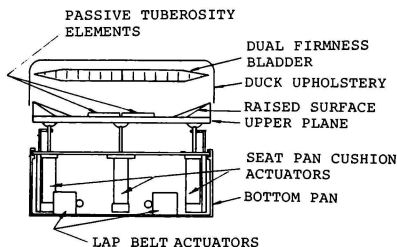


FIG. 2 FRONT VIEW OF SEAT PAN CUSHION SHOWING MOVING PLANE AND FIRMNESS BLADDER DESIGN

been termed "moving plane and firmness bladder" for it cascades the benefit in terms of tactile pressure and area of con-

tact cuing available from a thin bladder on top of a rigid plane capable of moving through the excursion range necessary to provide compatible skeletal position and attitude change, flesh scrubbing, and visual perspective alteration. A similar approach is employed in the backrest as pictured in Figure 3. The approach reduces the number of servo loops from 32 used in the first generation G-seat to 14 employed in the advanced seat while increasing the number of drive modalities as earlier mentioned.

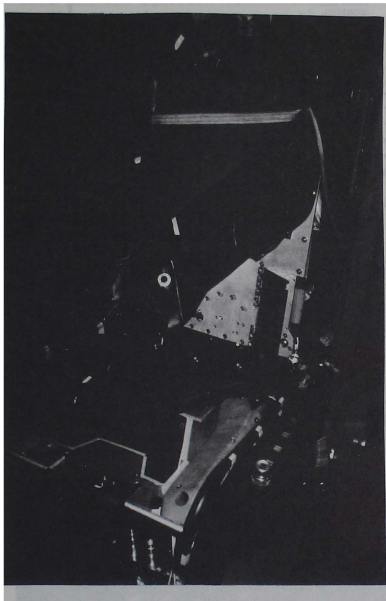


FIG. 3 ADVANCED G CUING SYSTEM G SEAT WITH UPHOLSTERY AND FIRMNESS BLADDERS LAID BACK SHOWING MOVING PLANES, PASSIVE THIGH RAMPS, AND ACTIVE BACKREST RADIAL ELEMENTS

A typical seat pan cushion response to positive G (eyeballs down) simulated acceleration would cause the moving plane to settle, lowering the body, causing skin tension in that area adjacent to the backrest, and shifting eye point downwards. Simultaneously firmness bladder pressure is lowered to permit the body to settle more firmly on the moving plane. Thus, a greater portion of the body's normal 1 G load is concentrated in the area of the ischial tuberosities locally increasing flesh pressure. Likewise, a larger portion of the buttock area is permitted to

lightly contact the upward contour of the outboard edges of the moving plane, thereby increasing tactile area of contact.

Mechanical Configuration

In order to establish an integrated cuing system, control is centralized in an electronics cabinet patterned after platform motion system control cabinets. The electronics cabinet is the interface between the various system components, and as such, contains the operational logic and servo control electronics for all aspects of the system. Figure 4 shows the interaction and interdependencies within the ALCOGS structure.

The G-seat, the most complex of the three cuing sources, consists of two major assemblies: the seat pan cushion and the backrest cushion. Utilizing the motion of these two assemblies, the seat provides excursions in four degrees of freedom.

The seat pan consists of a total of six hydraulic actuators. Three actuators form a three-post support system and drive the seat pan upper plane in pitch, roll, and heave. Each of these actuators has an excursion range of ± 1.25 inches. The two lap belt actuators are located in the seat pan and drive the lap belt in the longitudinal and vertical axis and differentially in the lateral axis. The seat pan upper plane consists of an undercarriage and top plane. The longitudinal actuator is mounted on the undercarriage and drives the top plane in fore and aft motion. This motion is cascaded on seat pan pitch, roll and heave capability. Mounted on the top plane are the passive tuberosity blocks and thigh ramps, and this assembly is covered by a dual cell firmness bladder. The thigh ramps contribute to an increase in flesh area of contact while the tuberosity blocks provide an increase in localized buttock pressure, both occurring during deflation of the firmness bladder. All of the above are mounted within the volume of the seat pan box, which is approximately $15" \times 15" \times 6"$. The seat pan cushion assembly is in turn mounted in the seat frame utilizing the volume normally occupied by the aircraft seat survival kit.

The backrest assembly contains five hydraulic actuators packaged in a volume $15" \times 21" \times 3 \frac{3}{4}"$. Three actuators drive the top plane in the same manner as in the seat pan. The other two actuators drive the radial wings located in the lower corners of the top plane causing an increase in area of contact in the lower back region as the wings are extended. Mounted on the top plane is a single cell firmness bladder.

The anti-G-suit system is patterned after prior systems in which a standard unmodified anti-G suit is employed. Suit

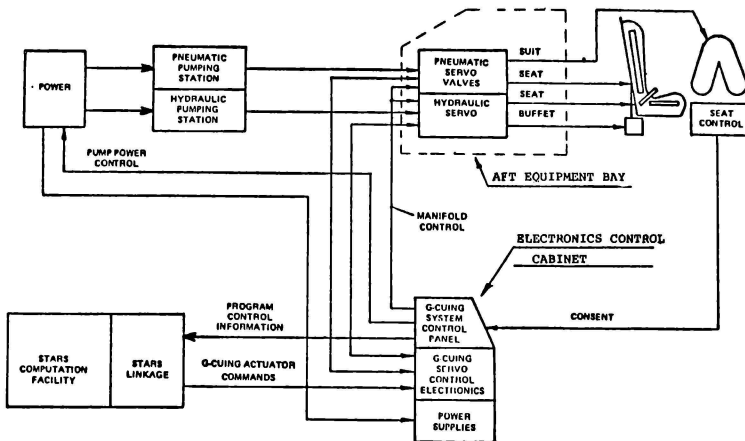


FIG. 4 SCHEMATIC ORGANIZATION OF THE ADVANCED G-CUING SYSTEM

internal pressure is regulated by a pneumatic servo valve assembly as a function of simulated aircraft acceleration.

The seat shaker consists of a short body hydraulic actuator mounted to the rear of the seat frame providing both discrete and continuous vibratory cues through seat frame motion. The shaker produces continuous vibratory cues over a 0.25 Hz to 40 Hz spectrum at levels up to 0.5 g.

ALCOGS is intended to operate in either a free standing test bed or cockpit environment. The seat is mounted on a frame assembly which is bolted to an aft equipment bay behind the seat. Adjustment of this frame assembly permits ALCOGS to adopt an upright F-15 type attitude or the 30° reclined attitude of the F-16. The aft equipment bay, containing the controls for hydraulic and pneumatic power distribution along with the pneumatic servo valve/booster manifold assemblies for firmness bladder and G-suit control, is bolted to the research test bed. A T-38 flight simulator cockpit was acquired by AFHKL which was modified to house ALCOGS. By unbolting the aft equipment bay from the test bed, the seat and aft equipment bay can be slid through the rear of the simulator where the system can be operated in a cockpit environment.

A design philosophy adopted during system development allows maximum access to drive elements in a minimum amount of time and facilitates actuator set up and test. A modular package was developed resulting

in easily accessible and separately removable actuator subassemblies. There are four such modular subassemblies in the seat pan; the front actuator, two combination side and lap belt actuator subassemblies as shown in Figure 5, and the undercarriage containing the longitudinal actuator and the vibration monitoring accelerometer.

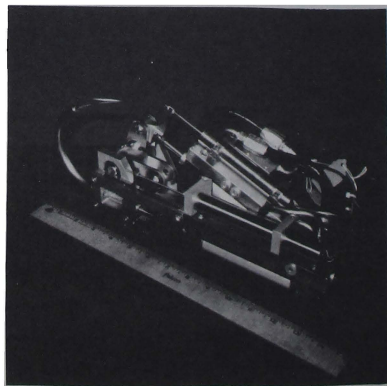


FIG. 5 SEAT PAN COMBINATION SIDE AND LAP BELT ACTUATOR MODULAR SUBASSEMBLY

The backrest cushion also contains four modular subassemblies; the three backrest actuators and one subassembly containing the radial actuators and wings. Once removed from the seat pan or backrest, an actuator can be serviced on a universal test manifold capable of porting hydraulic fluid to any one of the eight modular subassemblies. In addition, both seat pan and backrest cushions can be easily removed as a unit from the seat frame.

Pneumatic Bellows Drive

One of the original drive concepts that was expected to be employed in the G-seat was a pneumatically driven metal bellows providing the backrest top plane drive. A three post system similar to that actually implemented using hydraulic actuators was to be utilized to develop the three degrees of backrest motion. The radial wings were also intended to be driven pneumatically.

It was expected from the outset that simply closing the servo loop on position and utilizing existing G-seat components would not yield the required response characteristics of a 30 millisecond rise time (roughly equivalent to a 10 Hz bandpass for a second order system). To determine the system characteristics necessary to achieve the specified response, several aspects of the pneumatic system were investigated. One principle component affecting system response was the pneumatic servo valve. Flow analysis, based on a Link-imposed specification of 1 Hz full stroke operation with no flow limiting, indicated that the valve must be able to pass better than 6 SCFM (5 inch diameter bellows, 20 pound load), a capability beyond that of the valve used in the first generation G-seat open loop pneumatic servo.

A flapper-type pneumatic valve was purchased as a possible replacement valve. The pneumatic flow characteristics of this valve were modeled in a computer program which indicated the valve would not meet the 1 Hz full stroke specification. However, this valve had superior frequency response characteristics compared to the prior valve. Therefore, a similar valve with larger orifices and greater flapper travel, permitting greater flow, was purchased. Unfortunately, this valve exhibited poor stability characteristics and was not used. A manifold flapper-type valve booster relay combination was designed that would meet the flow and frequency response requirements. This development will be discussed later.

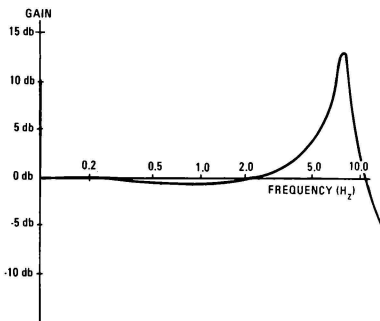


FIG. 6 RADIAL BELLOWS AMPLITUDE RATIO (POSITION/PRESSURE) VS. FREQUENCY

It was apparent that the bellows actuator assembly would require high spring rate and external servo loop compensation in order to provide the desired response. Manufacture and test of a sample bellows indicated that the spring rate parameter would be difficult to achieve, particularly in the 5 inch diameter bellows utilized to drive the backrest top plane. Experimental data taken on the radial element bellows, a 2.55 inch diameter bellows, indicated problems would also occur due to poor bellows damping characteristics. The data shows a damping ratio of 0.125. Amplitude ratio vs. frequency is plotted in Figure 6 for the radial bellows.

These parameters pose an interesting control problem. The open loop valve/bellows model is shown in Figure 7. Root locus analysis shows simple unity feedback would cause the system to become unstable when the gain was increased enough to achieve 10 Hz response, due to the low bellows natural frequency and poor damping (Figure 8). A cascaded compensator of the form:

$$G_c(s) = \frac{K(s+a)}{(s+b)} \frac{(s^2 + c_1s + c_0)}{(s^2 + d_1s + d_0)} \quad (1)$$

was developed to stabilize the system, resulting in the root locus of Figure 9. However, further analysis indicated that the system open loop poles were sensitive to changes in load, as shown in Figure 10, and that there was no simple optimal compensation that would stabilize the system

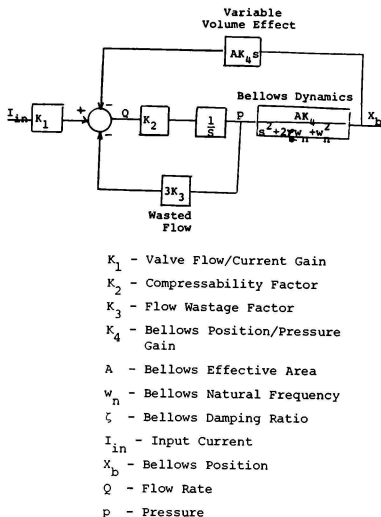


FIG. 7 VALVE-BELLOWS OPEN LOOP BLOCK DIAGRAM

for large variations in load while meeting the response specification. In a related effort the bellows actuator was driven electronically closed loop on pressure. A bandpass of 2.2 Hz was achieved however, 30% overshoot on bellows depressurization was experienced and considered unsatisfactory. The conclusion was reached that these problems were not without a solution, but would require more effort than time allowed. Hence, it was decided to employ hydraulic actuators for the backrest and radial element drives in a manner similar to that being employed in the seat pan.

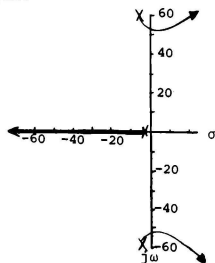


FIG. 8 FIVE INCH BELLOWS SYSTEM ROOT LOCUS-UNITY GAIN FEEDBACK

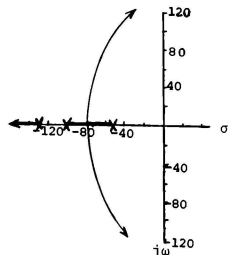


FIG. 9 FIVE INCH BELLOWS SYSTEM ROOT LOCUS-IDEAL COMPENSATION

Firmness Bladders

With the conversion of the backrest and radial elements drive mechanisms to hydraulic actuators, the firmness bladders and G-suit remained the only pneumatically driven elements. Bladder volume as a function of pressure was measured as 24 in³ at 1.75 psi for one cell of the seat pan bladder and 104 in³ at 0.8 psi for the backrest bladder. From this valve flow requirements were established as 3.6 SCFM for each cell of the seat pan bladder and 10.3 SCFM for the backrest bladder. Thus, as in the case for the backrest bellows, valves with flow capabilities greater than that previously employed for first generation G-seats were needed.

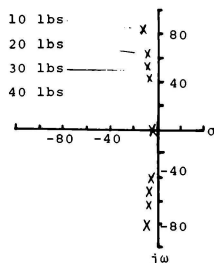


FIG. 10 FIVE INCH BELLOWS SYSTEM OPEN LOOP POLE SENSITIVITY TO STATIC LOAD VARIATIONS

As stated previously, the larger flap-per-type valve exhibited instabilities, and therefore an alternative approach was

developed. The original flapper valve was augmented by high flow booster valves wherein the flapper valve provides a pilot signal to the boosters which act as flow amplifiers. This servo is operated closed loop on pressure and has a rise time of 25 msec. in response to a step input and provides enough flow to meet the 1 Hz full stroke specification. The seat pan bladder cells required two booster augmentation, while the backrest bladder, because of its greater volume, required four boosters to pass the necessary amount of air. The bladders are operated at low pressure, typically 0-2 psi, and the evacuation of the bladders during dynamic operation was a problem due to the low pressure differential between bladder pressure and atmospheric pressure. Therefore, a vacuum assist was added to aid in bladder evacuation. Vacuum was applied at the exhaust ports of both the flapper valve and boosters. Tests run on the bladder system with different configurations of atmospheric and vacuum exhaust show vacuum applied to both exhaust ports to provide the best response.

These tests were run utilizing an apparatus that applied a load to one cell of the seat pan bladder similar to that of a person's buttock. A force transducer was located under the bladder at the location of the ischial tuberosity. Using this set-up, pressure and force step response and frequency response data was gathered for the various configurations mentioned above. A typical step response is shown in Figure 11.

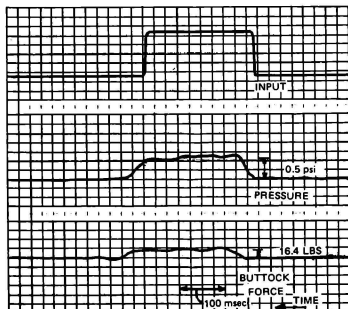


FIG. 11 SEAT PAN BLADDER PRESSURE AND ISCHIAL TUBEROSITY FORCE RESPONSE TO STEP INPUT

As previously stated, the drive servo is electronically closed loop on pressure. It is a servo in which a constant error signal is required to maintain a constant bladder pressure. The feedback signal is provided by pressure transducers located in the seat pan and backrest cushions. The bladders are set up such that the trainee's body is lifted by the bladders to the point where contact is lost between the body and seat pan and backrest top planes. For the seat pan, preliminary tests indicated that this point corresponded to a pressure of 1.8 psi, and the backrest neutral point was 0.8 psi. However, during installation these pressures were reset to 1.2 psi and 0.6 psi for the seat pan and backrest respectively.

Hydraulic Actuator Drive

In developing the hydraulic drive for the seat pan top plane, various actuator configurations were examined. It was determined to be advantageous in terms of response and minimization of oil column resonance to have the valve situated as close as possible to the cylinder. Thus, the servo valve, cylinder, and follow-up device were compactly packaged as one unit.

As earlier mentioned a design objective was to package all servo actuators within the normal confines of the seat pan cushion/survival kit and backrest parachute pack volumes. A rotary actuator appeared attractive for this reason; however, actuator frequency response was too low and breakaway friction was too high. A second approach, the one finally implemented, uses a bellcrank mechanism. Utilizing a bellcrank with a mechanical advantage of 1.25:1.0, the stroke of the hydraulic actuator was reduced from ± 1.25 inches to ± 1.0 inches, resulting in a shorter actuator body.

Similar to the pneumatics, the hydraulic servo valve was sized to meet the 1 Hz full stroke specification. Valve flow tests were run to confirm vendor flow data and valve and cylinder leakage flow was measured to determine its effect on system performance.

With the decision to utilize hydraulic actuators in place of the backrest pneumatic bellows, another packaging problem arose. The backrest assembly is only three inches deep in the fully settled state. Two different subassembly designs emerged. One was a modified version of the bellcrank assembly used in the seat pan, and the other was a slide link mechanism. Both subassemblies would have a mechanical advantage of 2:1 resulting in ± 0.625 inch stroke actuators. Both actuators showed equivalent response characteristics. Due to the thinness of the backrest package and the modular design objective, the low profile slide link was

a more attractive assembly, incorporating servo valve, cylinder, and follow-up device in one unit. The bellcrank configuration would require the servo valve be mounted apart from the cylinder and follow-up, adversely affecting serviceability. Therefore the slide link approach was incorporated in the backrest cushion design.

During the frequency response tests in which the slide link actuator was consistently run at frequencies of up to 40 Hz under static loads up to forty pounds, it was found that the brass bearings used in the slide link mechanism deteriorated to the point where they were unusable. The brass bearings were replaced with steel bearings which have performed satisfactorily with no evidence of deterioration.

The hydraulic actuator servos are closed loop on position. The follow-up device providing position feedback is a linear variable differential transformer (LVDT). This device provides a clean feedback signal with infinite resolution.

Anti-G-suit

In G-suit implementations prior to ALCOGS, suit inflation was regulated by a pneumatic servo valve coupled with a single booster relay. The deflation rate for this system was slower than desired which suggested the usage of the vacuum assisted two stage booster valve designed to drive the firmness bladders. The four booster relay configuration provides ample flow and significantly improves G-suit pressurization and exhaust rates. Vacuum exhaust of -5 psi applied to the booster exhaust ports further aids depressurization of the suit.

The ALCOGS G-suit also incorporates a pilot initiated press-to-test. A linear potentiometer is connected to the press-to-test button. As the button is depressed, a pressure proportional to the button position is applied to the suit. The commanded pressure signal from the press-to-test button is combined with the commanded pressure signal from the software or maintenance potentiometer to permit functional press-to-test capability at all times.

Seat Shaker

The seat shaker system provides vibration and buffet cues of a sinusoidally continuous and/or discrete form for use in replicating events such as stall buffet, background rumble, speedbrake buffet, gear buffet, runway joint bumps, and a discrete touch down bump. The ALCOGS approach permits these effects to be displayed to the pilot either by vibrating the total seat frame or superimposing the effects on the G-seat seat pan cushion hydraulic actuators.

The shaker system provides vibratory cues between frequencies of 0.25 to 40 Hz at amplitudes up to ± 0.25 inches. The system can provide accelerations of 0.5g throughout the 4.5 - 40 Hz frequency spectrum. The shaker actuator is driven by the summation of two variable frequency oscillators (VFO) and a discrete channel input. Each VFO constructs a sinusoidal signal from two inputs, a voltage proportional to the desired signal frequency and a voltage proportional to the amplitude of the signal. The shaker actuator servo loop is closed loop on position through an LVDT follow-up device.

To protect against mechanical resonances in the seat assembly, the output of each VFO is limited to provided a maximum of 0.5 g. The limiter circuit limits the amplitude signal according to the equation

$$A = \text{MIN} \left[A, \frac{K_1 f^2 + (K_2 f)}{0.5} \right] \quad (2)$$

where A = amplitude of signal

f = frequency of signal

K_1, K_2 = limiter gain constants

K_1 attenuates the permissible amplitude to alleviate problems in the region of mechanical resonance, which is 14 Hz to 17 Hz. The second term, $K_2 f$, increases the permissible amplitude for frequencies above 16.5 Hz to compensate for system roll-off above that point.

Safety

The fact that the hydraulic actuator assemblies can develop hundreds of pounds of force has caused considerable thought to be given to safety in the design of ALCOGS. Several areas of concern were addressed. First, an interlock inhibits the seat cushions from erecting to their neutral point upon powering up if the seat is occupied. This prevents someone from sitting in the seat, buckling up the lap belt, and then erecting the seat, which would force the lap belt tighter around the user's midsection. The interlock is activated by pressured sensitive switches on the seat pan and backrest top planes.

Another concern was that of a foreign object becoming trapped between the moving surfaces of the seat pan and backrest top planes and the seat frame. Pressure activated tape switches line the areas where an item, such as a finger, might stray. The switches trip at an applied force of 12 ounces, causing the system to go into an emergency shutdown. This problem is somewhat diminished by the fact that all moving elements are confined within the upholstered seat pan and backrest cushions. There are no moving parts, with the exception of the shaker actuator, outside the seat frame.

All the hydraulic actuator assemblies were designed such that in emergency shutdown any actuator can be extended immediately to free the trapped object. Upon emergency shutdown, the hydraulic supply is immediately ported to return and a check valve in each actuator assembly allows the actuator to be manually moved in extension, regardless of the position of the servo valve spool at shutdown.

V. SYSTEM PERFORMANCE

The ALCOGS performance characteristics at installation are shown in Table I.

TABLE I. ALCOGS PERFORMANCE CHARACTERISTICS

Component	Axis	Excursion	Response
Seat Plan	Roll, Pitch	$\pm 12^\circ$	30 ms, 10 Hz
	Heave	$\pm 1.25"$	
	Fore-Aft	$\pm 1.0"$	
Backrest	Pitch	$\pm 6^\circ$	30 ms, 10 Hz
	Yaw	$\pm 9^\circ$	
	Surge	$\pm 1.25"$	
Seat, Backrest, Bladders	Roll, Heave, Surge	1"	30 ms, 6 Hz
Seat Shaker	Heave	$\pm 0.25"$	34 Hz
Lap Belt	Fore-Aft	$\pm 1.5"$	30 ms, 10 Hz

Typical hydraulic actuator frequency and step responses are shown in Figures 12 and 13 respectively. A typical firmness bladder frequency response is shown in Figure 14.

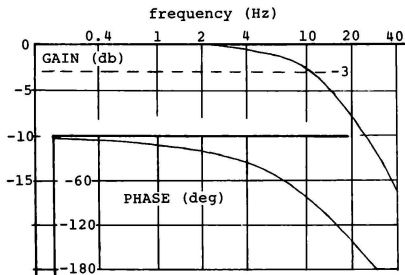


FIG. 12 TYPICAL HYDRAULIC SERVO FREQUENCY RESPONSE

ALCOGS was integrated with the Air Force Human Resources Laboratory Simulation Training and Research System (STARS) at Wright-Patterson AFB. At this time the ALCOGS hardware was integrated with its

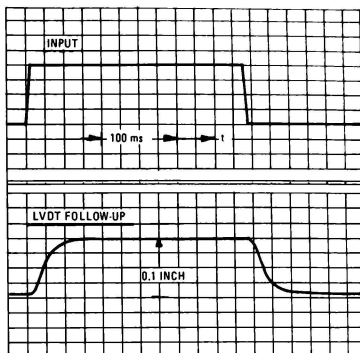


FIG. 13 TYPICAL HYDRAULIC SERVO STEP RESPONSE

drive software for the first time. The software consists of separate modules to drive the G-seat, G-suit, and seat shaker, a module for vibration exposure monitoring (VIBCOUNT), and a dynamic driver test module for seat operation in the absence of flight acceleration inputs which were not available at the time of integration.

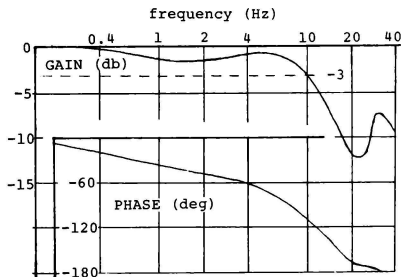


FIG. 14 SEAT PAN FIRMNESS BLADDER SERVO FREQUENCY RESPONSE

During hardware/software integration, a stepping effect was noticeable in actuator motion due to the 20 per second program iteration rate of the STARS. ALCOGS, displaying a 10 Hz bandpass, is capable of responding to the discrete digital changes in actuator drive signals at this iteration rate. Anticipating this problem Link designed and incorporated variable band-

pass filters as part of the input signal path to each servo which function in series with the high bandpass filter section of the linkage D/A circuit. The filters smooth the computer-originated drive signal such that the stepping in the actuator motion is eliminated and are variable so that the filter bandpass can be increased as the iteration rate is increased as per the Human Resources Laboratory research plan. As set up during installation, the filters were adjusted for a 2.5 Hz bandpass, yielding a servo bandpass of approximately 2.0 Hz. As the program iteration rate is increased, the variable bandpass filters can be rolled out and overall servo bandpass increased so the system can be utilized to its full potential.

In order to determine optimum G-cuing hardware and drive algorithms for use in tactical aircraft simulators, AFHRL has embarked on a program of engineering and psychophysical testing and evaluation. Evaluation and characterization will be made of the ALCOGS cuing capabilities and dynamic performance. This will be followed by an investigation into the cuing capabilities of the system with restrictions placed on seat excursion and/or response and an investigation of alternate drive algorithms, in particular the application of onset cuing. At present tests are being conducted to determine Weber fractions for the tactile sensitivity levels for the regions of body contact with seat.

References

1. Kron, G. J. Advanced Simulation in Undergraduate Pilot Training: G-Seat Development. AFHRL-TR-75-59(III), Wright-Patterson AFB, Ohio: Advanced Systems Division, Air Force Human Resources Laboratory, October 1975.
2. Albery, W., McGuire, D. Emulation of an Advanced G-seat on the Advanced Simulator for Pilot Training, AFHRL-TR-78-4, Wright-Patterson AFB, Ohio: Advanced Systems Division, Air Force Human Resources Laboratory, April 1978
3. Kroemer, K. H., Kennedy K. W. Involuntary Head Movements and Helmet Motions During Centrifuge Runs with up to +6 G's. Aerospace Medicine 44(6): 639-644, 1973
4. Kleinwaks, J. M. Advanced Low Cost G-Cuing System, Unpublished AFHRL report, July 1978

THE EFFECT OF HELMET LOADER G-CUEING ON PILOT'S SIMULATOR PERFORMANCE

B. R. Ashworth
and
B. T. McKissick
NASA Langley Research Center
Hampton, Virginia

Abstract and Summary

In high performance aircraft the g forces on the pilot's helmet provide important feedback concerning the aircraft's dynamic state as well as limiting the pilot's ability to move his head when the g forces are high. A helmet loader has been designed to provide the effects of these forces in aircraft simulators. The design is such that the forces applied to the helmet are independent of the pilot's head and shoulder position.

The device is easily installed in a simulator cockpit, quickly attaches to the pilot's flight helmet and is safe for use in simulators. The helmet loader has been installed in Langley Research Center's Differential Maneuvering Simulator (DMS) and subjectively rated as providing realistic forces on the head and shoulders during high g simulator tasks.

In order to determine the effect of the helmet loader on a pilot's performance, an experiment was performed in the DMS, consisting of a tracking task using an F-14 aircraft simulation. Pertinent system states were recorded and analyzed using univariate and multivariate statistical algorithms. Analysis of the data indicates that pitch control increases significantly during the transition phases of the task when the helmet loader is activated. Overall, the variation in the performance measures are reduced under the helmet loader activated condition indicating more precise control of the aircraft simulator for this task.

I. Introduction

Providing the motion induced (kinesthetic) cues which the pilot uses in control of the aircraft has always been a concern in piloted aircraft simulations. This concern is magnified in high performance aircraft simulations where the pilots tend to rely more heavily on these motion induced cues. Simulator engineers have historically used various devices in an effort to provide realistic cues to the simulator pilot. At LaRC such devices have included g-suits, arm harnesses, g-seats, control loaders, blackout/grayout controls, and cockpit buffet as well as motion based cockpits. Another very important kinesthetic cue to the pilot is the increased load on the neck and shoulders due to the increased weight of the head/helmet combination. Helmet loaders have had very little utilization to date due primarily to the problems associated with providing the proper cue without other false cues such as the restriction of head motion.

A helmet loader has been designed and tested in LaRC's Differential Maneuvering Simulator which

provides the proper cues without restricting the pilot's movement or requiring cumbersome attachments. The loader follows the pilot's movement while providing the proper forces and requires only two small strings to be snapped to the helmet. An experiment was conducted to determine the effect of the loader on both LaRC test pilots and operational F-15 pilots. Both the objective and subjective data from the experiment was used to determine the effect of the helmet provided acceleration cues on the simulator pilot's performance.

II. Helmet Loader Design

The helmet loader is designed utilizing force feedback in order to follow the pilot's movements while providing proper helmet forces. Figure 1 shows the helmet system as installed in the DMS cockpit and Figure 2 shows the design in schematic diagram form. The two small pulleys attached to the pilot's shoulder straps provide a loosening of the straps as force is exerted downward on the helmet for positive g. The excess cable between the helmet and the force transducer allows for unrestricted turning of the head while the torque motor has sufficient cable wound on its reel to allow for all body and head movements of the pilot.

The helmet loader is essentially a 0.4 damped second order system with a 20 millisecond steady state time delay. Full amplitude sine and triangular response data are plotted in figures 3 and 4 for commands representative of changes in normal acceleration of 1g to 6g in 1 second, which is representative of current high performance aircraft. Figure 5 shows a 50% step response with a 0-90% rise time of approximately 50 milliseconds.

The helmet loader has been scaled at approximately 2/3 the inflight helmet loads. The loader exerts 40 newtons (9 lbs.) of force at the selected full scale command of 6g. The loader uses break away snaps on the helmet, current and voltage limiting, and small torque motors to ensure that the pilot does not experience excess forces.

III. Simulation Facility

The helmet loader was installed in NASA Langley's Differential Maneuvering Simulator (DMS) in order to carry out this study. The DMS provides a realistic means of simulating two aircraft or spacecraft operating in a differential mode and has a wide F. O. V. visual display where all servos involved in projecting the visual scene are synchronized with a .7 damped, 25 rad/sec. second order transfer function. An F-14 simulation was used as the test aircraft. A more detailed description of the DMS is given in reference 1. Detailed information about the F-14 simulation is found in

reference 2.

IV. Statistical Analyses and Experimental Design

Experimental Task

A tracking task (approximately 70 seconds in length) was used in performing the experiment. The target aircraft was driven by a taped maneuver consisting of a three g wind-up turn at a constant airspeed of 325 knots. The pursuit aircraft was required to track the target while maintaining a 457 meters (1500 feet) range. During the task, the pursuit pilot's tracking reference (reticle) was switched from a 10° lead position to a 5° lag and back to a 10° lead. These changes in reticle position (occurring every 10 seconds) forced the pilot to reacquire the target after each change in the tracking reference (Figure 6) thus increasing and decreasing "g" from the nominal 3g point. Range information was provided by a standard reticle range analog bar scaled for 914 meters (3000 feet). This caused the required 457 meters (1500 feet) range to appear at the 6 o'clock tab.

Subjects and Procedure

Two groups of pilots were used as test subjects in this study. The first group consisted of two Langley test pilots with many hours in fighters and in simulators. These two test pilots were used during the helmet-loader developmental phase and as a result were very familiar with this simulation. The second group consisted of five F-15 pilots with no experience flying this simulation. The amount of flight time in high performance fighter aircraft varied from a pilot just out of flight school to ones having several thousand hours of flight time.

The experiment was conducted by flying the task in sets of ten 70 second runs. Each set of ten runs (a session) consisted of ten randomly chosen runs, five with the helmet-loader activated and five with the helmet-loader deactivated. Each pilot was allowed 3 to 5 practice runs to familiarize himself with the simulator and task. After the practice runs, each pilot flew two sessions per day. Previous experience indicated that two sessions was about the maximum amount of time a pilot could fly this task before his performance started to deteriorate due to fatigue. Each member of the first group flew a total of 7 sessions, while each member of the second group flew a total of 4 sessions. The first two sessions for each pilot were treated as learning sessions and the remaining sessions were used to analyze the experiment.

Performance Measures

During each data run, eleven state variables were recorded every 1/16 second. Variables recorded were vertical tracking error (TKE), lateral tracking error (TKL), total tracking error (TKE), normal acceleration (NZ), pitch rate (TD), roll rate (PDT), range to target (RT), longitudinal stick deflection (DE), lateral stick deflection (DA), rudder pedal deflection (DR), and time (T). In order to calculate the performance measures, the tracking task was broken down into four basic phases as shown in figure 6. These phases are: (1) transitioning from -10° (lead) reticle setting to $+5^\circ$ (lag) reticle setting (positive transition, denoted by +T), (2) tracking at $+5^\circ$ reticle setting (positive tracking, denoted by +S), (3) transitioning from

$+5^\circ$ reticle setting to -10° reticle setting (negative transition, denoted by -T), and (4) tracking at -10° reticle setting (negative tracking, denoted by -S). The pilot is considered to have transitioned when the vertical tracking error reaches 80% of the required value (-10° or $+5^\circ$). Four measurement calculations (arithmetic mean, variance, maximum and minimum) were applied to the four parts of the task to develop the measures as shown in Table 1.

Statistical Analyses

The univariate analyses included F-ratio test and the student's t-test for paired data. The multivariate analyses included Hotelling's T^2 and linear discriminant analysis for paired data. In each of the tests, performance measures were tested under the helmet activated condition versus the helmet deactivated condition. As previously mentioned, the first group flew 5 sessions for analysis, while the larger second group flew 2 sessions for analysis. This resulted in 150 replicates of a performance measure for each of the two helmet conditions.

V. Results and Discussion

The results for both sets of pilots are similar, therefore, only the data from the five F-15 pilots will be presented.

The performance measures for the helmet activated data (Fig. 7 thru 14) are normalized with respect to the data for the helmet deactivated condition. The center horizontal lines of the figures represent the means of the performance measures for the helmet deactivated condition. The two outer horizontal lines represent the one sigma limits of the performance measures for a deactivated condition. The vertical lines represent the one sigma limits and mean of a performance measure for a helmet activated condition. The numbers on the figures give the $1-\alpha$ levels at which the F-test (upper numbers) and paired student's t-test (lower numbers) are significant. For example, figure 9 indicates that the mean stick deflection for pitch during a positive transition (MDE +T) is significantly lower ($1-\alpha = .96$) when the helmet loader is activated. The variance of this performance measure for positive transition is reduced significantly ($1-\alpha = 1$) when the helmet-loader is activated as compared to when it is not activated.

Examination of the univariate analyses (fig. 7 thru 14) shows that the helmet-loader had more effect on pilot performance during the transition periods of the task. In particular the effect of the helmet-loader shows up mainly in the longitudinal axis. Significantly more pitch control (MDE) is applied when the helmet-loader is activated (a measure is judged to be significant if $1-\alpha > .9$.) This results in significantly more pitch rate (MTD) during a negative transition and significantly less MTD during a positive transition. Other measures that show significant mean differences during a negative transition are TDMAX, NZMAX, MTK, and TS-. The most apparent effect, however, is not the mean differences but a significant lowering of the variances when the helmet-loader is activated. Fifteen out of thirty measures for the transition portion have significantly lower variances. Of the measures that aren't significantly lower, only two have significantly higher variances (TDMAX and

NZMAX for negative transition) and there is no statistical difference in the remaining measures. Therefore, although more control is used when the helmet is activated the pilots exhibit less variation in their control inputs during a transition.

A similar trend is evident in the tracking portion of the task. But this time more significant results appear in the lateral axis. The variation in lateral stick input (MDA) is significantly reduced for positive and negative tracking. Other measures that show reduced variances for the lateral axis are MDR, MTKL, and PDTMAX for positive tracking. MDA and MPDT show reduced variances for negative tracking. Hence, with the helmet-loader activated there is less variation in the pilots roll input while tracking.

While the most important result from the univariate analyses is reduced control variation, the measure that most strongly differentiates between helmet activated and not activated is TS-. The pilots performed negative transitions significantly faster on the average (3.05 sec. vs 3.22 sec) when the helmet-loader was on. There was also reduced variation in the negative transition time. The importance of TS- is also reflected in the multivariate analysis.

In the multivariate tests, two basic groups of ten performance measures were analyzed: (One) primarily for the longitudinal degree of freedom and (the other) for the lateral degree of freedom. The performance measures for these groups are given in Table 1. Initially all ten measures were analyzed. Next, based on the discriminant analysis, the dimension (number of measures) was reduced and the remaining measures were reanalyzed. The results of the reduction in dimension is given in Table 2. It can be seen that TS- ranks high in all the groups. The two groups for the negative transition provide the strongest differentiation between helmet-loader on and helmet-loader off; the probabilities of these two groups (.971, .978) are higher than the probabilities for any other group. In the four groups for the transitions, the measures contributing most to distinguishing between helmet-loader activated and helmet-loader deactivated are TS-, MTD, TDMIN, and PDTMIN. All of these performance measures with the exception of TS-, are highly correlated (.7 or greater) with control activity. TS- indicates that the helmet-loader is providing a cue that enables the pilots to transition faster during the negative transition. This is not surprising since the strongest normal acceleration cue should be during a negative transition when the pilots are increasing their g loads.

VI. Conclusions

Analysis of the simulation data indicates that the helmet-loader does have measurable effect on the pilot/simulator system. The effect is mainly seen in the transition portion of the task. The pilots significantly increase their control outputs for pitch which causes a significant increase in aircraft pitch rate. This is accomplished while more precise control of the aircraft is being executed. A significant reduction in the variances of 50% of the measures for transition indicates more precise control of the aircraft. Subjective data indicates that the cue provided through the use of the helmet-loader is realistic, and there is no noticeable time delay in the presentation of the cue. However, the

pilots had mixed opinions about the effect of the helmet on their performance. Tests to determine the effect of the helmet-loader on the linear pilot transfer function and an experiment in which the helmet-loader and g-seat (Ref. 3) are used together are planned.

VII. References

- ¹Ashworth, B. R.; and Kahlbaum, William M., Jr.: Description and Performance of the Langley Differential Maneuvering Simulator. NASA TN D-7304, 1973.
- ²Gilbert, W. P.; Nguyen, L. T.; and Vangunst, R. U.: Simulator Study of Applications of Automatic Departure and Spin Prevention Concepts to a Variable Sweep Fighter Airplane. NASA TMX-2928, 1973. (CONFIDENTIAL).
- ³Ashworth, B. R.; McKissick, B. T.; and Martin, D. J., Jr.: Objective and Subjective Evaluation of the Effects of a G-Seat on Pilot/Simulator Performance During a Tracking Task. Tenth NTEC/Industry Conference; Orlando, Florida; November 15-17, 1977.

TABLE 1.- LONGITUDINAL AND LATERAL
PERFORMANCE MEASURES

LONGITUDINAL

MEAN STICK DEFLECTION FOR PITCH (MDE)
MEAN VERTICAL TRACK (MTKL)
MEAN PITCH RATE (MTD)
MEAN NORMAL ACCELERATION (MNZ)
MAXIMUM PITCH RATE (TDMAX)
MINIMUM PITCH RATE (TDMIN)
MAXIMUM NORMAL ACCELERATION (NZMAX)
MINIMUM NORMAL ACCELERATION (NZMIN)
POSITIVE TRANSITION TIME (TS+)
NEGATIVE TRANSITION TIME (TS-)

LATERAL

MEAN STICK DEFLECTION FOR ROLL (MDA)
MEAN RUDDER DEFLECTION (MDR)
MEAN LATERAL TRACK (MTKL)
MEAN ROLL RATE (MPDT)
MAXIMUM ROLL RATE (PDTMAX)
MINIMUM ROLL RATE (PDTMIN)
NZMAX
NZMIN
TS+
TS-

TABLE 2.- RESULTS OF MULTIVARIATE ANALYSES

GROUP	+T TASK	PROB.	GROUP	+S TASK	PROB.
LONG.	MTD TDMIN TS- MDE MNZ	0.972	LONG.	TS- TDMAX NZMIN TDMIN	0.921
LAT.	TS- PDTMIN PDTMAX	0.930	LAT.	TS- MDR NZMIN	0.956
GROUP	-T TASK	PROB.	GROUP	-S TASK	PROB.
LONG.	MTD TDMIN NZMIN TS- MTK TDMAX MDE MNZ	0.971	LONG.	NZMIN TS- NZMAX TDMAX MNZ TDMIN	0.939
LAT.	TS- PDTMIN NZMIN MPDT	0.978	LAT.	TS- NZMIN MTKL MPDT	0.946

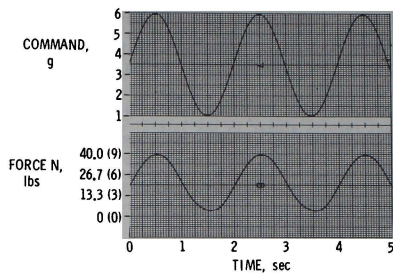


Figure 3. Sine response.

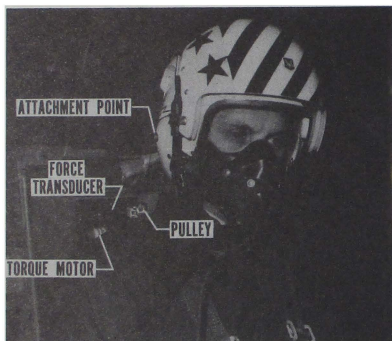


Figure 1. Helmet loader installed in DMS.

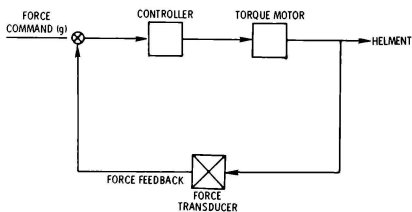


Figure 2. Helmet loader controller.

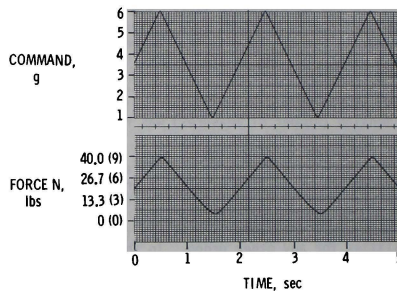


Figure 4. Triangular response.

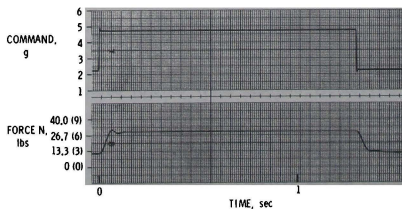


Figure 5. Step response.

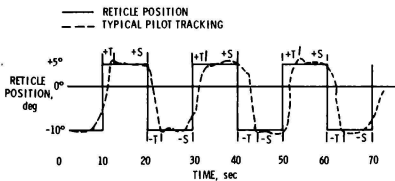


Figure 6. Structure of one computer run.

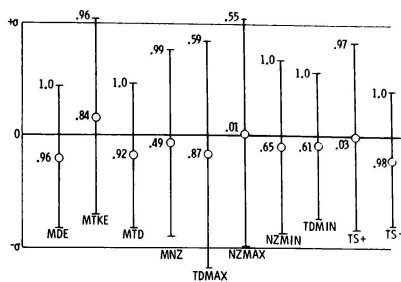


Figure 9. Normalized longitudinal measures for positive transition.

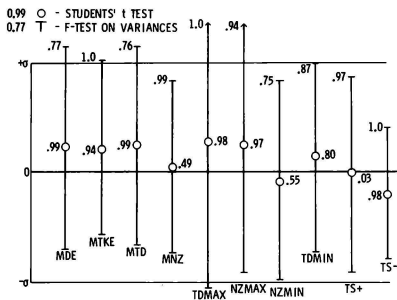


Figure 7. Normalized longitudinal measures for negative transition.

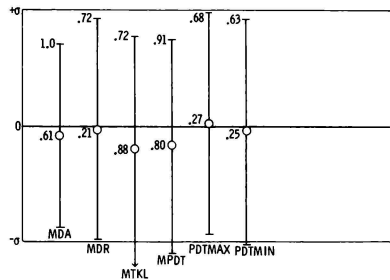


Figure 10. Normalized lateral measures for positive transition.

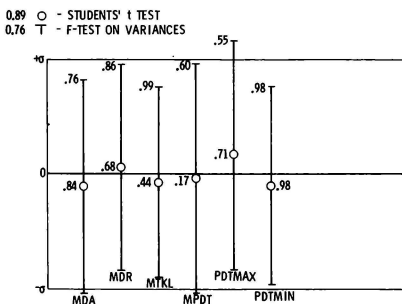


Figure 8. Normalized lateral measures for negative transition.

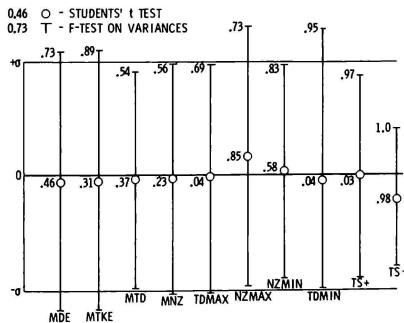


Figure 11. Normalized longitudinal measures for negative tracking.

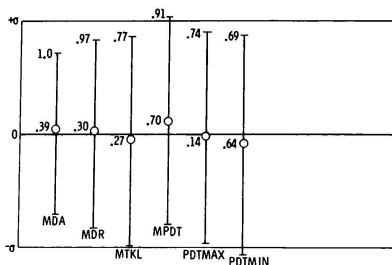


Figure 12. Normalized lateral measures for negative tracking.

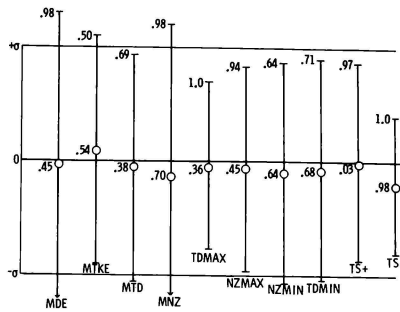


Figure 13. Normalized longitudinal measures for positive tracking.

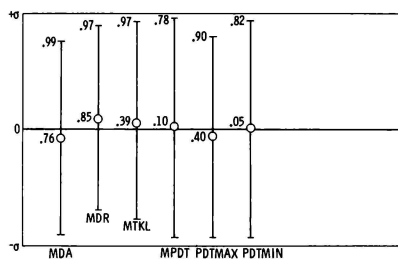


Figure 14. Normalized lateral measures for positive tracking.

PLATFORM MOTION FOR FIGHTER SIMULATIONS -- LET'S BE REALISTIC

R. V. Parrish
NASA Langley Research Center
Hampton, Virginia

Abstract

In light of the controversy that has been raging for the past several years over the value of platform motion for fighter simulations, an effort has been undertaken to determine, not the training effectiveness of platform motion, but whether or not "realistic" motion cues can even be presented with a conventional synergistic platform. "Realistic" cues are defined here to mean cues that are representative of an airplane, that are of sufficient magnitude to be sensed, that are in the proper direction arriving at the proper time, and yet that are within the presentation capabilities of the washout/motion base system.

I. Introduction

The emotionalism that one encounters on the motion/no motion issue for tactical fighter simulations is quite high, with proponents and antagonists of platform motion hurling at each other such terms as cost-effective training, more rapid asymptotic performance, transfer of training, maneuver cues, alerting cues, time lags, wide field-of-view visual predominance, asymmetric thrust, improved "G-seats" and "G-suits," etc. As stated in a recent USAF Scientific Advisory Board report¹, the studies to date, based on performance data comparisons, present no convincing case either for or against motion for fighter simulators. In light of this lack of convincing objective data, conventional resolution, at least in the past, would be based on subjective data. Unfortunately, the issue is not clearly settled by past results in this arena either. Motion antagonists cite non-acceptance by some pilots and the inability of other pilots to differentiate between motion on or off conditions². Proponents cite time lags, asynchronization with visual cues, and inappropriate cueing systems³ in response to adverse pilot opinions.

It is interesting to note that transport/VTOL motion is not nearly as inflammatory a subject, perhaps because pilot acceptance of transport/VTOL motion simulation is quite high. The motion cues presented for this class of aircraft simulation are apparently very "realistic." Recent motion experiences at Langley with the Visual Motion Simulator (VMS) have been mainly confined to transport/VTOL categories^{4,5} and pilot acceptance has been quite favorable.

The success of the washout/motion system used on the Langley simulations has been attributed to the Nonlinear Adaptive Washout^{6,7} that was utilized and to the meticulous effort to reduce time delays in visual/motion cue presentations^{8,9}. Application of this washout/motion system to the tactical fighter simulation problem was undertaken with the goal of pilot subjective acceptance at the

forefront. Studies of motion utility (in training, in tracking, etc.) would be ignored, or at least postponed, in order to concentrate solely upon "realistic" cue generation and evaluation. "Realistic" cues are defined here to mean cues that are representative of an airplane, that are of sufficient magnitude to be sensed, that are in the proper direction arriving at the proper time, and yet that are within the presentation capabilities of the washout/synergistic platform system.

II. The Simulator Characteristics

Pilot acceptance is as nebulous a term as realism, but when applied to a simulator, one can assume that it is dependent on the fidelity of the mathematical model of the flight vehicle, the computer implementation, the cockpit hardware (control loader, instrumentation, etc.), and the visual, motion, and aural cues provided.

Aircraft Mathematical Model

A variety of high performance aircraft math models are in use at Langley Research Center in conjunction with the Differential Maneuvering Simulator¹⁰ (DMS), a fixed-base, dual dome simulation system. The YF-16 simulation model was chosen for the purposes of this study because of its force actuated (minimum displacement) side-arm controller, which could be implemented in the Motion Base cockpit; the VMS currently has a control loader system for wheel and column controls, rather than for stick controls. The mass and geometric characteristics of the simulated aircraft are presented in Table 1. Complete details of the model are documented in reference 11. Additional special features of the configuration with motion cue implications included: (1) the use of a normal-acceleration command longitudinal control system which provides static stability, normal-acceleration limiting, and angle-of-attack limiting; (2) the use of a roll-rate command system in the roll axis; and (3) the use of an aileron-rudder interconnect and a stability-axis yaw damper in the yaw axis.

Computer Implementation

The mathematical model of the aircraft and the simulation hardware drives were implemented on the Langley Real-Time Simulation System. This system, consisting of a CYBER 175 with the necessarily associated interface equipment, solved the programmed equations 32 times a second. The average time delay from input to output (1.5 times the sample period) was approximately 47 milliseconds.

Cockpit Hardware

The general purpose transport cockpit of the VMS was modified to represent a fighter by removing the wheel and column and installing a side-arm force-actuated controller. The rudder pedals were configured as force-actuated pedals. The pilot seat was of the general transport type, rather than the special inclined seat of the YF-16. No special armrest was provided to support the forearm, although the elbow rest of the transport seat mimicked this function due to the placement of the controller in the same general location as the controller in the actual airplane. Primary instrumentation consisted of an attitude indicator, vertical speed indicator, an altimeter, angles of attack and sideslip meters, an airspeed indicator, a Mach meter, a turn and bank indicator, and a compass card.

Visual Display

The Langley VMS is provided with an "out-the-window" virtual image system of the beam splitter, reflective mirror type. The system, located nominally 1.27 m (4.17 ft) from the pilot's eye, presented a nominal 48° width by 36° height field of view of a 525 TV line raster system and provided a 46° by 26° instantaneous field of view. The system supplies a color picture of unity magnification with a nominal resolution on the order of 9 minutes of arc.

The scene depicted in the virtual image system was obtained by video-mixing a terrain model board picture with a target aircraft and reticle display. The state-of-the-art TV-camera transport system used in conjunction with a sophisticated terrain model board is described in reference 9. The maximum speed capability of the system is 229 m/sec (444 knots), with vertical speed capabilities of ± 152 m/sec ($\pm 30,000$ ft/min). The translational lags of the system are 15 msec or less and the rotational lags are 22 msec or less. The target aircraft/reticle display was generated by the small model, closed-circuit television system described in reference 12. Elevation and azimuth changes, as well as target roll, were accomplished electronically. Relative pitch and yaw were obtained by rotation of the two-gimbal support mount. The average total visual delay, including computational through-put delay, was thus less than 70 msec.

The target aircraft maneuvers were provided by taping the attitude and position time histories of the simulated YF-16 as it was flown over the terrain model board for real-time playback. Any one of the many stored flights could be called up instantly for playback, or a new tape could be generated and stored on the spot. This target capability was very useful, as it not only created a pilot task during motion evaluation, leading the pilot through a series of maneuvers, but it also served to keep the pilots flying within the terrain board boundaries.

Motion System

The motion performance limits of the Langley six-degree-of-freedom base are shown in figure 1. These limits are for single-degree-of-freedom operation. References 8, 13, and 14 document the characteristics of the system, which possesses

time lags of less than 50 msec. Thus, the average total motion delay, including computational through-put, is less than 100 msec (ignoring the lead introduced by washout) and is quite compatible with the visual delays. The washout system used to present the motion-cue commands to the motion base is nonstandard. It was conceived and developed at Langley Research Center and it is documented in references 7, 15, and 16. The basis of the washout is the continuous adaptive change of parameters to (1) minimize a cost functional through continuous steepest descent methods and (2) produce the motion cues in translational accelerations and rotational rates within the motion envelope of the synergistic base. The specific parameters of the nonlinear coordinated adaptive washout used in this study are presented in Table 2. Modifications to the system to attempt to improve pilot acceptance of fighter motion are suggested in this paper.

III. Motion Cueing

The approach taken in this study followed the successful approach previously utilized in transport/VTOL work; that is, to present as much of the motion cues as possible using nonlinear techniques, without major concern for physiological considerations. As in the past, the fixed parameters of the washout system were chosen off-line by an "analog matching" technique on fixed-base generated data. The body axis translational accelerations and rotational rates of the aircraft were displayed and the motion command time histories were then compared. Piloted evaluations of these selections resulted in suggested modifications to the roll axis system only. Discussion of the motion cue problems encountered follows in terms of coordinated degrees of freedom.

Vertical Acceleration

Since the subject is "realistic" motion cues, it is natural to dispose of the vertical degree of freedom first. Beyond use for buffet and turbulence simulation (cues of high frequency content requiring small amplitude motions), the vertical capabilities of the conventional synergistic platform are best reserved for nonrestriction of the pitch and surge envelopes. Onset cues for other changes in normal acceleration, while supplied by the nonlinear washout system as result of the buffet/turbulence implementation, are of small magnitude, 15.24 cm (1/2 ft), and are below threshold. Several pilots have insisted that a vertical cue is sensed at the inception of stall; however, the perception must arise from the longitudinal acceleration, as the heave cue supplied is well below threshold. Augmentation of platform motion with g-seat¹⁷ and/or helmet loader¹⁸ devices in order to provide the missing vertical g cues is anticipated to be effective.

"Realism" in the vertical degree of freedom is thus restricted to buffet/turbulence cues, a situation that can be satisfied without a platform motion system.

Longitudinal Acceleration and Pitch Rate

The representation of sustained longitudinal force cues through rotational tilt to align the gravity vector is almost standard practice in motion simulation. Reference 19 introduced the idea of coordination of rotation and translation to remove

Induced translational cues as well. The nearly in-phase relationship that generally occurs in aircraft (including the YF-16) between pitch rate, q , and longitudinal acceleration, a_x , makes the coordination of pitch and surge motions convenient, as a positive pitch angle induces a positive surge force on a motion simulator⁴. However, because the sustained longitudinal accelerations of the YF-16 model range from about 1.7 G's with full afterburner to -0.4 G with idle thrust and extended speed brakes, cue scaling is mandatory. In addition to the conventional scaling of $0.5^{19,20,21}$, the Langley washout scheme¹⁵ allows for nonlinear scaling. Additional acceleration above 0.25 G was scaled at 0.15 rather than 0.5. This nonlinear scaling resulted in tilt angles of +20° and -9° to represent the range of sustained longitudinal acceleration cues of the YF-16.

Figure 2 presents time history comparisons of the simulated aircraft a_x and q with the motion base commanded \hat{a}_x and \hat{q} for the following sequence of maneuvers:

From trimmed flight at 0.35 Mach, the pilot (a) put the throttles to idle; (b) extended the speed brakes; (c) pitched up to induce stall; (d) applied full thrust after the stall; (e) applied full afterburner; (f) applied idle thrust; (g) extended speed brakes; (h) initiated a 75° dive; (i) pulled out of the dive; and (j) using full afterburner, pulled up and through a vertical loop although the pitch rates used to obtain the necessary tilt angles on the motion base were sometimes in excess of 6°/sec; i.e., (f), generally the pilots interpreted these cues as translational acceleration cues rather than false pitch cues. Overall, both longitudinal acceleration and pitch rate cues were judged to be realistic, even at the reduced values of longitudinal G (0.3 G versus 1.7 G's).

Yaw Rate

When asked to judge the realism of the yaw cues of the simulator, a pilot inevitably includes some discussion of the accompanying roll cues. Roll stick inputs invariably produce preceding roll cues, and rudder inputs produce trailing roll cues, that dominate the yaw cues produced. However, once the roll and yaw comments are separated, it is apparent that the yaw degree of freedom is adequately represented.

Lateral Acceleration and Roll Rate

The coordination burden in the lateral axes is significantly increased over that of the longitudinal axes because a negative roll angle induces a positive sway force on a motion simulator, as opposed to the generally desired coordinated turn of an aircraft (zero side force regardless of bank angle). The initial parameter selection for the YF-16 washout gave the results shown in figure 3 for: (a) a quick 30° roll from straight and level and (b) a roll back to straight and level, followed by (c), a steady state sideslip maneuver. The side force representation is poor in (a) and (b) for two reasons. First, the roll rate cue is subjectively the overriding cue -- the most important cue of all¹⁵, and therefore must be represented (thus inducing a false side force cue). Second, the y axis capabilities of

the platform are too limited to both remove the false translational cue induced by the bank angle of the base and to then represent the proper side force in the opposite direction¹⁵. However, because the roll rate cue is dominant, the pilots are not particularly observant of the side force cue, especially if the base bank angle is less than five or six degrees.

In fact, during the washout evaluation, all of the pilots were so concerned about the roll representation that side force comments had to be elicited. The reason for this overwhelming concern was that the roll cue was not realistic. A roll cue is presented on the motion base upon stick release that is not present, at least subjectively, in the air. The times of occurrence of the objectionable cues, at stick release, are marked with asterisks in figure 3.

A survey of all of the real-time fighter simulation models currently available at Langley (DMS models for the F-14, F-15, F-16, A-10, F-4, etc.) revealed the same type of aircraft response for a roll stick step to zero command. Most of those models included actuator servo models and they cover a wide range of control systems. The aircraft response referred to is the large reversal in roll acceleration necessary to return the roll rate to zero upon stick release (fig. 3). Since the model responses are similar, it is presumed that the objectionable roll cue would be present in moving base simulation of these models, also. It should be noted, however, that the cues may be eliminated by easing the stick back to zero position, rather than releasing the stick. Whatever the physical or physiological explanation of the presence of these cues on the motion base and their absence in flight, the pilots felt that realism was lost completely by this anomaly.

A similar objectionable roll cue that occurred upon wheel release (or zero rate command) in a 737 simulator is described in reference 15. This objectionable cue was imputed to be a false rotational rate cue. This false cue was eliminated by the nonlinear adaptive washout, which resulted in significantly higher pilot acceptance, or subjective "realism." Figure 4 presents 737 time histories for an aileron pulse, displaying the results from a linear washout and the nonlinear adaptive washout. The fact that wheel release is delayed some 5 seconds from initiation of the roll command allows the adaptive parameters time to change and eliminate the objectionable cue. Fighter inputs are typically much shorter, about 1 second in figure 3, and the adaptive parameters are thus ineffective for fighter motion simulation; since the parameters have little time to adapt, the nonlinear filter behaves as a linear filter.

A second order filter, as opposed to the first order filters utilized in the majority of this study, does not remove the objectionable cue presented at stick release, either. Indeed, driving the base with no washout, that is, with aircraft bank angle, still does not eliminate these anomalous cues which are not present in flight.

IV. The Anomalous Cue

Having identified the anomalous cue of the 737 to be a false rotational rate cue¹⁵, an identification which is now to be recanted, one hesitates to attempt identification again. However, regardless of just what the fighter cue is, the presence or absence of the cue in subjective terms is easily identifiable. Figure 5 presents time histories obtained by driving the motion base with a sequence of three sine waves in rotational acceleration. Two pilots subjected to this input felt it to be representative of roll motion in an airplane, although the level of washout, a negative roll rate of 0.05 rad/sec, was above threshold and therefore noticeable. The pilots could not detect any cue indicative of stick release with this input.

Figure 6 presents a different sequence of sine waves that does provide a cue indicative of stick release. The cue occurs about the time of maximum negative acceleration, -0.4 rad/sec^2 . The washout rate of 0.025 rad/sec for this case is acceptable.

A lower maximum negative acceleration, -0.1 rad/sec^2 , was used in the sequence shown in figure 7. No cues indicative of stick release or of washout were noted, although the misalignment of the gravity vector was quite noticeable over a long period. Figure 8 illustrates a sequence that the pilots found quite suitable for aircraft roll representation. The maximum negative acceleration is -0.25 rad/sec^2 , which is well above the accepted threshold, and yet no cue indicative of stick release was produced. The previously accepted washout rate level of 0.025 rad/sec was also used.

The contention of the participating pilots was that a washout scheme which invoked motion cues for roll inputs similar to those invoked by the sine wave sequence of figure 8 would be potentially realistic. Such a scheme would require extensive logic to provide for interruption of a sine sequence in order to produce responses to new inputs. However, similar logic circuits have been successfully assembled in the past (i.e., the logic circuits of the digital controllers of reference 7).

V. Concluding Remarks

The motion cues for fighter aircraft produced by the Langley nonlinear adaptive washout/synergistic motion base system are unacceptable in the roll axis representation. However, a method for producing potentially realistic roll cues has been identified. The motion cues in the other degrees of freedom were judged realistic, although these judgments were tempered based on the desire for overall system evaluation.

VI. References

- ¹Report of the USAF Scientific Advisory Board Ad Hoc Committee on Simulation Technology, April 1978.
- ²Brown, Charles D., "Current Deficiencies in Simulation for Training," AGARD Meeting on Piloted Aircraft Environment Simulation Techniques, Brussels, Belgium, April 1978.
- ³Caro, Paul W., "Platform Motion and Simulator Training Effectiveness," Seville Research Corporation Report, April 5, 1977.
- ⁴Parrish, R. V., and Martin, D. J., Jr., "Comparison of a Linear and a Nonlinear Washout for Motion Simulators Utilizing Objective and Subjective Data From CTOL Transport Landing Approaches," NASA TN D-8157, May 1976.
- ⁵Parrish, R. V., Houck, J. A., and Martin, D. J., Jr., "Empirical Comparison of a Fixed Base and a Moving Base Simulation of a Helicopter Engaged in Visually Conducted Slalom Runs," NASA TN D-8424, May 1977.
- ⁶Parrish, R. V., Dieudonne, J. E., Martin, D. J., Jr., and Bowles, R. L., "Coordinated Adaptive Filters for Motion Simulators," Proceedings of the 1973 Summer Computer Simulation Conference.
- ⁷Parrish, R. V., Dieudonne, J. E., Bowles, R. L., and Martin, D. J., Jr., "Coordinated Adaptive Washout for Motion Simulators," Journal of Aircraft, Vol. 12, No. 1, pp. 44-50, January 1975.
- ⁸Parrish, R. V., Dieudonne, J. E., Martin, D. J., Jr., and Copeland, J. L., "Compensation Based on Linearized Analysis for a Six-Degree-of-Freedom Motion Simulator," NASA TN D-7349, November 1973.
- ⁹Rollins, John D., "Description and Performance of the Langley Visual Landing Display System," NASA TM-78742, 1978.
- ¹⁰Ashworth, B. R., and Kahlbaum, W. M., Jr., "Description and Performance of the Langley Differential Maneuvering Simulator," NASA TN D-7304, June 1973.
- ¹¹Gilbert, W. P., Nguyen, L. T., and Van Gunst, R. W., "Simulator Study of the Effectiveness of an Automatic Control System Designed to Improve the High Angle-of-Attack Characteristics of a Fighter Airplane," NASA TN D-8176, May 1976.
- ¹²Miller, G. K., Jr., and Riley, D. R., "The Effect of Visual-Motion Time Delays on Pilot Performance in a Simulated Pursuit Tracking Task," NASA TN D-8364, March 1977.
- ¹³Dieudonne, J. E., Parrish, R. V., and Bardusch, R. E., "An Actuator Extension Transformation Applying Newton-Raphson's Method," NASA TN D-7067, November 1972.
- ¹⁴Parrish, R. V., Dieudonne, J. E., and Martin, D. J., Jr., "Motion Software for a Synergistic Six-Degree-of-Freedom Motion Base," NASA TN D-7350, December 1973.
- ¹⁵Parrish, R. V., and Martin, D. J., Jr., "Empirical Comparison of a Linear and Nonlinear Washout for Motion Simulators," AIAA Paper No. 75-106, January 1975.
- ¹⁶Martin, D. J., Jr., "A Digital Program for Motion Washout on Langley's Six-Degree-of-Freedom Motion Simulator," NASA CR-145219, July 1977.

¹⁷Ashworth, B. R., McKissick, B. T., and Martin, D. J., Jr., "Objective and Subjective Evaluation of the Effects of a G-Seat on Pilot/Simulator Performance During a Tracking Task," Proceedings of Tenth NTEC/Industry Conference, November 1977.

¹⁸Ashworth, B. R., and McKissick, B. T., "The Effect of Helmet Loader G-Cueing on Pilots' Simulator Performance," AIAA Paper No. 78-15, September 1978.

¹⁹Schmidt, S. F., and Conrad, B., "Motion Drive Signals for Piloted Flight Simulators," NASA CR-1601, 1970.

²⁰Sinacori, J. B., "A Practical Approach to Motion Simulation," AIAA Paper No. 73-931, September 1973.

²¹Conrad, B., Schmidt, S. F., and Douvillier, J. G., "Washout Circuit Design for Multi-Degrees-of-Freedom Moving Base Simulators," AIAA Paper No. 73-929, September 1973.

TABLE 1. MASS AND DIMENSIONAL CHARACTERISTICS USED IN SIMULATION

Weight, N (lb) 73 480 (16 519)

Moments of inertia,

kg-m² (slug-ft²):

I_X 12 662 (9339)

I_Y 53 147 (39 199)

I_Z 63 035 (46 492)

I_{XZ} 179 (132)

Wing dimensions:

Span, m (ft) 8.84 (29.0)

Area, m² (ft²) 26.0 (280)

Mean aerodynamic chord,
m (ft) 3.335 (10.94)

Surface deflection limits:

Horizontal tail -

Symmetric (δ_h), deg ± 25

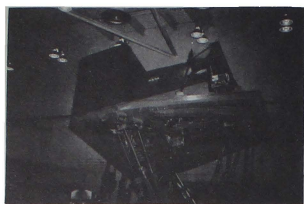
Differential (δ_p), deg ± 5 per surface

Ailerons (flaperons), deg ± 20

Rudder, deg ± 30

TABLE 2. VALUES FOR NONLINEAR ADAPTIVE WASHOUT PARAMETERS

Name	Value	Name	Value
RX	15.25	CY	1.414
RY	2.25	DY	1.6
RZ	2.2	EY	0.64
XI	8	GAMY	0.015
SX0	0.5	KLY	0.5
YI	4.0	KDY	0.00286
SY0	0.5	KILY	0.5
ZI	50	KIDY	2.625
SZ0	0.5	LAMYL	0
PI	0.25	LAMYU	0.32
SPO	0.7	DELYL	0
QI	0.15	DELYU	0.4
SQ0	0.7	LAMYDL	-0.2
RI	0.15	DELYDL	-0.2
SRO	0.7	LAMOY	0.32
WX	0.1	DELYO	0.4
BX	1.0	BZ	63.8
CX	1.414	CZ	95.8
DX	1.6	DZ	1.1313
EX	0.64	EZ	0.64
GAMX	0.05	KEZ	0.00075
KLX	0.5	KIEZ	3.5
KDX	0.01	ETAZL	0.0046
KILX	0.5	ETAZU	0.02
KIDX	0.1	ETAZDL	-0.0229
LAMXL	0	ETAZO	0.02
LAMXU	0.6	BPS	1
DELXL	0	EPS	0.3
DELXU	0.8	KEPS	100
LAMXDL	-0.15	KIEPS	1
DELXDL	-1,000	ETAPSL	0
LAMXO	0.6	ETAPSU	1
DELXO	0.8	ETAPSDL	-0.1
WY	100,000	ETAPSO	1
BY	1		



	POSITION	VELOCITY	ACCELERATION
PITCH	+30, -20°	±15°/sec	±50°/sec ²
ROLL	±22°	±15°/sec	±50°/sec ²
YAW	±32°	±15°/sec	±50°/sec ²
VERTICAL	+0.762, -0.991m	±0.610m/sec	±0.6g
LATERAL	±1.219m	±0.610m/sec	±0.6g
LONGITUDINAL	+1.245, -1.219m	±0.610m/sec	±0.6g

Figure 1. The visual-motion simulator.

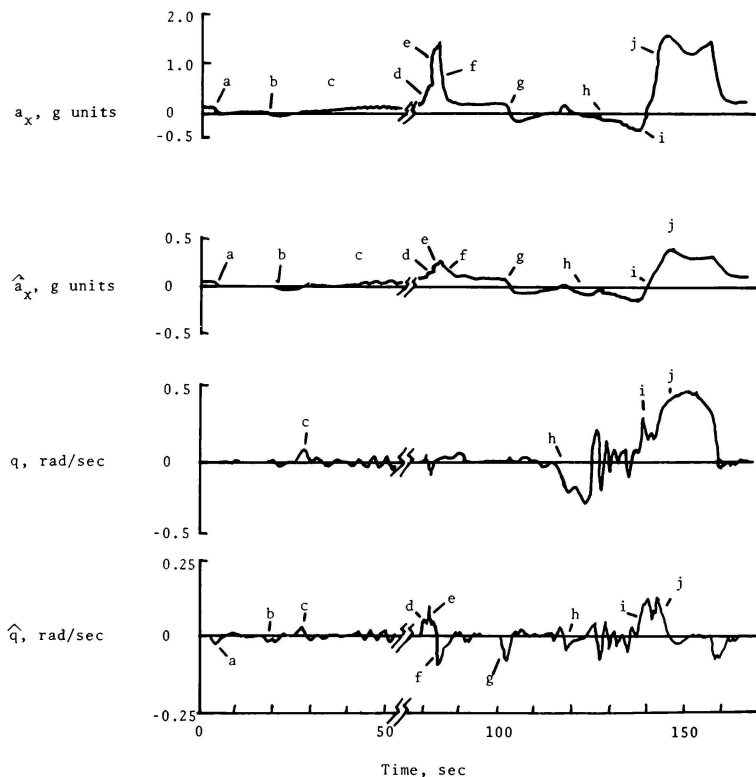


Figure 2. Longitudinal maneuvers.

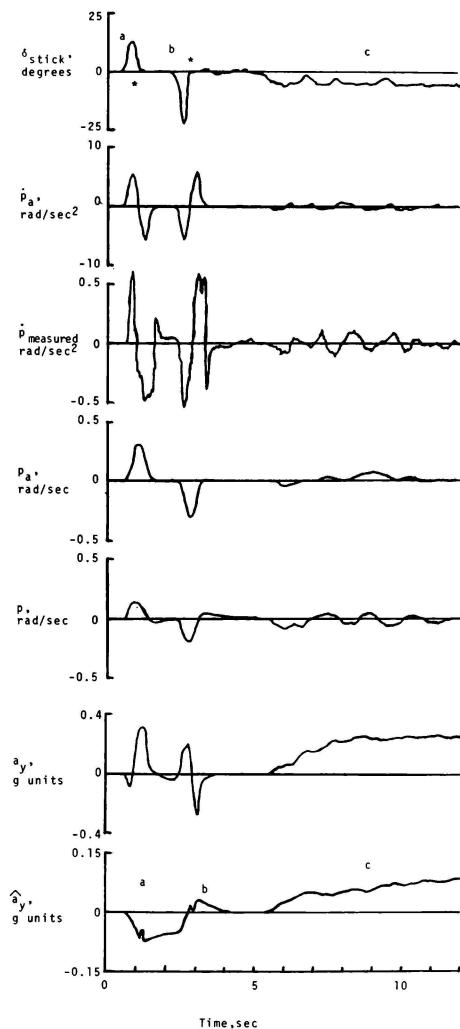


Figure 3. Lateral maneuvers.

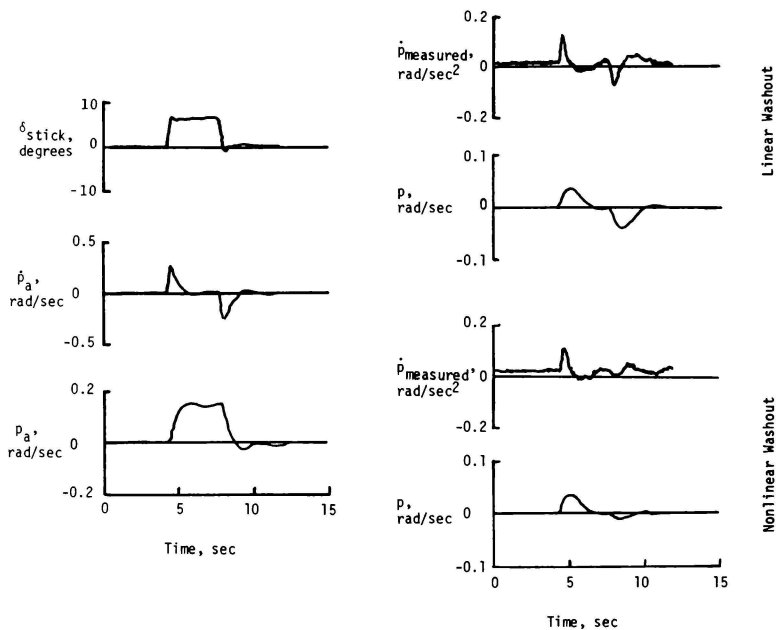
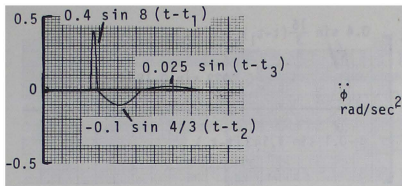
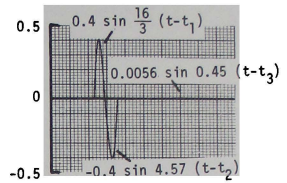


Figure 4. Aileron input on 737 simulator.

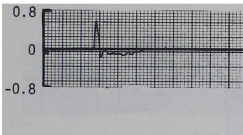
$\ddot{\phi}$,
rad/sec²



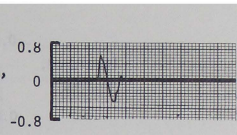
$\ddot{\phi}$,
rad/sec²



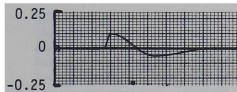
$\dot{\phi}_{\text{measured}}$,
rad/sec²



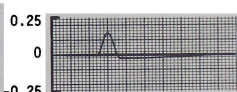
$\dot{\phi}_{\text{measured}}$,
rad/sec²



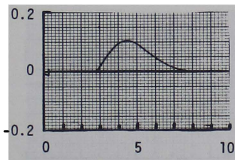
$\dot{\phi}$,
rad/sec



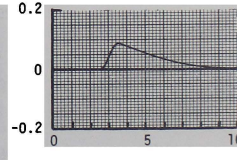
$\dot{\phi}$,
rad/sec



ϕ ,
rad



ϕ ,
rad



Time, sec

Time, sec

Figure 5. Sine wave sequence #1.

Figure 6. Sine wave sequence #2.

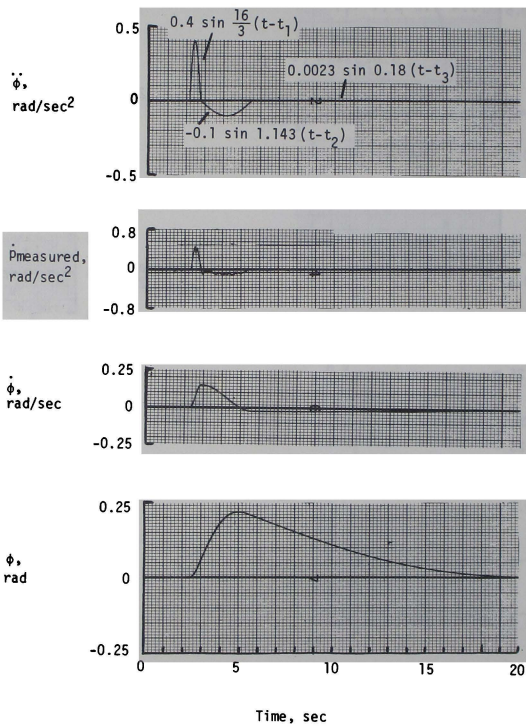


Figure 7. Sine wave sequence #3.

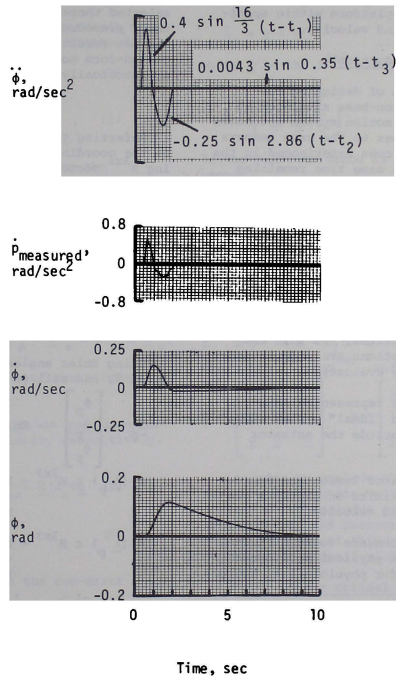


Figure 8. Sine wave sequence #4.

Robert L. Kosut
Link Division of Singer Company
Binghamton, New York

Abstract

The platform motion cue-shaping problem is formulated as an Optimal Tracking Control Problem with a non-quadratic cost function. Applying current concepts in Non-Linear Optimal Control Theory results in a non-linear control which is asymptotically stable and the non-linearity is exploited to maintain the platform within specified bounds on excursion and velocity.

I. Introduction

The fundamental problem of designing cue-shaping filters for a motion-base simulator is to generate inputs to the motion system actuators so as to provide motion cues to the crew members which simulate the motion cues experienced in the real vehicle, while at the same time remaining within the simulator performance envelope. Motion cue-fidelity is determined by comparing the platform centroid state trajectory with an equivalent point on the simulated vehicle, whereas the performance envelope is limited by the actuator state trajectory.

The primary motivation of this paper is to formulate the above problem in such a way that Optimal Control Theory can be utilized to develop a non-linear cue-shaping filter. To this end several simplifying assumptions are made in order to allow for a preliminary evaluation:

- (1) The motion base is represented as a linear model of an "ideal" system whose dynamics do not include the actuator hydraulics.
- (2) The platform actuator limits are represented as static limits on platform centroid excursion and velocity.
- (3) A measure of performance to be minimized is based solely on physical motion and does not account for physiological factors.

II. Linear vs. Non-Linear Cue-Shaping

Linear cue-shaping filters limit the performance of the motion platform below the actual limits of performance for a given task. This problem is inherent in the use of linear filters. Linearity implies that the transient response to input aircraft cues of different magnitudes but of the same wave-form will have the same onset duration. Thus smaller cues are sustained the same as larger cues thereby unnecessarily reducing the onset for a low-magnitude cue. The advantage of a non-linear filter would be the ability to increase the onset duration for a decrease in cue magnitude.

III. Approach

In recent years there have been several attempts to develop non-linear cue-shaping filters

from optimization techniques 1, 2, 3. One advantage of deriving the filter in this way is that the measure of performance is contained in a single cost functional which need only have a few adjustable parameters. Thus the cue-shaping filter is determined once these parameters are selected thereby greatly reducing the trial and error procedure to find all the control gains. The new result presented here gives rise to a closed-form non-linear optimal control which is asymptotically stable.

IV. Notation

Referring to the platform centroid in neutral as the coordinate system origin define the following $R^{3 \times 1}$ vectors in this inertial-frame:

$$\begin{aligned} \underline{x}_p & - \text{centroid position, where } \underline{x}_p = \begin{bmatrix} x_p \\ y_p \\ z_p \end{bmatrix} \\ \underline{v}_p & - \text{centroid velocity } (\underline{v}_p = \dot{\underline{x}}_p) \\ \underline{\dot{v}}_p & - \text{centroid acceleration } (\underline{\dot{v}}_p = \dot{\underline{v}}_p) \end{aligned}$$

$$\underline{g} = \begin{bmatrix} 0 \\ 0 \\ g \end{bmatrix} - \text{gravity vector}$$

Using Euler angles (order of rotation = yaw ψ , pitch θ , and roll ϕ) define

$$\underline{\lambda}_p = \begin{bmatrix} \phi_p \\ \theta_p \\ \psi_p \end{bmatrix} - \text{Euler angle vector}$$

$$\underline{E}(\underline{\lambda}_p) \in R^{3 \times 3} - \text{Euler angle transformation matrix from inertial to body axes.}$$

$$\underline{N}(\underline{\lambda}_p) \in R^{3 \times 3} - \text{Euler angle rate transformation matrix from inertial to body axes.}$$

$$\underline{w}_p = \underline{N}^{-1}(\underline{\lambda}_p) \dot{\underline{\lambda}}_p - \text{Angular velocity vector in body-axes.}$$

Referring to the aircraft define the following $R^{3 \times 1}$ vectors with respect to a moving coordinate system attached to the airframe with origin at the CG,

$$\underline{v}_a - \text{aircraft CG velocity in body-axis.}$$

$$\underline{w}_a - \text{aircraft angular velocity vector about the CG.}$$

V. Definition of Cue-Error

Although subjective there are physical quantities which are at least sufficient to $\mathbf{R}^{3 \times 1}$ measure of motion. These are defined by the $\mathbf{R}^{3 \times 1}$ vectors:

$\underline{\mathbf{f}}_i$ - Specific force, the total force experienced by the pilot, including gravity, in the body-axis.

$\underline{\mathbf{w}}_i$ - Angular velocity experienced by the pilot, in the body-axis.

The subscript $i = a, p$ for either aircraft or platform. Referring to the platform centroid,

$$\underline{\mathbf{f}}_p = \underline{\mathbf{E}}(\underline{\lambda}_p) [\underline{\dot{\mathbf{v}}}_p - \underline{\mathbf{g}}] \quad (1)$$

$$\underline{\mathbf{w}}_p = \underline{\mathbf{N}}^{-1}(\underline{\lambda}_p) \underline{\dot{\lambda}}_p \quad (2)$$

Referring to an equivalent point on the aircraft

$$\underline{\mathbf{f}}_a = \underline{\mathbf{F}}_a - \underline{\mathbf{E}}(\underline{\lambda}_a) \underline{\mathbf{g}} \quad (3)$$

$$\underline{\mathbf{w}}_a = \underline{\mathbf{N}}^{-1}(\underline{\lambda}_a) \underline{\dot{\lambda}}_a \quad (4)$$

where

$$\underline{\mathbf{F}}_a = \underline{\dot{\mathbf{v}}}_a + \underline{\mathbf{w}}_a \times \underline{\mathbf{v}}_a + \underline{\dot{\mathbf{w}}}_a \times \underline{\mathbf{R}}_a + \underline{\mathbf{w}}_a \times (\underline{\mathbf{w}}_a \times \underline{\mathbf{R}}_a)$$

and $\underline{\mathbf{R}}_a$ is the relative position of the aircraft CG to the centroid location.

Define the $\mathbf{R}^{3 \times 1}$ vectors $\underline{\mathbf{f}}, \underline{\mathbf{w}}$, as cue-error in specific force and angular velocity respectively, thus

$$\underline{\mathbf{f}} = \underline{\mathbf{f}}_p - \underline{\mathbf{f}}_a = \underline{\mathbf{E}}(\underline{\lambda}_p) [\underline{\dot{\mathbf{v}}}_p - \underline{\mathbf{g}}] - \underline{\mathbf{F}}_a + \underline{\mathbf{E}}(\underline{\lambda}_a) \underline{\mathbf{g}} \quad (5)$$

$$\underline{\mathbf{w}} = \underline{\mathbf{w}}_p - \underline{\mathbf{w}}_a = \underline{\mathbf{N}}^{-1}(\underline{\lambda}_p) \underline{\dot{\lambda}}_p - \underline{\mathbf{w}}_a \quad (6)$$

Define the $\mathbf{R}^{6 \times 1}$ vector $\underline{\mathbf{e}}$ as the cue-error vector, where

$$\underline{\mathbf{e}} = \begin{bmatrix} \underline{\mathbf{f}} \\ \underline{\mathbf{w}} \end{bmatrix} \quad (7)$$

VI. Platform Dynamics

From the previous definitions, specifically (5) and (6), the platform dynamics can be expressed as,

$$\left. \begin{aligned} \underline{\dot{\lambda}}_p &= \underline{\mathbf{v}}_p \\ \underline{\dot{\mathbf{v}}}_p &= \underline{\mathbf{E}}(\underline{\lambda}_p) [\underline{\mathbf{F}}_a + \underline{\mathbf{f}}] + [\underline{\mathbf{I}} - \underline{\mathbf{E}}(\underline{\lambda}_a - \underline{\lambda}_p)] \underline{\mathbf{g}} \\ \underline{\dot{\lambda}}_p &= \underline{\mathbf{N}}(\underline{\lambda}_p) [\underline{\mathbf{w}}_a + \underline{\mathbf{w}}] \end{aligned} \right\} \quad (8)$$

since $\underline{\mathbf{E}}^{-1}(\underline{\lambda}_p) = \underline{\mathbf{E}}'(\underline{\lambda}_p)$ and $\underline{\mathbf{E}}'(\underline{\lambda}_p) \underline{\mathbf{E}}(\underline{\lambda}_a) = \underline{\mathbf{E}}(\underline{\lambda}_a - \underline{\lambda}_p)$ are properties of the Euler's matrix. Linearizing (8) about the equilibrium state at neutral with

$$\underline{\mathbf{r}}_p(0) = \underline{\mathbf{0}}, \underline{\mathbf{v}}_p(0) = \underline{\mathbf{0}}, \underline{\lambda}_p(0) = \underline{\mathbf{0}}$$

results in the linear equation of motion,

$$\left. \begin{aligned} \underline{\dot{\lambda}}_p &= \underline{\mathbf{v}}_p \\ \underline{\dot{\mathbf{v}}}_p &= \underline{\mathbf{f}} + \underline{\mathbf{F}}_a + \underline{\mathbf{G}}(\underline{\lambda}_a - \underline{\lambda}_p) \\ \underline{\dot{\lambda}}_p &= \underline{\mathbf{w}} + \underline{\mathbf{w}}_a \end{aligned} \right\} \quad (9)$$

where $\underline{\mathbf{G}}$ is the $\mathbf{R}^{3 \times 3}$ matrix given by

$$\underline{\mathbf{G}} = \begin{bmatrix} 0 & g & 0 \\ -g & 0 & 0 \\ 0 & 0 & 0 \end{bmatrix} \quad (10)$$

If the platform state is defined by the $\mathbf{R}^{9 \times 1}$ vector,

$$\underline{\mathbf{x}} = \begin{bmatrix} \underline{\mathbf{r}}_p \\ \underline{\mathbf{v}}_p \\ \underline{\lambda}_p \end{bmatrix} \quad (11)$$

then with $\underline{\mathbf{e}}$ previously defined the state equations are,

$$\underline{\dot{\mathbf{x}}} = \underline{\mathbf{A}} \underline{\mathbf{x}} + \underline{\mathbf{B}} \underline{\mathbf{e}} + \underline{\mathbf{B}} \underline{\mathbf{z}}, \underline{\mathbf{x}}(0) = \underline{\mathbf{0}} \quad (12)$$

$$\begin{aligned} &\text{where } \underline{\mathbf{A}} \in \mathbf{R}^{9 \times 9}, \underline{\mathbf{B}} \in \mathbf{R}^{9 \times 6}, \text{ and } \underline{\mathbf{z}} \in \mathbf{R}^{6 \times 1} \text{ (input cue)} \\ &\text{are } \underline{\mathbf{A}} = \begin{bmatrix} 0 & \underline{\mathbf{I}} & 0 \\ 0 & 0 & -\underline{\mathbf{G}} \\ 0 & 0 & 0 \end{bmatrix}, \underline{\mathbf{B}} = \begin{bmatrix} 0 & 0 \\ \underline{\mathbf{I}} & 0 \\ 0 & \underline{\mathbf{I}} \end{bmatrix}, \underline{\mathbf{z}} = \begin{bmatrix} \underline{\mathbf{F}}_a + \underline{\mathbf{G}} \underline{\lambda}_a \\ \underline{\mathbf{w}}_a \end{bmatrix} \end{aligned} \quad (13)$$

In order to include the hydraulics/platform dynamics a new state vector would have to be defined which includes position, velocity, acceleration, and pressure from all six actuators. For the purpose of this paper the model (12) will represent an "ideal" platform system.

VII. Linear Optimal Tracking Control (LOTC)

Assuming (12) represents the platform, and if both the platform and the aircraft are initially at identical equilibrium states, then $\underline{\mathbf{e}} = \underline{\mathbf{0}}$ means that platform and aircraft motions are identical for any input cue $\underline{\mathbf{z}}$. However, given bounds on platform excursion ($\underline{\mathbf{r}}, \underline{\lambda}$) and velocity ($\underline{\mathbf{v}}, \underline{\mathbf{w}}$) it is clear that $\underline{\mathbf{e}} \neq \underline{\mathbf{0}}$ is definitely more likely. Therefore, define the following optimal control problem:

Given the linear time in-variant system

$$\left. \begin{aligned} \underline{\dot{\mathbf{x}}} &= \underline{\mathbf{A}} \underline{\mathbf{x}} + \underline{\mathbf{B}} \underline{\mathbf{e}} + \underline{\mathbf{B}} \underline{\mathbf{z}}, \underline{\mathbf{x}}(0) = \underline{\mathbf{x}}_0 \\ \underline{\mathbf{x}} &\in \mathbf{R}^{n \times 1}; \underline{\mathbf{e}}, \underline{\mathbf{z}} \in \mathbf{R}^{m \times 1}, m \leq n \end{aligned} \right\} \quad (14)$$

choose \underline{e} such that J is a minimum where

$$J = \frac{1}{2} \int_0^{\infty} (\underline{e}' \underline{R} \underline{e} + \underline{x}' \underline{Q} \underline{x}) dt, \quad \underline{R}, \underline{Q} \text{ positive definite}$$

The quadratic term $\underline{e}' \underline{R} \underline{e}$ and $\underline{x}' \underline{Q} \underline{x}$ penalize respectively cue-error and platform performance limitations. This problem (14) is known as an Optimal Tracking Control 4, 5 where the optimal control is given by

$$\underline{e} = \underline{F} \underline{x} + \underline{R}^{-1} \underline{B}' \underline{g} \quad \text{with } \underline{F} = -\underline{R}^{-1} \underline{B}' \underline{K} \in \mathbb{R}^{n \times n} \quad (15)$$

where $\underline{K} \in \mathbb{R}^{n \times n}$ is the positive definite (symmetric) solution of the Ricatti equation,

$$\underline{A}' \underline{K} + \underline{K} \underline{A} - \underline{K} \underline{B} \underline{R}^{-1} \underline{B}' \underline{K} + \underline{Q} = \underline{O} \quad (16)$$

and \underline{g} can be found from,

$$\underline{\dot{g}} + (\underline{A} + \underline{B} \underline{F})' \underline{g} + \underline{F}' \underline{R} \underline{z} = \underline{O}, \quad \lim_{t \rightarrow \infty} \underline{g}(t) = \underline{O} \quad (17)$$

or in integral form,

$$\underline{g}(t) = \underline{e}^{-(\underline{A} + \underline{B} \underline{F})' t} \int_0^{\infty} \underline{e}^{(\underline{A} + \underline{B} \underline{F})' \tau} \underline{F}' \underline{R} \underline{z}(\tau) d\tau \quad (18)$$

In addition with \underline{Q} positive definite and $(\underline{A}, \underline{B})$ controllable, the eigenvalues of $(\underline{A} + \underline{B} \underline{F})$ all have negative real parts, thus the closed loop system

$$\underline{\dot{x}} = (\underline{A} + \underline{B} \underline{F}) \underline{x} + \underline{B} \underline{z} + \underline{B} \underline{R}^{-1} \underline{B}' \underline{g}, \quad \underline{x}(0) = \underline{x}_0 \quad (19)$$

is asymptotically stable for all $\underline{z}(t)$ such that

$$\int_0^{\infty} \|\underline{z}(t)\|^2 dt < \infty.$$

The difficulties with the LOTC as presented are:

- (1) The closed-loop system is linear and thus the inherent disadvantages of linear cue-shaping (Section II) still apply.
- (2) The feedforward control $\underline{g}(t)$ in (18) require the future knowledge of the aircraft input cue $\underline{z}(t)$.

The difficulty of (2) can be mitigated by designing for a specific test input (step, ramp, etc.) or assuming $\underline{z}(t)$ is the solution of a known differential equation 4, 5 by using a linear model of aircraft dynamics. In any event the difficulty (1) remains. The desired control should have the form,

$$\underline{e} = \underline{e}_L + \underline{e}_{NL}(\underline{x}) \quad (20)$$

where the linear control \underline{e}_L is given by (15) and the non-linear control $\underline{e}_{NL}(\underline{x})$ becomes more active as \underline{x} approaches the performance boundary.

VIII Non-Linear Optimal Tracking Control (NLOTCT)

A control of the form (20) can be found by following the work of 6, 7, 8 and solving an Isoperimetric Optimal Control Problem:

Given the controllable system:

$$\underline{\dot{x}} = \underline{A} \underline{x} + \underline{B} \underline{e} + \underline{B} \underline{z}, \quad \underline{x}(0) = \underline{x}_0$$

Choose \underline{e} such that J is a minimum, where

$$J = \int_0^{\infty} \left[\frac{1}{2} \underline{e}' \underline{R} \underline{e} + \frac{1}{2} \underline{x}' \underline{Q} \underline{x} + q(\underline{x}) \right] dt \quad (21)$$

subject to the isoperimetric inequality constraint,

$$\int_0^{\infty} m(\underline{x}) dt \leq \rho, \quad m(\underline{x}) \text{ positive (semi) definite}$$

The NLOTCT solution is

$$\underline{e} = \underline{e}_L + \underline{e}_{NL}(\underline{x}) \quad (22)$$

with

$$\underline{e}_L = \underline{F} \underline{x} + \underline{R}^{-1} \underline{B}' \underline{g}, \quad \underline{F} \text{ and } \underline{g} \text{ given by} \quad (23)$$

(15) and (18),

where

$$\underline{e}_{NL}(\underline{x}) = -\underline{R}^{-1} \underline{B}' \nabla_{\underline{x}} \phi(\underline{x}) \quad (\nabla_{\underline{x}} \equiv \partial/\partial \underline{x} \text{ gradient}) \quad (24)$$

provided that

$$m(\underline{x}) = \frac{1}{\rho} \underline{e}_{NL}'(\underline{x}) \underline{R} \underline{e}_{NL}(\underline{x}) \quad (25)$$

and $\phi(\underline{x})$ is a Lyapunov Function which solves the partial differential equation,

$$q(\underline{x}) + \langle (\underline{A} + \underline{B} \underline{F}) \underline{x}, \nabla_{\underline{x}} \phi(\underline{x}) \rangle = 0 \quad (26)$$

In addition the closed-loop system

$$\underline{\dot{x}} = (\underline{A} + \underline{B} \underline{F}) \underline{x} - \underline{B} \underline{R}^{-1} \underline{B}' \nabla_{\underline{x}} \phi(\underline{x}) + \underline{B} \underline{R}^{-1} \underline{B}' \underline{g} + \underline{B} \underline{z} \\ \underline{x}(0) = \underline{x}_0, \quad \int_0^{\infty} \|\underline{z}(t)\|^2 dt < \infty \quad (27)$$

is asymptotically stable about the zero state.

It can be shown 6 that given the positive (semi) definite form,

$$q(\underline{x}) = \sum_{i=1}^{\eta} (\underline{x}' \underline{Q}_i \underline{x})^{\alpha}, \quad \alpha = \text{even integers} \quad (28)$$

there exists a solution $\phi(\underline{x})$ of (26) such that

$$\phi(\underline{x}) = \sum_{i=1}^n (\underline{x}' \underline{p}_i \underline{x})^{\alpha} \quad (29)$$

which is also positive (semi) definite and where the $\underline{p}_i \in R^{n \times n}$ can be uniquely determined from (26) by solving N linear equations for the N unknowns in \underline{p}_i , $i \in [1, n]$, where

$$N = \frac{(n+2\alpha-1)!}{(2\alpha)!(n-1)!}, \quad n = \dim \left\{ \underline{x} \right\} \quad (30)$$

If $n=9$ as in (11) and $q(\underline{x})$ is quartic ($\alpha=2$), then $N=495$. This is quite formidable but can be greatly reduced by de-coupling the axes and defining a cost functional for each axes. For example, one possible system is the four-axis model given by:

Longitudinal

The state equations are

$$\begin{aligned} \dot{\underline{x}} &= \underline{v} \\ \dot{\underline{v}} &= \underline{f}_{xa} - g\theta + \underline{f}_x \\ \dot{\theta} &= \dot{\theta}_a + q \end{aligned} \quad (31)$$

Thus

$$\underline{x} = \begin{bmatrix} \underline{r}_x \\ \underline{v}_x \\ \theta \end{bmatrix}, \quad \underline{e} = \begin{bmatrix} \underline{f}_x \\ \underline{v}_x \\ q \end{bmatrix}, \quad \underline{z} = \begin{bmatrix} \underline{f}_{xa} - g\theta \\ \dot{\theta}_a \end{bmatrix}$$

$$\underline{A} = \begin{bmatrix} 0 & 1 & 0 \\ 0 & 0 & -g \\ 0 & 0 & 0 \end{bmatrix}, \quad \underline{B} = \begin{bmatrix} 0 & 0 \\ 1 & 0 \\ 0 & 1 \end{bmatrix}$$

and $n=3$ implies $N=15$.

Lateral

The state equations are

$$\begin{aligned} \dot{\underline{x}} &= \underline{v}_y \\ \dot{\underline{v}} &= \underline{f}_{ya} + g\phi + \underline{f}_y \\ \dot{\phi} &= \dot{\phi}_a + p \end{aligned} \quad (32)$$

Thus

$$\underline{x} = \begin{bmatrix} \underline{r}_y \\ \underline{v}_y \\ \phi \end{bmatrix}, \quad \underline{e} = \begin{bmatrix} \underline{f}_y \\ \underline{v}_y \\ p \end{bmatrix}, \quad \underline{z} = \begin{bmatrix} \underline{f}_{ya} + g\phi \\ \dot{\phi}_a \end{bmatrix}$$

$$\underline{A} = \begin{bmatrix} 0 & 1 & 0 \\ 0 & 0 & g \\ 0 & 0 & 0 \end{bmatrix}, \quad \underline{B} = \begin{bmatrix} 0 & 0 \\ 1 & 0 \\ 0 & 1 \end{bmatrix}$$

and $n=3$ implies $N=15$.

Vertical

The state equations are

$$\begin{aligned} \dot{\underline{z}} &= \underline{v}_z \\ \dot{\underline{v}} &= \underline{f}_{za} + \underline{f}_z \end{aligned} \quad (33)$$

Thus

$$\underline{x} = \begin{bmatrix} \underline{r}_z \\ \underline{v}_z \end{bmatrix}, \quad \underline{e} = \underline{f}_z, \quad \underline{z} = \underline{f}_{za}, \quad \underline{A} = \begin{bmatrix} 0 & 1 \\ 0 & 0 \end{bmatrix}, \quad \underline{B} = \begin{bmatrix} 0 \\ 1 \end{bmatrix}$$

and $n=2$ implies $N=5$.

Yaw

The state equations are

$$\dot{\underline{\psi}} = \dot{\underline{\psi}}_a + r \quad (34)$$

Thus

$$\underline{x} = \underline{\psi}, \quad \underline{e} = r, \quad \underline{z} = \dot{\underline{\psi}}_a, \quad \underline{A} = 0, \quad \underline{B} = 1$$

and $n=1$ implies $N=1$.

The total number of computations needed to solve (26) is then $N=36$, by using this model.

IX Example: Vertical Degree of Freedom

Consider the vertical degree of freedom system

$$\begin{aligned} \dot{\underline{z}} &= \underline{v} & , & \quad r(0) = r_0 \\ \dot{\underline{v}} &= \underline{e} + \underline{z} & , & \quad v(0) = v_0 \\ \underline{z} &= \underline{f}_{za} \end{aligned} \quad (35)$$

Thus

$$\underline{x} = \begin{bmatrix} \underline{r} \\ \underline{v} \end{bmatrix} \in R^{2 \times 1}, \quad \underline{A} = \begin{bmatrix} 0 & 1 \\ 0 & 0 \end{bmatrix}, \quad \underline{B} = \begin{bmatrix} 0 \\ 1 \end{bmatrix}$$

Let the cost be

$$J = \frac{1}{2} \int \left\{ \left(\frac{\underline{e}}{E} \right)^2 + \sigma_L \left[\left(\frac{\underline{z}}{X} \right)^2 + \left(\frac{\underline{v}}{V} \right)^2 \right] + \sigma_{NL} \left[\left(\frac{\underline{z}}{X} \right)^4 + \left(\frac{\underline{v}}{V} \right)^4 \right] \right\} dt \quad (36)$$

where σ_L , σ_{NL} weigh the relative effect of e_L and e_{NL} . Thus

$$\begin{aligned} \underline{R} &= 1/E^2, \quad \underline{Q} = \begin{bmatrix} \sigma_L/X^2 & 0 \\ 0 & \sigma_L/V^2 \end{bmatrix} \\ q(\underline{x}) &= \frac{\sigma_{NL}}{2} \left(\left(\frac{\underline{z}}{X} \right)^4 + \left(\frac{\underline{v}}{V} \right)^4 \right) \end{aligned} \quad (37)$$

Solving for the LOTC from (15) gives

$$\begin{aligned} \underline{E} &= [-\alpha, -\beta], \quad \alpha = \sqrt{\sigma_L^2} E/X, \\ \beta &= E(2\sqrt{\sigma_L^2}/EX + \sigma_L^2/v^2)^{1/4} \end{aligned} \quad (38)$$

Assume $z(t)$ is a pulse of magnitude z_0 and duration T_0 then from (18),

$$\underline{g}(t) = \underline{\Phi}(t) \underline{\Omega}^{-1} \left(\underline{\Phi}(-T_0) - \underline{\Phi}(-t) \right) \underline{E}' \underline{R} \underline{Z}_0, \quad (39)$$

for $t \in [0, T_0]$ where

$$\underline{\Phi}(t) = \exp(-\underline{\Omega}t), \quad \underline{\Omega} = (\underline{A} + \underline{B} \underline{E})'$$

If T_0 is sufficiently small so that

$$\underline{\Phi}(t) \approx \underline{I}, \quad t \in [0, T_0] \quad (40)$$

then $\underline{g}(t) \approx \underline{0}$ and the linear portion of the control is

$$e_L = -(\alpha r + \beta v) \text{ with } \alpha, \beta \text{ given from (38)}. \quad (41)$$

Thus the LOTC gives rise to the form presently employed in the linear cue-shaping filter.

Since $n = 2$ implies $N = 5$ select the Lyapunov function as

$$\phi(\underline{x}) = p_1 x^4 + p_2 x^3 v + p_3 x^2 v^2 + p_4 x v^3 + p_5 v^4 \quad (42)$$

Substituting this into (24), the non-linear portion of the control is,

$$\begin{aligned} e_{NL}(\underline{x}) &= -E^2 \nabla_v \phi(\underline{x}) = -E^2 \left(p_2 x^3 + 2p_3 x^2 v \right. \\ &\quad \left. + 3p_4 x v^2 + 4p_5 v^3 \right) \end{aligned} \quad (43)$$

Where the p_i are found from (26) which results in the linear equation,

$$\begin{bmatrix} 0 & \alpha & 0 & 0 & 0 \\ 4 & -\beta & -2\alpha & 0 & 0 \\ 0 & 3 & -2\beta & -3\alpha & 0 \\ 0 & 0 & 2 & -3\beta & -4\alpha \\ 0 & 0 & 0 & -1 & 4\beta \end{bmatrix} \begin{bmatrix} p_1 \\ p_2 \\ p_3 \\ p_4 \\ p_5 \end{bmatrix} = \begin{bmatrix} \sigma_{NL}/2X^4 \\ 0 \\ 0 \\ 0 \\ \sigma_{NL}/2V^4 \end{bmatrix} \quad (44)$$

Selection of the following parameters,

$$\begin{aligned} E &= .18g, \quad X = 20 \text{ in}, \quad V = 24 \text{ in/sec}, \\ \sigma_L &= .1, \quad \sigma_{NL} = .9 \end{aligned} \quad (45)$$

Results in the non-linear system

$$\dot{z} = v$$

$$\begin{aligned} \dot{v} &= f_{za} - 1.0977r - 1.7433v - .0124r^3 - .0171r^2v \\ &\quad - .0066rv^2 - .0050v^3 \end{aligned} \quad (46)$$

Fig I shows the acceleration response to step inputs of 0.3g and 0.1g. Fig II shows the state-space trajectory. Note that the acceleration response is sustained longer for the low cue while position and velocity are attenuated by approximately two, whereas in the linear filter the onset duration would be identical and the (r, v) attenuation would be three. This is the anticipated desirable effect of the non-linear filter.

Acceleration

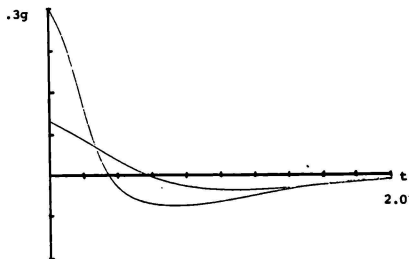


Fig I - Acceleration Response

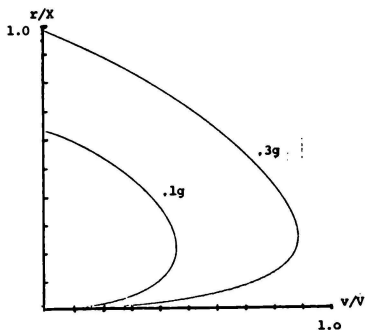


Fig II - State-space trajectory

X Concluding Remarks

Preliminary evaluation of the non-linear Optimal Control presented indicates improvement over linear cue-shaping in regard to utilizing more of the available platform performance envelope. This method suffers from a computational burden (30) which can be alleviated by decoupling the axes as suggested in (31) to (34). The next step in studying this approach would be to remove the assumptions of Section I so that:

(1) A linear system model is developed which includes the actuator hydraulics and platform geometry.

(2) A transformation (linear) from static actuator limits to dynamic platform centroid limits is developed and is incorporated in a cost functional.

(3) The cost functional should contain terms involving cue-error phase, angular acceleration, and translational jerk.

Research along these lines is being conducted at the present time.

XI References

- 1 Friedland, B., Ling, C.K., "Quasi-Optimum Design of Control Systems for Moving Base Simulators", NASA CR1613, Oct. 1970
- 2 Parrish, R.V., Dieudonne, J.E., Martin, D.J., Bowles, R.L., "Coordinated Adaptive Filters for Motion Simulators", Proceedings of the 1973 Summer Computer Simulation Conference.
- 3 Friedland, B., Ling, C.K., Hutton, M.F., "Quasi-Optimum Design of a Six-Degree-of-Freedom Moving Base Simulator Control System", NASA NAS 2-3636, Jan. 1973
- 4 Athans, M., Falb, P., "Optimal Control", McGraw Hill Book Company, 1966, pp. 793.
- 5 Asseo, S.J., "Application of Optimal Control to Perfect Model Following", Cornell Aeronautical Laboratory Report, Air Force Contract No. F33657-67-C-1157, July 1967.
- 6 Sandor, J., Williamson, D., "Design of Non-Linear Regulators for Linear Plants", IEEE Trans. Aut. Contr., Feb. 1977
- 7 Moylan, P.J., Anderson, B.D.O., "Non-Linear Regulator Theory and an Inverse Optimal Control Problem", IEEE Trans. Aut. Contr., Oct. 1973
- 8 Bass, R.W., Webber, R.F., "Optimal Non-Linear Feedback Control Derived from Quartic and Higher-Order Performance Criteria", IEEE Trans. Aut. Contr., July 1966.

W. T. Harris, J. A. Puig,
G. L. Ricard and D. G. Weinman
Naval Training Equipment Center
Orlando, Florida 32813

Abstract

At the present time, the role of motion cues in the effectiveness and efficiency of simulator training is not certain. Before valid training effectiveness studies can be accomplished for motion cueing, the nature of the drive signals for motion platforms and their relations to actual aircraft motions must be accurately determined.

This paper reports plans to: (1) Assess the training effectiveness of several of the flight simulator motion-system drive algorithms in current use, (2) Select the most training effective, (3) Develop them for specific Navy tasks, and (4) Relate them to characteristics of the motion systems. The stages of this project; engineering analysis, preliminary algorithm selection, and training effectiveness evaluation are presented herein.

Introduction

Background

Prior to the introduction of wide angle visual display systems into flight simulators used for training and research, several characteristics were attributed to cockpit motion-cueing systems. In particular, they were reported to:

- . Alert pilots to changes in state of the simulated aircraft.
- . Promote the formation of habit patterns in the simulator more akin to those found in the actual aircraft.
- . Provide a sense of realism to the simulations that fixed base simulations did not have, thus adding to the intangible pilot acceptance factor.
- . Improve pilot control responses during in-simulator tracking experiments.
- . Affect aircraft control tasks.
- . Provide secondary task loading.
- . Have benefits which are related to task and pilot experience level.

Based upon all of these apparently positive factors associated with cockpit motion cueing systems, a formidable array of cockpit motion hardware is in use today. The Navy currently uses:

- 17 -- 3 Degree of Freedom (DOF) Cockpit Motion Systems
- 6 -- 4 DOF Cockpit Motion Systems
- 50 -- 6 DOF Cockpit Motion Systems

in their training programs.

Since the introduction of wide angle visual systems, questions have arisen as to the effectiveness and efficiency of cockpit motion cueing for training and whether the wide angle visual display systems could replace the cockpit motion effects (if they exist) or expand upon them.

To date, the relations between training effectiveness, efficiency, cockpit motion hardware capability (acceleration, velocity, excursion limits), algorithm (gains, frequencies, damping), mission or task and subject experience level have never been drawn. There is no universally accepted drive philosophy. One or several types may prove to be better suited to the training task than others. If so, these beneficial algorithms should be used to retrofit the existing motion systems (and possible future procurements).

It is not likely that all 73 cockpit motion equipped simulators the Navy currently uses in training will be equipped with wide angle visual display systems; hence, the need exists to answer the questions of how to best use the existing motion equipped simulators, with and without visual display capability, and whether to procure additional motion bases. We must determine how much motion (hardware characteristics) of what kind (drive philosophy) is necessary to perform our ultimate goal of better training pilots. The approach taken by the Navy to answer these questions is the subject of this paper.

Scope and Approach

The primary objectives of the research program being described here are: (1) To assess the training effectiveness of several of the flight simulator cockpit motion drive algorithms in current use today, (2) Select those most training effective, (3) Develop them for specific Navy tasks, and (4) Relate them to motion system characteristics (excursion, velocity and acceleration requirements). The approach taken to investigate the problem addressed by this research is summarized into the phases shown below:

Phase I - Engineering Analysis

During this phase, the preliminary work necessary to select the most training effective cockpit motion algorithm(s) as well as to provide a thorough understanding of the drive philosophies in use, is performed. To conduct any valid comparisons of experimental results, replications of experiments, or generalizations of experimental data, it is necessary to perform the following analyses and publish the results in some retrievable form:

- a. The hardware performance capabilities of the equipment used in the experiments should be established. This capability must be published so that excursion, velocity and acceleration limits, and frequency response for each degree of freedom

of each piece of hardware e.g., cockpit motion and visual display hardware are reported. The intent here is to ascertain the capabilities and limitations of hardware for which there is training data. This requirement is being satisfied by compiling the results of various semi-formal testing programs to which the hardware systems have been subjected into NAVTRAQIPQCEN TN-59.²

- b. An evaluation of the fidelity of the simulation of the reference aircraft flying qualities and performance must be made. Errors such as extensive delays or improper simulation of characteristics such as damping and frequency coefficients for the various oscillatory modes can adversely affect pilot and simulator performance and hence, obfuscate the results of any research performed on the simulator. This is particularly true if training effectiveness studies are to be undertaken, even though positive transfer does occur when simulators of low fidelity are used in training. It is probably not as important to have identical flying qualities and performance simulation of a specific aircraft but the simulation must be similar to that of a typical aircraft. The TRADEC research tool was subjected to acceptance testing in late 1969. The results of that testing program appear in a Technical Report.³ The flying qualities simulation in the AWAWS research tool are based upon the Navy 2F101 series (T-2C) of flight simulators which were thoroughly evaluated by teams of test pilots and flight test engineers during the 2F101 acceptance program. Those test results appear in a Naval Air Test Center Technical Report.⁴ The AWAWS itself was further tested by a test pilot and flight test engineer team. The results of that testing program are as yet unpublished.
- c. An evaluation of the drive algorithms in use in the cockpit motion research. The cueing provided to the subject by the motion base is bounded by either the performance capability of the hardware or by the algorithm used and its associated gains, frequencies and damping coefficients. That is, the same hardware can deliver totally different cues depending upon the particular driving philosophy chosen for that particular simulation. This type of evaluation may explain some of the equivocal results of research on the training benefits of motion-cueing currently being published. To be most useful, this evaluation should include time histories of normalized engineering inputs to the algorithm, and outputs, as well as a frequency response for each degree of freedom of the system. This testing should determine system iteration delays as well as phasing delays of the system caused by the algorithm or analog filters on its hardware. The analysis of the algorithms undertaken in this research consists of the following forms of analyses:

Transfer Function Analysis

An analysis of the types of transfer functions frequently encountered in cockpit motion simulation has been performed. Normalized step, ramp, and pulse inputs are provided for comparison of transfer function outputs. Frequency response data were obtained over the frequency range of interest. The purpose of these analyses is to quantify the effects of the various filter types for later use in distinguishing the relative learning effects of the various algorithms. Figure 1 displays responses of a typical transfer function. In this figure, normalized frequency is " $\omega/\omega_{\text{natural}}$ " and normalized time is " time/τ ." Thus the figures represent responses for families of transfer functions.

Drive Algorithm Analysis

The next portion of the cockpit motion algorithm analysis involves programming selected cockpit motion models and providing standardized inputs to each degree of freedom of the model. This means that if an algorithm normally employs roll angle, rate, and acceleration as operating inputs to the lateral channel, only one of the inputs will be excited at a time; using the standardized inputs. Recognize, that in general, this constitutes a form of excitation that would not occur during normal flight simulation, e.g., a pulse roll rate input with no attendant roll acceleration or angular change inputs would not be physically realizable. The purpose of this form of excitation is to determine the effects of the algorithm on specific inputs. For example, various static and dynamic couplings of degrees of freedom may be readily determined in this fashion. Data typically obtained include: step, pulse and ramp responses along with the frequency response for each input. The specific outputs vary with gain, frequency and damping coefficient adjustments, however, trends are apparent. Figure 2 is representative of this portion of the analysis.

The final portion of the algorithm analysis still involves engineering inputs, but they are not supplied into the cockpit motion modules directly. Instead, they are provided, as aircraft control excursions, into a flight simulation whose outputs constitute the inputs to the cockpit motion models. This configuration replicates, with reproducible inputs, the typical application a cockpit motion model would be subjected to in normal operation. A technical report⁵ is being prepared which addresses the transfer function and cockpit motion drive analyses.

Phase II - Preliminary Algorithm Selection

One purpose of this phase is to screen the motion drive algorithms selected from Phase I. The myriad combinations of algorithms, with associated frequencies, gains, damping values, degrees of freedom, etc., will be screened to a more manageable quantity such that the actual aircraft time required for the transfer studies will be reduced to a minimum.

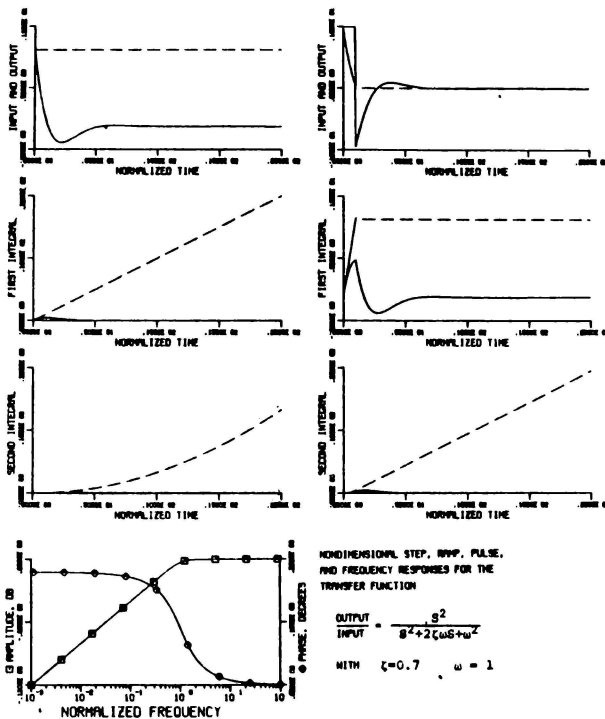


Figure 1. Sample Transfer Function Analysis

Another purpose of this phase is to conduct a preliminary investigation, or pilot study, which will determine the feasibility of the proposed research method. It will enable us to gain some idea of the sample size needed by noting the variability within and between subjects. It will also provide a test bed for our measurement techniques.

An in-simulator study will be conducted in which pilot subjects fly specific maneuvers in the simulator using combinations of algorithms, gains, etc. Both system performance measures (altitude, bank angle, pitch angle, etc.) and control measures (pilot control activity) will be recorded. The algorithms with the 'best' scores will be retained for further investigation as likely candidates for effectiveness studies.

It is intended to perform this preliminary study in the Naval Training Equipment Center (NAVTRAEQUIPCEN) Computer Laboratory's Training Device Computer (TRADEC) Figure 3. This will set

the stage for a simulator comparative study to determine if the algorithms selected by the TRADEC study will be as effective in NAVTRAEQUIPCEN's Aviation Wide Angle Visual System (AWAVS) research simulator (Figure 4). This might be considered a simulator transfer of training study.

Experimental Design

Statistically, the main point of the experiment is to provide an optimum setting for the motion algorithms (including no motion) to exhibit their differential effects, if any exist. To this end, all other sources of variability will be identified, so their effects can be separated from the effects of the motion algorithms. Major sources of variability will generally be considered as factors in the experiment. Some sources, such as training conditions, will be controlled by holding them constant. Other sources will be controlled by providing balance: let every subject use every algorithm, for example.

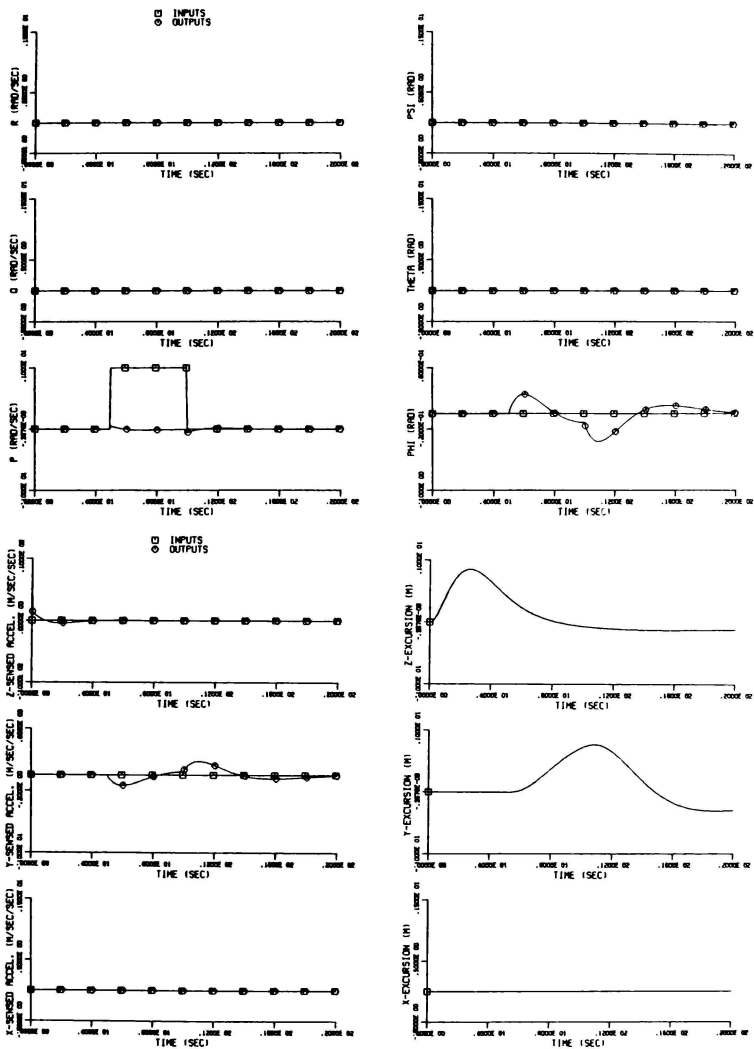


Figure 2. Sample Algorithm Response to Roll Rate Pulse Input

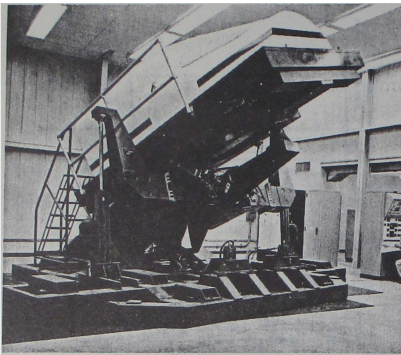


Figure 3. TRADEC Research Simulator

Some of the obvious major sources of variability are subjects, tasks or maneuvers, and trials. These will be considered as factors in the experiment. Certain other variables, such as age and experience, should be considered covariates, and their effects removed by multiple regression or analysis of covariance. A search will be made for other covariates (field dependence, for example) which might account for some variability in subjects' performances.

Subjects will be given the same maneuver to perform using all algorithms. The algorithms will be divided into subsets and presented in an order that will allow analysis of partial results. To be more specific, suppose there are 25 algorithms (or 10 algorithms with multiple adjustments-gain, etc.) and 5 subjects. The algorithms would be randomly divided into 5 subsets of 5 algorithms each, and these subsets would be designated A, B, C, D, E. (A, for example, might contain algorithms 2, 7, 10, 18, and 23). The algorithms would be presented to the subjects as follows:

Algorithm Subset Order

Subject	1st	2nd	3rd	4th	5th
1	A	B	C	D	E
2	B	C	D	E	A
3	C	D	E	A	B
4	D	E	A	B	C
5	E	A	B	C	D

Each column contains every algorithm once, so each column is, in a sense, a replication of the experiment. It is not a true replication since we would probably give all the algorithms to subject 1 before running subject 2, etc. Nor can we get any reasonable estimates from the first column alone, because there will be 25 observations in that column, from 25 algorithms and 5 subjects.

However, with 2 columns, or 20 observations per subject, we can get estimates of the algorithm effects as well as subject effects. Assume for the moment that the observation of interest is the

*See measurement section.

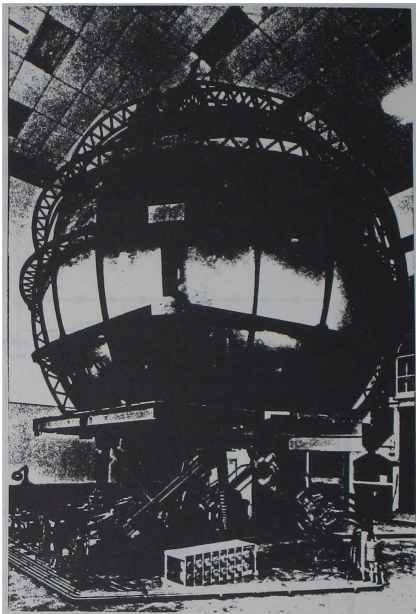


Figure 4. ANAVS Research Simulator

Basic Instrument Flight Maneuvers* (BIFM) system performance measure, Y. Then we have:

$$Y_{ijk} = \mu + \alpha_i + \beta_j + \gamma_k + \epsilon_{ijk}$$

where: Y_{ijk} is the Y for subject i on algorithm j presented on trial k;

μ is the overall mean;

α_i is the effect due to subject i;

β_j is the effect due to algorithm j;

γ_k is the effect of the k-th trial.

Note that $i = 1, 2, 3, 4, 5$ (subjects), $j = 1, 2, \dots, 25$ (algorithms), and $k = 1, 2, \dots, 10$ (trials in the first 2 columns). We do not have all combinations of i, j, and k though. Subject 1 has only 10 of the possible 25 algorithms and algorithm 1 occurs only twice in the first 2 columns.

There are 50 observations in the two columns, leaving 49 degrees of freedom (df). The 25 algorithms require 24df, the 5 subjects 4df, and the 10 orders 9df, leaving 12df for error.

Source of Variability	df (2 columns)	df (k columns)
Subjects	4	4
Algorithms	24	24
Order	9	5k-1
Error	12	20k-28
TOTAL	49	25k-1

As we increase the number of columns by 1, we gain 25df total, 5 of which must be used for order, leaving an extra 20df for error (since subject and algorithm df remain constant).

Analysis

Generally, the analysis of a scheme such as the one in the previous section can be done by analysis of variance (and/or covariance) or by multiple regression. Analysis of variance with fixed effects can be considered a special case of multiple regression. In this situation, subjects should certainly not be treated as fixed effects. Minor modifications to multiple regression can take the randomness of subjects into account.

First, regress the dependent variable Y on subjects and covariates (if any) to obtain an estimated score for each observation. If there are no covariates, this estimated score is just the mean for the particular subject involved. Subtract the estimated score from the observation to obtain a residual score, called y_p . Now perform an analysis of variance on the residual y_p 's, using algorithms and order as the only factors. (Since a computer program will be used, the df need to be adjusted by subtracting from the total df the number of df used by the covariates. If subjects are the only "covariate," 4df will be subtracted from total and from error. Algorithms and order still have their original df.)

Assuming we have all 5 columns (or all 25 algorithms for each subject), we have a full "subjects by levels" factorial experiment, but we cannot analyze the interaction of subjects and algorithms, since no df would be left for error. The 24df can be examined for order in the following way: consider the five "columns" in the design as having 4df; then each column has 5 orders inside (i.e., column 1 has 1, 2, 3, 4, 5 while column 3 has 11, 12, 13, 14, 15, etc.). Then the order effects we will look at are the interactions of the columns with subjects, requiring $4 \times 4 = 16df$. If there is a significant interaction, it can be separated into interactions of subjects with: the first 2 columns; columns 1 and 2 versus the 3rd column, etc.

If there are significant interactions in almost all of these, they would be taken out (as a new factor) and the algorithms reanalyzed. This might prove satisfactory (show that the algorithms are indeed different). If not, and the significant interactions are mainly in effects involving the last 2 columns, for instance, then it would suggest using more subjects and only running them on 15 algorithms (the first 3 columns).

Twenty-five algorithms and five subjects were used simply as an example. The actual numbers will be dependent upon the results of the Phase I

engineering analysis and the availability of qualified subjects.

As a result of the Phase II analysis, those algorithms with the best scores (lowest errors) will be retained for the transfer experiment. Some thought will be given, however, to keeping one (or more) algorithm that produces high errors. Perhaps greater difficulty in the simulator will lead to better transfer of training.

Experimental Tasks. The group of algorithms selected will be expected to produce discernably different cues during the simulated flight tasks. The experiment will contain two maneuvers one of which will consist of instrument flight rules (IFR) and the second will consist of a task which is primarily visual (VFR). The subjects' tasks will involve: (1) maintaining straight and level flight (with and without turbulence) which will merge with, and end in a vertical S-3 pattern; and (2) a carrier controlled approach (CCA).

For the preliminary work, only maneuver (1) will be used as it has complex descending, ascending and turning components which will provide a wide range of movement for the motion platform. This type of maneuver will provide a good basis upon which to differentiate algorithms. This maneuver will also provide advantageous and disadvantageous effects of motion.⁶ According to this classification, turbulence will cause disadvantageous effects whereas the aircraft motion caused by pilot control of the aircraft is considered advantageous.

Subjects. For the preliminary study, novice private pilots from civil aviation will be used. It is planned to limit the age range from 18 to 30 years since we have found from previous studies that age is an important variable that affects performance. This age range will match that of most of the naval aviator population which will be used in the later studies. The experience levels of these novice pilots range from about 4 to 1000 hours in light aircraft. All subjects will be trained to proficiency in the basic control of the simulator. Generally, this requires from two to six hours of practice per subject.

For the follow-on studies, subjects will be naval aviators, both "nugget" and experienced. In view of logistics costs in bringing military subjects to the Naval Training Equipment Center, it will be necessary to keep the total number of subjects as small as possible and attempt to attain a sizable data base by taking a large number of data points from each subject. The minimum number of subjects will be six but observing the variability from the preliminary study should help us determine the required number.

Experimental Equipment. The TRADEC facility which will be used for this initial study consists of a 4 degree of freedom moving base platform (with cockpit instruments) driven by an XDS Sigma 7 computer with F4E aircraft mathematical model. Associated peripheral equipment includes four 9-track 800 BPI tape transports, one high-speed printer, one card punch, random access devices and A/D and D/A equipment. A Brush recorder is used to display analog signals in real time and a Cal Comp plotter is used to plot power spectra. A Varian 6201 minicomputer and associated IDIOM graphics processor are

interfaced with the Sigma 7 to provide subject performance data and a means to exercise experimental control.

Performance Measurement. Both subjective and objective measurement techniques will be used. The subjects will be asked to judge the fidelity of the motion cues encountered during the tasks on both an absolute and comparative basis. The subjects will score separately the translational and rotational motion cues relative to a rating scale. These scores will also be used to provide a combined fidelity score. The overall handling qualities will be subjectively evaluated on the Cooper-Harper Rating Scale. The algorithms will also be compared to each other on a comparative rating scale.

For objective measurement, the Basic Instrument Flight Maneuvers (BIFM) training package developed for laboratory studies of automated or adaptive training techniques will be used. The BIFM package uses a technique for segmenting flight tasks that separates psycho-motor (control) performance from system performance. A sample student record is shown in Figure 5.

Validation

After completion of the simulator study, a validation study will be conducted to compare system performance and pilot control performance in the simulator with the same maneuvers performed in flight. Again, both subjective and objective data will be collected. For objective measures, an instrumented aircraft will be required to be equipped with a recording capability equivalent to that of the simulator. The algorithms which elicit performance in the simulator most resembling that of flight will be retained for Phase III.

Phase III - Training Effectiveness Evaluation

This part of the study will be concerned with the practical question of the effects of the particular type of motion represented by the "best" algorithms on transfer of training. The ability to control the simulator in a manner similar to that employed in controlling the aircraft is only of academic interest if it does not have a positive and significant effect upon training.

In order to conduct the transfer study, a group of naval aviators who did not receive simulator training should be used as a control group. However, since all student naval aviators will have received simulator training (Device 2F101, T2C Operational Flight Trainer), in-flight performance measures will be taken prior to AWAWS simulator training. This will provide a basis for comparison to determine if learning has taken place as a result of the various algorithms or the no motion condition in the AWAWS simulator.

Epilog. - We have attempted to describe our plans to evaluate the training effectiveness of several of the currently available flight simulator motion system drive algorithms. We are aware that there may be some discrepancy between our current plans and their finalized version. In order to achieve our objectives successfully, we realize that changes will probably be required.

References

1. Smode, A. F. "Human Factors Inputs to the Training Device Design Process," NAVTRADEVEN 69-C-0298-1, September 1971.
2. Harris, W. T., "A Description of the Cockpit Motion Hardware used at the Naval Training Equipment Center," NAVTRAEEQUIPCEN TN-59, in preparation.
3. Wychorski, H. J. "Final Test Report on Research Tool Digital Computer System as a Fixed Wing Simulator," NAVTRADEVEN 67-C-0196-10, December 1969.
4. Walker, L. A.; Galloway, R. T.; "Flight Fidelity Evaluation of the T-2C Operational Flight Trainer, Device 2F101," NAVAIRTESTCEN FT-3R-75, January 1975.
5. Harris, W. T., "An Investigation of Drive Philosophies Encountered in Flight Simulation," NAVTRAEEQUIPCEN IH-299, in preparation.
6. Gundry, A. J. "Thresholds to Roll Motion in a Flight Simulator," Journal of Aircraft, July 1977. (Also as Paper 76-1717 of the AIAA Visual and Motion Simulation Conference, Dayton, Ohio, 1976).

```

*****
FLIGHT 0004 RUN 0005 PIM 0007 ENTRY 0005 LEVELS 0008 CURRENT 0005
MANUEVER: VERTICAL S-3 CG: AFT TURBULENCE: NONE

ASSIGNED ALTITUDE AIRSPEED HEADING CLIMB RATE TURN RATE YAW ANGLE ANGLE/ATTACK ROLL ANGLE ROLL RATE
(FEET) (KNOTS) (DEGREES) (FT/MIN) (DEG/SEC) (DEGREES) (UNITS) (DEGREES) (DEG/SEC)

19967-054 314.951 0.027 -534.507 0.020 0.010 7.753 0.168 0.447

SEGMENT 0001
SEGMENT SCORES SYSTEM NONE CONTROL NONE PROCEDURE 0001 TIME 14.949 SECONDS

SEGMENT 0002
FAM DSRD XFM RAW WF WEIGHTED TYPE
A/S 300.0 RMS *** NONE *** NONE ***
BETA 0 RPS *** NONE *** NONE ***
ELVS 0 SDEV *** NONE *** NONE ***
AILS 0 SDEV *** NONE *** NONE ***

SEGMENT SCORES SYSTEM NONE CONTROL NONE PROCEDURE 0001 TIME 0 SECONDS

SEGMENT 0003
FAM DSRD XFM RAW WF WEIGHTED TYPE
TURN 1.250 RMS 0.449 50.0 24.979 S
HDOT 1000.0 RMS 1326.537 0.100 132.653 S
A/S 300.0 RMS 7.881 5.0 39.409 S
BETA 0 RMS 0.236 50.0 16.817 S
ELVS 0 SDEV 0.570 10.0 5.707 C
AILS 0 SDEV 0.221 10.0 2.211 C
INNER/MIDDLE/OUTER COUNT TRANSFORM DATA
FAM DSRD INNER % MIDDLE % OUTER %
TURN 1.250 46.2 24.4 29.2
HDOT 1000.0 27.1 12.2 60.6

SEGMENT SCORES SYSTEM 53.444 CONTROL 3.459 PROCEDURE NONE TIME 47.199 SECONDS

SEGMENT 0004
FAM DSRD XFM RAW WF WEIGHTED TYPE
TURN 1.250 RMS 0.617 50.0 30.866 S
A/S 300.0 RMS 7.127 5.0 35.636 S
BETA 0 RMS 0.381 50.0 17.598 S
ELVS 0 SDEV 0.660 10.0 6.608 C
AILS 0 SDEV 0.189 10.0 1.899 C
INNER/MIDDLE/OUTER COUNT TRANSFORM DATA
FAM DSRD INNER % MIDDLE % OUTER %
TURN 1.250 21.8 31.2 47.0

SEGMENT SCORES SYSTEM 28.033 CONTROL 4.254 PROCEDURE 0001 TIME 16.148 SECONDS

*****

SEGMENT 0010
FAM DSRD XFM RAW WF WEIGHTED TYPE
A/S 300.0 RMS 1.879 5.0 9.305 S
BETA 0 RPS 0.564 50.0 29.239 S
ELVS 0 SDEV 0.254 10.0 2.844 C
AILS 0 SDEV 0.239 10.0 2.392 C

SEGMENT SCORES SYSTEM 15.317 CONTROL 2.418 PROCEDURE NONE TIME 4.449 SECONDS

SEGMENT 0011
FAM DSRD XFM RAW WF WEIGHTED TYPE
HDOT 0 RMS 400.186 0.100 40.018 S
A/S 300.0 RMS 9.258 5.0 46.293 S
BETA 0 RMS 0.161 50.0 8.052 S
ELVS 0 SDEV 0.401 10.0 4.017 C
AILS 0 SDEV 0.218 10.0 2.189 C

SEGMENT SCORES SYSTEM 31.454 CONTROL 3.103 PROCEDURE 0001 TIME 10.0 SECONDS

FINAL 19998.121 238.165 356.819 -329.337 0.008 -0.0102 7.436 -1.608 1.842

RUN TERMINATED BY SUCCESSFUL COMPLETION
MANUEVER FINAL SCORES SYSTEM 50.285 CONTROL 3.443 PROCEDURE 6.666
RUN TIME 25.4 SECONDS TOTAL RUNS THIS FILE 0005 SC FLEIGHT RUN ADJUSTMENT
ADAPTIVE LOGIC INCREMENT = NONE

```

Figure 5. Sample Student Record for Vertical S-3 Maneuver

DEPTH PERCEPTION AND MOTION CUES VIA TEXTURED SCENES*

Richard V. Reynolds
William O. Dungan Jr.
George J. Suttly
Technology Service Corporation
Santa Monica, California

Abstract

The need for depth perception cues in flight simulators is illustrated. Traditional depth perception cues are discussed: accommodation, relative size, interposition, linear perspective, aerial perspective, monocular movement parallax, convergence and binocular disparity. Several psychophysical experiments that yield insight into the depth perception process are discussed. The TSC approach for generating textured scenes is presented. Finally, the relevance of texture and texture gradients is discussed in both static and dynamic scenes.

I. Introduction

When pilots try to land on homogeneous surfaces, e.g., calm water or snow, there is a problem in judging the height above the surface. This situation results from a lack of depth perception cues. The bush pilot usually takes action to resolve the situation by providing depth perception cues, e.g., he tosses one or more red blankets out of the plane. Then he lines up the approach track accordingly and flairs with the blanket or blankets continually providing the necessary cues.

Flight simulators that generate untextured surfaces must utilize nontextural cues for generating depth perception. In general, scene complexity is a severe restriction and is usually expressed in edges per scene. How to allocate the edges over scene elements is always a taxing problem. For example, the lack of depth perception cues caused one user to augment the scene with groups of clustered diamonds on the sides of a runway in order to provide depth perception cues to pilots. A good experiment to demonstrate the need for depth perception cues in a flight simulator would be to attempt a landing in a large homogeneous region.

Today's state-of-the-art flight simulators generate real time untextured scenes. Currently there are many approaches being pursued to efficiently generate realistically textured scenes.¹ The approach² taken by Technology Service Corporation (TSC) is predicated on tiling areas of a scene with primitive texture tiles. These tiles are arrays containing digitized photographs of textured material such as trees and grass. This technique

has matured to the point where complex scenes containing multiple areas of various textures can conveniently be generated. By means of pre-filtering, the periodic boundaries between tiles are not distinguishable. In addition, scene filtering and level-of-detail data structures for the texture tiles are other means which significantly reduce spatial aliasing.

As a natural extension to the static generation of textured scenes, TSC has produced two 20-second video tapes: one textured; and one untextured. The scenario is for an aircraft to descend from an altitude of 3000 ft over a large tree-textured area toward a complex of buildings in a clearing at an angle of 10° with a field of view of 60° by 45°. The intent is to observe the perceptual effects induced by the motion of textured materials. The perception of depth is the primary effect to be investigated.

However, by viewing the first few seconds of video imagery, an unexpected phenomenon appeared. There were bands of scintillating textured materials. These bands occurred at the boundaries between levels of detail of textured material. Textured scenes when viewed individually were judged to be acceptable renditions, i.e., spatial aliasing was under control. However, when viewed in real time, 30 frames per second, temporal aliasing appeared in the form of scintillating bands. At the present time this phenomenon is under intensive investigation and will subsequently be reported.

II. Depth Perception Cues

The three primary cues of depth perception are accommodation, binocular disparity, and convergence. Traditional secondary cues are: relative size of similar objects, interposition, linear perspective, aerial perspective, and monocular movement parallax. These traditional cues have in recent years been supplemented by both spatial and temporal retinal gradients of texture material.³ The following sections will expand on these cues and emphasize those motion cues that yield information on depth perception.

Depth perception induced by CIG images is equivalent to viewing two dimensional imagery and determining which information present in the image

* This research was sponsored by the Air Force Human Resources Laboratory, Contract F33615-C-0063.

yields the perception of depth. There traditionally have been two points of view of experimental research: (1) pick various three-dimensional transformations, view their two-dimensional projections, and determine which information in the two-dimensional projection is used in the perception of three-dimensional information, and (2) generate two-dimensional pattern variations without regard to three-dimensional transformations. Clearly, the former method is the one employed by TSC in the generation of textured images. These experimental techniques have images projected onto translucent surfaces, i.e., the light is able to pass, but the image is diffused.

Accommodation is the ability of the eye to adjust in such a manner as to bring an object into focus. The image of that object is focused sharply onto the retina. Other objects at different distances have blurred images focused onto the retina; therefore, relative distance of depth can be perceived for objects close to the observer.

Relative size of retinal images of familiar objects are cues for determining a feeling of distance. Larger retinal images of objects in the same class usually indicate that the larger object is closer.

Interposition is the overlapping of one object by a closer object. This information yields an ordering of objects. Not every visual flight simulator adequately solves this hidden surface, masking, or occultation problem. For example, in some systems the view from one side of a hill has a building correctly in front of the hill. However, from the other side of the hill the building appears to float through the scene. Other CIG techniques properly occult objects, but only if two objects are involved. The image of a third object is superimposed on the proper images of the other two objects.

Linear perspective describes the condition that a constant distance between points subtends a smaller and smaller angle as the points recede from the observer. This is the common railroad effect as the tracks converge toward the horizon.

Aerial perspective represents the case of viewing an object from a considerable distance through the atmosphere which both absorbs and scatters light. This obscures surface detail and visual contrast and causes an observer to report an object as far off. Smog and haze are excellent absorber and scatterers of light.

Monocular movement parallax occurs when a subject's eyes move with respect to the environment or conversely. When such movement occurs, there exists a differential angular velocity between the line-of-sight of a fixated object and any other object in the field of view. This provides a means to discriminate between objects.

Convergence is the rotation inward of two eyes such that each eye fixates on the same point. This is effective for distances of several meters.

Binocular disparity, i.e., stereoscopic vision, is the condition of different retinal images existing in each eye when viewing an object in space. It turns out that binocular disparity even in random patterns is enough to indicate depths.⁴

III. Depth Perception Experiments

Psychophysicists have conducted a series of experiments designed to elicit reports from subjects as to their perceptions of depth and direction of rotation. A prelude to the types of experiments that shall subsequently be discussed is the case of the windmills in Holland during the early 1800's. Dutch farmers reported, and some even tried to sue the contractors, that their windmills were rotating in reverse. This phenomenon was usually observed near dusk with the observer placed at an angle to the windmill.

The following series of experiments consisted of shadows or bright figures cast onto a translucent surface. A wire figure was oscillated through an angle of 42 degrees. The subjects perceived depth, but most were unable to correctly perceive the shape. Thus perception of depth is partially independent of the correct perception of shape.⁵ In another experiment a truncated cylinder was rotated to produce a one-dimensionally changing shadow. It was perceived only as a shadow changing in one dimension with no perception of depth. Straight rods were then rotated to produce shadows that changed in both length and direction. Subjects then perceived depth, but sometimes incorrectly perceived the direction of rotation. Another experiment in which the distances between objects was varied demonstrated that if the two-dimensional projection contained contour lines, either real or imaginary, then the simultaneous changes in length and direction would induce a perception of three dimensions.

IV. Texture Gradients

The CIG texture project at TSC generates scenes that consist of textured surfaces. Gibson hypothesized that space perception is reducible to the perception of visual surfaces and argued that the texture density gradient was sufficient stimulus for the perception of slant surfaces. Therefore, the ability to identify planes greatly enhances the perception of a scene. The attributes of texture that affect perception are size, shape, and distribution. By slanting the textured planes in a scene, the projected images have very discernible texture gradients. This is true for static scenes, but when displayed in a dynamic sequence, i.e., realtime, there exists clearly discernible patterns of texture flowing across the display screen.

Summary

In summary, this paper has discussed the TSC approach to generating textured scenes, the traditional depth perception cues, and the usage of texture and texture gradients to induce more realistic perception of depth. Since the TSC project has just crossed the threshold of providing a viable means for investigating textural cues for flight simulators, the direction of CIG research in texturing is at an important junction. It is not clear what the future directions and impetus will be. However, it is clear that texture makes a difference in depth perception and that the future research should have as a goal the refinement of how and why texture makes a difference.

References

1. Reynolds, R., "Scene Realism via Texture", to be published, S. P. I. E., 1978.
2. Dungan, W., A. Stenger, and G. Sutt, "Texture Tile Considerations for Raster Graphics", to be published, Siggraph, 1978.
3. Gibson, J. J., "Perception of Distance and Space in the Open Air", from Motion Picture Testing and Research, AAF Program, Report No. 7, 1946.
4. Julesz, B., "Binocular Depth Perception of Computer Generated Patterns", Bell System Technical Journal, Vol. 39, pp. 1125-1162, 1960.
5. Wallach, H. and D. N. O'Connell, "The Kinetic Depth Effect", Journal of Experimental Psychology, Vol. 34, pp. 205-217, 1953.

CIRCLES, TEXTURE, ETC.
ALTERNATE APPROACHES TO CIG SCENE DETAIL

Dr. W. Marvin Bunker
General Electric Company
Daytona Beach, Florida
and

Capt. M.L. Ingalls
U.S. Air Force
AFHRL/ASM, Wright-Patterson AFB, Ohio

Abstract

Since its inception, visual scene simulation using computer image generation (CIG) has been applied to training tasks requiring increasingly extensive visual cues. Early systems had only one type of entity, or "primitive" from which this scene detail could be created - the edge. Early requirements for increased detail were met by increasing system edge capacity. Edges have a range of natural application where they are both the most efficient and the most valid means of defining features. Runways and rectangular buildings are examples. When they are used beyond their natural application (to approximate circles, for example), efficiency is low since large numbers must be used, and scene validity suffers from the stylized nature of the approximation. This has led to continuing effort to develop new primitives which in their areas of application will be the most efficient and effective tools for providing scene detail. The CIG system users - the military training establishment - have most seriously felt the need for the added CIG capability and have initiated action leading to some of the more significant developments. This paper discusses the recently developed ellipsoidal features and surface-map texture, and illustrates their use.

a stylized, approximated appearance. The use of edges to define runways is a natural application; the use of edges to define circles is not - both efficiency and quality suffer.

Introduction

The Problem

CIG systems have traditionally defined scene features with edges - straight-line segments bounding planar faces. These have been processed by an image generator and shown by a display system to form the scene detail making up the visual cues required for training. A given CIG system will have a specific edge capacity available for use in meeting the requirements of the training missions it supports. Let's examine a couple of types of problems this led to.

Fig. 1 shows a scene near touchdown on a runway. There is a variety of detail - the runway itself, stripes and runway markings, taxiways, fields, etc. In a dynamic mission, ample cues are provided to detect motion, attitude, elevation, and their rates of change. Not only are these cues present, but they have full spatial validity - they look real. Further, there is high efficiency in the scene definition and processing. A 10,000-foot runway can be defined with only four edges (the base runway without markings). Fig. 2 shows a bomb circle simulated with edges. There are four circles, each approximated with 16 edges - 64 edges are used for this one feature, and yet it still has

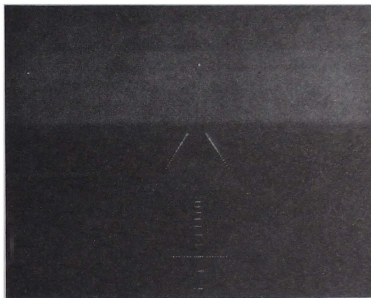


Fig. 1 Runway scene with detail.

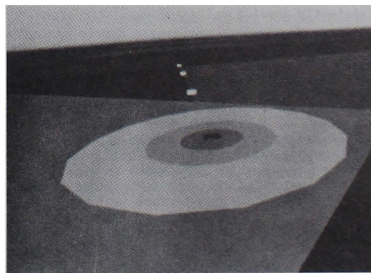


Fig. 2 Bomb circle simulated with edges.

Fig. 3 illustrates another problem. It shows a highly detailed aircraft flying over terrain that is almost devoid of detail. The edge capacity of the system was devoted to detail on the KC-135, leaving little for the ground. Flying over such a depiction of the ground surface gives very little impression of motion or of attitude or altitude change. Much more surface detail is needed.



Fig. 3 KC-135 flying over sparse terrain.

All visual cue requirements could be met with edges alone, if there were no limit to system edge capacity. Consider the bomb circle of Fig. 2. If it were approximated with a sufficiently large number of edges, it would be indistinguishable from a true circle. Consider a 200-mile square gaming area. One surface-detail feature for each 64-foot square of the surface could be defined with some 1,000,000,000 edges. While system edge capacity will continue to increase, and while more efficient and effective ways to process and use edges will be devised, there is obviously need for approaches not limited by the characteristics of edges. The edge can be considered the first primitive available for supplying detail in CIG systems. It seems logical that other primitives could be developed; each of which in its area of natural application would efficiently provide valid and realistic scene detail.

Background

Strictly speaking, the edge was the second primitive applied to solid-surface CIG visual scene simulation. A system delivered to NASA in Houston in 1964 had no edges, only ground-map texture. This provided valid motion and attitude cues. Edge capacity was added to this system in 1967. Fig. 4 shows the nature of the results provided by the technique used. The map-texture implementation at that time depended for its feasibility on a constraint that the raster lines of the display device be parallel to the horizon. Because of this constraint, and the desire for greater realism which could only be provided by edges, there was no further development of the map-texture technique for a number of years.

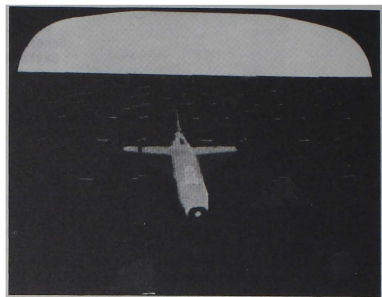


Fig. 4 Early results of map-texture approach.

The 1967 retrofit on the NASA system provided it with 240-edge capacity. The 2F90 visuals delivered to the Navy in 1972 had 512-edge capacity. The Air Force ASPT system increased CIG per-scene edge capacity to 2400 edges. Systems currently being built can process up to 8000 edges, and even greater capacities seem certain for the future. These numbers, however, do not preclude the need for additional primitives to provide detail outside the range of natural application of edges.

The next primitive to be added to operational systems after edges was point-feature capability - first in the role of point lights. Applications such as runway lighting require large numbers of point lights. These could be formed with edges, but this is both inefficient and awkward. Each point light uses four edges in its definition. As distance from the light changes, the edge-definition of the light must change to keep its image the proper size on the display. Further, complex perspective processing is being applied to each edge, and this processing is not necessary for point lights. When the requirements for point-light simulation are considered alone, significant efficiencies are possible as compared to edge processing. This additional primitive was first operational in real time in 1971, and has since been a capability of a number of operational systems. As compared with earlier implementations, the number of point features a system can process is now greater, fully effective quantization smoothing is applied as they move or change size, and designs currently under way will allow the view window image of the point feature to be circular rather than square.

Benchmark Status

The status at the time of the start of the developments discussed in this paper can be summarized as follows: Two primitives were common in operational systems - edges and point features. Their capabilities, both quantitative and qualitative, were continually being improved. A map-texture technique had shown its value in providing visual cues, although with a dead-end implementation.

Finally, the most commonly expressed criticism of existing systems was the lack of scene detail, surface texture, over broad expanses of terrain away from the airports, and other areas in which available detail was concentrated.

Approaches to Surface Detail

The goals of the investigations to be discussed were originally defined in a somewhat narrow manner - to develop techniques for providing the missing, and badly needed, scene detail over large gaming areas. As the effort proceeded and insight was gained, the goals were expanded to take advantage of the broader applicability of the techniques developed.

The major part of this report deals with map texture and with ellipsoidal features. A couple of other approaches to the goal as initially stated are also discussed briefly.

Surface Detail with Edges

In spite of earlier comments and numbers, much more could be done toward meeting surface detail requirements with edges, than has been done. Consider a system whose per-scene edge capacity will provide sufficient surface detail on any individual scene. Now if we fly outside the region where detail has been defined, the cues are unsatisfactory and the major portion of the entire CIG system is sitting idle. What is needed is something at the "front end" of the system, to keep the remainder supplied with detail edges at all times.

Two approaches to this appear quite feasible. These edges can be defined off line and stored in a mass memory, then transferred to current scene memory as the flight proceeds and they are needed. As an alternate approach, assume we have an algorithm that considers current location of the viewpoint and uses some pseudorandom processing to generate feature definitions in terms of edges. This would eliminate the great numbers of edges in mass memory, yet provide large numbers of edges for detail wherever we fly in the gaming area.

Some work has been done on both the above. More should be done, along with effort on new primitives.

Use of Noise

Surface detail with a high degree of randomness has the appearance of visual texture. The appearance is similar to that produced by noise on the video applied to a display device. The idea of actually using noise in this manner to provide surface detail for visual cues is one that occurs early in the consideration of approaches to the goal. Upon further investigation, the probability that this will be a fruitful approach seems rather low. A brief discussion later will deal with the reasons for this.

Ellipsoidal Features

In radar display simulation, a circular target generator has proven very valuable. Not only can it generate individual targets, but excellent simulations of irregularly shaped features are provided by clumping a set of individual features of

appropriate size and location. In radar displays, a circular pond is of constant size and shape independent of its location on the display. In the perspective display simulation produced by CIG, the image of a circular feature is in general an ellipse, and its size is a function of distance. This complicates the processing. Nevertheless, it is true that if an efficient means could be devised to process such features, they could be scattered in large numbers over the terrain, meeting the goal of surface detail for visual cues. As development proceeded not only did this appear feasible, but the new class of features turned out to have applicability far beyond that of meeting the initial goal.

Map Texture

The original map texture not only had an implementation which was not applicable to most systems, but exhibited artificial and obvious directional cues, repetition patterns, and scintillation in the distance. However, it had the very powerful characteristic that, once implemented, it would provide its surface detail over a gaming area of infinite extent. This motivated an effort to overcome the deficiencies so the full potential of this powerful tool could be applied to CIG requirements.

Noise Texture

Either true or pseudorandom noise of selected characteristics may be applied to the video produced by a radar display simulation system, and the result is a clumping, grainy texture closely resembling some types of ground texture. It has provided a valuable addition to realism in such simulations.

Similar noise may be added to video in simulation of FLIR and LLTV displays, to reproduce the effects of the noise which is present in actual systems.

Upon looking at photographs made on the above systems, the idea of applying similar noise to CIG texture in visual scene simulation naturally arises.

Let's consider some of the factors involved.

If we use actual noise, we know right away what the effect will be—we've all seen "snow" in television sets when the incoming signal is weak.

If we use pseudorandom noise, locked to the beginnings of the scan line, we can produce texture that will look fine as long as there is no movement. However, as we move, the clumps created by the texture will remain stationary on the display, while the faces they are supposedly a part of move by and leave them behind.

In radar simulation, the much longer time to generate each full display (corresponding to the actual radar), and the memory fading rate for such small detail, have prevented either of the above problems.

We might consider locking a pseudonoise generator to the leading edge of a face. We would have to include features to assure that when our viewing angle to a face changed, the image of a blob would change perspective in a valid manner.

Also as distance increases, the texture blobs must become smaller and closer together in a perspective valid manner. No approach to solving these problems has as yet shown promise. Thus, this approach is not currently being considered.

CIG Processing

A brief discussion of some of the fundamental operations involved in CIG image generation will help in understanding of some of the following material. The functions are conveniently grouped as scene-rate functions, line-rate functions, and pixel-rate functions.

Scene-Rate Functions

The scene-rate functions must be performed once for each scene to be shown. These include definition of the view window (or view windows for a multichannel system) based on viewer position and attitude for the current scene, and determination of which features are potentially visible in the view window as defined. Each potentially visible feature must have its view window image computed. This involves a perspective transformation from the three-dimensional feature definition to the two-dimensional view window coordinates. It also includes truncation of features at view window boundaries. Another significant scene-rate function is the determination of priority relationships. For any two features part of whose images may occupy the same region of view window space, an order must be determined designating which masks or occults the other. The hardware implementing these scene-rate functions is sometimes referred to as the "vector processor."

Line-Rate Functions

The line-rate functions must be performed for each scanline of the display device. For each scan line, the features "active" on that scan line are identified - those which appear in the scene for that scan line. For each active feature, the definition of the feature truncated to the scan line is determined. Next is the ordering function - the feature information must be ordered left-to-right, since the time-order of the output video must conform with this scan direction along the line. Next is the priority resolver function. When feature information indicates conflicts along a portion of a scan line, these must be resolved. This function must provide information in a form suitable for implementation of quantization smoothing - the area times color rule that must be applied when a given pixel contains portions of several features.

Pixel-Rate Functions

The pixel-rate functions, which must be performed each 25 nanoseconds or so, depending on the number of lines and elements of the system, generate the video for application to the display system. These functions use the information from the priority resolver and from other system functions. Final area-times-color implementation is done here, and fog or haze effects are introduced.

Ellipsoidal Features

Circular Features

Initial implementation, following from the experience with radar display simulation, was limited to horizontal circular discs on the ground. Such a circle transforms to an ellipse in the view window, whose full spatial definition is contained in the six coefficients of:

$$R1I^2 + R2J^2 + R3IJ + R4I + R5J + R6 = 0; \quad (1)$$

where scan line number is designated by I, and pixel number along a scan line by J.

Scene-Rate Functions. The scene-rate functions for circular features must define them in form suitable for the subsequent line-rate and pixel-rate functions to work from. The fundamental function is determination of the six coefficients spatially defining the feature in the view window coordinate system. Using these coefficients, the vector processor determines the values of I and J defining the ellipse extrema - top, bottom, left, and right.

Line-Rate Functions. For each scan line, the ellipses active on that scan line must be determined. The values of J at which the ellipse intersects both the top and the bottom of the scan line must be determined. From these points, and the extremum points, a set of two to four line segments which closely approximate the portion of the ellipse on the current scan line, is defined. These segments join those derived from actual edges by the edge generator, and in subsequent processing no distinction is made based on the source. Thus if circular features are being added to a system, no modification is necessary past this point. The circuitry implementing these functions is referred to as the circular-feature edge generator.

Assume the viewer is near an airport which contains a full complement of detail formed from edges. The bulk of the system, the hardware following the edge generation function, is devoted to processing this detail. Later in the mission the viewer is in an area with very few edges, but with detail provided by large numbers of circular features. Now the same hardware is kept busy processing them. This is a definite efficiency-enhancing characteristic of the basic approach used.

Results. Fig. 5 shows an application of these circular features, to produce a circular bombing target. This may be compared with the bomb circle in Fig. 2.

Extension of the Concept. In addition to circles, ellipses; spheres; and ellipsoids of any orientation map into ellipses on the view window. By adding to the scene-rate functions the capability of performing these transformations, with no change in the subsequent functions from the above discussion, this entire family of primitives can be included in visual scene simulation.

capability. Design is currently under way to provide this capability with hardware implementation in real-time systems.

Surface-Map Texture

Concept

The concept involved in surface-map texture is simply stated. On the surface to be textured - whether a face of a building or the unlimited ground surface - a set of bits is associated with each surface point. For each pixel containing an image of part of this surface, computation determines the bits for the portion of the surface contained in the pixel. The bits or a subset of them are used as the address to a table-look-up memory. The memory output is used to modify the tone or color of the face, thus simulating texture. Alternately, the bits may be used in a quantitative manner to modulate tone or color.

The bits may be assigned to a surface with a high degree of flexibility. The subsets to be used may be selected in any of a number of ways. The contents of the memories may be selected to achieve an unlimited variety of effects. The surface-map texture concept constitutes an extremely powerful tool for providing valuable visual cues. This tool has not been a feature of most previous systems because of implementation difficulty. To determine the set of bits mapped onto a textured surface requires in general several high-precision divides - and this must be done each pixel time. Consider the ASPT visuals - a 14-channel system. A straightforward implementation would require in excess of 10^9 such divides per second.

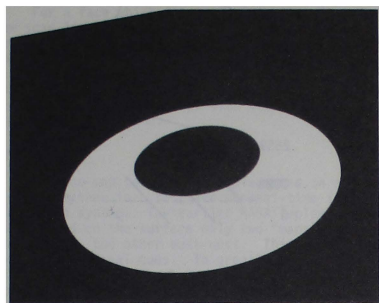


Fig. 5 Bomb circle simulation using circular features.

Fig. 6 illustrates some of the ways in which this new capability can be used. Spheres can be clumped to form clouds. Concentric circles can form curved segments of roads. Circles form the tops of cylindrical storage tanks. A spherical top of a water tower, and circular settling ponds, are efficiently and validly simulated.

Status. The ellipsoidal feature illustrations were made on a nonreal-time software scene generation system, which has been programmed to add this

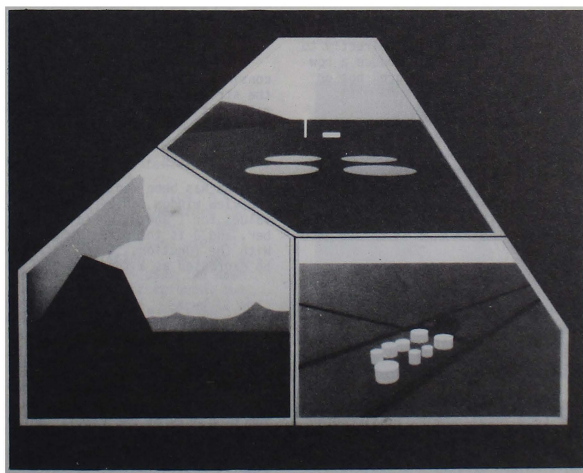


Fig. 6 Applications of ellipsoidal features.

In the following, the concept will be further clarified; illustrations provided on various ways of applying it; and some comments on implementation will be included.

Some Variations

Consider a quantitative function, q , which varies linearly across the surface of a face. Assume that when perspective transformation is applied to the face to determine its image on a display window, the pattern of numbers transforms validly. There are a number of ways in which such a pattern or function can be used.

Fig. 7(a) shows a plan view of a face with the gradient vector of a function q . Assume that the plot of q versus position on the face is as shown in Fig. 7(b)—a continuous, linear variation of magnitude. Such a function is used directly in curved surface simulation. It is applied to the assigned face color to produce a smooth continuous gradation of intensity across the face. In the curvature application, the range of magnitude of the function is such as to produce only a small percentage variation in brightness across one face.

Fig. 7(c) shows $q_a = q \bmod (1024)$, plotted to an enlarged scale. Thinking more in hardware terms, q_a constitutes the ten least significant bits of q . In a texturing application, q_a could be used to control intensity variation of a face, over a specified range of total brightness variation. The variation would be smooth from minimum to maximum brightness with an abrupt change back to minimum.

Function q_b would be quite easy to derive from q_a — it is a q_a folded around 511 and based at zero. If this is used for quantitative variation, we no longer have the abrupt changes. Tonal modification is continuous across the entire face.

Function q_c is a logical signal produced by comparing q_b with a threshold. If used directly to control color or intensity, it would produce a row of parallel stripes (parallel on the face, not on the image).

Several functions or patterns of numbers can be combined to produce texture. Fig. 7(f) shows the result of using a logical combination of q_c with a similar signal from a second function, made purposely nonorthogonal to the first function. Several such functions can also be combined in a quantitative mode. As another possibility, three functions could be used, controlling intensity of the three primary colors.

Another approach involves use of sets of bits from several functions as addresses to color register memories, whose output is converted to video. This was the technique used on the NASA system to produce indefinitely extended surface patterns. Or, the output of a table-look-up memory can be used to modulate assigned face or surface colors.

A flexible approach involves definition of several functions for each face. Their relative orientation and their orientation on one face relative to another are unconstrained. A code that is part of the face definition can specify the desired manner of using the functions, several of which have been mentioned above. This will provide a very

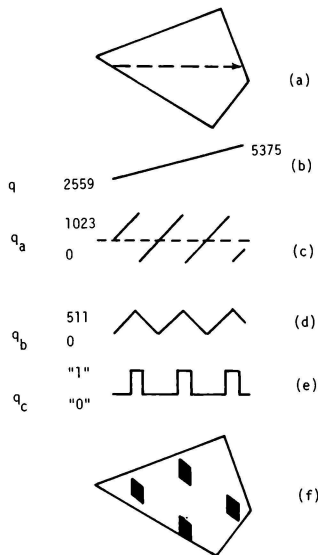


Fig. 7 Linear texture function.

powerful and versatile system for providing motion and attitude cues along large faces that are currently a uniform color.

In considering implementation details, we can consider separately the processing that produces the streams of values of "q", changing at element rate, and the subsequent steps involved with the use of these q values.

Implementation

As has been mentioned earlier, any location on the view window can be specified by giving a set of values for I and J , where I is the scan line number, and J is the pixel number along a scan line. With the functions "q" as defined above, any q can be expressed as a function of I and J as follows:

$$q = \frac{K_1 + K_2 I + K_3 J}{K_4 + K_5 I + K_6 J} \quad (2)$$

This has the merit that updating the numerator and denominator for each new pixel involves only incrementing. If a face has several q 's defined, the denominator will be the same for all — it is a function only of the spatial definition of the plane of the face. Each q will have its own set of numerator coefficients. This leads to a slight simplification in implementation in such cases. The reciprocal of the denominator is determined,

after which a sequence of multiplications by the respective numerators serves to give all desired q 's for the face.

For a face which is parallel to the view window scan lines, K_x is zero. Thus, following some setup work for each new scan line, each q can be updated for each pixel by a single increment. It was this simplification which was utilized in the NASA system to make possible implementation of the surface-map texture concept with the technology available at the time.

Some Results

Surface-map texture was implemented in a very flexible manner in a software nonreal-time image generation system. The earlier NASA implementation had defined on the surface only two "maps", one north-south, the other east-west. This led to the undesired cardinal cues. To greatly reduce this effect, a set of six equally spaced maps was defined for this test, as illustrated in Fig. 8.

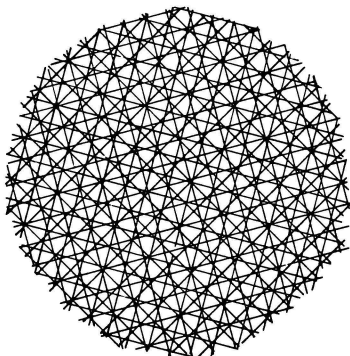


Fig. 8 Set of six maps for texture.

The test scene is shown in plan view in Fig. 9. Faces 1 through 8 are untextured - they form two vertical towers to help give perspective to the scene. The background behind the faces uses all six maps for the texture modulation. Each map accesses a separate memory. Face 14 uses the same maps, in the same manner, as the background, but with a different assigned face tone. Faces 12 and 13 use the maps in the described manner, but each uses a subset of two of the six maps. Face 10 uses the X and Y maps, but in a quantitative manner rather than via a memory. Face 9 uses only the X map, also in a quantitative manner, but with different spacing than that defined for face 10. Faces 11 and 15 use the tables, but with further variations applied.

Fig. 10 is a closeup view of this test scene, with texture contrast deliberately set quite high for algorithm evaluation. It effectively illustrates the variety of effects that can be achieved.

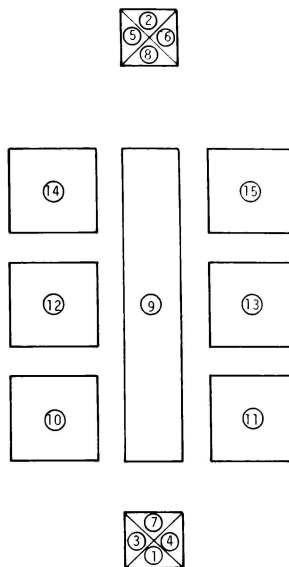


Fig. 9 Map texture test data base.

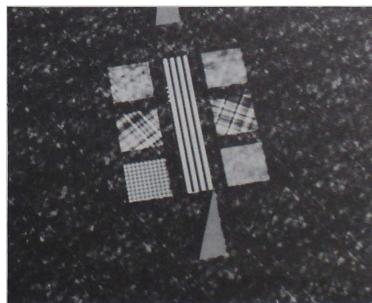


Fig. 10 Texture test scene closeup.

Fig. 11 shows a different view of the test scene, with texture turned off. The effect of solid objects against an artist's backdrop is familiar to users of CIG systems. In Fig. 12, texture

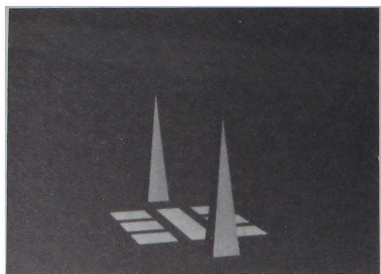


Fig. 11 Test scene with texture off.

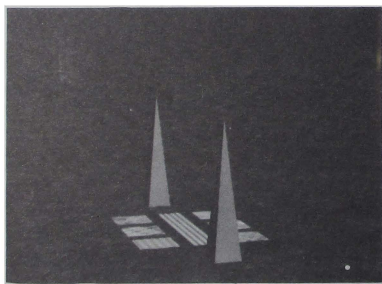


Fig. 12 Test scene with texture on.

is turned on. Now it is obvious that the objects are on an extended horizontal surface.

Each of the maps contributes a set of parallel zones to the texture structure. Gibson¹ concluded that the primary source of distance information is in the "stimulus gradient" of horizontal surfaces, that this may be derived from any one or combination of a variety of stimuli, and that among these are the texture gradient and the gradient of convergence of parallel lines. A part of the observed effectiveness of this texture can be attributed to the fact that it contributes two sources of stimulus gradient, which reinforce each other. There will be cases, however, where the nonrealism of the parallelism is undesirable. The parallelism results from the fact that we use a subset of bits

from the X map as the address to one memory, a subset of bits from the Y map as the address to a second memory, and similarly for the remainder of the six maps.

The alternate approach will be described for a set of two maps. Let us form an address from five bits of the X-map appended to the corresponding five bits of the Y-map. We now have a unique address for each square of size determined by the magnitude of the least significant bit of the five. Using this as the address to a memory, we get a unique value for each such square, with none of the extended parallel zone effect seen earlier. If this is extended to form a single address from a combination of the bits from all six maps, then there is a separate output for each small polygon formed by the set of maps in Fig. 8 - very random-like texture results.

Fig. 13 illustrates the result of this mode of operation. It is an enlarged, high-contrast, test scene. The small squares are not from the map structure - they are enlarged pixels.

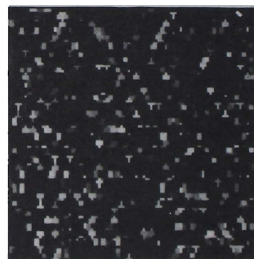


Fig. 13 Texture with alternate address-formation scheme.

Fig. 14 shows the effect of varying the rule by which the table-look-up memory contents are determined. In the earlier scenes, they were loaded from a pseudorandom number generator. For this scene, the X-map was loaded using a sinusoidal function. In making the scene, the magnitude of the modulation from the X-map was increased, and that from the other five maps was reduced.

If we combine the addressing scheme which provides a unique address for each point on the surface with no banding, with the freedom to obtain memory contents as desired, an interesting variation becomes possible which appears to have merit in some applications. The memory can be loaded by digitizing a photograph of a textured area. If the original area is planar, then the result of using the surface-map texture approach with this

shadow with a single ellipse, as compared with earlier tree approximations.

Applying Scene Detail to Training - The User's Viewpoint

Data bases are constructed with the tools available to the modeller. The preparation of data bases may be done manually, interactively, or automatically. The ultimate utility of the resultant data base is limited by the modeller's imagination and more importantly, the modeller's medium. To date, his medium has been limited to the use of color, edges, linear shading algorithms, and point features. The capability to generate elliptical and ellipsoidal objects by means other than a polygonal or polyhedral approximation in the data base has introduced an additional tool for the modeller to use. The edges, shaded surfaces, point lights, elliptical and ellipsoidal objects are the primitives, used either singularly or in combination, from which environments are synthesized. Each primitive suggests a natural application and, when used in a manner other than that, realism can be expected to suffer. For example, runways and markings are most effectively and efficiently modelled with edges. To approximate the same shapes with ellipses would be wasteful of the capability and would result in an image of less than comparable quality. This suggests that new primitives ought to be sought where their application efficiently represents what would otherwise require vast amounts of edges, point, and elliptical features. An obvious candidate for development is texture.

Texture might be thought of as a level of detail. The object or surface which is said to be textured is at such a distance that the shapes of

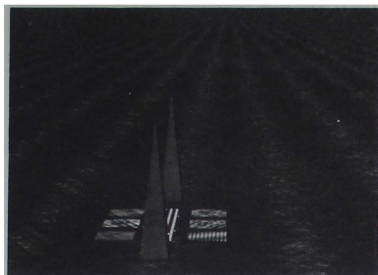


Fig. 14 Texture using sinusoidally-loaded memory.

source of memory contents will be a perspective valid image of the textured area.

New Primitives Combined

Fig. 15 is a scene containing edges, ellipsoidal features, and surface-map texture. The contribution of the combination to realism and richness of visual cues is striking. Note the efficiency of forming a tree with a single ellipsoid, and its

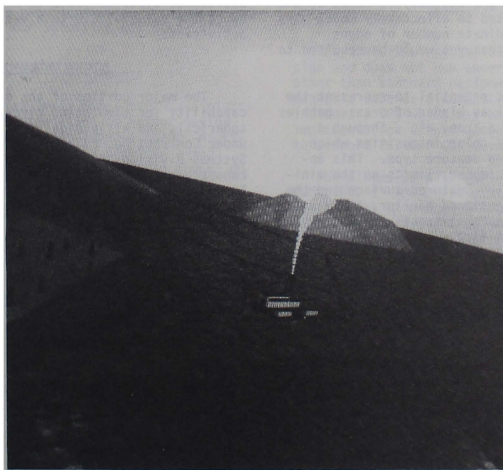


Fig. 15 Scene containing ellipsoidal features and surface-map texture.

the constituents comprising the texture are not singularly identifiable. It is the boundaries in conjunction with the granular structure interior to those boundaries that provides the information. And the information is developed by viewing the bounded granules as a whole. For example, it is the combinatorial effect of each blade of grass that enables one to identify an area as being grassy. The observer can conclude with reasonable assurance that he sees grass long before he actually sees each blade of grass. Just as the grassy area is said to be textured, there will be a point at which the individual blades of grass may be seen. The texture now belongs to each blade of grass.

The importance of texture on the majority of manmade things does not appear to be as important as the need to texture natural features. For example, the architecture of a building expressed solely in terms of edges, elliptical, and point features may provide an adequate and sufficient representation of a building. The addition of texture to the buildings' surfaces may only be desired if it were necessary to distinguish, for example, a brick building from a wooden one. However, in the case of a runway, the texture corresponding to the roughness of the material from which the runway was made, would provide at close range the appearance of a surface fixed in space as opposed to the dimensionless appearance exhibited by current image generation systems. Much of a CIG primitive capacity is consumed when modelling man-made features and, in general, these features are concentrated in operational areas of interest. The remaining capacity is used to depict the national characteristics of the environment. The natural areas of the data base represent a far greater area than that occupied by the manmade features. If primitive density were used as a measure of data base adequacy, and adequacy is based on the number of primitives used to effectively model man-made features, an inordinate number of edges, elliptical, and point features would be required to model the terrain.

Texture offers the potential to represent the presence of such detail as blades of grass, pebbles in a desert, leaves on a tree, etc., through a spatial distribution of color intensities which characterize the desired feature type. This approach to scene detail imposes limits on the minimum distances between the textured surface and the view point since, as mentioned earlier, there will be a point at which the constituents of the texture can be singularly identified. In a practical situation where the variations in height of the texture constituents is small with respect to its distance from the viewpoint, a two-dimensional representation may be sufficient. The forested area presents a difficult problem since the probability is great that the pilot could see individual trees, as well as the underlying surface. The leaves on the tree may be represented with textural techniques, however, the tree must be processed as a three-dimensional object in order to depict the proper masking relationships.

The objective of texture is to increase the density of the displayed information and provide the pilot with cues that have a counterpart in the real world. Texture becomes important, if not crucial, when the viewpoint comes in close proximity to the surface of the terrain.

Approaches which result in unrealistic textures may not facilitate effective transfer of training. Although these abstract textures may exhibit granularity and gradients, they do not provide the cues of the real world. They are in a sense meaningless. It is certainly possible that the trainee could learn to use abstract textures especially in light of the fact that, until the trainee learns to use them, even the real-world textures may appear to be equally abstract. Ineffective training transfer may be realized when the pilot returns to the real world and must develop his reactions with the real-world textures just as he had to do with the abstract.

Conclusion

The effort to develop new primitives for CIG scene detail has been fruitful. The ellipsoidal features and surface-map texture have significant areas of application in which they are more efficient and more effective than edges in contributing to training requirements.

Just as has been true with edges, there will be a period in which experimentation and exploration of a variety of approaches helps determine the best way to use these new tools. They are currently being designed into operational systems.

It cannot be said that all CIG needs are now met, or that all primitives of value have been discovered. Continuing effort is expected to lead to additional types of features which will further enhance the value of CIG to a variety of training activities.

Acknowledgement

The major portion of the development of the capability for simulating circular, elliptical, spherical, and ellipsoidal features was performed under Contract No. F33615-76-C-0038, for Advanced Systems Division, Air Force Human Resources Laboratory, Wright-Patterson Air Force Base, Ohio. The work was done under the direction of Capt. Michael L. Ingalls of the Simulation Techniques Branch.

References

1. Gibson, James J., The Perception of the Visual World, Houghton Mifflin Company, Boston, 1951.

Dr. Ron Swallow, HumRRO
Roscoe Goodwin and Rudolph Draudin, ATS
Roselle, New Jersey 07203

Introduction

In preparing this paper several important considerations became immediately evident. We recognized that we could not do justice in describing our CGI development within the time constraints of the technical sessions nor the page limitation of the published proceedings. Thus we have elected to describe the basic elements of our design: what makes it different from conventional systems and what new capabilities it offers. We will highlight the most asked for features in the hope that it will satisfy the interests of the audience majority.

Background

For those not acquainted with Advanced Technology Systems, please permit a slight digression. We are an operating division of The Austin Company, an organization of engineers, designers, and builders established in 1878 and operating coast-to-coast in the United States and 11 foreign companies. Advanced Technology Systems was organized as the Special Devices Division to handle classified Research and Development projects and has been devoted to the advancement of the state-of-the-art of visual simulation since its founding in 1943. Our credits include:

- A Torpedo Attack Trainer which features the first spherical domed visual system of the simulated world environment in which the trainee maneuvered.

- Every Submarine Periscope Training System used by the U.S. Navy. Many now include our 40:1 diffraction limited zoom lens which revolutionized the performance of our Submarine Periscope View Simulator.

Early CGI Developments

Our first Computer Image Generator was a nighttime system for the simulation of harbor navigation. ATS designed and developed a color, nighttime, dynamic CGI system which provided a 360° view capability with simulated own ship speeds up to 60 knots. The system had 300 point lights, some of which were hooded to permit viewing to a restricted FOV. The simulated buoy lights blink at controllable rates which permits the maneuver into and out of a simulated harbor.

This early system also simulated aircraft flight providing maneuverability for takeoff, landing, and airborne maneuvers. Recognizing the inadequacies of current daytime CGI techniques, ATS embarked upon the development of the COMPUTROL Day/Dusk/Night Image Display and Control System.

The goal of this development was increased capability for the real time manipulation of perspective views of three-dimensional objects. The resulting system design will be capable of generating enhanced detail for terrain, cultural features, and moving target models while also displaying such special effects as contrails, weapon impacts, and transparencies.

Upon becoming acquainted with the accomplishments of the Human Resources Research Organization's (HumRRO) CHARGE System, the two organizations decided to combine Technical and Financial Resources for the fulfillment of common goals.

The CHARGE (Color Half-tone Area Graphics Environment) System, part of a HumRRO study conducted in 1971 and 1972, addressed Computer Aided Instruction (CAI) techniques. The purpose was to develop specifications for a total CAI system with components that included hardware, software, lesson plans, and instructional decision models.

Image generation techniques were first modeled in software so that alternative algorithms and hardware architectures could be studied, simulated, and verified before committing image generation functions to hardware. The resultant hardware/software design exceeded expectations, rivaling in sophistication and performance any CGI system then on the market.

As a result of a continuing effort in the study of image generation techniques, ATS/HumRRO has evolved the basis for the current advanced design. While committing certain image generation functions to hardware to achieve an order of magnitude increase in processing capability, the system still retains immense versatility both in hardware and software flexibility. The main advantage is that it can handle more edges in real time at less cost. Any additional or new image generation algorithms can be incorporated since algorithms are not completely frozen into special purpose hardware.

The COMPUTROL* system is a special purpose design and does not use general purpose hardware other than standard peripheral equipment such as magnetic tape or disc units. The special design includes a CPU which may be utilized to facilitate implementation of new computational algorithms and to support further CGI development.

The slides we will project illustrate COMPUTROL's* image processing capability. These photographs have been taken from a standard 15" 525 line TV monitor that has been modified by increasing the bandwidth of the video amplifiers by a factor of five and the vertical "resolution" to 1200 lines by a means of a 5:1 interlace.

- Dulles terminal, as viewed from the cockpit window of a taxiing aircraft consists of 2,162 edges.

- The simulated view of a CONCORDE in the landing configuration consists of 910 edges. Color shading capability may be appreciated by a close examination of the fuselage. Motion of control surfaces (wheels, nose section, flaps, etc.) is updated in each new TV frame.

*Registered Trademark.

- . The dining room scene consists of 9,125 edges and is representative of the detail possible with the 16,000 edge early development system.
- . The simulated chair cushion consists of 400 edges and is presented as an example of the shading and texture representation possible with only edge description.

Design Capabilities

COMPUTROL uses a numerically stored model and data on the real world to generate "out the window" visual scenes. All objects in the data base are modeled in three dimensions so that the observer can move about at will, throughout the playing area, with no restriction on movement, direction, altitude, or velocity.

Features of aircraft or other vehicles (targets) will be of sufficient detail as to be visually identifiable at a range equal to the range in real life. As range decreases the motion of control surfaces will become visible. These surfaces will move as if they were actually controlling the motion of the aircraft.

The COMPUTROL is designed to interface with multiple terminals. The terminal screen will act as a window into a three-dimensional world containing representations of:

- . Physical objects
- . Symbols
- . Graphic Images
- . Surfaces
- . Physical events

The representations in this 3D world may:

- . be solid, liquid, or gas
- . have any color, brightness, sheen, transparency
- . be point light sources
- . have any location, orientation, scaling, and magnification
- . have any shape

All parameters in the definition of the world and all parameters in the specification of the "window" into that world may be dynamic in real time. Allowed functions of time or of user input include:

- . Polynomial functions, i.e., constant velocity, constant acceleration, etc.
- . Analytical functions such as sine (kt), square root (kt), e^{kt} , log (kt), 1/log (kt), etc.
- . Numerical functions
- . Arbitrary space/time trajectories

Object/objects interactions include:

- . Illumination shading of object surfaces
- . Collision dynamics (i.e., collision detection and conservation of momentum and energy)
- . Object lock-on (i.e., two objects colliding will stick together during and following trajectory -- useful when one of the objects is under the control of a hand or joystick input device)
- . Planar scalping and "window" clipping (i.e. selective cross-sectioning of subsets of objects)

The image generation capability of COMPUTROL will:

- . Display up to 30K edges in any single channel or throughout a wide angle FOV. Edges may be utilized to model point light sources, ellipsoidal surfaces, etc.
- . Provide up to 1,000 "X" intercepts/scanline. 2K, 3K, etc. intercepts may be handled by expansion of hardware buffer size.
- . Within the edge capability, provide for unlimited high resolution targets.
- . Display point light sources.
- . Display ellipsoidal and elliptical objects with capability for smooth and color shading.
- . Be limited only by the mass storage device for those portions of the world outside the FOV.

Basic System Hardware Configuration

The general configuration of the COMPUTROL system consists of essentially three components: Image Generator, Memory/Decoder Units, and Disc Storage Units.

The image generator performs in real time all functions required to generate a perspective view from a compiled world whose unspecified parameters are derived from the user's input devices or from another computer.

The memory/decoder units receive from the image generator the edges representing the selected two-dimensional projection of three-dimensional objects and buffers and decodes the edges for display on the monitor screen. One or more memory/decoders can be assigned to a color monitor.

The disc storage units store the 3D definition of objects and surfaces comprising the data base gaming area. This representation of the real world is logically segmented into related object sets so that a "user" may roam through a world, not all of which can be held in the image generator's main memory at once.

The image generator consists of two parallel processors: the projection processor and the visible surface processor. Each processor consists of custom designed high speed controllers and arithmetic units which communicate with a specially designed high speed CPU and main memory.

CPU

Initially, the architecture of the CPU was designed with the intent that image generation be accomplished utilizing a high speed CPU in combination with a high speed arithmetic unit. Further study, however, indicated that by putting more of the image generation work into special purpose subsystems, an enormous increase in speed could be realized. Thus, the major workload of image generation has been moved into the special purpose subsystems and placed under the control of the CPU. Its high speed architecture has been retained not only to provide the speed necessary to control the arithmetic and special circuitry, but also to provide the versatility for further system growth.

This growth capability accommodates further research and development by permitting the simulation of additional features.

The ability to permit host computer functions to reside in the CPU may also be accommodated. This ability may be useful to permit stand-alone applications, to relieve the host computer of its workload, or even to provide look ahead computations to enhance image generator output.

Physical Characteristics

The development CGI system, exclusive of displays and input terminal, is housed in four vertical, joined cabinets suitably finished and covered. Cable access is from the rear and circuit board access is from the front.

One cabinet contains the wire wrap logic boards for all CPU, processing, controller, cache, and interface functions required for the projection and visible surface image generators.

The second and third cabinet similar to the first houses main memory (MOS) mounted on PC cards, interconnected via edge connectors, mounted on a "mother board" chassis, and two dual disc drives. Blowers and power supplies are distributed in the fourth cabinet to support system requirements. A basic control panel is also included.

Functional Operation of the CGI System

In the time allotted for this presentation, we can best address the system components and their functional duties within the CGI. The components, of course, operate on digital data and we can start by describing information entry by the author language.

The author language is divided into an atom language, and an object/world language. The atom language permits the creation of "primitive" objects out of xyz data, such primitive objects being termed atoms. The object/world language permits the modification or building of more complex objects/worlds out of other objects and atoms.

Worlds, objects, and atoms, portions thereof and operations thereupon, may be given symbolic names (labels) for their construction and manipulation.

The basic library contains standard two and three dimensional atoms, such as cubes, spheres, cylinders, wedges, circles, squares, and triangles. Special atoms are created for such items as an airplane aileron when it cannot be adequately represented by combining standard shapes. Once created, the atom is added to the library and is available for use wherever needed. The atoms are created in one or more of the following ways:

- . By polygon input method
- . By contour input method
- . From other sets of points by interactive and/or analytical techniques
- . By modification of another atom, its points, contours, etc.

Additional capabilities are techniques to warp, bend, and cut. Logical functions between atoms (volume common to two atoms defines a third atom, etc.) along with parametric specifications of an atom are also included.

Objects or worlds may be created by assembling them out of transformations of one or more objects or atoms. Allowable transformations on objects are:

Translation (move in xyz)

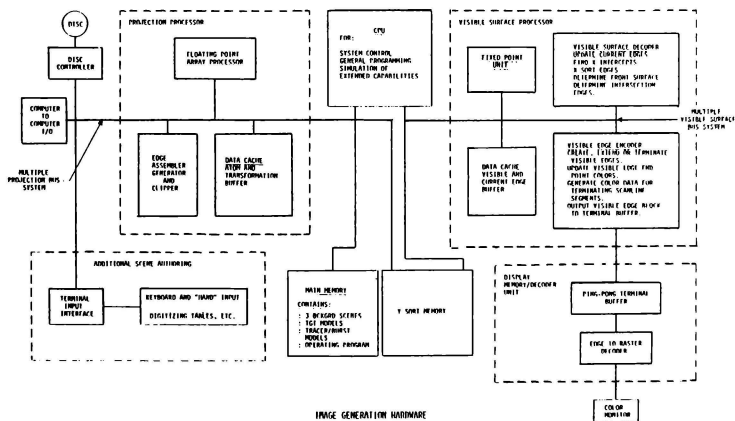


Figure 1

- . Rotation (about xyz)
- . Size scaling
- . Surface or point recoloring (the color within a surface is a linear interpolation from the color at the edges defining the surface)

Image Handling

An image is encoded by a set of edges. An edge is a real or an imaginary line to the right of which is displayed a color. The data word which defines an edge contains such characteristics as color, hue, saturation, brightness, and magnitude in xyz space. There are many atoms which could be described, but let us explore the cube as an example.

A polygon of arbitrary shape and color is represented by these edges. Figure 2 depicts a perspective of a cube represented by nine edges. Because the color may vary linearly along edges bounding the polygon and linearly in x between edges, a polygon can also represent a portion of a curved surface. By means of these polygons, both flat and curved surfaces can be represented in any illumination environment.

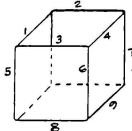


Figure 2

When objects are occluded by other objects, new edges are created called "intersection edges". These intersection edges are created in real time and do not reduce the basic 30K edge capability of the system. They are, therefore, not counted as additional visible edges.

We foresee that a later generation of COMPUTROL will provide the capability of computing 60K potentially visible object edges (depending on the requirement for texture) and displaying them in any single window or combination of windows throughout the FOV.

Data Input

Data entry sequence is used by the modeler to create and manipulate descriptions of two and three dimensional objects and display real time perspective views of these objects at his monitor. The major software components involved in managing the data are described below.

Operating System

The monitor program handles all physical input/output requirements of the CGI software. These input/output devices include:

- . Visual display channels
- . Mass storage disc drives and controllers
- . Card reader/punch
- . Printer
- . Teletype
- . Alphanumeric CGI and keyboard

- . Digitizing tablet
- . Operator's monitor
- . Link with the host computer

The mass storage discs are arranged into libraries and entries within libraries. A library is generally a logically related collection of entries such as object codes for programs, atom descriptions and compiler output listings to be printed or displayed via CRT, etc. Libraries and entries may be created, deleted, or modified either under program control or under user control via interactive commands. There is no restriction upon the number or size of disc libraries permitted other than the physical restriction of disc storage size. A library may contain either fixed length data block entries for random access or variable length data.

Using the CGI system to advantage, the programmer may do such things as:

- . delete an entry from a library
- . delete an entire library from a disc
- . copy an entry from one library to another
- . copy a library of entries to another disc
- . rename an entry or library
- . merge two libraries together
- . copy an entry or entire library to another medium, e.g. card punch or printer
- . load a library from another medium, e.g. card reader
- . list the names of library entries, libraries on a disc or discs currently on the system.

Text Editor

The text editor allows a user to create, update and store text in a general form. Each collection of text is stored by name in a disc library and may be retrieved at any time for subsequent inspection or modification. While the text may be any arbitrary sequence of symbols in general, more specifically it will be used to contain the descriptions or atoms and objects created by a modeler. This text may be initially entered by using a keyboard and CRT terminal, by using a card reader as input or by using an interactive digitizing tablet program which generates text as its output. The modeler specifies point coordinate locations and point linkages, with the program generating the modeling language statements as if the modeler had typed these statements directly. Thus, subsequent keyboard modifications to the data, such as the appending of comments or other features, are permitted, regardless of the original source of the input text.

Atom Compiler

The atom compiler processes a user's text description of the three-dimensional structure of an atom and generates an encoded description of the atom for subsequent processing by the image generator. The resultant compiled atom is stored by name in a disc library for later use in constructing objects. As delivered, the system library will contain a wide assortment of atoms reflecting geometric shapes and other special shapes encountered in modeling the data base. There is no limit imposed by the CGI hardware design on how many additional atoms and objects can be defined by the

user. Optionally, a listing file is produced by the compiler containing the source input statements, a sorted cross referenced list of all mnemonic names used in the atom description text and error diagnostic messages if errors were encountered during compilation. This listing file may be examined on-line using the text editor, printed on a hard copy device, retained on disc for later reference or deleted from its listing library.

Object Compiler

The object compiler processes text describing a collection of previously defined atoms and objects and creates one or more new, more complex objects from them. The input text identifies a set of atoms and objects by their names and specifies such things as the color, size, and location of each with respect to the others. The resultant compiled object is stored by name in the specified disc library for subsequent viewing or use in constructing other objects. As with the atom compilation process, a listing may be produced by the object compiler.

World Compiler

The world compiler prepares a group of objects for processing by the image generator. A world consists of an object and a set of viewing parameters. The viewing parameters define such things as the color and brightness of the background area, the location and brightness of the sun and so forth. The world compiler is also responsible for segmenting large logically related sets of objects into "sub-worlds" and organizing linkages among these various sub-worlds so that a user may "roam" through the world, not all of which can be held in the image generator's main memory at once. The compilation process is in no way sensitive to the number of image generator channels to be used in displaying the world.

Image Generator Control

The image generator control software controls the operation of the various image generation hardware units. It first performs parameter substitution of all numeric parameters of a given world which were left unspecified at compilation time. These parameters are supplied by the modeler's control devices or by the digital computation system, whichever is controlling the image generator. After parameter substitution the resultant compiler world is treated as a command list which causes the image generator control program to command the individual special purpose hardware units to transform the data list portion of the compiled world into a set of projected edges in the user's CRT screen domain. Finally, the projected edges are transformed into visible edges by commanding the arithmetic units of the visible surface processor.

The modeler user creates his world from atoms and objects as detailed in the preceding paragraphs. He combines objects and atoms to make other objects and scenes. This is done in the coordinates of a "scratch" world so that he can monitor his progress without the distraction of other objects which might occult the object being

worked on. When complete, the objects are given real world coordinates and orientation to place them properly in the playing area data base. It is also possible to remove any object from the data base to the scratch world for making modifications or corrections.

Atom Library

The library of "standard faces, objects, and models" which comprise the atoms and objects of the ATS author language has been illustrated in Figure 3. The ability to generate new atoms and objects is only limited by the modeler's imagination. The various methods of constructing the basic shapes have already been described with illustrations of the variations possible shown in Figure 4. These atoms were specially developed to conform to the real world atoms of the Dulles Airport complex.

In Figure 5 we model a car. A basic car "cube" atom has been extended and flattened to represent the car body. A similar atom is added to represent the top. Other modifications of the basic shape produces a car image with recognizable detail. The modifications may be reformulated until the car has the fidelity of an artist's rendering of a car.

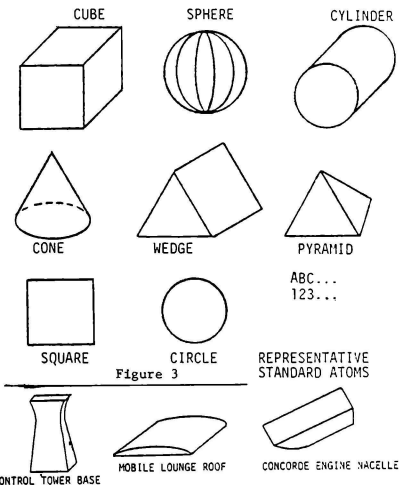


Figure 3

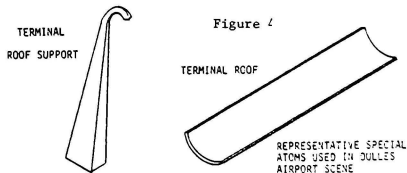


Figure 4

1. Body
2. Partial Top
3. Completed Top
4. Wheels & Hubcaps
5. Grille & Headlights

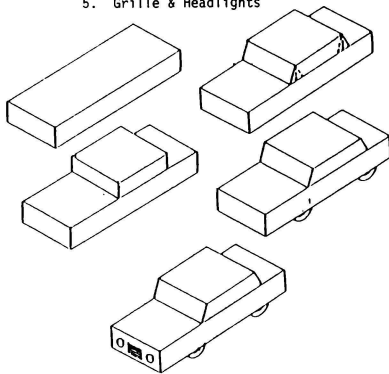


Figure 5 . Authoring a Car

CGI Operators Station

The primary work station for the modeler is at the location of the monitor and keyboard. Since modeling is done during off-line periods, the teletype and CRT will be shared between the CGI and the simulation computing systems. Normally the keyboard is used to input new data or to make changes to the existing library. The CRT is used to monitor progress by displaying source text from the text editor program. The operator's monitor is used to view the completed atom, object, or world and can be commanded to display the scene from any vantage point and viewing direction. If a single object is of interest, a single command will show it centered in the field of view and sized to fill the screen.

Hard copy output from the text editor showing all the author inputs will be available on the teletype or line printer.

CGI Operators Manual

The CGI Operators Manual will be organized into four major sections: General Description, System Operation, User Commands, and Modeling Rules. The General Description will describe the purpose, scope, intended usage, and capabilities and limitations of the CGI. The System Operation will describe the system turn-on/check out procedure and will provide the procedures for routine, emergency, and manual operation of the CGI. User Command section will contain all commands required for the creation, compilation, and modification of images. All user commands will be segregated by compiler level (atom, object, or world) and will be alpha-numerically sequenced based on the command acronym. Each command will be provided with supporting text describing the command syntax, function, a description of output, user oriented notes, and, if necessary, applications. The Modeling Rules section will describe rules for the genera-

tion, modification, or edit of the CGI environment data base. This section will relate the interaction between compilers (atom, object, world), their usage, and relationship in compiling a real world scenario.

Occultation

For any given viewpoint, the CGI system will generate the appropriate perspective scene of the symbolic world, eliminating all hidden lines and resolving all conflicts between overlapping surfaces. As conflicts between overlapping surfaces are resolved, intersection edges are created for display of proper occultation relationships.

Curved Object Simulations

The CGI system provides realistic curved object simulation by assigning color to vertices and linearly varying the color between the vertices and along the scanline between edge intersections. Color interpolation solutions are performed in parallel with the decoding of edges and do not affect the linear geometric processing or display capability of the image generator.

Color

The CGI system generates images coded in nine bits for each of the red, green, and blue channels of the TV display. This corresponds to 512 intensity levels for any color. The data base is stored by specifying for each object its color in the visible spectrum.

Programmable Field of View

The field of view for each of the windows is completely programmable. Thus, for any given window the FOV need not be defined as that required to completely fill the window but instead can be that FOV defined by any portion of the window. This is possible since the window/clipping parameters are programmable and can be altered or varied as described.

System Overload

Overloads, caused by excessive edge capacity in a computed scene, is eliminated by employing frame to frame coherence monitoring. This type of monitoring senses the number of visible edges in a scene and utilizes this number to cause logical simplifications of the world when overload conditions are approached. Thus, if the number of visible edges in the FOV approaches the limit during a frame solution, certain objects will be simplified to assure maintaining the edge count below the maximum capable of display by the system.

If, despite the logical detection and subsequent object simplification an overload does occur, the system design is such that the solution is completed while the last solution is used to refresh the display. With this approach, an overload will not cause picture disintegration, but will merely cause a momentary and slight delay. The frame to frame coherence will prevent this overload condition from persisting and of course will minimize the probability of its occurrence.

Point Lights

The CGI system permits the display of a minimum of 10,000 colored point light sources. Lights can be modeled whose intensity is constant or varies in accordance with slant range and time (blinking). There are no restrictions on placement.

Perspective Lights

Perspective lights are modeled individually by the author language. Several different types of perspective lights are possible, including omni-directional, such as taxiway lights and directional, such as VASI lights. In addition, a certain number of the perspective lights can be designated as light emitting. These will emit colored light with appropriate color mixing and surface absorption as observed in a real physical environment (a blue object illuminated by a red light will appear black). The directional lights are modeled with hoods such that the cone of visibility may be specified.

Aerial Perspective

"Aerial perspective" is an important ingredient in any visual presentation. A certain amount of visibility-limiting haze or fog almost always exists, so that a scene without it lacks realism. It provides an additional altitude cue by causing the horizon to seem lower as the pilot goes higher, and is a factor in his ability to judge the range of targets within the blanket of haze. The fog blanket also provides a hiding place for ground, or low flying, targets and so is essential in combat simulation situations.

The visibility restriction is simulated as a low-lying layer of haze, fog, or smoke. It is densest at ground level and thins out with height. The operator selects the thickness of the layer as well as the density at ground level. The CGI system computes the visibility and observed color of each component of the data base as a function of the altitudes of the object and the observer, and the slant distance between them.

Moving Model Simulation

The CGI system puts no limit on the number of items in the data base that can be dynamic. Likewise, there is no restriction on the degrees of freedom of this motion. Any part of an object can be addressed separately so that incremental movements are also simple, that is, an aileron will move with the airplane but also rotate about its hinge line.

Texture

To provide surfaces with a realistic textured appearance, it is necessary to display the texture pattern with the same perspective processing applied to object or polygon edges. There is, therefore, a need to obtain a perspective of each discernable "characteristic" of a texture pattern. It is appropriate that each "characteristic" be represented and processed so as to contain all the features inherent in edge representation (perspective, size, brightness, occultation, etc.)

Clouds

The CGI system provides for operator selection of cloud condition ranging from overcast to clear skies. The bottom of clouds can be placed at any height above ground level while cloud tops can be at any altitude above the bottoms.

Clouds are treated as objects and are able to be placed where needed and given appropriate motions, with appropriate shape and size functions of time. Solid cloud covers and scud clouds are, therefore, modeled in the data base.

Sun Simulation

The sun's glare and horizon glow is modeled by a two-dimensional model at infinity. Since shading of all objects is computed at execution time, the location of the sun can be dynamic. It can thus be updated every "frame" along with its effects upon the shading of the world.

When the sun is masked by clouds, it results in a diffuse illumination of the world. This kind of light source, which is not truly directional is handled by altering the brightness fall-off function from an angle defining the direction of the light source and the direction of the surface. The fall-off function is a slower fall-off function than normally encountered with a point light source at infinity.

Summary

In recent years, we have come to realize that physiological motion cues are but one part of a total simulation experience. It must be augmented by the "visual" cue which appears to have become accepted as the more important aspect of the two. In the past, we have seen a transition of Visual System techniques from Film Projection to Terrain Model Boards with current enthusiasm for Computer Generated Image Systems. In the competitive struggle for increased realism, the COMPUTROL Computer Generated Image System has come of age due to its ability to dynamically change scene content in real time. Not only is there freedom of eye movement around a particular CGI model, but also the capability to effect a "complete" change of gaming area in reasonable time. The goal of our Research and Development efforts has been to incorporate current "chip" technology, resulting in a new computer design capable of high speed data handling. The objective was to create a full color raster scan simulation of a three dimensional real world. We recognized that the product of our Research and Development efforts should match the following criteria.

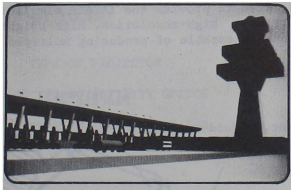
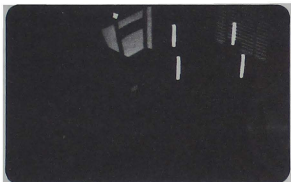
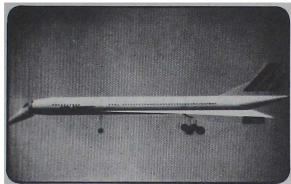
1. Resolution and fidelity of the final scene should closely equate to that of optical or high quality film systems.
2. Inherent capability to quickly change entire gaming areas.
3. Gaming area size sufficient to permit extended flight simulation without reaching the limit of stored data.

4. High speed computation to permit dynamic movement of objects within the displayed scene, e.g. moving vehicle (land, sea, or airborne).
5. System design sophistication to permit miniaturization of the entire system.
6. Minimal power requirements for economical operation.
7. Reasonable purchase price and cost of ownership. Affordable by a majority of customers.

We feel confident that our research efforts have met these 7 basic criteria. A 16,000 edge full color static demonstrator has been developed. Capability to generate high definition pictures with variable sun angle, smooth shading, and the occultation of hidden surfaces has been proven. Occulting of objects through the visible edge solution guarantees non-bleed through of hidden lines. Another feature of the COMPUTROL system is the ability to portray transparent objects which provides much improved realism within the scene. Windows look like windows rather than holes in buildings. The transition to and from clouds is also much more convincing. System architecture and special algorithms are used to permit the incorporation of texturing with respect to trees, grass, clouds, and water. The key ingredient of the system design is the "atom" philosophy of geometric forms used as building blocks for the total scene model. The basic forms are stretched, squashed, lengthened and/or added to other geometric forms to develop a particular scene. The modeling and use of atoms is performed in the off-line mode where there is the ability to generate and modify scenes as well as to edit and assemble programs. With the exception of flight data or any other vehicle interface which is resident within a simulator "host computer", the visual system is a self-contained digital image generator with bulk storage of specific geographic areas. The current design has the capability of displaying 30,000 edges. The surfaces can be planar, or spherical due to the systems' ability to smooth-shade curved surfaces. There is virtually no limit to the number of edges that can be contained within the gaming area data base. The special purpose CPU used with the image generation system has been especially developed to provide the computational speed necessary within the total system. Risk normally associated with specially designed computer systems has been substantially reduced due to the use of standard MOS chips and straight-forward computer architecture. The resulting CGI technology promises to set the standard for visual simulators for many years to come.

COMPUTROL

A COMPUTER GENERATED DAY • DUSK • NIGHT IMAGE DISPLAY AND CONTROL SYSTEM



The technology to produce a Day-Night-Dusk COMPUTER GENERATED IMAGE DISPLAY SYSTEM with full color, smoothly rounded curves, and infinite texturing has been developed. This system represents a genuine breakthrough in the state-of-the-art, in that the quality of the picture far exceeds all currently available systems.

The outstanding features of the Advanced Technology Systems' COMPUTROL are:

- A full color, day-dusk-night picture including blue lights.

- The ability to display 30,000 edges or 7,500 light points at a given time.

- Ease of generating a new picture, i.e. a new airport can be programmed in one working day. Its ability to drive additional, independently controlled displays.

- Realistic special effects such as horizon glow, variable cloud cover, variable visibility, correct sun angle, moving traffic and lights whose intensity varies with slant angle.

- No blooming of lights.

- Independent control of lighting for at least two objects per scene.

- Realistic attenuation of intensity with distance — no lightpoint "piling".

- Realistic "fog" presentation without "curtain" effect.

- Independent aircraft left / nose / right landing light simulation, with each light presenting a parabolic light pattern on the runway surface.

- Stable display — free from "swimming", "waver", and "whip" effects.

- Tapered horizon glow, above and below clouds.

- Adequate horizontal field of view (48° per window). Added windows increase the F.O.V.

- Programmable focus.

- Bright images without saturation or afterglow.

William B. Albery*
George J. Dickison**
Advanced Systems Division
Air Force Human Resources Laboratory
Wright-Patterson AFB, Ohio 45433

ABSTRACT

The Air Force is currently pursuing an advanced development program for the development and demonstration of an advanced Tactical Air (TACAIR) combat visual simulation system technology. The program, called Advanced Tactical Air Combat Simulation, or ATACS, has as its main objective the development of the technology necessary to provide full visual simulation of TACAIR missions, at an affordable cost, suitable for the next generation fighter/attack visual simulators. This paper gives an overview of the objective, approach and payoff of such a program.

INTRODUCTION

Visual simulation technology has developed at a rapid pace in recent years and has advanced to a point where most commercial and some military flying tasks requiring visual interaction can be simulated. However, current visual simulation technology is unable to provide the optimum required simulation capability for visually simulating military TACAIR combat missions in areas such as target resolution, multiple friendly and aggressor targets, color, display brightness, and cues via computer generated imagery. Development of hardware and software to provide increased capability in these areas is necessary for the operating commands (principally USAF Tactical Air Command) to attain greater utilization of simulation in their training programs.

The objective of ATACS is to develop and to demonstrate the technology necessary to provide full visual simulation of TACAIR combat missions, at an affordable cost, suitable for the next generation fighter/attack visual simulators. TACAIR combat missions are those missions involving visual contact for delivery of air-to-surface weapons and visual air-to-air combat.

BACKGROUND

Visual systems with a wide field-of-view (FOV), high image content, and color are desired in aircraft simulators for aircrew training to provide efficient ground based training. The development of the mosaicked in-line, infinity display visual systems, such as those on the Advanced Simulator for Pilot Training (ASPT) and the Simulator for Air-to-Air Combat (SAAC) provided a quantum step forward in the capability for

simulating air combat missions. However, there are certain improvements which would increase their capability to provide effective training for a wide range of tactical air combat/missions. Specific areas where improvements are required include multiple targets in the air-to-air mode for realistic 2 vs 1 and 2 vs 2 aerial combat, high resolution of all targets at all ranges, increased detail of the ground plane for air-to-surface missions and multiple targets and color in the ground plane for air-to-surface combat training.

This project builds upon technology already demonstrated in previous advanced development programs such as the ASPT (CIG technology) and the SAAC (mini-raster for high resolution target presentation) and also utilizes the recent exploratory developments sponsored by AFHRL such as the low cost, light weight, holographic, in-line, infinity optical display and the high resolution, high brightness, liquid crystal color projector technology developed under a previous advanced development efforts and CIG image improvement studies under exploratory development efforts. These previous developments have brought forth technology which has great promise of providing relatively low cost, wide field-of-view color imagery with multiple high-resolution moving targets applicable for both air-to-surface and air-to-air tactical training simulation.

APPROACH

The key components which must be developed and integrated to provide the TACAIR simulation capability are: high-resolution, high-brightness color projectors capable of producing multiple high-

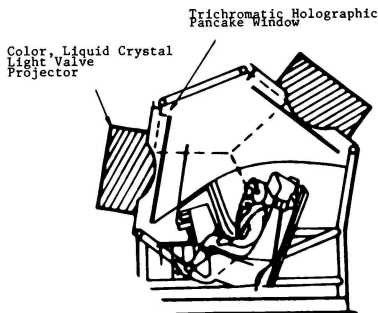


Figure 1. GENERAL ATACS CONFIGURATION. A three channel display system mounted on a dodecahedron

Copyright 1978 W. Albery and G. Dickison with release to AIAA to publish in all forms

*Program Manager, Project 2363, Member AIAA

**Simulation Techniques Branch, Member AIAA
Advanced Development Projects Manager

resolution targets on a color background; in-line, color, infinity optics utilizing a holographic analog of the glass mirror-beamsplitter element for lower cost and weight; and advanced algorithms developed for real-time operation to provide texturing, simulation of terrain contours, and feature generation in the computer generated scene. The general configuration of the ATACS is depicted in Fig 1. The ATACS visual system characteristics are listed in Table 1.

Liquid Crystal Light Valve Projector (LCLVP)

The Hughes LCLVP (Fig 2) is the AFHRL specified approach to satisfy the image input requirements of the project, including high resolution, high brightness color imagery. The Hughes LCLVP currently represents the only apparent technology capable of meeting the demanding requirements imposed by TACAIR needs. AFHRL believes that since the LCLVP is such a rapidly evolving, dynamic technology, that by virtue of its basic simplicity it will result in high availability, low life-cycle cost visual systems. The LCLVP to be employed will be based upon the experience gained with a color LCLV projector recently developed under a separate effort with Hughes. The general layout of the Hughes LCLVP

when packaged and mounted on a dodecahedron type structure is depicted in Figure 3. A side view of the LCLVP and triochromatic holographic pancake window is depicted at the bottom of Figure 3.

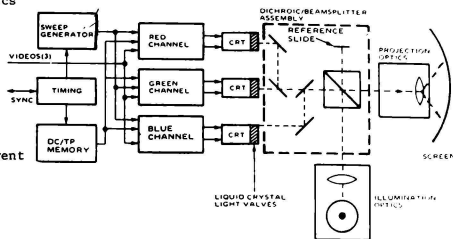


Figure 2. FUNCTIONAL DIAGRAM OF FULL COLOR LIQUID CRYSTAL LIGHT VALVE PROJECTOR, LCLVP

TABLE 1. ATACS FEATURES

TYPE OF DISPLAY	IN-LINE INFINITY OPTICS
COLOR	YES
RESOLUTION	TARGETS, 2 ARC MIN, 1 ARC MIN GOAL BACKGROUND, 4 ARC MIN, 3 ARC MIN GOAL
DISPLAY CONFIGURATION	3 CHANNELS OF DODECAHEDRON EXPANDABLE TO 9
OUTPUT BRIGHTNESS	6 FOOTLAMBERTS
MULTITARGET	YES, 3 HIGH RES MINIRASTERS SIMULTANEOUSLY DISPLAYED
TYPE OF PROJECTOR	HUGHES
TYPE OF INFINITY OPTICS	FARRAND
TYPE OF IMAGE GENERATOR	CONTRACTOR SPECIFIED
	6000 EDGES
	2000 POINT LIGHTS
	1000 ELLIPTICAL FEATURES
	3 MINIRASTERS
	4 MOVING MODELS
	TEXTURE, ELLIPSES
	ACCOMMODATES FUTURE FEATURES
DIGITAL COMPUTATION SYSTEM	MULTICOMPUTER/MULTIPROCESSOR
SYSTEM CONTROL CONSOLE	OPERATING/DBMS CONSOLE
EVALUATOR STATION	GENERIC HIGH PERFORMANCE A/C CKPT

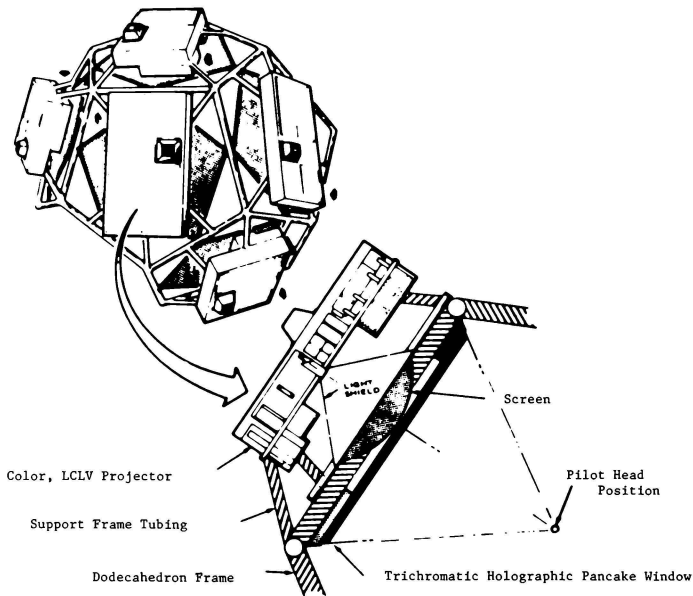


Figure 3. OVERVIEW OF A MULTIPROJECTOR/HOLOGRAPHIC PANCAKE WINDOW VISUAL DISPLAY SYSTEM LIKE THE ATACS

Trichromatic Holographic Pancake Window (TCHPW)

The Farrand TCHPW (Fig 4) is the AFHRL specified approach to satisfy the in-line infinity optics requirements of the ATACS system. Farrand developed the pancake window and installed the all-glass versions in both the ASPT and SAAC simulators. Under Project 1958, AFHRL has developed on a previous effort with Farrand, a holographic pancake window 32" in diameter. This window contains an element which is a hologram of the heavy, expensive glass beamsplitter mirror. When light of the proper wavelength is used to illuminate the hologram, it diffracts the light rays and performs like the glass beamsplitter mirror used as the model. The holographic pancake windows fabricated to date are monochromatic and principally sensitive to a narrow bandwidth of the visible spectrum, (green response holograms). ATACS being a color system, requires holographic windows sensitive to the red, blue and green wavelengths. Therefore a hologram of the beam-splitter mirror must be developed in each primary wavelength. These holograms are then placed together in layers aligned and cemented with the birefringent package to make up the trichromatic holographer pancake window. The fabrication of such a display for the ATACS would be routine

except that the system must be designed around a trichromatic holographic beamsplitter mirror. In order to use these holographic beamsplitter mirrors in a full color display, techniques will be developed to produce them with a spectral response approaching the entire visible spectrum.

Computer Image Generation (CIG)

The CIG system is not contractor specified on the ATACS program although an equal amount of technology risk is assumed in the development of the ATACS CIG system. Originally conceived as just an image input device to the LCLVP/TCHPW channels, the ATACS CIG system has evolved into the third advanced development area of the project. CIG advancements required include generation of special effects as texture, the investigation of new CIG system architectures to reduce cost and hardware, and the investigation of noninterlaced scan in order to eliminate the distractions imposed by dynamic imagery displayed via an interlaced scan. In order to size the system for bidding purposes, 6000 edges, 2000 ellipsoidal features and 1000 point lights are specified. After the CIG data base has been developed, the final edge count of the system will be determined

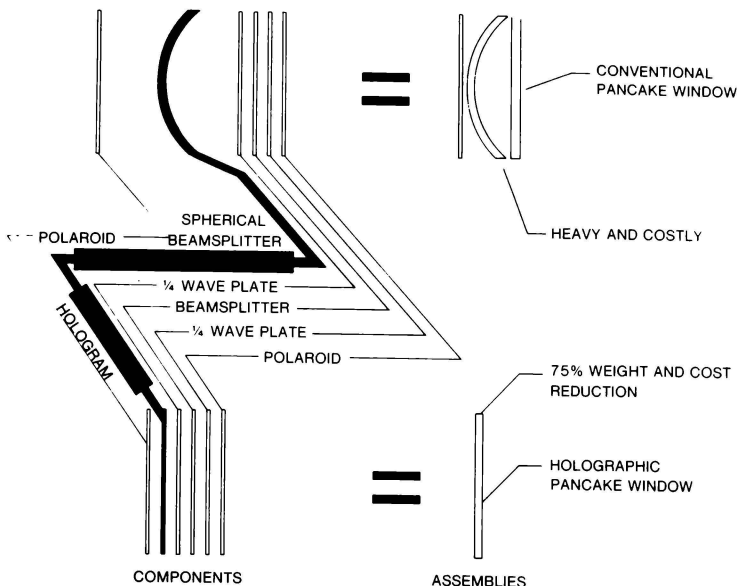


Figure 4. COMPARISON OF ALL-GLASS AND HOLOGRAPHIC PANCAKE WINDOW

based upon the size of the data base required to demonstrate TACAIR combat missions.

Other ATACS Systems

In order to demonstrate and evaluate the ATACS developed visual technology and to perform follow-on engineering and psychophysical studies on the system, the three channel system will be supported by an evaluator's station (simplified cockpit), an operator's station and a digital computer system. These subsystems will be developed in the spirit of support systems and will not function in the sense as a "full mission simulator". AFHRL will be able to demonstrate the ATACS technology via these subsystems, but full mission TACAIR training will not be practical on the delivered ATACS visual simulation system.

TECHNOLOGY ADVANCES

Technology advances of the ATACS will be principally in the visual display and CIG areas. The LCLVP makes it possible to display target controlled high resolution rasters. There is no need for a head slaving or area-of-interest type approach to providing high resolution targets. Multiple high resolution targets can be electronically inset with the Hughes LCLVP. Another

advancement in this program will be the investigation of a noninterlaced scan. Interlaced scan TV systems cause many CIG related undesirable visual effects. Imagery movement perpendicular to the scanlines can appear to separate into parallel bands as if every other scanline were missing. This effect is present in all interlaced television systems and occurs as the eye tracks a surface which moves across the display at a rate of about a one scanline/field. Such an effect could be very distracting to pilots performing rapid air-to-air and air-to-surface maneuvers in a simulator. The noninterlaced scanning requirement will have a significant impact on the electronics driving the LCLVP. Another advancement is high resolution imagery. For the background data 4' and 3' of arc, and for the target data, 2' and 1' of arc resolution at 20 percent MTF have been set as the minimum and design goal resolutions, respectively. Even the minimum required background resolution represents a considerable improvement over the ASPT system while the target resolution of 1' of arc represents a significant advance over the capability of current image input devices.

The trichromatic holographic pancake window represents another significant technology advancement of this program. Perhaps the most risky development item of the ATACS, the TCHPW represents one of the most fruitful products of

the project. The potential payoff is in terms of up to 75% cost and weight savings when compared to the conventional all-glass window. Although green response hologram windows have been fabricated, the blue and red response holograms will present new unknowns such as laser power requirements, photo-sensitization techniques and film sensitivity. In addition, these three holograms must be manufactured to close tolerances on radius of curvature as a function of the wavelength, optical axis and other parameters, so that when assembled they will respond as a single mirror with respect to collimation and magnification.

The third area of technology advancement will be in the CIG system. Not only will CIG technology be pushed in the area of improved imagery, but also CIG system architecture technology will be advanced. AFHRL has been a leader in developing CIG technology. The ASPT was the Air Force's first simulator with a CIG visual system. Such CIG image improvements as "edge smoothing" and "curved-surface shading" were introduced on the ASPT CIG system. This technology advancement will be furthered on the ATACS with the requirement for developing new primitives, or basic CIG building blocks. Image improvement advancements include ellipsoidal features, shading, and texture. Since the Air Force has purchased or intends to purchase a number of CIG visual simulation systems for training, it would be advantageous to keep the cost of these systems down. In an effort to improve the reliability and efficiency of CIG systems while keeping the life-cycle-cost down, AFHRL will also be applying advanced CIG component technology and system architecture on the ATACS program. CIG systems consist primarily of Medium Scale Integration (MSI) integrated circuits and memories and most of these operate at extremely high speed. More reliable, more stable and faster components are required to improve MTBF. Improved CIG system architecture with respect to alternate processor approaches and new component technology will be pursued.

SUMMARY AND CONCLUSIONS

The Advanced Tactical Air Combat Simulation visual simulation system is truly an advanced development program. It represents the only DOD visual simulation research effort directed towards providing the TACAIR requirements for ground based training including presentation of multiple targets, high resolution color imagery and increased ground detail. Since the development of the ASPT in 1975, AFHRL has pushed technology in the three areas of computer image generation (CIG image improvement studies), in-line infinity optics (holographic pancake window) and high brightness, high resolution input devices (liquid-crystal projector). These advanced developments have demonstrated the potential to satisfy the demanding requirements of the TACAIR combat missions in areas such as target resolution, multiple friendly and aggressor targets, color, display brightness and enhanced computer generated imagery. Improvements in visual simulation technology as a result of the ATACS program will provide an effective solution to the TACAIR training needs.

CORRELATED DATA BASES FOR THE PRESENT AND FUTURE

Thomas W. Hoog*
Aeronautical Systems Division
Wright-Patterson Air Force Base, Ohio

Abstract

The paper identifies a problem facing simulator acquisition and production organizations for providing correlated environments for aircrew training. A method for obtaining correlated topographic data bases using present day technology is discussed based on the Defense Mapping Agency data base. Both the source material and data base generation aspects are discussed. Some long range goals are presented along with plans for reaching these goals.

Introduction

Aircrew simulators are becoming more and more complex as Using Commands demand increased performance due to reduced flying hours, lack of real world hostile training environments and safety considerations. The increased performance being demanded in these simulators has resulted in some stiff challenges for the simulation industry, particularly in the functional areas dealing directly with tactics, sensor and visual simulation and coordinated aircrew activities. This paper will discuss the part of the overall simulation problem that deals with topographical data used in the simulation of ground mapping sensors, out the window visual scenes, electronic warfare environments and navigation aids environments. A solution to the problem of maintaining correlation of these functional areas is proposed which emphasizes correlation of data bases at the source.

The Problem

Confusion in the Cockpit

Consider the following situations:

An aircrew is returning to its home base in bad weather to complete a simulator mission. The radar operator advises the pilot that the runway is straight ahead at a range of two nautical miles. The pilot's navigation aids indicate the airfield is just to the right at a range of five nautical miles. The aircraft breaks through the low clouds and the pilot sees the runway lights on his left.

A fighter pilot of a single seat aircraft takes off for an air to ground weapon delivery mission. As he approaches the target area, his ground mapping radar shows fairly rough terrain

and his electronic warfare threat receiver indicates the presence of a hostile radar. As he drops his altitude, the radar display shows the opening in the hills that is the entry point for the low level penetration run. He looks out the window and sees flat plains and the electronic warfare receiver continues to indicate the presence of a hostile radar just beyond the hills shown on the radar display.

These situations may be somewhat exaggerated but they demonstrate what can happen if the radar, visual, electronic warfare and navigational aids environments are modeled independently without regard for each other. The following is representative of the data sources used in a typical modern Air Force Simulator.

A Reason for the Confusion

The radar data base is derived from the Defense Mapping Agency (DMA) Digital Landmass Simulation (DLMS) data base. The simulated threat radars are located per intelligence data. The navigation aids are located per data in the Flight Information Publications (FLIPs). The computer image generation (CIG) visual data base is produced from airfield civil engineering drawings, aerial and ground photographs, and some large scale local area maps.

All these data base sources (DMA DLMS data, maps, photographs, etc) have various accuracies associated with them and each may be referenced to a different datum. Thus, objects that appear in each data base source may have a different horizontal and/or vertical position relative to each of the other sources. Similarly, terrain elevation information is different in these various data base sources. Furthermore, position discrepancies can be inserted through the actual modeling process due to the precision of the final stored data base and the techniques used in the modeling process. Figure 1 illustrates the source data error problem.

Each of these functional area simulations may be adequate by itself, since it can provide the required training environment. However, just as an aircrew is thrust into an integrated real world environment, the simulated environment must also replicate an integrated environment. Otherwise, the aircrew can become confused, frustrated, "turned-off" towards simulators and improperly trained. In the military arena today, this can be critical. The remainder of this paper will discuss an approach to achieving a correlated ground truth environment which can be applied to simulators which involve all or just some of the functional areas mentioned earlier.

*Technical Area Coordinator for Radar Simulation and Data Base, Simulator Systems Program Office
Member AIAA

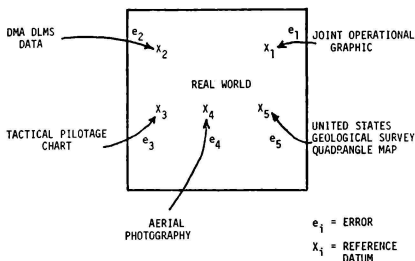


FIG. 1 EXAMPLE OF SOURCE DATA ERROR DIFFERENCES

The Key - Correlation at the Source

Independent Simulation

Simulated environments can become uncorrelated for many reasons--differences in data base source materials, the modeling process and the real time processing associated with the simulation. The real time processing contribution to an uncorrelated environment can be ignored for now, since it normally represents the real world situation with respect to accuracy of the equipment, uncertainty of information presented to the aircrew due to equipment characteristics and precise knowledge of current aircraft position. For example, the radar simulation model must compute object locations and account for such things as radar pulse length error and beamwidth error; the electronic warfare simulation model must compute emitter locations and account for such things as processor and display range and azimuth error. The visual simulation must compute object locations to sufficient fidelity to avoid overlapped objects and proper relative location to provide consistency within the visual scene. Thus, if a correlated environment is presented to the real time processing for each functional area, a correlated environment should be presented to the aircrew.

As discussed earlier, there is no assurance that this correlated environment will be presented to the real time processing subsystems. Before proceeding a more detailed discussion of how the on-line data bases are produced should be presented. The following relates to Figure 2.

Radar Data Base

The on-line radar data base is a set of data that describes the topography in terms of a reflectance code and elevation. The data is formatted into two files, terrain elevation and planimetry, each being addressable in small sized

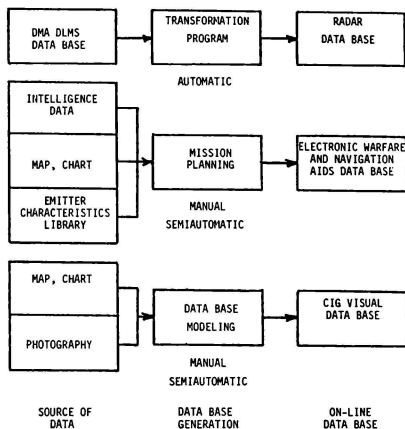


FIG. 2 FUNCTIONAL FLOW FOR DATA BASE GENERATION

blocks representing specific geographic areas. The terrain elevation data may be stored in a variety of ways and the elevation for any geographic location can be determined via an interpolation scheme. The stored data is transformed from the DMA DLMS data base and compressed to the stored format consistent with the reconstruction algorithm. The planimetry data defines the reflectance of objects (buildings, vegetation, ground cover, etc) along with their elevation above terrain. This information is derived from the DMA DLMS data base files through the use of a transformation program. The transformation program is not a part of the real time system, but operates on a DMA computer and is designed to automatically transform data into a useable form for a specific system. The transformation program formats the data for direct loading into the real time system, assigns the reflectance codes based on the radar being simulated and provides additional codes based on the topography for use by the simulation logic. The content of the radar data base is defined by the DLMS production specification, the transformation program requirements and the radar simulation requirements.

Electronic Warfare/Navigation Aids Data Base

The electronic warfare threat and navigation aid data base is normally a list of geographical locations of each emitter and the associated characteristics of that emitter. These emitters are either permanently located in a mission file or are called from a library file and placed along the planned flight path during mission preparation. Electronic warfare threats are often assigned locations, using various maps and charts, during the mission planning phase, thus providing another source of correlation error.

Visual Data Base

The on-line CIG visual data base is a set of data that describes the topography in terms of a color, elevation and a set of coordinates defining the edges of planes. The terrain is treated the same as the planimetry. The data is formatted into addressable blocks representing specific geographic areas. Additional data may be present which identifies the level of detail, non-planar surfaces, point light sources, texture associated with a feature, curved surface shading, etc. This additional data is used by the real time processing to generate the visual scenes. The on-line CIG data base is produced through a largely manual process. There have been some efforts to automatically transform DMA DLMS terrain elevation data as is done for radar. However, the planimetry data base automatic transformation is more complex and has not progressed as far. Planimetry CIG data bases have been created from various maps and charts, aerial and ground photography, personal observations and verbal descriptions of areas to be modeled. The data base modeler digitizes objects from a source on a graphics tablet or light table and, with the aid of computer programs, sorts the data into some logical order. This process is very time consuming and considerable resources are required to model large geographical areas. The modeler must also be sure that the real time processing subsystem capabilities have not been exceeded, for example, too many edges in one area may overload the CIG system. The content of the data base is largely up to the data base modeler and how he uses the various data base source materials available to him.

A New Start

As stated earlier, a correlated environment should be presented to the aircrew if the environment description presented to each of the functional real time processing systems is correlated. This assumes that the simulated equipment (radar, navigation aids, electronic warfare) correctly emulates the actual aircraft equipment and the visual simulation image generation and display is highly accurate. It was also noted earlier that the modeling processes and specific sources of data base information can vary widely. A key to obtaining a correlated on-line environment is to start with correlated information. However, since the modeling processes can also insert considerable variations, there must also be some control placed on them.

There are several problems/issues which must be considered in determining what data base source(s) should be used. The Air Force has a requirement to simulate the environment of many parts of the world. There are also requirements to simulate missions over large areas, e.g., 40,000 square nautical miles for the C-130 including visual, several million square nautical miles for the B-52, etc. Often times a visual system is only used during specific portions of a mission, i.e., takeoff and landing. Even if a local reference system is used for two different airfields, the ground mapping radar would be used continuously as would the navigation aids. Thus, the coordinate reference system must accommodate the requirements for large continuous gaming areas for any part of the world. The content of the radar data base is defined since the DMA DLMS data base is specified

for use. The content of the visual data base is often left to the individual modeler. Thus, features which are significant in both the radar and visual domain may not be represented in both on-line data bases. To compound this, additional variations can be inserted through the local data base modifications generated at individual operating sites. It is also recognized that simplifications can occur when the visual data base modeler intentionally modifies a feature or several features due to CIG image generation limitations, i.e., edge crossings per raster scan line, number of edges in a scene, etc. This type of simplification is normally not necessary in a radar data base since the radar processing has a much grosser resolution and can resolve conflicts within a much larger processing interval (depending on radar pulse length and display resolution). Thus, there must be some control for the content of on-line data bases. The method(s) chosen for creating on-line data bases must be flexible enough to allow for state-of-the-art advances in simulation technology and allow for higher fidelity simulation due to improved aircraft equipments, e.g. higher resolution radars.

Two questions that are very important are -- What is the minimum data base content required for satisfactory training; and, how much needs to be correlated? Until these questions are answered, the methods used to create on-line data bases must remain flexible.

Based on experience to date, there is a good chance current procedures will not assure that data bases are correlated. The following is a discussion of a method for creating correlated data bases that is built around the DMA DLMS data base.

A Solution A Common Ground Truth Data Base Source

The DMA DLMS Data Base

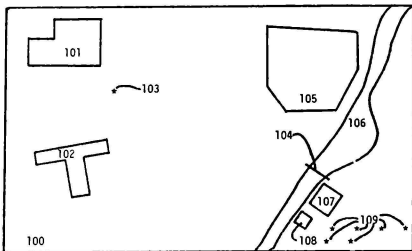
The DMA DLMS data base is a source of ground truth information with extensive coverage. Current plans call for initial coverage of 18 million square nautical miles before 1990. Since the basis for creating correlated data bases is the DLMS data base, a brief description will be provided.

The DMA DLMS data base consists of two files -- the terrain elevation file and the planimetry file. Each file can be used separately or they can be used together. The vertical datum is mean sea level and horizontal datum is the World Geodetic System, 1972 (WGS 72), i.e., an earth centered reference.

The terrain elevation file is a matrix of elevation values with a spacing of three seconds of arc in latitude and longitude. The longitude spacing increases to 6 seconds at 50 degrees latitude, 9 seconds at 70 degrees, 12 seconds at 75 degrees and 18 seconds at 80 degrees, in an attempt to maintain an approximately square matrix. Data is stored in one degree by one degree squares.

The planimetry file describes the content of the earth's surface. This file contains two basic levels of information, i.e., resolution levels, compilation levels, etc., based on the size and separation of objects. The file describes objects as areal, linear or point features depending on

their shape and size. Each feature is also described by its predominant surface material, height above terrain, its identification and other characteristics depending on its type. Figure 3 is an example of several features. Level 1 data (the coarsest level) is provided over the entire area. Level 2 data (a higher resolution level) is provided only when identified as being required for higher level of detail by a user. This concept was adopted since Level 2 data is about 15 times as costly to produce as Level 1 (the factor actually varies depending on the specific area being produced, i.e., urban versus rural).



NOTE: Additional information can be found in Reference 1

FIG. 3 TYPICAL DMA DLMS PLANIMETRY FILE DESCRIPTION

Advantages and Applications

The advantages of using the DMA DLMS data base are many. It has an earth centered datum making it directly useable anywhere without complex transformations to account for shifts from one local datum to another or projection errors (as is common with maps and charts). By 1990, Level 1 data will cover over 18 million square nautical miles thus providing the most extensive topographic description at that level of data compilation. The data files are expandable to include additional levels (resolutions) of data, additional feature identifications and additional descriptors (this latter change could have significant impact on the data base if major changes were made). Other advantages will be brought out later.

Radar Data Base

The radar simulation application can remain as before, i.e., automatic transformation of the DLMS data files into a useable form. The allowable error criteria for the entire simulation process is a function of the radar characteristics, primarily the pulse length, pulse repetition frequency, antenna scan rate and display characteristics. These overall errors must then be allocated to the transformation program and simulation system.

The DMA DLMS data base need not be used directly in the location of navigation aids and electronic warfare threats. The sources of information for these data can remain as before. However, there must be some assurance that the geographical location of these emitters correlates with data in the DLMS data files. For example, airfield navigation aids must have the same geographical location as the same airfield in the DMA DLMS data base and emitters must be located such that the terrain occulting is correct. A brief check of some navigation aid locations listed in the FLIP charts has shown sufficient agreement with the DLMS planimetry file that correlation should result. Final checks for emitters, particularly the threats associated with electronic warfare environment simulation, should be performed as part of the simulated mission planning/creation effort. Some relatively simple verifications, if necessary, can be performed with a software support program to assure correlation with the radar and/or visual data base.

CIG Visual and Sensor Systems Data Base

For CIG system applications there are two approaches available. The first is to use the Level 1 DMA DLMS data base as a basic source of information for the CIG data base and let it be the reference source for all CIG data base modeling. This is the basic policy being adopted by ASD in the development of CIG data bases. Since the DMA DLMS data base alone is insufficient to support visual and some sensor systems, some enhancements will be required. The sources for these enhancements can be large scale maps, charts, and photographs, i.e., some of the same sources used previously. However, the DMA DLMS Level 1 file is established as the reference. In addition, the Level 2 DLMS data can be used as an additional enhancement data source. This approach will help assure correlation with the radar data base since both will utilize the same data source and it will permit the addition of detail required to support visual simulation.

A more advanced application is to create CIG data bases automatically via a transformation program as is currently done for radar data bases. It must be noted that there are additional complications which must be considered because of the way visual data bases are utilized by the image generation processor. This is primarily due to the limited number of edges that can be generated in each scene, the transition between levels of detail when approaching fixed objects and the need to establish object priorities and occulting data within geographical areas. Another major consideration is the problem of merging the transformed terrain elevation and planimetry CIG data bases since they are separate DMA DLMS data files but treated the same by the CIG image generation processor. For example, checks must be included to assure that hydrographic features do not appear on the slopes of hills, bridges, cross rivers, etc. Even with automatic transformation of the DLMS data base, the CIG data base can be enhanced using other sources.

ASD plans to initiate a program to develop a CIG transformation program and attempt to solve the above noted problems. This program expects to utilize a new level of DMA DLMS data base developed specifically to support CIG visual systems. This will help to crystallize some unknown factors relating to the required content of visual data bases to support various types of air to ground training, the resources required to produce these data bases, the limitations of automatic transformation of the data bases and the amount of enhancement necessary to make them acceptable for training use. Since the new level DLMS data base will be compatible with the existing file structure, it will also be available for use by the radar transformation program thus maintaining correlation of data at the source. Additionally, this new program will address some longer term goals discussed later in this paper.

Some Long Range Goals

Within DOD there have been many discussions about standardizing data bases. There can be advantages to this but more information is needed before any practical methods can be adopted. Some basic questions are: Where do you standardize? How do you prevent stagnation of technology? How can data bases be interchanged since data formats relate to the processing design? How does standardization of one area such as visual data bases affect other areas such as radar data bases? I will not attempt to answer these questions here, but will outline what ASD is doing in an attempt to reduce overall on-line data base production costs, obtain a form of standardization and in the process provide some information pertinent to these questions.

As stated earlier, ASD has adopted the DMA DLMS Level 1 data base as the reference for ground truth topographical data. There is presently a joint ASD-DMA effort to study methods for synthetically breaking up the planimetry file, i.e., use software to create mini-features out of features produced using normal production processes. This can help add information to the data bases. The basic concept is discussed in a paper by Hoog and Stengel presented at the 1977 IMAGE Conference.⁶

Creation of radar data bases is fairly stable and has been demonstrated to work. The DMA DLMS data base is the standard source data. Additional efforts similar to those done for radar data bases are needed in the CIG data base area. ASD has adopted some procedures to promote a form of standardization and to provide some information regarding how to standardize. Contractors who produce simulators with CIG data bases are now required to deliver a contract data item that describes in detail the contents of the delivered data bases. The contents of these data bases could then be used on other contracts thus saving the modeling costs. A growth possibility is to adopt a standard format for these delivered data bases. This format need not necessarily be a normal on-line format since an on-line format can be obtained via a software program. A second thing to be done is to standardize the sources of data used to model geographic areas for CIG data bases. A first step has been taken by specifying Level 1 DMA DLMS data for use. Supplementary data

should have a preferred order for use in the enhancement process. With this approach, some consistency can be retained in the CIG data base content whether it is created via a transformation program and enhanced or modeled manually or semi-automatically. Because of differences in the availability of data sources suitable for use for enhancement, the preferred sources may vary for different parts of the world. If the sources of the initial on-line data base modeling are controlled and individual site updates to delivered data bases are controlled, the data base configuration management system can be used to help assure that data bases remain correlated. With controls such as these, there can be consistency in CIG data bases and correlation with other sensor data bases.

Summary

Because of the increased reliance on simulators in the Air Force's aircrew training programs, it is essential that real world environments be presented to the aircrews. A means of assuring this is to strive for correlation of individual environments at their source. A means of achieving this is to adopt a standard reference source of topographic data and to develop some consistency in the development of on-line data base models. ASD has chosen the DMA DLMS data base as a reference for the following reasons:

- a. The extensive geographic coverage.
- b. A world-wide reference datum.
- c. Expandable to include additional resolution levels.
- d. Adaptable for use with other data sources for enhancement of localized areas.
- e. Reduces the quantity of data sources required to model specified geographical areas.

The content of radar data bases is well defined and controlled. Additional efforts are required to develop the needed control of CIG data bases. Some of these efforts are:

- a. Expand the use of the DMA DLMS data base, including DMA's production of data specifically for CIG systems.
- b. Standardize the type of data sources used for enhancement purposes.
- c. Standardize the format for delivery of CIG data bases developed under each contract.
- d. Establish a library of CIG data bases for use on any CIG system.

The development of automatic transformation methods to create CIG data bases from the DMA DLMS data base will aid in the reduction of costs to create CIG data bases over large areas and will help assure the correlation of environments since a common topographical data source would be used for several purposes.

References

1. Defense Mapping Agency Digital Data Base Description Document, SSP0-07878-9000, Revision A, 10 February 1978.

2. Hoog, Thomas W. and Stengel, John D., Captain, "Computer Image Generation Using The Defense Mapping Agency Digital Data Base", Proceedings of the 1977 IMAGE Conference, 17-18 May 1977.

Frank M. Cardullo*
Senior Staff Engineer
Link Division, Singer Company
Binghamton, New York

Abstract

The problem of providing motion cues for the full crew of a tank simulator has been investigated. The motion cuing requirements were first established based on training objectives, vehicle dynamics and physiological considerations. To satisfy these requirements hardware was configured and evaluated. Several motion cuing devices were considered and trade-off analyses were performed. A drive signal philosophy was developed to provide the appropriate cuing as a function of vehicle dynamics. State-of-the-art drive techniques were employed. The resulting algorithm is presented along with the preferred hardware embodiment.

Introduction

The need for simulators to train the flight crews of aircraft and spacecraft has been well established. This aircraft simulator need has been emphasized in recent years by diminishing fuel supplies. The spacecraft need has been recognized by NASA due to safety and other conditions. However, the recognition of similar needs in the training of crews for other vehicles has come more slowly. This is particularly true of land borne vehicles such as tanks. Part task training aids with low level fidelity have been in use for some time for tank drivers and gunners. But it is only recently that the need for simulators has become evident. As a consequence of this, the state-of-the-art of tank simulators is behind that of aircraft simulators. It follows then that the requirements for these devices is also less developed than for flight simulators.

Since the state-of-the-art of training simulators has been advanced primarily through the development of flight simulators, it is logical then to attempt to apply flight simulation techniques to any less developed training simulator application. The important consideration,

though, is to analyze the application sufficiently to determine the validity of the flight simulator approach in a certain area to another vehicle.

This caveat applies, of course, even to various applications in flight simulators. For example, if a particular single narrow FOV display is sufficient for a take-off and landing flight simulator, it may not necessarily be sufficient for an air-to-air combat simulator.

Therefore, the simulation requirements for the particular training device must first be established in the absence of the existing technology. These requirements must be established considering the vehicle being simulated, the mission for which training will be accomplished, and the fidelity required.

Once these criteria have been established, then the existing technology should be applied where possible. Where the existing technology is inadequate, an economics vs. training value assessment must be made to determine the future course. This methodology is applied to the motion simulation problem herein. In the main, armor training devices have been task trainers, (such as driver trainers). Some of these devices have had motion systems. In general, however, the motion stimulation has been provided with available hardware or hardware that provided "motion sensations".

Analysis

It is the attempt here to systematically arrive at a configuration of cuing hardware to meet the requirements of a simulator for a full tank crew. This is accomplished by analyzing the motion experienced by each crew station; due to locomotion of the vehicle, turret traversing and main gun firing. These motion sensations were then analyzed in light of the training requirements, physiological considerations and drive signal philosophies to arrive at a final configuration.

Determination of Simulation Requirements

The methodology involved accumulating data, consideration of physiological factors and training objectives, and ultimately performing a cue analysis consistent with the foregoing.

*Member AIAA

In order to define the motion environment of crew members, data from several sources were accumulated. These data were derived from accelerometer measurements made at Ft. Knox, Kentucky on an M60A1 tank, tank manufacturer's test results, various published reports and papers, and an analysis of the physics of tank motion.

These data are summarized in Table 1 for the hull and Table 2 for the turret.

A brief discussion of these data is required. Longitudinal acceleration of the hull and turret is due to accelerating from a stop based on maximum tank performance on a paved road as determined by Chrysler data. Deceleration is that which results from brake application (not from impact with an object which obviously could produce greater decelerations). Main gun recoil data is based on either over the front or nearly over the front firing. Accelerations on the hull can be derived for other gun azimuths as a function of the ratio of the moments of inertia and the azimuth angle.

Terrain effects data are generally worst-case for going over bumps. Normal undulating terrain exhibits significantly lower accelerations ($<0.02g$ vertically). Slope operations angles are based on the maximum capabilities of the vehicle. No lateral accelerations were measured or observed due to sloping on sideslope operations.

TABLE 1 M60A1 DATA

HULL	
MANEUVER	PARAMETERS
LONGITUDINAL ACCELERATION	$0.1g, -0.6g$
MAIN GUN RECOIL (long)	$-0.2g$
(pitch)	$+1.0 \text{ rad/sec}^2$
(heave)	$+0.2g$
TERRAIN EFFECTS (heave)	$+1.0g^* f=1.0Hz$
(pitch)	$+0.02 \text{ rad/sec}^2$
	$+0.15 \text{ rad}$
	SLOPE $+0.64 \text{ rad}$
(roll)	SLOPE $+0.30 \text{ rad}$
(lateral)	NONE MEASURED
ENGINE VIBRATION (long)	NO DATA
(heave)	$0.025g @ 30 \text{ Hz}$
(lateral)	NONE MEASURED
TURNING (yaw)	NO DATA
(lateral)	NONE MEASURED
MACHINE GUN VIBRATION	NO DATA
TURRET ROTATION (lateral)	$+0.5g$

*Does not include the effects of bump stop or idler impact. Peaks of 3 to 6g are possible in these cases.

TABLE 2 M60A1 DATA

TURRET		PARAMETERS
MANEUVER		
TURRET ROTATION (yaw)		$+2.15 \text{ rad/sec}^2$
		$+0.392 \text{ rad/sec}$
MAIN GUN RECOIL (long)		$-0.4g$
(pitch)		$+1.0 \text{ rad/sec}^2$
MAIN GUN ELEVATION		$0.025g$
(SAFETY STOP IMPACT)		$0.2g$
LONGITUDINAL ACCELERATION		$0.1g, -0.6g$
TERRAIN EFFECTS (heave)		$+1.0g^* f=1.0 \text{ Hz}$
(pitch)		$+0.02 \text{ rad/sec}$
		$+0.15 \text{ rad}$
(roll)		NO DATA
SLOPE EFFECTS (pitch)		$+0.64 \text{ rad}$
(roll)		$+0.30 \text{ rad}$
ENGINE VIBRATION (long)		$+0.035g @ 5 \text{ Hz}$
		$(<0.01g)^{**}$
		$+0.018g @ 15 \text{ Hz}$
		$(<0.01g)$
(heave)		$+0.11g @ 5 \text{ Hz}$
		$(0.04g)$
		$+0.03g @ 15 \text{ Hz}$
		$(<0.01g)$
(lateral)		$+0.077g @ 5 \text{ Hz}$
		$(0.022g)$
		$+0.028 @ 15 \text{ Hz}$
		$(<0.01g)$
TURNING (yaw)		NO DATA
(lateral)		NONE MEASURED
MACHINE GUN VIBRATION		NO DATA
COAXIAL GUN FIRING		NO DATA

**Average values

Engine vibration data were not recorded longitudinally at the hull; but since the levels (vibration) at the turret in this degree of freedom are low, it can be assumed that they would be low at the hull. The 30 Hz vertical vibration at the turret is assumed to be a harmonic of what is observed at the hull. Higher frequencies resulting from engine vibrations have been recorded, these are harmonics of the lower frequencies and the power spectral density analyses result in such low power spectra that it was felt these should be disregarded at the outset.

No data are available for yaw motion on turning. Also, no lateral acceleration was measured due to turning. Observations of personnel who drove the tanks were that

neither was felt at the driver's station. Occupants of the turret reported some yaw sensations when the tank was turning. It is difficult, however, to determine if this sensation was induced by some other stimuli. Turret rotation effects can produce start/stop transient accelerations of up to 0.5g at the driver's station.

Effects of these data on the motion training problem are discussed subsequently.

Physiological Perception of Motion

In order to fully analyze the motion simulation requirements for any vehicle, it is important to understand how a human perceives motion, i.e. which physiological receptors are affected, how they function, and how they may be stimulated by a simulator motion system.

Motion is perceived by the human body primarily through three physiological receptor systems: the vestibular (non-auditory labyrinth) system, the haptic system, and the visual system. The auditory system also has some effect on the perception of motion but it is probably a second-level effect. That is, the association of certain sounds with past experiences of motion.

In a modern flight simulator, these sensory systems are stimulated by various means. The vestibular system is stimulated by motion systems, vibration systems, and to some extent, G-seat systems (devices for producing sustained acceleration cues). The haptic system is stimulated by G-seat systems, motion systems, anti-G-suit systems, and control feel systems. The visual sensory apparatus is stimulated by both out-the-window visual systems and cockpit instruments. For simulators of other types of vehicles analogs of the above vehicle systems require similar stimuli. These stimuli might be provided by the same types of simulation hardware, for armored vehicle simulation.

The physiology of these various receptor systems has been treated extensively in other works; (1,2,3,4,6,7). Therefore, no discussion is deemed necessary herein.

A discussion of the response characteristics of physiological receptors is required. There has been a significant amount of research done on the thresholds of perception of these receptors. Some of the work dates back to the 19th century. However, the single fact that has become most obvious is that the range of thresholds of the population is fairly large and therefore averages are simply mathe-

matical quantities which do not necessarily fit any individual. However, these averages can be useful tools in a cue coordination analysis. Table 3 presents a compendium of threshold of perception data for the vestibular, and visual systems. These data reflect the results of many studies which attempted to answer this question, however, each study essentially indicated need for further study. These thresholds are difficult to parameterize since they are multi parameter functions. There is a dependence on task loading, ambient conditions such as existing motion, duration and the natural variation among the population.

The frequency response of the vestibular and haptic system are given by Lum to be 0.1 Hz and 2 Hz respectively. Young indicates a 10 Hz response for the semicircular canals, but this is based on a velocity input and approximately 0.1 Hz for the otoliths. The frequency response data are primarily useful for determining the requirements for the simulator which will stimulate these receptors.

Another performance parameter of importance is the adaptation time of these receptors. According to Young, the semicircular canals have an adaptation time of 30 seconds, while the haptic system adapts in approximately 1.0 second. The rapid adaptation characteristics of the haptic system is no doubt why motion systems which use onset cuing philosophy with subliminal washout seem feasible.

One further comment to conclude the discussion of the physiological aspects of motion sensitivity is the effect of the absence of any of these stimuli. For example, if there is no stimulation of the vestibular or haptic systems, and only of the visual apparatus, will the crewman perceive motion correctly? It is thought not. This may be illustrated by the familiar railroad station paradox. That is the situation where a passenger in one railroad train thinks he is moving when he sees the train on an adjacent track move. However, he is confused by this phenomenon because he did not "feel" motion; he only "saw" it. Of course, in this situation there has been no vestibular or haptic stimulation. There are many levels of stimuli which may be considered in this type of discussion and some are far more subtle than the railroad station paradox. Some examples of these areas of uncertainty are: Is it necessary that the organ be stimulated at the correct magnitude or is it sufficient that the direction be correct, or can small components be left out?

TABLE 3 THRESHOLDS OF PERCEPTION

MOTIONSemicircular Canals

0.5°/sec ²	Vertical	MEIRY 1965
0.14°/sec ²	Horizontal	MEIRY 1965
0.2 - 0.5°/sec ²	Z Axis	JOHNSON 1959
0.41°/sec ²	X & Y Axes	STEWART 1970
0.67°/sec ²	Y Axis	STEWART 1970
0.2°/sec ²	Z Axis	TUMARKIN 1937
0.3 - 0.5°/sec ²	All Axes	WENDT 1966
0.12 - 0.15°/sec ²	Z Axis	CLARK & STEWART 1962
0.5°/sec ²	Yaw	GROEN & JONGKEES 1948
0.06 - 0.35°/sec ²	Z Axis	WANN & RAY 1956
0.02 - 0.06°/sec ²	Roll	HOSMAN & VAN DER VAART 1978
0.04 - 0.07°/sec ²	Pitch	HOSMAN & VAN DER VAART 1978

Otoliths

0.005g	All Axes	GUM 1972
0.02 - 0.08g	All Axes	WENDT 1966
0.01 - 0.03g	Z Axis	GURNEE 1934
0.03 - 0.08g	Z Axis	FOGEL 1963
0.08 - 0.13g	X & Y Axes	FOGEL 1963
0.04 - 0.08g	Z Axis	HOSMAN & VAN DER VAART 1978

VISUALFovea

1-2 min/sec	w/Ref	AUBERT 1886
10-20 min/sec	w/o Ref	AUBERT 1886
10 sec/sec -		Injury Research Council
40 min/sec		

Periphery

18 min/sec @ 9°	w/Ref	OGLE 1962
180-360 min/sec	w/o Ref	OGLE 1962

Consider the case of rotation. If the observer is situated some distance from the center of rotation, there is a translational component associated with the rotation proportional to the radius of curvature. Therefore, the vestibular system senses the rotation via the semicircular canals and the translational component via the utricle. Clearly, if the radius of curvature is large, the utricular stimulation is important. However, other factors such as the task loading, the preexisting motion, the dynamics of the control loop, the absence or existence of disturbing influences, etc., are important. This discussion could continue for quite some length, but this is not intended to be a treatise on the perception of motion, but rather a means of illustrating the complexity of the problem.

The foregoing indicates that for any different application, empirical methods should be used to determine which stimuli are necessary.

Motion Cue Analysis and Simulation Philosophy

In a previous section tank kinetics, which influence motion simulation were tabulated and discussed and the motion sensing physiological apparatus was explained. The objective of this section is to evaluate this data in order to establish a motion training requirements and motion simulation philosophy.

Data were tabulated separately for the driver station and the turret, the rationale being; it was considered that cuing requirements could be different for the two stations. This approach did not preclude the possibility of applying the same cuing to both the driver and the occupants of the turret. It became obvious, however, that unless the kinetic relationship between the hull and the turret could be maintained, separate cue sources would be required. The imposition of this requirement emanates from two major considerations:

- 1) The turret, being suspended within the hull, has different mechanical response characteristics than the hull.
- 2) As the turret slews, its occupants sense motion of the hull differently as a function of the turret deviation angle.

The first consideration is supported by the data; the second is a simple statement of fact. The second can be appreciated easily by the following example: consider the situation where a simulated tank is proceeding due north with the main gun pointing due east. Motion cues, which to the driver are sensed as pitch, would be sensed as roll to the occupants of the turret facing in the same direction of the gun. It further follows that longitudinal motion to the driver would be lateral motion to the turret crew, etc. Of course, non-orthogonal orientation of the turret relative to the tank requires combinations of degrees of freedom. The foregoing implies a requirement for continuous turret rotation capability in the simulator or separate crew stations for the driver and turret crew. That is, if onset cuing is used for turret rotation, separate crew stations must be used for the driver and the turret crew.

However, even if continuous turret rotation is provided, the correct driver-to-turret crew geometrical relationship must be maintained. Also, the simulated turret must be suspended in the simulated hull such that the structural coupling transmits the motion dynamics "similar to" the actual vehicle. The phrase "similar to" is obviously vague, but not intended to be deceptive. It is not known what effect on transfer of training a degradation of fidelity of cues in this area might have. However, some more conclusive statements may be made about this problem. First of all, consider the transmission of vibratory cues across the turret/hull structural interface. It has

been shown that man is much more sensitive to the frequency and amplitude of a vibratory stimulus, than its phase shift. Therefore, the important parameters to preserve are frequency and amplitude. The question now is: to what extent must frequency and amplitude relationships be maintained? While a person's ability to estimate these parameters absolutely is low, he does possess capability for relativistic discrimination. That is, he might be able to say that a particular cue has a frequency which is too high or too low but is not able to quantify it as being 12 Hz instead of 13 Hz, for example, or 0.2g instead of 0.3g. Actual thresholds cannot be absolutely quantified because they are a function of too many variables; ambient motion, task loading, intensity, etc. Therefore, a reasonable approach might be to incorporate sufficient flexibility into the laboratory model to vary the structural coupling between the turret and the hull in order that the actual requirements may be determined empirically. One method to implement this decoupling would be the incorporation of separate motion systems for the turret and the driver station.

To firmly establish requirements for turret rotation motion cuing, the first question which must be answered is: "Is any vestibular/haptic stimulation required to adequately simulate turret rotation or is it sufficient to provide motion cuing solely with visual and aural effects?" As was stated previously, the absence of stimuli to any of the physiological receptors may cause vertigo or motion sickness. However, how much motion cuing is actually required is a much more difficult question to answer. The cues could run the gamut from a jolt to indicate starting and stopping, to onset cuing, to full continuous turret rotation in replication of the real-world turret. The concept of onset cuing has been demonstrated to provide adequate stimulation for continuous rotation, particularly when no realignment of the gravity vector is required. Therefore the question reduces to whether a jolt would provide sufficient training value. It is felt that the only way to conclusively establish this is to have the capability for onset cuing available in a laboratory model, and degrade it to a jolt for experimental purposes. To date, this experiment has not been performed.

Pitch and roll are required at the turret to provide the cues associated with along- and cross-slope operations. It is further recommended that these 2 degrees-of-freedom be driven kinematically (platform angle proportional to tank angle) rather than employing an onset philosophy.

Longitudinal and lateral motion would be desirable to provide acceleration/deceleration cues as well as main gun firing effects, although pitch and roll may be

substituted without significant loss of training value.

Heave is required at the turret to provide cues indicating rough terrain and vibration effects. The heave mode could also provide main gun safety stop bump. Therefore, definite requirements for 3 degrees of rotational freedom (pitch, roll and turret rotation) and one translational (heave) have been established. A desirability for longitudinal and lateral motion has also been identified.

The degrees-of-freedom required for driver's station motion are pitch and roll, driven kinematically, to provide cues of slope operations; longitudinal, to provide acceleration and deceleration cues; and heave, for vibration and bounce. Either lateral or yaw would be a useful adjunct for turret start/stop transients, and if available on the simulator, could be used to investigate the usefulness of either degree-of-freedom for turning cues.

Table 4 summarizes the requirements for driver and turret crew members. These data constitute the performance requirements in each degree-of-freedom, in terms of displacement, velocity, and acceleration. Also tabulated are the vibration requirements listed as frequency and amplitude. The table is configured to illustrate which degrees of freedom are considered to be necessary or useful. The absence of an entry (-), implies no requirement.

In general, the table implies full fidelity simulation and does not consider limitations due to cost and other factors. Pitch and roll for both stations was considered to be driven kinematically with the constant of proportionality equal to unity. Velocity and acceleration requirements are a result of subjecting the commanded angle to linear second order cue shaping.

Yaw is not considered essential at the driver's station but is used to provide onset cues of turret rotation at the fighting station. Since the semicircular canals are sensitive primarily to rotational velocity, it is desirable to provide the stimuli associated with turret rotation by means of a position proportional to velocity drive signal. Therefore, to provide the full velocity capability of the turret a platform yaw rate of 0.39 rad/sec is required. The excursion and accelerations presented in Table 4 are the result of the second order cue shaping dynamics.

Translational cues (longitudinal, lateral, and vertical) result from stimulation of the utricles and are therefore acceleration sensitive. The appropriate drive concept for these three-degrees-of-freedom would be a position proportional to acceleration approach. For full accel-

eration stimulus, the constant of proportionality is chosen such that the platform acceleration equals vehicle acceleration. The excursion and velocity shown in the table are the result of employing the second order cue shaping dynamics. Longitudinal and vertical cues are required at both crew stations. Lateral cues are of limited value at the driving station. It is, however, required at the fighting station if continuous turret rotation is not provided.

Finally, during analysis of vibration requirements, it became evident that while there are measurable vibrations in the orthogonal directions and at several harmonics of 5 Hz, not all are significant. The amplitudes, as indicated both in terms of acceleration and power spectrum analysis, are small in the lateral and longitudinal direction as compared to the vertical. Also, frequencies other than 5 Hz and 15 Hz also produce low amplitude at the fighting station.

The only vibration data available for the driver's station indicates that a relatively high frequency, low amplitude signal is required in the vertical direction.

As previously stated, there are several types of devices currently in use to provide stimulation of the motion sensory apparatus. First consider the application of platform motion systems. If this type of apparatus was to be used to satisfy the motion requirements, a comparison of single vs. dual motion platform approaches is first presented, dual platform approaches are then discussed, discussion of methods to provide vibration cues to the crew is presented following those and finally the application of a G-seat is considered.

Single vs. Dual Motion System

The single platform approach has some distinct advantages over a dual platform approach. These are: lower facility costs, larger visual field-of-view, and lower motion system costs. This approach would also place the entire crew together at one crew station. There are also several disadvantages. Only those directly associated with motion simulation will be discussed herein.

The disadvantages of a single motion system approach, from a motion simulation point of view, can be separated into two main categories -- flexibility and cuing. Flexibility is an extremely important attribute if a simulator laboratory model is to be used to establish future simulation requirements; for either interactive or individual crew member training. The standard approach with this type of simulator (as employed on the U.S. Air Force's Advanced Simulator for Pilot Training (ASPT)), a simulator to establish require-

TABLE 4 MOTION EXCURSIONS, VELOCITIES AND ACCELERATIONS

MOTION REQUIREMENTS				
Degree of Freedom	Mode	Required	HULL Useful	TURRET Required
PITCH	DISP.	+0.64 rad	--	+0.64 rad
	VEL.	± 1.11 rad/sec	--	± 1.11 rad/sec
	ACC.	± 17.3 rad/sec ²		± 17.3 rad/sec ²
ROLL	DISP.	+0.3 rad		+0.3 rad
	VEL.	± 0.52 rad/sec	--	± 0.52 rad/sec
	ACC.	± 8.11 rad/sec		± 8.11 rad/sec ²
YAW	DISP.			+0.23 rad
	VEL.	--	--	± 0.39 rad/sec
	ACC.			± 6.12 rad/sec ²
LONGITUDINAL	DISP.	+10 in		+10.0 in
	VEL.	± 15 in/sec	--	± 15 in/sec
	ACC.	$\pm 0.6g$		$\pm 0.6g$
LATERAL	DISP.		+10 in	+10.0 in
	VEL.	--	± 15 in/sec	± 15 in/sec
	ACC.		$\pm 0.6g$	$\pm 0.6g$
VERTICAL	DISP.	+15 in		+15 in
	VEL.	± 25 in/sec	--	± 25 in/sec
	ACC.	$\pm 1.0g$		$\pm 1.0g$
VIBRATION	FREQ.	30 Hz	--	5 Hz 15 Hz
	AMPLITUDE	0.03g		1.0g 0.05g

ments for fighter training was to provide the capability in the laboratory model to systematically degrade performance to establish the minimum training requirements.

For motion simulation, it is particularly important to be able to independently degrade degrees of freedom for the driver and for the occupants of the turret. This can only be accomplished by employing separate motion systems. There must be no contamination of results from one crew station to the other. Furthermore, the types of motion cuing necessary at each crew station may be more easily determined in an environment of separate motion systems.

Another advantage of the flexibility offered by the dual platform approach is that the devices may be used directly and independently as a driver trainer and as a turret crew trainer. A major point is that separate research can be accomplished simultaneously in the two devices.

The area of cuing is where additional benefits may be realized by employing dual motion systems. As indicated previously: if one motion base is used, the option of using onset cuing for turret rotation is forfeited and continuous turret rotation must be employed. Continuous turret rotation means that the turret must have essentially the same rotational capability in

the simulator as it does in the tank. Simply using 360 degrees of rotation is not adequate because of the reverse cue from reinitializing the turret. Using a continuously rotating turret introduces other problems such as video transmission across a rotating interface.

In addition, the geometry of the tank, i.e., the driver's position relative to the turret crew, must be maintained or false cues will be introduced on rotation. This precludes any possible foreshortening of the device to facilitate visual system implementation. Finally, the simulated turret would have to have the same structural characteristics as the tank to properly transmit cues between stations. Therefore, a dual platform approach is selected as the appropriate configuration.

Vibration Methods

There are three methods of providing vibratory cues to the various crew members. Before discussing these methods, some background information concerning vibratory cues is in order. Vibration is generally considered to be a continuous, periodic motion of either fixed or varying frequency and/or amplitude. Vibration, in this application, should not be confused with the "shudder" which might propagate through the vehicle as a decaying sinusoidal disturbance resulting from a shock.

Experience has shown that a vibration cue is not necessarily required in a specific degree of freedom. It seems that humans are more concerned with the frequency and amplitude or existence of the disturbance than with its direction. Therefore, two of the three methods of providing vibration cues involve only one degree of freedom.

The three methods to be discussed herein are:

- o Seat shaker
- o Crew station shaker
- o Motion system

The seat shaker simply vibrates the crewman's seat; the crew station shaker vibrates the entire crew station; and the motion system option allows the presentation of vibration cues via the motion system hardware. With this option, vibration can possibly be introduced in any of the motion system's degrees of freedom.

All three methods have been successfully employed in flight simulators. Usually, seat shakers and cockpit shakers are employed when high-frequency vibration (3 Hz to 20 Hz is required. Motion systems can provide up to 10 Hz vibration frequency. After analysis of the available data, it has been concluded that tank requirements do not warrant the addition of hardware beyond that presently available in the motion system. Significant vibrations occur at 5 Hz or below. Therefore, use of a motion system would be quite satisfactory. In addition, the motion system would provide the capability of introducing vibrations into the various degrees of freedom to ascertain training value.

Vibrating a motion system at higher frequencies reduces component life, may excite resonances, and requires considerable structural stiffening of components mounted on the platform.

G-Seats

Finally, since in aircraft simulators the tendency is to replace platform motion systems with G-seats, the question arises; can the motion requirements be provided by G-seats? The answer to that question is no, for the following reasons.

The G-seat is a device which is designed to provide sustained cues by stimulating the haptic system. It is true that in the process some vestibular stimulation may be achieved. However, it is questionable as to whether sufficient displacement is available in the case where the cuing is kinematic such as roll and pitch to properly stimulate the semi-circular canals. In the case of translation or yaw where kinematic cuing is not possible,

there certainly is not sufficient stroke available to provide onset and washout.

In the cases of roll and pitch a further disadvantage of a G-seat is the movement of the line of sight relative to a fixed reference on the tank.

If platform motion systems are to be used, what should the platform be capable of providing for cues in terms of state vector components in each degree of freedom?

If two crew stations are used, on the basis of commonality, two types of six degree-of-freedom motion systems could be developed to satisfy the requirements - a cascaded motion system or a synergistic system. A cascaded system is one in which the excursion in any one degree of freedom is independent of excursions in any other. A synergistic system may be characterized as one in which motion in any degree of freedom degrades the instantaneous capability in all other degrees of freedom. This, however, is the only advantage of a cascaded system. It tends to be heavier, more expensive, and have servo loop stability problems. Synergistic systems, on the other hand, do not have those problems and offer the additional advantages of simplicity, ease of maintenance, superior performance, and greater flexibility.

In the 3 translational degrees of freedom (longitudinal, lateral and vertical), values for displacement, velocity, and excursion are the result of the application of onset cuing with second-order shaping to a "commanded position proportional to vehicle acceleration" philosophy. The motion system should have this capability to effect the appropriate cues.

The yaw axis for the fighting station should employ onset cuing with "commanded angle proportional to turret rotational rate." The resulting characteristics are tabulated in Table 4. The value of 6.12 rad/sec^2 for yaw imposes rather severe constraints and is somewhat unrealistic since it is the result of applying a maximum turret velocity step (0.39 rad/sec) in one iteration. Recorded data reveals that it would actually take about 3 computer cycles before the turret reaches maximum velocity. Reanalyzing on this basis, the required acceleration would be $+2.0 \text{ rad/sec}^2$. This level is more reasonable and is a result of a unity ratio between platform turret as well as relatively high poles in the cue shaper function. Hence, the acceleration requirements could quite readily be reduced further, but it would be advantageous to have this capability for laboratory experimentation.

The pitch and roll requirements for the ideal case; i.e., a one-to-one relationship between platform angle and tank angle, impose performance capabilities in

excess of virtually all state-of-the-art motion systems. This same situation confronts the designer in aircraft simulation where an airplane can pitch to 90° and the simulator obviously cannot. Therefore, the ratio of pitch (or roll) angle of the platform to the corresponding angle of the aircraft is less than unity. This approach works quite well and if necessary can be augmented by adding onset cuing to initiate rotation. This augmentation does not appear to be necessary since the tank is not able to pitch or roll very rapidly unless it is falling. In this instance, the cue terminates quite rapidly so a mere saturation of the system would be sufficient. Therefore, the maximum capability in pitch and roll should be no greater than that required for fighter and transport aircraft. Those parameters are: excursion 50° total in pitch and ±20° in roll, a velocity of 20°/sec for pitch and roll and accelerations of ±60 deg/sec².

The recommended requirements for the 6 degrees of freedom are provided in Table 5.

TABLE 5 DEGREE OF FREEDOM REQUIREMENTS

Degree of Freedom	Disp.	Velocity	Accel.
YAW	±13°	±20°/sec	±114°/sec ²
PITCH	50° Total	±20°/sec	±60°/sec ²
ROLL	±20°	±20°/sec	±60°/sec ²
VERTICAL	±15"	±25"/sec	±1.0g
LONGITUDINAL	±10"	±15"/sec	±0.6g
LATERAL	±10"	±15"/sec	±0.6g

These characteristics can be met by most systems currently available in the industry and would require no development.

Vehicle dynamics simulation provides required information concerning the vehicle orientation, velocity, and acceleration to the motion module. This information is then processed to compute the actuator commands to properly position the motion platform.

Platform pitch and roll could be kinematically computed by equations of the form:

$$\theta_P = K_\theta \theta_T \quad \& \quad \phi_P = K_\phi \phi_T$$

where θ_P and ϕ_P are the desired platform pitch and roll angles respectively, K_θ and K_ϕ are constants of proportionality and θ_T and ϕ_T are the pitch and roll angles of the tank. The two constants of proportionality should be easily variable by the

experimenter in order to determine the crewmember's sensitivity to the proportion of the real-world angle being produced in the simulator.

At the fighting station, compensation for turret pointing angle must be provided. For example, when the tank is proceeding with the turret pointing 90° to the right, what is perceived as pitch in the hull is roll at the fighting station and vice versa.

The governing equations are of the form:

$$\theta_P = \theta_T \cos \alpha_T + \phi_T \sin \alpha_T$$

$$\phi_P = \phi_T \cos \alpha_T + \theta_T \sin \alpha_T$$

where α_T is the pointing angle of the turret.

To provide onset cues for turret rotation, the position drive command should be a function of turret rotation rate. The drive equation should be:

$$\psi_P = K_\psi \dot{\alpha}_T$$

where $\dot{\alpha}_T$ is the turret rotation rate.

This drive signal is then passed through a cue shaping, second order filter with a transfer function such as:

$$G(s) = \frac{1}{(s+a)(s+b)}$$

where a and b are the poles which are under the control of the experimenter. The above transfer function is represented in the Laplace domain and must be expressed in the time domain for mechanization in the digital computer. The poles of this transfer function can be manipulated to control the slope of the onset cue and the shape of the washout profile.

The translational axes drive equations should all be a function of vehicle acceleration. These equations:

$$q_{P_i} = K_i \ddot{q}_{T_i}$$

where q_i are the generalized coordinates X , Y and Z ; are then used as drive parameters for the cue shaping functions which are of the same form as the yaw axis (although the poles may be different).

Next, a compensatory term should be added in the vertical and lateral directions, to establish the appropriate center of rotation. This additional term is a function of the distance to the center of rotation and the tank rotation angle.

The next set of computations provided, should enable the experimenter to degrade capabilities in any degree of freedom proportionately to zero; if, for example, the experimenter desires to validate the training effectiveness of cue in any degree of freedom.

An example of how degradation factors could be employed is shown here for the pitch axis:

$$\theta_{pO} = k_{\theta D} \theta_F$$

Therefore, if $k_{\theta D} = 1$, the full effect of cues in the pitch axis are experienced. If $k_{\theta D} = 0$, no cues in the pitch axis are provided. Also, cues may be partially reduced by inserting $0 < k_{\theta D} < 1$.

Special Effects

Vibratory cues are computed for any periodic type phenomena such as engine or road vibration. Discrete cues might arise from weapon strikes or collisions. The advantage of using this channel to provide these pulses is that it is unfiltered. The vibration drive equations may be configured to provide engine vibration as a function of engine RPM. Two drive signals, frequency and amplitude, are required. They may be of the form:

$$f = K_f (\text{RPM})$$

$$a = K_a (\text{RPM})$$

where f is the commanded frequency and a is the commanded amplitude. These signals control the output of a variable frequency oscillator which is summed with the leg commands from the primary cues section and the discrete channel.

Cue Synchronization

Cue synchronization has become a significantly more important parameter of simulator design in recent years, and since the motion system is one of the most important constituents of the synchronization problem, it deserves treatment here. Many studies have been conducted over the years concerning this subject. It appears that the more recent studies have shown that more delay is acceptable than some of the earlier, that is 1940's and 1950's, studies have shown. For example, Ricard, Norman and Collier in 1976 state that virtually no difference was seen between delay and no delay conditions in the control of aircraft pitch angle. However, on the roll, axis control became progressively worse as display delay lengthened. Roll errors and control stick deflections tended to increase when the delay exceeded 100 milliseconds.

These preceding data are for strictly visual delays and do not consider motion. Since motion cuing is thought to be re-

quired prior to visual cues, must motion delays obviously be less? It is interesting that from the work in 1975 using 100 milliseconds delay, and subjects flew carrier approaches with and without the delay inserted, there was no difference in the mean number of trials needed to reach the criterion, but the pilot's exercise their skills differently under delayed conditions -- particularly these differences were noted on the lateral axis. Work by Miller and Kiley 1976 indicates no increase in tracking errors until the overall delay was 250 to 375 ms, depending on the control characteristics of the vehicle. It seems then the precise criterion has yet to be determined.

The question is, how do all these time delay analyses done for aircraft simulators, apply to the simulation of other types of vehicles? It was stated previously that the later data differed significantly from the earlier data. Perhaps this difference in the results may have been due to the fact that most of the early data had involved tracking tasks considerably different from the task of flying an airplane. Therefore, one might conclude that similar discrepancies would be found if aircraft data would be extrapolated to include the simulation of other types of vehicles. One must be especially careful in using any of these cue synchronization data for the following reasons:

The field of view of the visual system on which the data were taken has a significant effect on the synchronization of the cues. Wide field of view visual systems provide cues in the periphery which are not present in narrow fields of view systems which tend to stimulate primarily the foveal vision. Dawson states that discrimination of motion is greatest at the fovea, but the appreciation of motion seems highest in the periphery. This essentially means that motion is detected in the periphery, but the stimulus lacks information. Therefore, motion acuity is greatest in the fovea. It can be seen then that the field of view dimensions of the visual system has a significant impact on the amount of information that an operator has available for controlling this vehicle.

A second consideration is the control dynamics of the simulated vehicle. Miller and Kiley have indicated that the lesser responsive the simulated vehicle, the longer the time delays that can be tolerated. The characteristics of the simulator motion system also can affect the results of the study. Also of importance is the qualification/experience of the operator in the actual vehicle. For example, if the operator is highly experienced in the vehicle being simulated, he would become more disoriented with poor synchronization than an inexperienced operator, since the inexperienced person may not

detect an improperly synchronized set of cues.

How does all this information relate to the synchronization of tank cues? The tank presents some unique control problems relative to airplanes. In most modes of operation, a tank has relatively slow dynamic response to control inputs. However, in certain modes, the response is extremely rapid and may indeed surpass the aircraft. However, for the most part, when the tank is involved in any of these high response situations, there is not much that an operator can do to alter the situation. In general, the control loop can be termed looser in the tank than in an aircraft, particularly for the driver.

The most critical aspect of cue synchronization is the correlation of the visual and motion systems. Instrument synchronization is less of a problem than in aircraft simulation since there are no navigational or high-response attitude instruments -- only a tachometer and speedometer. Control inputs are used to compute vehicle dynamics. These parameters are then used to update the visual display through the visual system image generator and the motion system through the motion drive equations. Motion commands are converted to analog signals to drive the motion servo systems.

Each transfer of data and computation is additive to the delay from the time of input to the time of motion or visual response. If individual steps are not organized, controlled, and properly executed, resultant delays could become unacceptable (from the crewmembers' viewpoint).

System Flexibility

As indicated, the system flexibility is considered to be of significant importance. Increased flexibility provides the experimenter with a wider latitude for verifying simulation requirements which optimize transfer of training.

A major step in the achievement of system flexibility is the 6 degree-of-freedom motion system. The utilization of the 6 degree-of-freedom system permits experimental determination of how many degrees of freedom are actually required.

Software configuration also contributes to overall motion system flexibility. Software formulations permit module interchangeability, ease of modification of drive signal philosophy, alteration of motion control low gains (constants of proportionality; i.e., K_0), poles, and washout profiles.

Degradation of overall motion performance and degrees of freedom add additional flexibility.

Conclusion

A systematic approach to determining the motion requirements for a training device for the crews of tanks. These requirements were then translated into a hardware configuration and a determination that for separate training devices, a driver trainer could probably be configured with four degrees of freedom (pitch, roll, longitudinal, and vertical) and the turret crew would require all six degrees of freedom.

References

1. Davson, H. ed, "The Eye Vol. 4 Visual Optics and the Optical Space Sense", Academic Press, 1962
2. Gibson, J. J., "The Senses Considered as Perceptual Systems", Houghton Mifflin, 1966
3. Gillies, J. A. ed, "A Textbook of Aviation Physiology", Pergamon Press, 1965
4. Gum, D. R., "Modeling of the Human Force and Motion Sensing Mechanisms", Ohio State University, 1972
5. Hosman, H. J. A. W. and van der Vaart, J. C., "Vestibular Models and Thresholds of Motion Perception. Results of Tests in a Flight Simulator", Delft University of Technology, Delft, The Netherlands, LR-265, April 1978
6. Grimsby, C. C., "Model of human Dynamic Orientation", M.I.T. Cambridge, Mass, NASA CR-132537
7. Young, L. R., Meiry, J. L., Newman J. S., and Feather, J. E., "Research in Design and Development of a Functional Model of the Human Nonauditory Labyrinths", Space Sciences Inc. AMRL-1R-68-102, March 1969
8. Anon., "Design Definition Study Report Full Crew Interaction Laboratory Model Volumes II & IV", Link Division, The Singer Co., LR-895, Binghamton, N. Y., June 1978

B.W. McFadden* and John G. Joas
McFadden Electronics Co.
South Gate, California

Abstract

Areas covered in this paper are 1) the reasons for requiring accurate simulation of control force loading, 2) software and hardware deficiencies that preclude obtaining truly realistic feel characteristics in simulator cockpit controls, 3) a unique and different approach to mechanization of both software and hardware, and 4) some examples of successful applications of this control loader approach.

A variable control force loading system, with improved fidelity in generating forces pilots feel in flight simulators, has been developed. The heart of the system is a force servo rather than the positioning servo used in conventional control loading devices. This technique allows control forces simulating spring, damping, inertia, breakout, coulomb friction, deadband, etc. to be adjusted independently over a wide range and summed in proper proportions to easily synthesize desired feel characteristics. Attention to hydro-mechanical details in the hardware, such as bearings, linkages, actuator friction and valve characteristics allows servo performance to be optimized to achieve truly realistic cockpit control force loading.

Introduction

Cockpit Flight Simulators for both research and training are proving to be more economical, safer and more energy efficient than using real aircraft. However, if the components that comprise a flight simulator do not appear, feel, and react in a realistic manner, the fidelity of simulation will be impaired and valid results may not be achieved. This is particularly true for the feel characteristics of the pilot's controls.

If the controls look, feel and respond realistically to applied forces, the pilot will not be distracted from successfully completing his mission or task—e.g. learning in a trainer, or evaluating flying qualities in a research simulator. Poor control loading all too often results in negative training effectiveness and invalid research conclusions.

To be most useful, simulator controls should accept and respond to computer commands of force that are normally functions

of aerodynamic quantities such as airspeed and acceleration. In addition, since changes in the simulator might be required later in the field, to accommodate updated information describing the real aircraft, control loading changes should be easily accommodated by simply resetting dials or feeding in computer commands instead of crawling under the floor and making mechanical modifications. Each component of force such as spring, damping, breakout, backlash, friction, etc. should be independently variable over a wide enough range to facilitate quick, precise adjustments and easy incorporation of changes.

Weight ought to be kept to a minimum, especially when the simulator is on a moving base. A minimum of moving parts should be used to maximize maintainability and minimize down time. In other words, the system ought to be as reliable and fail safe as possible.

One straight forward method of obtaining correct static feel characteristics is to incorporate the entire control system of a real aircraft in a simulator. However, there are some limitations: 1) Dynamic control forces that are a function of air speed and normal acceleration in actual flight would be missing, 2) The real linkages, force producers and bell cranks are costly and take up a great deal of space and weight on board a moving base simulator.

Another method of providing a simulator with feel characteristics would be the use of a high performance control force loading system. Such a system could accept and respond to computer commands of force that are normally functions of aerodynamic quantities such as airspeed, buffet and acceleration. Installation and maintenance would be easier and less costly because reliability would be improved with fewer moving parts. Changes in the simulator that might be required later because of changes in the real aircraft control feel characteristics could be easily accommodated.

This latter method appears to be more desirable in establishing a set of cockpit controls capable of providing realistic, simulated stick and pedal feel forces at lower cost.

With this method in mind then, what are the problem areas associated with accurately obtaining good control feel characteristics?

*President and Technical Director
Member AIAA

Control Loader Problem Areas

A common complaint about flight simulators is, "It doesn't feel like the real aircraft". In such cases, the pilot does not always know why, but he is definitely aware that the control loading isn't right.

Incorrect control feel characteristics are usually caused by 1) a poor knowledge of real aircraft control force characteristics, and 2) incapability of the control loader to accurately reproduce desired forces.

If it is assumed that a satisfactory knowledge of actual control forces in the real aircraft are known, the problem then narrows down to reproducing these forces with sufficient fidelity to prevent the pilot from experiencing false cues.

Some key system performance problem areas are listed in Figure 1.

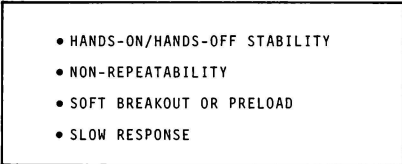
- 
- HANDS-ON/HANDS-OFF STABILITY
 - NON-REPEATABILITY
 - SOFT BREAKOUT OR PRELOAD
 - SLOW RESPONSE

Figure 1. System Control Loader Problem Areas

Mechanical design items that contribute to system problems are shown in Figure 2.

- 
- FRICTION
 - BACKLASH
 - THRESHOLD
 - ACCURACY
 - ALIGNMENT
 - COMPLIANCE

Figure 2. Mechanical Control Loader Problem Areas

All of these mechanical items contribute more or less to system performance deficiencies in all cockpit control force loaders. Hydraulic actuators have friction. Linkages have alignment problems, friction, backlash and compliance. Most servo valves have a significant threshold. Cable drives have friction and compliance. These are some of the problem areas that must be coped with in building a high performance, or high fidelity, cockpit control force loading system. With these items in mind then, what would constitute an ideal loader?

The Ideal Loader

An "ideal" loader should be capable of perfectly duplicating the pilot's control force feel characteristics of a real airplane. It should be capable of reproducing a wide range of force commands, including zero force, i.e. zero spring gradient, zero friction, etc. Thus, the loader itself should inherently have zero friction, zero backlash, zero force threshold, infinite stiffness and instantaneous response to force commands either electrically from a computer or manually from a pilot. The force feel parameters should be continuously adjustable. The loader should be capable of internal force programming as well as external programming from a computer. It should be very reliable and require virtually no maintenance.

Approaching the Ideal Loader

Although it is physically impossible to construct an "ideal" loader, or any "ideal" device, ideal conditions can be approached by careful design. As stated previously, the device should be a perfect force reproducer. Thus, in its basic sense, it should be a highly responsive and accurate force servomechanism. Since hydraulic systems are capable of fast response and have a high degree of stiffness, an electro-hydraulic servo-actuator is a good choice for a control loader. Hydraulic servo actuators generally have a high horsepower to weight ratio and, thus, are compact packages. Because the pilot's controls operate about pivot points, compact rotary hydraulic actuators can be directly coupled to each control. This approach eliminates the backlash and compliance problems associated with linkages, cables and bell cranks.

The major source of friction in such a system is usually the actuator itself. Actuator friction can be reduced to virtually zero by using bearings with hydrostatic lubrication under pressure. This can be accomplished using the same hydraulic fluid that drives the actuator.

If the control loader is a highly-responsive force servomechanism, control force feel characteristics can be easily and accurately programmed. From engineering mechanics, the composite force acting on a body, in this case the pilot's control, can be resolved into its' individual components. Typical force components that are felt in a pilot's stick are shown in Figure 3. Thus the optimum design of an electrical controller should allow for independent programming of each of these individual components of force on the pilot's control, summed typically as shown in Figure 4. Each individual component of force should be continuously adjustable over its expected range of variation. Such

a controller enables easy and accurate programming of the force feel, further enhancing the fidelity of the simulation. Additionally, adjustable electrohydraulic

hard travel limits (stops) should be provided, whenever control travel authority might need to be changed in the simulator.

- SPRING FORCES
 - Linear Spring
 - Non-Linear
 - Cable Stretch
 - Linkage Compliance
- BREAKOUT FORCES
 - Preloaded Spring
 - Detent
- DAMPING (VISCOUS) FORCES
 - Dashpot
 - Damper
- FRICTION (COULOMB) FORCES
 - Bearing Drag
 - Friction Clutch
- TRAVEL LIMIT FORCES
 - Mechanical Stops
- DEADBAND IN FORCES
 - Backlash (Gears)
 - Play, Slop (Linkages)
- DYNAMIC FORCES
 - Bob Weight
 - Stick Buffet Shaker
- LIGHT FORCES
 - Helicopter
 - VSTOL
- TRIM FORCES
 - Fighter, Transport
 - Helicopter

Figure 3: Typical Component Forces on a Pilot's Control

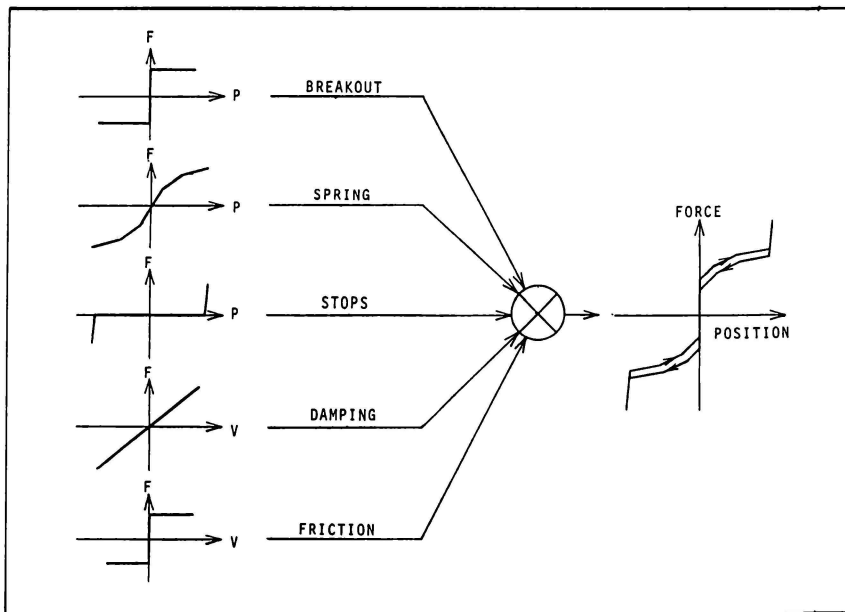


Figure 4: Typical Control Force Components

It should always be kept in mind that the accuracy of the simulation can in no way exceed that of the data provided to the programmer. Hence, provisions for easily updating feel characteristics after a trainer has been in service for a while would allow trainer updating to take advantage of better data or changes in the real aircraft.

As shown in Figure 5, a typical control force feel is made up of: breakout (preload), spring gradient, damping (viscous friction), and coulomb friction (ca-

ble and bearing drag). Breakout and spring gradient are functions of control position. Damping and coulomb friction are functions of control velocity. Additional functions of position are the stops and deadband, or backlash. Consequently, other than force, only control position and velocity, as feedback quantities, need to be sensed and varied. If desired, however, control acceleration might be sensed and utilized as feedback to vary the apparent inertia of the pilot's control. Such a control loader would not only provide accurate and "high fidelity" simula-

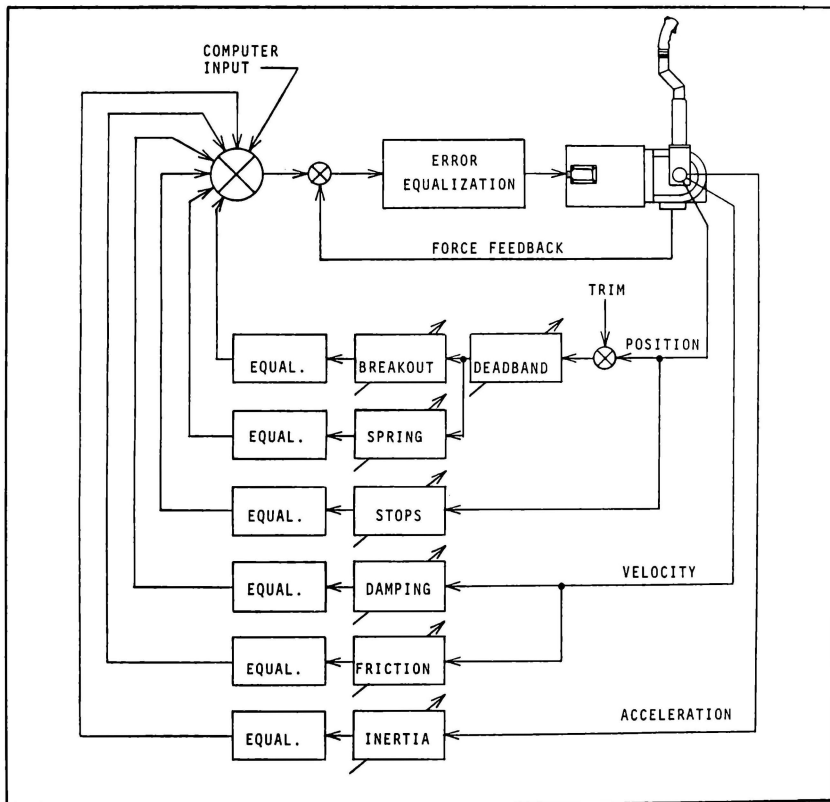


Figure 5: Control Loading System Block Diagram

tion, but would be adaptable to an extremely wide range of aircraft simulators; and should more accurate, updated information about the real aircraft become available, the simulator could be readily modified to reflect the new information.

A Practical "High-Fidelity" Loader

A control loader capable of providing accurate reproduction of pilot's control forces in a flight simulator has been developed. The design of the loader is based on the approaches described so far. The loader consists of electro-hydraulic servo actuators directly coupled to the pilot's controls and a set of control electronics for each axis of control. Salient features of this high performance control loader are presented in Figure 6. A stick, or cyclic, configuration is shown in Figure 7.

- Realistic Control Feel Simulation
- Stable, fast response
- No Static Friction; Hydrostatic Bearings
- Compact Light Weight Hydro-mechanical Packaging
- Extremely Low Force Threshold
- Smooth Response at Low Force Gradient
- Accepts Electrical Analog Force Commands
- Fail Safe Circuit; Stops Unsafe Motion
- Transducer Signals Available for External Generation of Special Non-Linearities or Other Functions of Force

Figure 6: Summary of Performance Features

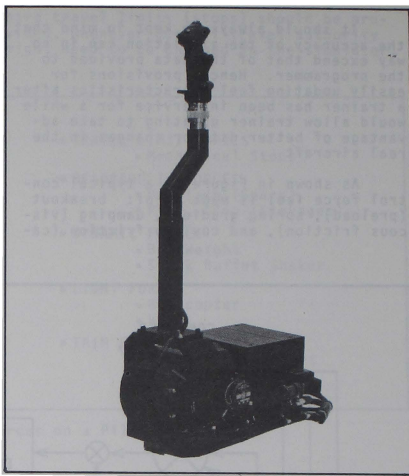


Figure 7: Fighter Stick (Cyclic) Control Loader

Actuator

Each axis has a rotary hydraulic actuator directly coupled to the pilot's control. Direct coupling not only provides a compact package, but eliminates the need for linkages, cables, and bell cranks. Thus backlash, friction, resonances, and alignment problems associated with linkages are not present. To reduce friction to virtually zero, the actuator shaft is floated on hydrostatic bearings. In a typical hydrostatic bearing, illustrated in Figure 8, oil under pressure is provided to the interface between the moving and stationary members of an actuator. Consequently, the actuator rotor "floats" on a thin film of oil under pressure. There is no metal-to-metal contact. A groove is cut in the stator at the free-air end of each bearing in the loader actuator. These grooves are connected to a vacuum scavenging system to retrieve the bearing oil that would otherwise leak out. Thus, there are no moving mechanical seals to cause friction. The actuator with hydrostatic bearings and no conventional mechanical seals will operate with a very low (virtually zero) force threshold and have long life coupled with high reliability. The unit will also require a minimum of maintenance.

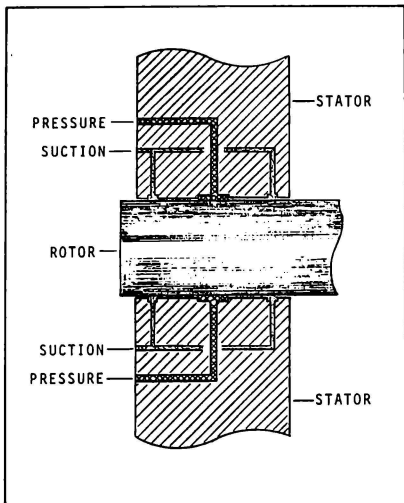


Figure 8: Hydrostatic Bearing

Controller

The electronic controller for the control loading system is, in essence, a special-purpose analog computer. A typical one is shown in Figure 9. The controller is all solid state and consists of a set of electronics with all components mounted on plug-in printed-circuit cards. Control dials, provided on the front panel, are used for manual programming of the control force feel and are shown in Figure 10. The electronic control for each axis is housed in a single chassis which is rack mountable. Remote computer programming is optional. The controller contains the electronics required to condition and scale the feedback signals, provide servo compensation, and force feel function generation. Buffered analog outputs of pilot's control force, position, and velocity are available and can be provided to the flight simulator host computer. Provisions for external input force commands, control trim position commands, and buffet commands are also incorporated.

The design of the electronic controller is based on the above described approaches. Basically, the control loader is a tightly-closed force feedback servo loop with a frequency response in excess of 50 Hz. Thus, the control loader is essentially a true voltage-to-force converter. The force is slaved to input voltage and/or feedback commands.

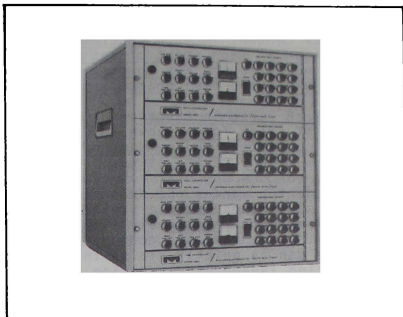


Figure 9: Electronic Control Console

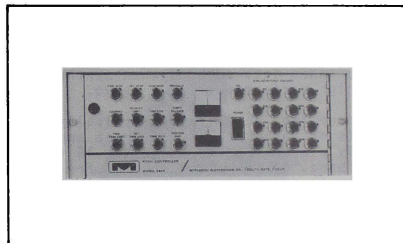


Figure 10: Typical Control Panel

System

The heart of the system is the high bandwidth force servo which is a voltage-to-force converter. The closed loop frequency response has a -90° phase point typically between 50 and 100 Hz, depending upon stiffness and inertia of the stick (or other control), the mounting points, the actuator oil column and load.

There are several advantages in having a high bandwidth inner force loop as shown in Figure 5.

1. Apparent inertia of the stick does not change whenever other force functions (gradient, breakout, friction, etc.) are varied. This is because only position and velocity feedbacks are changed. Force feedback is not changed to accomplish this.

2. Sharp, variable discontinuous nonlinearities such as breakout, coulomb friction, electrohydraulic travel limits, etc. can be developed to have

realistic "feel". Having high frequency content in each generated function at each point of motion discontinuity is the key to obtaining good simulated feel characteristics.

3. Each variable function or component of stick force shown in Figure 3 is completely independent of variations in any of the others. One knob, (or one computer command), independently varies one function. This makes the accurate synthesis of any feel system extremely simple and quick. Each variable component of force can be quickly dialed in and verified independently during calibration or trouble shooting procedures.

A typical cockpit control has a cantilever resonant frequency that occurs around 40 Hz. It is highly underdamped. A typical control loader actuator has an oil column load resonance between 50 and 150 Hz. It is also underdamped. Higher frequency resonances due to the valve and other sources are also present. All of these modes that are less than 1500 Hz must be taken into account when synthesizing a high performance force servo.

Force loop equalization typically consists of integration plus three appropriately placed lead terms in the 15 to 150 Hz band. Attenuation at high frequencies is accomplished with lags and notches.

Referring again to Figure 5, linear spring gradient is generated by feeding back stick position into the force servo. In this way, spring rate is directly proportional to the amount of position feedback. Similarly, linear viscous damping is directly proportional to velocity feedback. The force commands fed into the force servo may be any function of stick position or velocity. Non-linearities such as breakout, deadband, travel limits, and multi-gradient springs are feedback functions of position. Coulomb friction (bearing or cable drag) is a feedback function of velocity. Inertia is a feedback function of acceleration.

In addition, force commands that are not directly functions of stick motion may be fed into the force servo. These might be bob weight forces, buffeting, etc.

Buffered position and velocity signals are available to an external computer for generating other force commands. These externally generated commands can be functions of dynamic pressure (q), airspeed, Mach No., simulated aircraft control system failures, and other parameters.

A fast shut down, or abort, based on the derivative of force provides operator safety and minimizes chances of physical

damage caused by excessively large transients due to such things as power loss, computer switching, potentiometer opening, break in interconnecting cabling and even failure in the electronics. A remote abort, or disable, command also may trigger the safety shut down and additionally may be used in conjunction with a solenoid valve to shut off the hydraulic source of oil pressure.

The fast shut down safety circuit senses rate-of-change of velocity, or force onset. Whenever rate-of-change of velocity exceeds a preset level, a resistor is instantly inserted between the valve driver amplifier and the servo valve. This limits maximum possible valve opening (and, hence, actuator velocity) to a safe, low value while the system seeks null again. The safety circuit continues in the "abort" mode until the output of the valve drive goes essentially to zero. As the output of the valve driver amplifier approaches zero, the series resistor is shorted out, automatically reconnecting the valve directly to the amplifier to "enable" the system to full performance again. This technique results in safe engagement of the system to a full-power, operate condition without unsafe transient motions.

Trim is available on all axes and trim rate is variable. Trim authority is adjusted with Trim Travel Limits in each direction.

Variable electrohydraulic travel limits are independently adjustable in each direction in each axis.

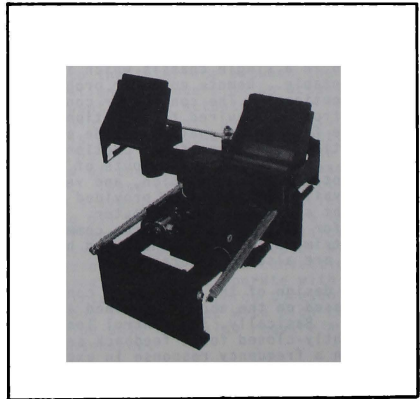


Figure 11: Pedal Control Loader

A bias, or initial condition, control in each axis is provided to locate the zero force position of each control anywhere within the limits of travel. Positioning is positive at all times except for the conditions of zero spring gradient and zero breakout force.

The pedals shown in Figure 11 may be adjusted fore and aft to accommodate each pilot. They are freed by pressing a push-

button placed near the pilot's seat or at the normal pedal-adjust handle location. The pedals will then be pulled toward the pilot by springs, or the pilot may push them away with his feet. The push-button, or handle, is released to rigidly lock the pedals in the new position.

A Navy (High Roll Axis) Type Stick is shown in Figure 12 and a Wheel and Column configuration (for transport and bomber type aircraft) is pictured in Figure 13.

A trainer configuration using real aircraft controls is shown in Figures 14 and 15.

A 2-Axis side arm controller with similar features is in the design stage.

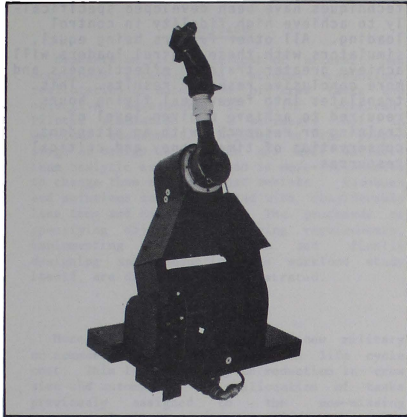


Figure 12: Navy (High Roll Axis) Stick



Figure 13: Wheel and Column

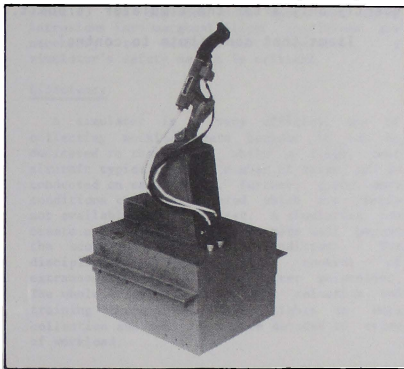


Figure 14: Trainer Stick Configuration

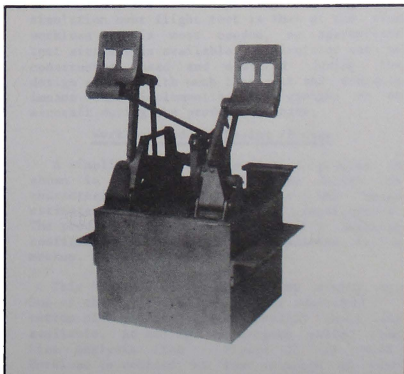


Figure 15: Trainer Pedals Configuration

Conclusion

A high performance control force loading system is an essential part of a cost-effective, safe and energy-efficient flight simulator. Lack of fidelity can ruin the training effectiveness of an otherwise excellent trainer, or result in invalid conclusions in a research simulator.

The problems associated with poor control loading fidelity are lack of band-pass in generating various control force functions; incapability of generating functions requiring light stick forces; and a lack of anticipation of independent adjustment of enough functions to accommodate real flight test data, available frequently only after the simulator is built.

Items that contribute to control

loading problems are usually attributable to small discontinuous non-linearities in the real hardware, making synthesis of high performance servo loops virtually impossible. Typical non-linearities are actuator and bearing friction, valve dead-band, slop and compliance in linkages and brackets, cable stretch, and linkage friction.

Special hardware and servo synthesis techniques have been developed specifically to achieve high fidelity in control loading. All other factors being equal, simulators with these control loaders will achieve greater training effectiveness and more conclusive research results. This translates into fewer real flying hours required to achieve a given level of training or research, with an attendant conservation of time, money and critical resources.

VERIFICATION OF WORKLOAD - A JOB FOR SIMULATION

T. C. Way
Boeing Aerospace Company
Seattle, Washington

Abstract

Emphasis on life-cycle cost of aircraft has occasioned interest in aircrew reduction, reallocation or automation of crew tasks, and objective assessment of pilot workload. Piloted simulation is a necessary tool in workload assessment. Applied at the proper stage of design, simulation has more validity than analytic assessment and is more responsive to change than a flight test vehicle. Feedback and solutions can be iterated with considerably less time and cost impact. The processes of specifying objectives, deriving requirements, implementing the simulation and finally designing and conducting the workload study itself, are discussed and illustrated.

Background

More and more, the selection of new military or commercial aircraft is based on life cycle cost. This leads directly to reduction in crew size and automation or reallocation of tasks previously assigned to the now-missing crewmen. It is also common to find that a new aircraft is more complex than the one it replaced. Frequently, then, in new aircraft there are fewer crewmen and at least as many functions to be performed as in older aircraft. The challenge to designers of flight decks and avionics suites, is to configure the crew station in such a way that required tasks can be accomplished by the allotted crew complement while holding crew workload within reasonable limits. The purpose of this paper is to outline the use of piloted simulation as an aid in meeting that challenge.

Advantages to Simulation

The advantages of simulation over flight test for workload studies include cost, safety, efficiency and timeliness.

Cost

Properly done, simulators are less expensive in acquisition, operation and maintenance cost. This is particularly true when the simulator is part of a larger simulation complex, sharing computers, operations and maintenance personnel and the visual system with other efforts. For a given program, simulation has uses beyond assessment of workload. These include, (1) development of flight control laws and handling qualities, (2) development of particular control or display concepts such as a head up display, (3) pilot

training and, (4) demonstration to customer, regulatory, program and management personnel.

Safety

As a ground-based system, a simulator is clearly safer than an aircraft as a test vehicle. In degraded mode operations where intrusions into marginal flight conditions are necessary, to define the boundaries, a simulator's safety margin is critical.

Efficiency

A simulator is a very efficient way of collecting workload data because it can be dedicated to that task, while a flight test aircraft typically has a number of tests to be conducted on each flight. Further, operational conditions can be simulated which are simply not available in flight test. A simulation can create a combat mission environment well beyond the scope of flight test conditions. The discipline of experimental control of extraneous variables can be better maintained. The whole effort, from subject selection and training through the test flights to data collection and analysis can be devoted to study of workload.

Timeliness

From the point of view of design development, the most compelling advantage for simulation over flight test is that at the time workload data is most needed, no appropriate test aircraft is available. A simulator can be constructed, used and modified during the design process with much less cost and schedule impact than implementing the changes on an aircraft during the production phase.

Workload and the Design Process

A simplified view of the design process is shown in Figure 1. Preliminary design is characterized by trade studies and broad estimates against the primary requirements. The product of preliminary design is a baseline configuration, frequently incorporated in a mockup.

This baseline is reviewed before moving on. One of the reviews is an analytic identification of workload drivers. Several tools are available. At Boeing, a program called Time Line Analysis (TLA - Figure 2) is used. Workload is defined in that program as time required to perform a task divided by time available for that task. Time available is

Simulation Objective and Requirements

The objective of simulation in this process is to provide a medium for further design validation, particularly with regard to crew workload.

Requirements

It is necessary to distinguish between a simulator and simulation. The requirements for both must be carefully developed and will be discussed here. A simulator is the device itself with its supporting hardware and software. Thus the flight deck with its controls and displays, the outside visual scene with the system which provides it, the supporting computer facility, its input and output devices and the computer programs are all part of the simulator.

A simulation includes the simulator and the scheme for using it. Selection and training of subjects and test personnel, the mission scenario, conduct of the test, data collection and analysis and reporting of the results are as important to the simulation as the simulator itself.

In an effort of this sort, using a simulation to test interactions between pilots and their airplane, it is critical to create and maintain for the pilots the illusion that they are in an actual aircraft on an actual mission. All elements of the simulation should have sufficient fidelity to both support that illusion and represent the flight deck being simulated.

Flight Deck Completeness. The simulator flight deck should be as complete as possible and, the features known or suspected to affect workload should look, feel and behave as much as possible like the real thing. Further, arrangement of these elements and geometry of the flight deck which contains them should be faithful to the airplane design. For example, the seats should be positioned and have range of adjustment to maintain proper eye reference point and postural support but how this adjustment is achieved is less important and seat color is not important at all.

Flight Control System and Aero Model. Modeling of the flight control system and aerodynamic characteristics of the represented aircraft should be sufficient to maintain our illusion. Pilots are very conscious of "how it flies." They will be, at best, distracted by a fighter simulator which flies like a C-5 or a STOL transport simulator with the characteristics of an F-18. Handling qualities should be appropriate throughout every phase of flight. On a study of a new fighter cockpit featuring subjective evaluation of advanced control and display concepts¹², the pilots wanted to talk about how difficult it was to fly the simulator at slow speeds and, consequently, paid less attention to the control-display concepts under test. In workload simulation, flying performance will be measured; this is another reason why control and aero models should adequately represent the aircraft.

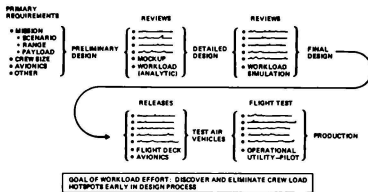


Figure 1. Workload in the Design Process

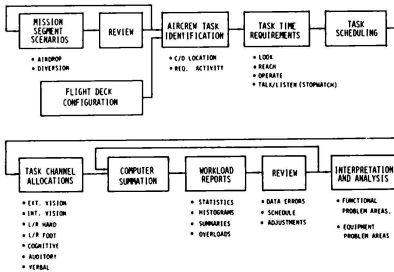


Figure 2. Time Line Analysis

derived from a detailed scenario and time required from a time-and-motion synthesis of task performance in that flight deck. These single task data are cascaded by the program so the designer can see overall workload and its breakdown into individual channel (two hands, two feet, internal or external vision, verbal, auditory and cognitive), channel groups (vision, manual, communicative), and particular functions or pieces of equipment (e.g., way-point selection or navigation control-display unit). The TLA program has been used with military customers, with FAA in the 747 certification process and with NASA-Langley in the 737-Terminally Controlled Vehicle program.

While the preliminary work produces a baseline design derived from primary requirements, the detail phase yields a complete configuration with particular elements specified and detailed. There is a higher degree of commitment here and greater functional detailing. At some point in the detailing, a design release is declared and the simulator is built. Timing for that release is critical since the simulator must be built and a workload simulation conducted after a fairly mature design is reached but before releases are made for aircraft avionics or flight deck purchase or construction. Fidelity of the simulation at this point is a combination of design commitment and judicious estimation.

Visual Scene. For most aircraft, takeoff and landing represent periods of quite high workload and must be well represented. Very few aircraft are equipped to take off or land under truly zero visibility and, even for these, there will be some visual cues available from outside the airplane during most low altitude operations. It follows that a workload simulation requires an external visual scene. This should be of sufficient quality and range to represent at least takeoff roll and rotation as well as approach from several miles out with landing through touchdown.

Motion. The use by pilots of both the alerting and directing functions of aircraft motion is well established. What is not established is the requirement for motion in simulators. Hopkins⁴, in a review of simulation, primarily for training, interpreted Koonce's⁶ results to show zero, or even negative transfer of training from simulation motion to aircraft motion. A similar comment was made by Ray McPherson⁷, a lead Boeing YC-14 test pilot. To an experienced pilot, simulation motion causes more confusion than benefit. For these reasons, and because motion systems are among the most expensive elements of an aircraft simulator, it is concluded that there is no compelling requirement for simulator motion in a workload study simulation.

Scenario. For a study of workload, it is critically important that what the pilots experience and what they are asked to do is similar to what would be encountered operationally. Scenarios for the simulated missions are completely developed beforehand to include a minute-by-minute account of simulation activity. On a workload simulation, the scenario should emphasize events or equipment known or suspected from earlier work to present high workload. For a military transport these might include air drops, formation flight, or enroute diversion. It should also include some failures - simulated degradations of capability which might be encountered operationally and which, again, would increase suspected workload. An extreme failure would be incapacitation of one pilot, forcing the other (in a two-man crew) to assume the whole workload.

Subject Selection. Selection of subjects for a workload simulation narrows rather quickly to one of two groups of experienced pilots. It is argued that the appropriate pilot population for a flight test, or a flight simulation is the group of professional test pilots. These are likely to be more skilled than operational pilots, more adaptable to peculiar test situations and more accustomed to responding to questionnaires developed for eliciting structured subjective opinion. Test pilots are, by training and experience, better test instruments for measurement of aircraft properties.

On the other hand, it is good experimental practice to draw a sample of subjects the population to which you wish to generalize. This would dictate using airline pilots for a workload study of a commercial transport flight

deck and pilots from the Military Airlift Command (MAC) for an Air Force transport. These operational pilots may be better subjects for measurement of the man-machine interface because they are more representative. This group also has the practical advantage of being more familiar with operational aspects of the missions to be flown in the simulation and so require less mission training.

In the Advanced Medium STOL Transport flight test recently completed at Edwards AFB, both approaches were taken. Some of the pilots were assigned on temporary duty from the Military Airlift Command and some were professional test pilots from the Air Force Flight Test Center. Similarly, the pilots for a workload simulation should be either professional test pilots or drawn from a user command or both.

Data Collection and Analysis. The importance of careful workload assessment of a new system or of a major modification to an existing system is clear. Both successful mission performance and flight safety are jeopardized if workload is too low or too high. However, as Roscoe⁸ noted in a very recent review, "Ideally, assessment or measurement of pilot workload should be objective and result in absolute values; at present this is not possible nor is there any evidence that this ideal will be realized in the foreseeable future. It is also unfortunate that the human pilot cannot be measured with the same degree of precision as can mechanical and electronic functions" (p.6).

Be that as it may, the subject of workload is of sufficient importance that it is being pursued on several fronts. First, methodological studies are continuing on the physical, psychological and physiological aspects of the problem in efforts to understand the determinants, mechanisms and consequences of workload. Discussion of these studies is beyond the scope of this paper. A number of good reviews are available^{3, 5, 8, 9, 11}.

Fortunately, there are two compatible, direct and intuitively appealing approaches which are particularly applicable in workload simulation. The first is subjective. A rating scale is developed and pilots are asked for their assessments of workload in the various mission phases. Ellis⁹ mounts some good arguments for use of a scale similar to the Cooper-Harper² scale for evaluation of aircraft handling qualities. The scale points are well defined and the technique is familiar to many pilots. Cooper-Harper like ratings are ordinal rather than interval in their mathematical properties. As such, they do not qualify for certain operations and certain analytic manipulations are inadmissible. Mean, standard deviation and product moment correlation coefficient are replaced by median, semi-interquartile interval and a rank correlation coefficient¹⁰.

The second approach to workload verification is measurement of performance. Performance measures have been criticized because they are not direct indices of workload. This is not particularly embarrassing since, for the

designers and users of a system, the real concern is with performance. If the pilots can use their aircraft to safely and completely perform their mission, then they have verified that workload is adequately bounded. This sort of measurement places emphasis on operational aspects of the simulation already discussed.

An Illustration of Workload Verification

Simulator

The requirements for the Advanced Medium STOL Transport (AMST) program dictated a two-pilot flight deck. Figure 3 shows the Boeing C-14A AMST. The aircraft will functionally replace the C-130 with four men in the flight deck. Quite reasonably, the Air Force has identified workload as an area of concern. In both the YC-14 prototype and C-14A programs, Boeing flight deck and systems designers have worked hard to reduce workload and automate a number of potentially high workload functions.

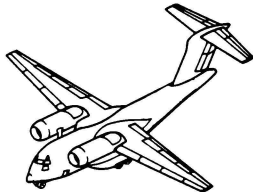


Figure 3. C-14A Advanced Medium STOL Transport

For C-14A, the time line analysis mentioned earlier identified potential workload hotspots in the area of communications and navigation. In the detailed design phase, these areas received particular attention and were included in a full-mission simulation conducted late last year. The simulator was built as part of the existing complex shown in Figure 4. Features of particular relevance to the C-14A simulation are the computer room with four Varian 74/75 digital computers interconnected through shared memory, the closed circuit TV system with cameras and carriages in the model room and projectors in the screen room and the wide-body simulator cockpit.

The simulation is supported by the mathematical model outlined in Figure 5. The software modules interact with the TV camera drive systems, the control console, data recorders and instruments, controls and the feel system in the cockpit. In addition, special purpose hardware and software packages operate the head-up displays and the integrated navigation control display unit.

Figure 6 shows one of the terrain board models. This is a 128:1 scale model used for takeoff, landing and rollout. A larger scale model is used for higher altitude work.

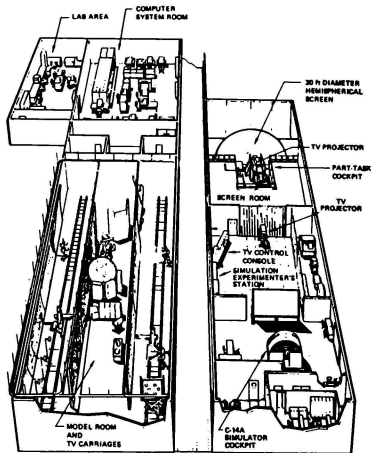


Figure 4. Visual Flight Simulation Laboratory

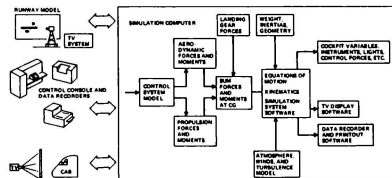


Figure 5. Mathematical Model for C-14A Simulator

In the cockpit of the simulator, pilots experience the geometry and features of the full flight deck. Figure 7 shows an earlier arrangement which is presently being modified to the current aircraft design. The instruments and controls are modularized so the flight deck can be easily reconfigured to support either part-task or full mission simulation.

Simulation Test

A preliminary workload simulation was conducted using test subjects who were current or recent C-130 or C-141 pilots. Figure 8 outlines their participation. Briefly, each crew of two pilots spent two days in the



Figure 6. Visual System Terrain Board

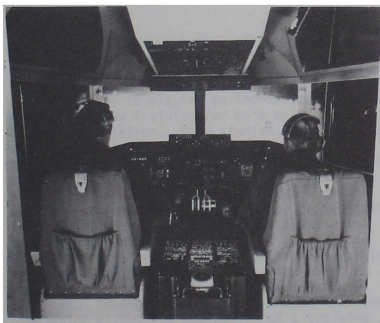


Figure 7. C-14A Simulator Flight Deck

simulation. The first day was primarily training and the second devoted to data collection. For each mission, pilots were briefed for one route, then diverted in flight. They had to both add and delete waypoints to successfully complete the mission. Normal checklists and operational communications were added to provide a realistic level of activity. Flight control and navigation performance was measured and debriefing questionnaires were used to collect subjective data.

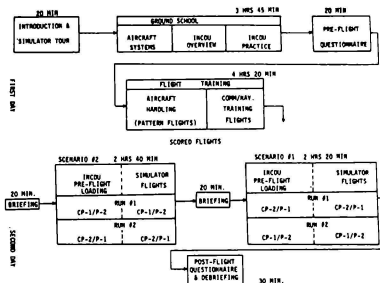


Figure 8. Pilot's Schedule-Preliminary Workload Study

The results of that simulation were gratifying in that adequate workload bounding was verified. Several areas of refinement were identified and the solutions will be tested in the follow-on simulation program.

Conclusion

This paper has discussed the importance of workload simulation, its place in the design process and some of the requirements for an adequate simulation. The state-of-the-art in fine-grain workload assessment (precise definition of the determinants and mechanisms of workload) is not particularly satisfying. However, it is possible to take the broader approach of designing and integrating a flight deck to minimize workload based on prior experience, industry standards and good human engineering practice. Simulation is then used to verify that workload has been adequately bounded. An illustration of that broader approach was given and it is concluded that such a program is a necessary part of a major aircraft project.

References

1. Anderson, A. F., "Time Line Analysis Program (T.L.A. Mod. III) Users Guide," Boeing Company, Seattle, WA, D6-44751, 1977.
2. Cooper, G. E., and Harper, R. P., Jr., "The Use of Pilot Rating in the Evaluation of Aircraft Handling Qualities," National Aeronautics and Space Administration, NASA-TN-D5153, 1969.
3. Gartner, W. B., and Murphy, M. R., "Pilot Workload and Fatigue: A Critical Survey of Concepts and Assessment Techniques," National Aeronautics and Space Administration, NASA-TN-D-8365, 1976.
4. Hopkins, C. O., "How Much Should You Pay for That Box?" Human Factors, Vol. 17, Dec. 1975, pp. 533-541.

5. Jahns, D. W., "A Concept of Operator Workload in Manual Vehicle Operations," Forschungsinstitute für Anthropotechnik, Mechenheim, Germany, Forschungsbericht No. 14, 1973.
6. Koonce, J. M. "Effects of Ground Based Simulator Motion Condition Upon Predictions of Pilot Proficiency," Unpublished doctoral dissertation, University of Illinois at Urbana-Champaign, 1974; also University of Illinois at Urbana-Champaign, Aviation Research Laboratory TR ARL-74-5/AFOSR-74-3, 1974.
7. McPherson, R. L., Personal communication, 1978.
8. Nicholson, A. N. Ed., Simulation and Study of High Workload Operations, North Atlantic Treaty Organization, NATO AGARD Conference Proceeding No. 146, 1974.
9. Roscoe, A. H., Ellis, G. A., and Chiles, W. D. "Assessing Pilot Workload," North Atlantic Treaty Organization, AGARDograph No. 233, 1978.
10. Siegel, S. Nonparametric Statistics for the Behavioral Sciences, McGraw-Hill, New York, 1956, pp. 18-30.
11. Spyker, D. A., Stackhouse, S. P., Khalafalla, A. S., and McLane, R. C., "Development of Techniques for Measuring Pilot Workload," National Aeronautics and Space Administration, NASA-CR-1888, 1971.
12. Way, T. C., and Premselaar, S. J., "Advanced Integrated Fighter Cockpit Simulation Programs," Air Force Flight Dynamics Laboratory, Dayton, Ohio, AFFDL-TR-72-119, 1973.

COMPUTER IMPLEMENTED GRADING OF FLIGHT SIMULATOR STUDENTS

F. L. Comstock
Staff Engineer
Link Division, Singer Company
Binghamton, New York

Hugo J. J. Uyttenhove
Department of Systems Science
School of Advanced Technology
State University of New York
Binghamton, New York

Abstract

An investigation into computer monitoring of aircrew performance and subsequent evaluation of that performance. The study presumes that it is possible to develop, for each training task, a General System model of aircrew skill development within the mathematical framework of set theory. Through the judicious selection of parameters to be monitored, and by utilization of a reasonable amount of computer resources, an evaluation can be made by comparing student performance to a performance optimum. The technique involves the development of a State Transition Structure difference matrix from the matrix representing the students performance and the matrix representing the optimum performance.

I. Introduction

Simulation is playing an increasingly important role in aircrew training for both military and commercial aviation. Many studies have established that the level of transfer of training to today's high fidelity simulators is extremely close to a one-to-one ratio in terms of training hours expended. Moreover training situations can be created in simulators that can never be duplicated in the real world. An often cited example is emergency training for which it is possible to establish simulated conditions offering valuable training in response to crisis situations that would be far too risky to duplicate in actual aircraft. Another example is in combat training. Simulation allows the concoction of a training scenario that could just not be contrived in a military exercise because of its complexity, because the equipment of the foreseen adversary is not available, because of the cost, and, again, because of the risks involved.

With the increasing substitution of simulator training for aircraft training, have come significant developments in automated training features made possible primarily by relatively inexpensive but powerful computers. These automated training features, in the nature of preprogrammed missions, demonstrations, automatic malfunction activation and the like, have done much to alleviate the workload and increase the effectiveness of the simulator instructor by relieving him of the

necessity for constant problem control inputs, thereby allowing him more time for monitoring, guiding, and evaluating student performance. But because the complexity of the equipment, especially in military aviation is increasing at a phenomenal rate, the burden on simulator instructors does remain significant. Currently work is underway to provide the simulator instructor with tools for making the tasks of monitoring, guiding and evaluating student performance less subjective. This work is frequently referred to as Computer Aided Instruction (CAI). This paper addresses a portion of that work specifically that area which is relevant to evaluation.

Computerized evaluation of flight simulator students has heretofore been limited to maneuvers and tasks for which the desired flight path or action is totally predictable and relatively simple. This has meant that computer monitoring and analysis of aircrew performance has been applicable to only navigation, instrument and procedure training and even here with minimal success. The problems can be categorized as follows:

1. The desired performance must be uniquely defined in terms of basic parameters of flight (from hereon called variables of flight) and procedural steps. This suffices for an Instrument Landing System (ILS) approach where the approach path is well defined and an acceptable tolerance band can be easily applied. However, in a combat maneuvering training problem such as two F-15 simulator cockpits pitted against a computer generated and controlled MIG 23, the situation is so fluid that there is no hope of predicting even a few seconds of the simulator flight paths.

2. Limiting the monitored performance parameters to the basic variables of flight because they were obvious, easily measured and traditionally accepted as the criteria for aircrew evaluation has imposed severe restraints on computerized evaluation of flight skills in simulators. It has been possible to grade a student on his flight along an airway but as yet no one has successfully graded aerobatic maneuvers, airborne formation join ups, and tactical weapon delivery maneuvers in which the significant measurements of performance may depend on the relationships among the basic variables.

3. The monitored performance has been limited to a relatively simple training situation because in a complex situation there were too many decision variables to handle. Thus, simple airborne radar intercepts in which a student performs a missile attack on a computer generated radar image have been evaluated. However, airborne intercepts of multiple threats in a dense emitter environment in which the student is employing a sophisticated weapon system such as the Navy's F-14 and Phoenix missile combination have not lent themselves to evaluation.

It is our belief that a computerized method of grading performance in flight simulators which handles not only the predictable flight maneuvers and tasks but also which is flexible enough to handle the unpredictable maneuvers and tasks is the key to performance evaluation.

We have turned to the field of General Systems Theory to find the proper methodology and tools which can aid us in the evaluation process. In particular, we have investigated the application of a General System Problem Solver² (from hereon abbreviated as GSPS) which is assumption free in its nature. The concepts involved are extensive but nevertheless relevant to our study. We present the basic outlines of these concepts in the following section.

II. Relevant Concepts

GSPS

The problem solving approach by the GSPS is based on a framework of taxonomies of systems, of problems, of the methodological tools which provide solutions to the problems, and of some systems modelling aspects.

The most fundamental classification is that of epistemological levels of systems, as suggested by Klir.³⁻⁵ The basic hierarchical categories are:

1. Source Systems (data-less systems) which define the object of investigation in terms of attributes and variables together with their possible appearances and states, respectively, and an interface between the attributes and the variables.
2. Data Systems consist of measured, observed or given data for the variables, usually appropriate parameters of some kind, such as time, space, population, etc.
3. Behavioral Systems or generative systems in the sense that the data systems can be predicted or generated by means of parameter invariant procedures.
4. Structure Systems defined in terms of a set of elements and some relation between them such that behavioral or lower level systems are fully described.
5. Metasystems at various levels are defined in terms of known systems corresponding to lower epistemological levels, together with a parameter invariant procedure which describes changes from

one system to another.

At each level the classification is extended by inclusion of various methodological distinctions. For further classifications see Cavallo and Klir² and Uyttenhove⁶.

The taxonomy of problems consists of problem types and particular problems defined in terms of system types, particular systems and requirements. Solutions for particular problems are provided, if possible, by the methodological tools. The latter are an assemblage of interactive computer programs which guide the investigator or modeller through the final stages of the GSPS.

We are thus dealing with systems and the identification of them at various levels of the hierarchy of epistemological levels.

Regardless of the level at which the system is defined, the variables involved in the system may be classified into input and output variables. This classification means that states of the input variables are viewed as conditions under which states of output variables are conditional: "If the input variables are in state x , then. . ." Input variables are thus not the subject of inquiry but are viewed as being determined by some agent which is not part of the system under consideration. Such an agent is referred to as the environment.

Systems whose variables are classified into input and output variables are called directed systems; those for which no such classification is given are called neutral systems. This dichotomy of systems holds for each of the epistemological levels.

The methodological criteria regarding the kinds of variables and relations are also part of the systems at each of the epistemological levels. We already noted above the distinction between input and output variables, while we also consider dichotomies such as variables being well defined or fuzzy, discrete or continuous, of nominal or ordinal scale, linearly or non-linearly ordered parameters, etc. Relations can be classified as being deterministic or probabilistic, memoryless or memory-dependent, linear or non-linear, etc.

These basic categories enable us to describe the mode of operation of GSPS in a more direct way. We must realize, however, that the computer-implemented GSPS (i.e., its interaction facilities and the tools) is constantly subject to changes in the sense that it (GSPS) learns from experience and as such stores information about problem types and particular problems for future reference. GSPS furthermore broadens its horizon by its expansion as an effort to solve more and larger problems.

In principle, the operation of the implemented GSPS consists of accepting inputs (i.e., the problem statement) and generating the correct sequence of tools and their output solution. Specifically, the output can be either a particular system of the type demanded by the problem,

or a relation between the initial and terminal systems. With regards to the input into GSPS, some interactive procedure should assist the investigator in identifying the entry to the GSPS. This means that the language and interaction should help to formulate the problem in an understandable general systems expression. The admissibility of the problem is largely dictated by the methodological tools. These, together with the specific sets of epistemological and methodological criteria, are coded on computer files. An interactive program activates the communication between the investigator and the user. The following sections of the algorithm are described from the standpoint of the GSPS.

- (i) Find out what the investigator defines as the initial system type and identify a particular system of that type.
- (ii) Determine the requirement types and the set of particular requirements from answers by the investigators.

(iii) Conclude, if possible, what the terminal system type is and, if the problem so requires, identify a particular system of that type.

(iv) Determine whether the problem is admissible and, if so, what the tool(s) is (are) to provide the solution(s).

(v) If no tool can be assigned or if the problem is not admissible, determine if useful information relevant to the problem is available and allow for respecifications of steps (ii) through (iv); else, the GSPS can offer no solution.

That part of the GSPS which is relevant to this paper is the description of systems at levels 1, 2 and 4 of the hierarchy. In the following section, we discuss some relevant formal concepts which are the backbone of the approach.

Formal Notions

Let $A = \{a_i | i \in I_n\}$ be a set of basic attributes chosen by the investigator to represent an object of interest for some specific purpose; $I_n = \{1, 2, \dots, n\}$ is an index set determined by the number n of basic attributes. Let A_i denote the set of potential appearances of the basic attribute a_i .

Let $B = \{b_j | j \in I_m\}$ be a set of supporting attributes (time, space, etc.) chosen by the investigator and let B_j stand for the set of potential appearances of supporting attribute b_j . Then, the neutral object system in the simplest form is defined by the pair

$$\alpha_N = ((\{a_i, A_i\} | i \in I_n); (\{b_j, B_j\} | j \in I_m))$$

Any useful relation (e.g. ordering) which can be recognized in the sets of appearances of the attributes should be added to the definition of the object system. Moreover, if there exists dependencies among the basic attributes which are solely due to observation or measurement

procedures (e.g. one attribute represents an arithmetic average of others), then these dependencies should also be included in the definition.

Let v_i and V_i ($i \in I_n$) denote basic variables and sets of states of the variables, respectively, and let supporting variables and their sets of states be denoted by w_j and W_j ($j \in I_m$) respectively. Note that $V = \{v_i | i \in I_n\}$ and $W = \{w_j | j \in I_m\}$. A neutral image system Γ_N compatible with the neutral object system α_N is then defined as the pair

$$\Gamma_N = ((\{v_i, V_i\} | i \in I_n); (\{w_j, W_j\} | j \in I_m))$$

This definition may be supplemented by some recognized relations in the sets of states and/or dependencies among the basic variables. The set $\bigcup_{j \in I_m} W_j$ is referred to as the parameter space, ω .

Assume now that a resolution level is introduced for each attribute of the object system which characterizes the meaning of data to be collected for the attribute. This can be accomplished by defining a partition $\pi_i(A_i)$ on each set A_i ($i \in I_n$) and a partition $\pi_j(B_j)$ on each set B_j ($j \in I_m$). The form each of these partitions takes depends primarily on the knowledge of the object of investigation, the purpose of the investigation and the measuring instruments as well as computing facilities which are available.

In order to get a meaningful basis for data gathering and data interpretation, a correspondence between the entities involved in the object and image systems must be introduced. This is accomplished by: (i) a one-to-one correspondence $f_a: A \rightarrow V$; (ii) a one-to-one correspondences $f_b: B \rightarrow W$; (iii) a family of one-to-one correspondences $G = \{g_i: \pi_i(A_i) \rightarrow V_k | i, k \in I_n; v_k = f_a(a_k)\}$; (iv) a family of one-to-one correspondences $H = \{h_j: \pi_j(B_j) \rightarrow W_k | j, k \in I_m; w_k = f_b(b_k)\}$. The collection of an object system, an image system, and a correspondence between them expressed in terms of the one-to-one correspondences (i) - (iv) form a complete frame for data gathering and interpretation referred to as the neutral source system.

Each data-less system (image or source system) implicitly contains all possible trajectories of states of basic variables in the parameter space, i.e., all possible functions from $\bigcup_{j \in I_m} W_j$ to

$\bigcup_{i \in I_n} V_i$. A meaningful restriction to one of the functions, say function δ , which in the modelling problem is determined by data gathering, constitutes data regarding the variables. When the neutral data-less system, say \mathcal{O}_S , is augmented with δ , we obtain a neutral data system (or a neutral system at epistemological level 1). Let \mathcal{I}_S stand for the neutral data systems, then,

$$\mathcal{I}_S = (\mathcal{O}_S, \delta).$$

(Systems S implicitly stand for neutral systems unless specifically subscripted by N or D (neutral or directed) for reasons of differentiation.)

Let a set of variables $s_k (k \in I_q)$, referred to as sampling variables, be introduced by the equation

$$s_{k,w} = v_{\lambda_r}(w),$$

where $s_{k,w}$ stands for states of sampling variable s_k at point w in the parameter space, and λ_r denotes a parameter-invariant translation rule which for any given point w in the parameter space determines one or several other points in the parameter space.

For instance, when the parameter space is totally ordered (as in the case of time parameter) and represented by the set of positive integers, each translation rule can be described by a simple equation

$$\lambda_r(w) = w + a,$$

where a is an integer; sampling variables are then defined by

$$s_{k,w} = v_{i,w+a}$$

When the parameter space is partially ordered $\lambda_r(w)$ may stand, e.g., for points in the parameter space which are predecessors (or successors) of w with a particular distance from w .

Let Λ denote the set of all translation rules under consideration and let the relation

$$M \subset V \times \Lambda$$

specify which translation rules are applied to which variables (including possible internal variables). Set M is called a mask.

Given a data-less system and a mask, a set of sampling variables is uniquely defined. A relation $R_1 \subset S$ defined on $S = \bigcup_{k \in I_q} S_k$ can be then

introduced. Elements of R_1 are q -tuples of states of the sampling variables defined by the mask. They are called data samples. When probabilities $p(c)$ are given with which samples $c \in S$ appear, we obtain set

$$\mathbf{B}(bb) = \{(c, p(c)) | c \in R_1, 0 \leq p(c) \leq 1, \sum_c p(c) = 1\}$$

which is referred to as basic behavior of the behavioral system under consideration.

To employ the basic behavior for generating data for the given primitive system, some order of states $w \in W$ must be chosen in which the data are generated. The order must be compatible with the natural order of the parameter space W . If the parameter space has no natural order, it may be artificially ordered in some suitable way.

Given an order of states in W (linear or partial), we let $w \leq w'$ denote that either state $w \in W$ precedes state $w' \in W$ or $w = w'$.

Once a generative order in set W is decided, a relation

$$R_2 \subset R_1 \times R_1,$$

whose elements are pairs (c, c') of successive samples with respect to the generative order, can meaningfully be defined. When probabilities $p(c, c')$ are given with which pairs (c, c') appear, we obtain a set

$$\mathbf{B}(bst) = \{((c, c'), p(c, c')) | (c, c') \in R_2, 0 \leq p(c, c') \leq 1, \sum_{c, c'} p(c, c') = 1\}$$

This set is called the basic state-transition relation (or basic ST-relation, in abbreviation).

The neutral behavioral system 2S is defined as a triple

$$^2S = ({}^0S; M; \mathbf{B}),$$

where 0S is a neutral data-less system with ordered set W , M denotes a mask, and \mathbf{B} stands for an element taken from the set $\{\mathbf{B}(bb), \mathbf{B}(bst)\}$.

Although the behavioral system does not explicitly contain any data, it contains a relation through which data can be generated. Hence, it consists of a source system, a generative relation invariant with respect to the state set W of supporting variables and, indirectly, a set of data systems, which can be generated through the relation. For the formal concepts regarding structure systems 3S we refer to Klir and Uytendhoeve ⁵.

When behavior or structure systems offer no solution to the problem investigated, one of the reasons may be that the parameter invariance does not hold. In other words, if time is a supporting parameter, then the system may turn out to be time-dependent. To determine the points in the data/system where this dependency becomes evident, an algorithm was developed by Uytendhoeve ⁶. The basic feature, for our application purposes, is based on the probability distribution for the samples c on which we calculate the uncertainty as

$$H = - \sum p(c) \cdot \log_2 p(c).$$

The samples are collected for larger and larger segments (\hat{S}) until the measurement for two successive segments shows a percentage change larger than an acceptable threshold, i.e., $\Delta H > \tau$. This process is carried out for a different segment increment sizes \hat{S} until a stable pattern emerges. For the nontrivial case of general parameter variance and larger masks we refer to previous work ⁶. Systems which are composed of a set of lower level systems and for which the procedure is known by which they "connect", are called metasegments. The metasegment is defined as a triplet

$$^4S = (T, S, P)$$

where T is the parameter space, S the set of lower level system and P the procedure.

System Identification Tools

The GPS contains several tools which will aid us in the identification of the proper systems. Identifying the behavioral system in state transition mode is a trivial operation. Identifying the meta system is accomplished by means of an algorithm META. During a full length application of the GPS, the investigator would be directed to these tools via an interactive program on a terminal time sharing device. Since it is our intent here to briefly state the GPS concepts relevant to our study, we refer to the previous references for full details of the methodology.

III. The Problem and Its Solution

The Problem Statement

The example chosen to illustrate the concepts presented in this paper is a relatively simple one. Extending the concepts to more complex and less predictable maneuvers requires further work but the basic framework exists here.

The data used are that for a typical TACAN approach (see Figure 1) as performed in a jet trainer. The attributes selected do not necessarily reflect all parameters that comprise the descriptors of a typical instrument approach but they do adequately define the essentials of an instrument approach. The intent is to describe a defined flight path relative to a fixed ground reference and monitor how well a student can control the simulator so that it adheres to that flight path and remains within the boundaries of the other restrictions imposed by the rules and regulations of the controlling agencies or the aircraft's performance limitations.

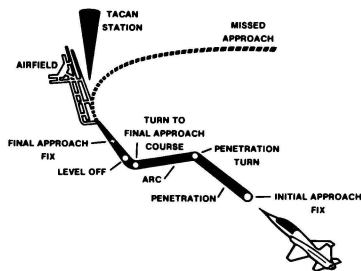


Fig. 1 Typical TACAN Approach

The parameters of altitude, TACAN radial and DME taken together totally describe the desired flight path for all points from the Initial Approach Fix to the Missed Approach Point (MAP). The airspeed parameter is a regulatory one imposed by controlling agencies and/or aircraft

performance characteristics. It was desired for purposes of this example to limit the monitored attributes to a small set; however, the system is capable of handling more attributes such as those describing aircraft attitude and procedure accomplishment.

The technique for student evaluation is based on a computer comparison of the ST behavior B(bst) for the aircraft under the control of the student against the optimum ST behavior established by the published approach path and procedures. The optimum values for a maneuver, taken at specific points and reduced to an ST matrix, are stored in the simulator computer. The parametric values for the simulator under student control are recorded as the student's flight progresses and this data is reduced similarly. The comparison of the stored optimum ST matrix is then made against the student's ST matrix. The student's grade is a matter of establishing his deviations from the optimum ST structure probabilities and outputting a standardized score based on a large data base that can easily be developed over a period of time.

Using the referenced data, an activity matrix was developed for a typical TACAN approach by a jet training airplane.

The Data System

The generated data matrix used as the standard in this study follows standard instrument procedures and covers the period from arrival at the Initial Approach Fix (IAF) through the missed approach. The appearances of the variables, airspeed, altitude, TACAN radial and TACAN distance or DME were described respectively in the common aviation units of knots, feet above sea level, degrees relative to magnetic north and nautical miles. Values were established for points approximately five seconds apart assuming a no wind conditions. A sample of the generated data array is given in Table 1. It should be clearly understood that the flight path generated and used as the standard against which student performance is to be measured, in this study, was strictly hypothetical. The variable values making up the activity array were estimates based on the writers' experience and judgement and do not represent actual recorded values. In implementation, the variable values used as a standard would be generated and recorded during actual aircraft or simulator flights performed by one or more highly qualified USAF Flight Instructors.

	TIME INTERVAL						
	0	1	2	3	4	5	6
Airspeed	250	250	250	265	280	280	280
Altitude	23000	23000	23000	22700	22100	21257	21414
Radial	102	087	082	082	082	082	082
DME	34.6	34.3	34.0	33.7	33.4	33.0	32.6

Table 1 Sample Data Array

Subsequent to the data collection, we carried out the mapping from appearances of the basic attributes to the states of the basic variables, according to set ranges of values (see Table 2). These ranges were not arbitrarily selected but were carefully chosen to create windows of acceptable performance at each of the points in the approach. For example with respect to airspeed, one range covers the penetration airspeed with a tolerance of -10 (no upper limit), one range covers the band of recommended final approach level off airspeeds (220-249) while a third covers the final approach airspeed with a tolerance of -5 knots and +14 knots to account for airspeed adjustments because of fuel. The other airspeed ranges cover the transitions from one approach phase to another. The tolerance bands can be tightened or loosened by adjustments in the ranges according to the proficiency level. The final approach airspeed range can also be more accurately modelled by requiring the computer to calculate the proper approach airspeed based on fuel remaining and applying the tolerance band to that figure.

The Metasystem Identification

The data system served as input to the META algorithm in order to determine points of change in the uncertainty measure. Although we only explored the computation for masks of depth 1,

we likewise carried out the identification procedure for masks of depth 2. Table 3 summarizes the results.

The selection of δ was based on the fact that $4 < |T|/\delta \leq 13$ was desirable from the point of view that 170 observations were available. Because of diversity in results and because points are difficult to uniquely identify, we average the results. How do these results confirm with the segments of the total descent course as we know it? System 1, for data from point 1 to 70 represents the penetration descent; system 2 for data from point 71 to 122 represents the flight along the arc and interception of the final approach course and system 3 is akin to data collected from the final and missed approach.

Since the metasystem identification was carried out successfully, we could continue investigating each of the smaller data systems on an individual basis.

Behavioral Systems (State Transition)

For each data system, a ST behavior ($B(bst)$) was obtained in matrix form. The matrix elements are probabilities associated with the plane moving to a particular state given that it was in a certain state just before. By inspection of Figure 2 (a, b and c), we notice that transitions

Table 2 Mapping of Appearances to States

ATTRIBUTES	VARIABLES		VARIABLE STATE SET MAPPING								SUPPORT
	NAME	ORDER MNEM	1	2	3	4	5	6	7	8	
Airspeed	1	S	150-169	170-219	220-249	250-269	>269	<150			Time is the Supporting Variable
Altitude	2	A	1700-1839	1840-2399	2400-2699	2700-4899	4900-6899	6900-22800	>22800	<1700	
Radial	3	R	0.0-71.9	72.0-92.9	93.0-112.9	113.0-121.9	122.0-360.0				
DME	4	D	0.00-2.59	2.60-13.59	13.60-20.59	>20.59					

Table 3 META System Identification Results

DEPTH OF MARK	TOLERANCE τ	INCREMENT SEGMENT SIZE δ	POINTS INDICATING UNCERTAINTY CHANGE $>\tau$ EACH POINT DENOTES BEGINNING NEW SYSTEM		
			SYSTEM 1	SYSTEM 2	SYSTEM 3
1	10%	13	1	79	131
		17	1	52	120
		21	1	64	127
		29	1	88	-
		42	1	-	127
2	10%	13	1	79	117
		17	1	69	120
		21	1	64	127
		29	1	-	117
		42	1	-	-
AVERAGE			1	71	123

are either to the same or one other state. This was expected since the airplane moved along a flight path that never intersected an earlier portion of the flight path nor, since the flight path was optimized, did the airplane ever leave the desired flight path (state) and then correct back again. In other words, a state was never entered more than once in the optimum approach. Each matrix in turn can be normalized per row; i.e., given that the aircraft is in state s_i , what is the probability that it is in a next state s_j , where the total of probabilities for s_j adds up to 1.

(a) NEXT STATE

	s8	s7	s6	s3	s2	s5	s4
PRESENT STATE	s8	.22	.00	.00	.00	.00	.00
s7	.01	.02	.00	.00	.00	.00	.00
s6	.00	.01	.07	.00	.00	.00	.00
s3	.00	.00	.00	.00	.00	.00	.01
s2	.00	.00	.00	.01	.02	.00	.00
s5	.00	.00	.00	.00	.01	.00	.00
s4	.00	.00	.00	.00	.00	.14	.00
	s4	.00	.00	.00	.00	.01	.46

(b) NEXT STATE

	s14	s13	s12	s11	s10	s9	s8
PRESENT STATE	s14	.46	.00	.00	.00	.00	.00
s13	.02	.04	.00	.00	.00	.00	.00
s12	.00	.02	.18	.00	.00	.00	.00
s11	.00	.00	.02	.02	.00	.00	.00
s10	.00	.00	.00	.02	.02	.00	.00
s9	.00	.00	.00	.00	.00	.04	.02
s8	.00	.00	.00	.00	.02	.00	.14

(c) NEXT STATE

	s17	s16	s15	s18	s19	s20	s21	s22
PRESENT STATE	s17	.09	.00	.00	.02	.00	.00	.00
s16	.02	.04	.00	.00	.00	.00	.00	.00
s15	.00	.02	.11	.00	.00	.00	.00	.00
s14	.00	.00	.02	.00	.00	.00	.00	.00
s18	.00	.00	.00	.09	.02	.00	.00	.00
s19	.00	.00	.00	.00	.00	.02	.00	.00
s20	.00	.00	.00	.00	.00	.04	.02	.00
s21	.00	.00	.00	.00	.00	.00	.07	.02
s22	.00	.00	.00	.00	.00	.00	.00	.40

Figure 2: State Transition matrices for system 1(a), system 2(b) and system 3(c), and the state representation in terms of values of the variables (d).

Conclusion

With the aid of the state transition matrices, we will now be able to carry out the evaluation of student pilots. Before reporting on this aspect of the study, let us first return to the ST matrix and see what we can expect. First of all, the airplane is ruled by the laws of physics and therefore the variables representing its location and movement cannot jump abruptly in value but must represent a gradual transition. There are no right angle turns or discontinuities in airspeed, altitude or ground track. It is a continuum and the transition of each state, either to itself or to some adjacent state is normal. It might, therefore, be argued that the whole system can represent the airplane's flight path just as well as the smaller systems. However, it must be remembered that one of the primary purposes of a grading system is to provide a learning tool. A good grading system should do more than rank students. It should also point out, to student and instructor alike, the student's weak areas and strong areas. When applied to flight training, this means that grades should identify the areas in which a student should be required to attain a higher level of skill development, an obvious need in a field in which substandard skill levels can be, and are all too frequently, fatal. To provide the detailed identification of weaknesses that is demanded, more than one overall grade is required. This leads quite naturally to task segmentation with grading of each segment and hence to sub-systems of the overall system that represents the flight maneuver. This segmentation is part of the considerations of implementing the obtained results for the GPS tools.

IV. Implementation Considerations

Hypothetical Implications

Now that a model for optimum performance exists, student evaluation is a matter of comparing his behavior with that of the model. The student's performance is recorded in the computer in terms of the data system, and the state transition matrix is calculated. By taking the difference between the optimum state transition matrix and the student's state transition matrix and summing the absolute difference values of the individual matrix entries, a raw grade within the range zero to two is obtained.

This range results because the probabilities for each state transition matrix sum to one. Thus, a student who follows the optimum flight profile will have a grade of zero (no differences) and a student who is constantly out of tolerance and therefore is constantly transitioning to an incorrect state will have a grade of two (no commonality with the optimum flight path). The basis on which every student's evaluation is made is: 1) does he attain the proper states, 2) does he remain in each proper state through the appropriate number of recorded points, and 3) does he transit to the next proper state when leaving a given present state.

The appearance of the correct states in the student's state transition matrix establishes

that he attained the correct states. The probability differences between the student's matrix and the optimum matrix, for those states which represent a transition to themselves, determine if the student remained in a given state through the proper number of recorded points. The probability differences between the student's matrix and the optimum matrix for the state transitions to new states determine if the student transits to the next proper state when leaving a given state. This information can be output in a hardcopy format that will identify the points in the maneuver at which the student strayed out of tolerance and the specific flight parameters that the student was negligent in controlling. This in itself will provide a valuable instructional tool for post mission debriefing of the student. Not only is the need for reliance on the instructor's memory obviated but the error data are specific and objective. The hardcopy output of this information can be expressed in the vernacular of aircrews and formatted for ease of reading so that it can be readily interpreted by instructor and student alike.

Application

For illustrative purposes, we assume a hypothetical behavioral system (i.e., ST matrix) as a given optimal model. We further assume a ST matrix which resulted from the student's interaction in the aircraft simulator. Both ST matrices are shown in Figure 3. The high probability associated with the student keeping the aircraft in state s2 reflects his delay in descent and acceleration beyond the initial approach fix. Due to this error, the transition to states s3 and s4 have been delayed.

In order to numerically evaluate this error, the absolute difference values of the corresponding matrix elements (probabilities) are calculated for each matrix. This results in an error value of 0.8. This value can now be presented to the instructor with optional comments in hardcopy format.

If the students are to be ranked by this evaluation scheme, some weighting should be applied to the raw scores. The individual probability differences make no distinction between

a student whose incorrect system states differ from the optimum states by only one variable state and a student whose incorrect system states differ from the optimum state by two or more variable states. This shortcoming can be overcome by multiplying the probability differences for those unique state transitions that appear only in the student's matrix by the number of variable states that differ from the optimum flight path state. This would have the effect of penalizing each student who deviated from the optimum flight path in accordance with the number of parameters he allowed to stray out of tolerance.

If the students are to be graded relative to other students for overall mission performance, further weighting applied to maneuver phases and some form of standardized scoring should be applied. In our example, system 3 represents the most critical phase of the instrument approach because the aircraft is nearing the runway in preparation for landing and therefore altitudes, airspeeds, and adherence to the course line are more critical than in the preceding phases. For this reason, the raw score for performance in system 3 should be more heavily weighted than performance in systems 1 and 2; however, the weighting factor to be applied to each phase of a maneuver is a subjective decision best left to those actively engaged in aircrew instruction.

The conversion of raw scores to a form of standardized scores is a matter of obtaining a sample of sufficient size to produce a statistically reliable base for the scoring curve. Obtaining a sample of valid subjects large enough for reliable results will require that the simulator be in use for training for an appreciable period. For this reason, the development of standardized scores based on the raw scores computed by this evaluation scheme also will be left to the using agencies.

It must be admitted that our illustrative example is based on a highly structured maneuver for which the desired behavior is totally defined. Such an example was purposely chosen to clearly demonstrate the mechanics of this method of evaluation. However, one might logically question how GPS tools can be applied to evaluate students performing less predictable flight tasks such as

(a) NEXT STATE					(b) NEXT STATE						
PRESENT STATE	s1	s2	s3	s4	PRESENT STATE	s1	s2	s3	s4		
	s1	0	0.2	0		0	s1	0	0.2	0	0
	s2	0	0.6	0.2		0	s2	0	0.2	0.2	0
	s3	0	0	0		0	s3	0	0	0	0.2
	s4	0	0	0		0	s4	0	0	0	0.2

(c) STATE				
4734	s1			
4724	s2			
4624	s3			
5624	s4			

(d) STATE	OPTIMUM PROBABILITY	STUDENT PROBABILITY	ABSOLUTE PROBABILITY DIFFERENCE
s1-s2	0.2	0.2	0
s2-s2	0.2	0.6	0.4
s2-s3	0.2	0.2	0
s3-s4	0.2	0	0.2
s4-s4	0.2	0	0.2

Total absolute probability differ. 0.8

Total absolute probability differ. 0.8

Figure 3: Sample ST Matrices for Model (b), Student (a) State Representation in terms of the values of the Variables (c) and Error Value Calculation (d)

in air combat maneuvering. The response to such a question is that as long as the proper variables and their states can be identified and the problems admissible, GSPS can attempt to complete the task. For instance, numerous studies of the problems of air combat maneuver training have been made 8, 9, 10 and based on these studies and other trainers such as Link's Simulator for Air-to-Air Combat (SAAC) have been designed. The highly successful SAAC employs a program to "fly" a computer generated target against students flying the fighter cockpits in a simulated environment. This program extrapolates the near term flight path of the student's simulated aircraft and based on that extrapolation, selects the most advantageous counter maneuver for the generated target. The program considers variables such as angle off, aspect angle, relative velocity total energy level (the sum of the fighter's potential and kinetic energy), relative position and the fighter's turn rate in making this selection of the best counter maneuver. It would be a small step for the computer to go through an identical decision process to establish the student's optimum next maneuver which is in essence the optimum next system state in terms of the above variables.

The methodological tools of GSPS impose no constraints on the real time development of the optimum ST matrix. In other words, at each point in the training exercise, the computer can determine and record the student's optimum next state as well as record the student's actual present state. These recordings are sufficient to establish the ST matrices on which this method of evaluation is based.

V. Conclusion

General Systems Problem Solving tools show promise as methods for computerized grading the performance of simulator students. Its advantages are:

1. It unburdens the instructor by relieving him of the necessity for maintaining a record of student activity, therefore, allowing him to spend a greater portion of his time in observing, guiding, and providing comments to the student during the on-going mission.
2. It is objective in that it is based on the attainment of specific goals.
3. It provides a valuable post-mission debriefing tool in the form of a hardcopy record of student performance that identifies the student's deviations from the desired flight conditions or states.
4. It is based on relatively simple concepts.
5. It can be applied to complex tasks that heretofore have been graded only by instructor opinion.

Nevertheless the implementation of student performance evaluation requires a thorough analysis of each maneuver or task, careful selection of the attributes and their appearances and judicious mapping of attributes and their appearances to variables and their states.

Despite the fact that general rules, techniques and procedures can be identified and described for all flight maneuvers and tasks, one drawback of performance evaluation routines is that in implementation they must be applied in a particular environment. Flight parameters and procedures must have specific values and sequences that fit the time, location and conditions under which the maneuver or task is performed. This evaluation technique is no exception. In order that it be applied, each maneuver must be thoroughly analyzed. This can be an arduous job where something as complex as an air combat situation is to be modeled. However, the first one is always the most difficult and once the initial maneuver or task in any group is completed, the others come more easily, be they TACAN approaches or air combat maneuvers.

References

1. Diehl, A. E. and L. E. Ryan, Computer Simulator Substitution Practices in Flight Training, TAEG Report No. 43, Orlando, Fl., 1977.
2. Cavallo, R. E. and G. J. Klir, A Conceptual Framework for Problem Solving, International Journal of Systems Science, Vol. 9, 1978.
3. Klir, G. J., An Approach to General Systems Theory, Van Nostrand, New York, 1969.
4. Klir, G. J., On the Representation of Activity Arrays, International Journal of General Systems, Vol. 2, No. 3, 1975.
5. Klir, G. J. and H. J. Uyttenhove, Computerized Methodology for Structure Modelling, Annals of Systems Research, Vol. 5, 1976.
6. Uyttenhove, H. J., Metasystem Identification. In: Applied General Systems Research, G. J. Klir (ed.), Plenum Press, New York 1978.
7. Uyttenhove, H. J., Computer-Aided Systems Modelling: An Assemblage of Methodological Tools for Systems Problem Solving, Doctoral Dissertation, State University of New York, 1978.
8. Campbell, T. K. and L. B. Hartsook, A New Approach to Onboard Real-Time Optimum Computations for Aerial Combat Games, AIAA 3rd Aircraft Design and Operations Meeting, 1971.
9. Lee, V. A. and R. J. Wenham, Air Combat Simulation, AIAA Aircraft Design for 1980 Operations Meeting, 1968.
10. Leatham, A. L. and U. H. D. Lynch, Two Numerical Methods to Solve Realistic Air to Air Combat Differential Games, AIAA 12th Aerospace Sciences Meeting, 1974.

John F. Lethert*
Engineering Division, Simulator System Program Office
Wright-Patterson Air Force Base, Ohio

Abstract

Electronic Warfare (EW) Simulation has been emphasized in recent Air Force Weapon System Trainer (WST) procurements (B-52, A-10, F-5E and F-16) because of the cost saving associated with simulator training and because a more realistic EW environment can be created in a simulator than can be encountered in an aircraft training mission. The paper will discuss the approaches to EW simulation that have been developed to provide this simulation. These include:

- Expansion of the simulated EW environment.
- Integration of extensive EW simulation capabilities into WSTs.
- Approaches to simulation of the on-board EW equipment.
- Simulation of war gaming.

Introduction

Air Force Manual (AFM) 51-3 defines Electronic Warfare as "Military action involving the use of electromagnetic energy to determine, exploit, reduce, or prevent hostile use of the electromagnetic spectrum and action which retains the friendly use of the electromagnetic spectrum."¹ In new Air Force Weapons Systems Trainers currently being procured (See Table 1) the primary emphasis is on Electronic Countermeasures (ECM) which is defined in AFM 51-3 as "any action taken to prevent or reduce an enemy's effective use of the electromagnetic spectrum."¹ The scope of EW for simulation purposes has been expanded to encompass many aspects of war gaming. These include interplay between the air vehicle and enemy EW systems as well as the simulation of weapons launched by enemy systems and their effects on the simulated air vehicle. The EW simulation is fully integrated into the WSTs. Thus, the cues received by operators being trained in the use of electronic warfare equipment must correlate with cues received from other cockpit systems, from the visual simulation, and from sensor (radar, infrared, and low light level television) simulation. This degree of sophisticated simulation has not been attempted on Air Force simulators currently in the field.

This paper will identify the reasons for increased sophistication in EW simulation, and discuss the major subsystems and interfaces of the simulation in terms of the major trends in EW simulation for WSTs.

*F-16 Weapon System Trainer Integration Engineer, Member, AIAA

TABLE 1 Air Force Weapon System Trainers with EW Simulation*

Program	Prime Contractor	EW Contractor
A-10	Reflectone	AAI
F-5E	Link	Link
B-52	Link	AAI
B-52	Boeing	Antekna/Boeing
F-16	Link	In procurement

Reasons for EW Simulation

It is a well documented fact that the use of simulation devices result in substantial savings in operation and support costs by substitution of simulator time for actual flying time. An example is shown in Table 2.

TABLE 2 Simulation Cost per Operating Hour versus Aircraft Cost per Operating Hour for B-52D, B-52G and B-52H Training**2

	<u>Simulators</u>	<u>Aircraft</u>
B-52D	260	3240
B-52G	249	3318
B-52H	249	3094

While the cost savings are obviously a major factor in the decision to use simulators for EW training there is another unique feature. Since potential enemies will not let the Air Force utilize their airspace and train against their EW systems, alternatives must be found. The principle alternatives are use of EW ranges or the use of WSTs.

*The A-10 WST includes one A-10 cockpit integrated with a Project 2360 visual system. The F-16 WST includes one F-16 cockpit integrated with a Project 2360 Visual System, Digital Radar Landmass and an EW Training Device.

**These devices include existing B-52 Flight, Bomb/Nav and Gunnery Trainers as well as the AN/ALQ T4 ECM Trainers. The devices are not integrated together.

Several ranges have been built, one of these being at Nellis Air Force Base.⁴ The ranges are made up of radar systems which duplicate enemy early warning radars, and the tracking and acquisition radars associated with enemy missile and anti-aircraft artillery systems. These systems are built by US contractors to match the characteristics of enemy systems and they are manned by Air Force personnel who operate them according to known enemy tactics. Ranges are also used for air-to-air combat training in which Air Force pilots fly US aircraft in accordance with enemy techniques in mock engagements with other US forces using US techniques.

While such ranges can provide very realistic training, there are limitations. These include:

- Since actual aircraft are used there are no savings in operation and support costs.
- The radar systems are expensive and must be manned by Air Force personnel so there are significant life cycle costs associated with them.
- Ordnance cannot be fired against the radar systems.
- Only a limited number of radar systems are available (27 at Nellis).⁴ Unless all are deployed close together and are operating simultaneously, they will not provide a saturation of environment. Furthermore, the limited number of systems available precludes aircrews from training against all types of systems in all mixes that they may encounter.
- Weapons are not fired at the aircraft; the crew cannot practice evasive maneuvers against missiles.
- Training in battle damage conditions is very limited.
- Range time for aircrews is very limited.

While a range provides many important psychological and physiological cues that an aircrew would not receive in a ground based training device, only the WST can overcome the limitations which have been cited. However for a WST to overcome these limitations it must provide very realistic simulation. In response to Air Force requirements for realism in the new WSTs, four major trends are evident. These are:

- Expansion of the simulated EW environment.
- New approaches to simulating EW equipment.
- Integration of extensive EW simulation with aerodynamic, visual, and sensor simulation to form WSTs.
- Simulation of war gaming.

The ECM Problem for WSTs

Before discussing the major trends some background is necessary. Air Force Regulation 50-11 defines a Weapons Systems Trainer as "a device

which provides a synthetic flight and tactics environment. It helps aircrews learn, develop and improve techniques that relate to their crew position in a specific aircraft. Aircrews work individually or as a team in completing simulated missions."³ At least in the broadest sense, all of the devices listed in Table 1 fall within the scope of this definition and the term WST will also be used to refer to the F-111, F-15, and F-4 simulators currently in the field. It will refer to both single seat fighters and aircraft with several crew members.

The ECM problem to be simulated in a WST may be envisioned as a set of dynamically related subsystems and interfaces as shown in Figure 1.* Figure 1 may be considered as applying to both the real world and WST since there is almost a one to one correspondence between subsystems denoted by S_1 to S_5 , one way interfaces denoted by I_{jk} , and two way interfaces denoted by I_{jkl} .

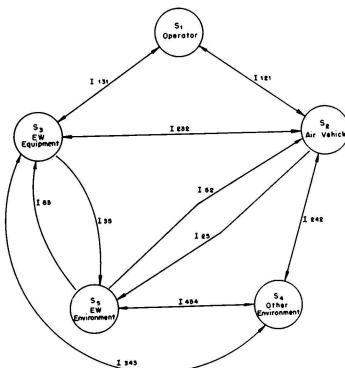


Figure 1 Conceptual ECM Problem WSTs

The Air Vehicle (S_2) and Other Environment (S_4). For purposes of this discussion the air vehicle (S_2) includes the aircraft of interest, all on-board equipment except EW equipment, and any crew members other than the operator. The other environment (S_4) consists of the terrain, vegetation, buildings, weather, etc., which may be sensed visually or by using various sensors. Although S_2 and S_4 interact with other subsystems in the WST ECM problem, discussion of their simulation, as well as the simulation of the interface between them (I_{242}), is beyond the scope of this paper.

*Figure 1 actually represents the simulation problem for any aircraft with an EW capability. The definitions of and distinctions between subsystems, one way interfaces, and two way interfaces are largely arbitrary. In this case they were chosen for convenience in discussing the ECM simulation problem for WSTs.

The Operator (S₁). Except for the B-52 WST, all other new WSTs represent single seat fighter aircraft. In these cases, the object of the EW simulation is to train the fighter pilot in electronic warfare. The pilot uses his EW equipment to observe the EW environment. The pilot can also observe other features of the EW environment visually (e.g. missiles) or by using sensors.

In the B-52 WST the object of the EW simulation is to train the EW officer. He uses his EW equipment to observe and counter the EW environment. The EW officer on the B-52 is not able to observe the EW environment through other means, although other crew members can observe it.

The operator as discussed herein is the pilot of single-seat fighters, and the B-52 EW officer. The operator's primary interface with the air vehicle (I₂₁) is through basic aircraft controls for a single-seat fighter and by verbal communications on other aircraft. The operator interface with the EW equipment (I₃₁) is through a series of controls, displays, and audio tones. All WSTs attempt to exactly duplicate I₂₁ and I₃₁ as they occur in the real world.

The EW Environment (S₅). The real world EW environment is a collection of friendly and enemy electronic and weapon systems. The WST EW environment attempts to duplicate the real world. It and its interfaces to other WST subsystems are affected by the first, third, and fourth major trends in EW simulation. The WST EW environment consists of a set of JARMS.* JARM is an acronym which stands for jammer, artillery, radar or missile system. It is generic term for all simulated friendly and hostile systems external to the simulated air vehicle which can search for the simulated air vehicle, track it, launch simulated weapons against it, jam its radar or communications, etc. It includes simulated airborne and ground based jamming systems, early warning radars, acquisition radars, ground control intercept radars, anti-aircraft artillery systems, surface-to-air missile systems, airborne interceptor systems, television stations, transponders, beacons and communications systems. In order to completely simulate the EW systems in the environment the JARM consists of various elements as illustrated in Figure 2. The emitter provides simulation of the electromagnetic characteristics of the real world system represented by a JARM; it forms I₃₃. For real world systems with a vehicle the JARM platform provides the simulated dynamics as well as the proper representation on the visual and sensor systems. A site provides the same function for real world systems which are fixed. JARM tactics provide the basic rules of JARM operation and with the JARM Countermeasures Evaluator (JARMCE) and

JARM Weapons is involved in war gaming simulation, JARM weapons also are represented on the visual and sensor simulation.*

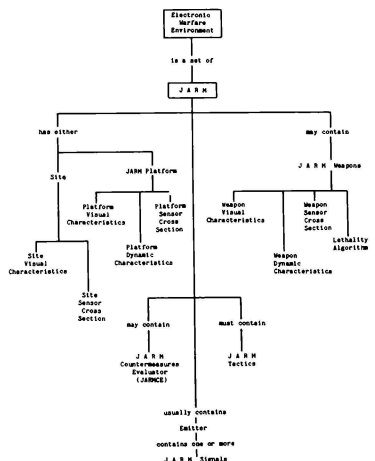


Figure 2 JARM Elements

The EW Equipment (S₃). Real world EW equipment is designed to perform the ECM task. The simulated EW equipment attempts to fully duplicate the real world EW equipment. The EW equipment and its interfaces to other WST subsystems are affected by the second, third, and fourth major trends in EW simulation.

Expansion of the EW Environment

The simulated EW environment has been significantly expanded on the new WSTs. However, to understand this expansion, we must first look at the various types of simulated EW environments.

Types of Electronic Warfare Environments. The EW environment has previously been defined as a set of JARMS. There are three types of EW environments that are of interest in WSTs. These are:

- The JARM list.
- The mission scenario.
- The instantaneous electronic warfare environment (IEWE).

*The term JARM and the remaining terminology in Figure 2 has recently been invented by the Engineering Division of the Simulator System Program Office, Aeronautical Systems Division in an attempt to obtain more precise meanings for terms used in EW specifications, etc. The terminology is not used in either new WST programs or other EW simulation devices. In defining the device capabilities in this terminology as is done in this paper, some minor approximations are used.

* Not all JARM elements are required to be simulated on all WSTs.

Relationships between these types are illustrated in Figure 3.*

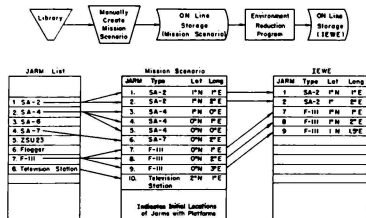


Figure 3. Simulated Electronic Warfare Environments

The JARM list is the list of real world systems represented by JARMS for a particular WST. It consists of a set of friendly and hostile systems, identified by a type designator (e.g. SA-1, ZSU-23, F-4E, etc.), which are available for inclusion in any WST training exercise. Each system must be programmed to include all applicable JARM elements and stored in a library for call-up by type designator for use in a mission scenario.

The mission scenario is the total set of JARMS encountered in a WST training exercise. It consists of a set of JARMS which result from a mapping of the JARM list into a set of locations (initial locations for platforms) as illustrated by Figure 3. The maximum mission scenario which can be provided for any WST is limited because data associated with JARMS must be stored in computer memory or real time accessible mass storage and some computer processing must be done to produce an IEWE.

The IEWE is a subset of the mission scenario consisting of all JARMS which interact with or act upon the simulated air vehicle or EW equipment at an instant of time. The maximum IEWE is limited by:

- The computer resources, time and memory, required to process each JARM.
- The capacity of special purpose hardware called audio/video generators to produce the audio and video associated with the real world system represented by the JARM.

The IEWE is produced from the mission scenario in real time by the environment reduction program.

Expanding the Environment. Most of the new WSTs represent an expansion of one or more of the three types of electronic warfare environments.

* Names for JARMS other than those representing US systems, which are used in Figure 3 and the rest of this text, are chosen from reference 15.

The concept of a JARM list is used on the A-10 and B-52 WSTs. It has been used in past WSTs. The JARM list for the F-15 WST, prepared in 1971, contained only 30 JARMS. The JARM list for the A-10 WST contains 94 JARMS, and the B-52 list contains 159 JARMS.^{5,6,7} The major impact of expanding the JARM list is that simulator contractors are forced to analyze intelligence data and program the elements for more JARMS.

Expansion of the JARM list allows easy creation of mission scenarios which represent almost all combat situations. Operators can practice missions in Eastern Europe one day, the Middle East the next, Asia the next. Mission scenarios for new "trouble spots" can easily be developed.

In WSTs prior to those listed in Table 1, there was a very limited mission scenario as illustrated by Table 3. This was compensated for by allowing the instructor to delete, reinitialize, relocate, and "fly" JARMS during training exercises. The concept of a large mission scenario allows the problem to proceed without instructor intervention. Thus, the instructor can concentrate on monitoring and evaluating student performance. The capability for instructor control of JARMS has been retained in the new WSTs, because many Air Force personnel believe it provides additional training flexibility.

TABLE 3 JARMS per Mission Scenario^{5,6,8,9,10,11}

New WSTs	Past WSTs
B-52 - 900	F-111 - 16
A-10 - 100	F-4 - 9
F-5E - 30	F-15 - 61

The use of an expanded mission scenario generates the need for an environment reduction program to convert the mission scenario to an IEWE.

The expansion of the maximum IEWE has had the most impact on EW simulation. As the maximum instantaneous electronic warfare environment grows larger, more computer time, computer memory, and audio/video generators must be devoted to generating it. The maximum IEWE is usually defined in terms of total JARMS, emitters, JARM signals, and JARM platforms. An emitter (See Figure 2) is the total simulated electromagnetic emission system associated with any JARM. It consists of one or more JARM signals. A JARM signal is a simulated transmitted electromagnetic impulse, or series of impulses, which may be defined in terms of parameters such as frequency, modulation, beam pattern, scan characteristics, pulse width, pulse repetition interval, etc. A JARM platform, as previously discussed, is the simulation of the vehicle associated with the real world system represented by the JARM.

Current B-52 EW training is done in the AN/ALQ-T4 simulator. The maximum IEWE is 24 JARMS with up to 52 total JARM signals.^{12,13} The

Expendables consist of chaff and flares. Chaff is released in an attempt to create false returns on enemy radar systems. Flares are released in an attempt to divert heat seeking missiles from the aircraft. Effectiveness of chaff and flares depends on many complex factors.

The preceding paragraphs have discussed real world EW equipment for the ECM missions of the aircraft simulated by new WSTs in a generic manner. As indicated in Figure 4, not all of the aircraft have all of this equipment.

New Approaches. This paper will discuss in detail only the simulation of panoramic and radar warning receivers. Jamming simulation will be discussed in terms of these receivers. Expendables are easily simulated in the WST computer program system. The receiver portions of transceivers are simulated using simplified versions of the technique for panoramic displays or by direct digital simulation in the WST computer program system.

Several new approaches to receiving equipment simulation have been developed within the last few years. These approaches are not necessarily unique to the new WSTs but they provide realistic simulations of dense environments. The approaches are:

- Stimulation of displays for panoramic receivers.
- Stimulation of aircraft processors for radar warning receiver displays.
- Direct digital simulation of radar warning receiver displays.

With each of these approaches, it is also necessary to generate the audio heard by the operator.

The ALR-20A found in the B-52 is the only panoramic receiver found in the new WSTs. The general approach to simulation is illustrated in Figure 5. The operator first turns the receiver on; this information is sent to the display logic programs which simulate warm-up. When warm-up is complete, the audio/video generator control programs access the IEWE data base. The audio/video generator control programs then process the data and assign parameters to the audio/video generators. There are several functions that may be simulated either in the audio/video generator control programs or the audio/video generator,

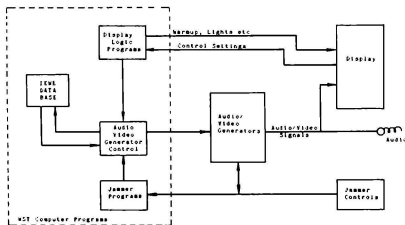


Figure 5 Panoramic Display Simulation

these include attenuation and tuning. The audio/video generator control programs can be performed at low iteration rates (2-10 Hz). The basic function of the audio/video generator is to update the display at the high rate necessary for audio and video fidelity. The audio/video generator runs asynchronously from computer between updates. It updates display and audio information hundreds of times per second. Since jammers also produce signals on the displays, it is necessary to generate these signals. This may be done with direct coupling to the audio/video generators or coupling through the computer programs depending on the update rates needed. This simulation method can be used with actual aircraft displays or facsimiles designed for simulator use.

There are two alternative approaches to simulation of radar warning receivers. Stimulation of radar warning receiver processors is used in the A-10 WST. The concept is illustrated in Figure 6. The actual aircraft processor and displays are used in the simulator. The display logic program operates as in panoramic receiver simulation. The audio/video generator control programs simulate the receiver front end which converts radar signals to video and operates as in panoramic receiver simulation to control the audio/video generators. The audio/video generators provide the same signals to the processor in the simulator as would be provided by a real world EW environment with a one to one correspondence with the IEWE. Jammer programs send information to the audio/video generator control program to control the audio/video generators and provide jamming video to the processor. Since the processor tries to remove such signals it may be possible to omit this jamming interface without degrading fidelity.

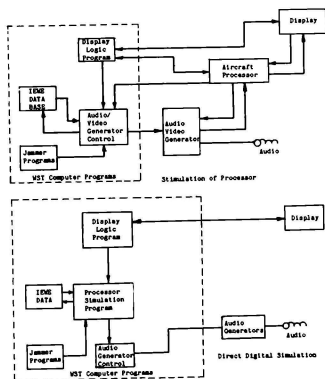


Figure 6 Radar Warning Receiver Simulation

The alternative approach to radar warning receiver simulation is also illustrated in Figure 6. In this approach the processor and video generation equipment to drive it are replaced by a WST computer program module which performs the same functions. This computer program must output

Integration of EW Capability into the WST

Integration of the EW Environment and Other Environment. The interface between the EW

Each JARM has either a JARM platform or a site. A JARM platform consists of:

b. Platform sensor cross section which is the simulation of the real world system on WST sensor system(s).

[illegible]

A site is similar to a JARM platform for a real world system whose simulated location remains fixed during a WST training exercise. JARM weapons, through, weapon visual characteristics, weapon dynamic characteristics, and weapon sensor characteristics provide the same interface for simulated weapons as the JARM platform provides for the JARM itself.

The integration of the EW environment with sensor and visual systems is illustrated in Figure 7. The platform dynamics characteristics compute the position and orientation of platforms. Data on site position is also available. For visual simulation this information used to control the platform or the site visual characteristics which are inserted into the visual scene. The process is accomplished by the WST computer at a high iteration rate (20-30 Hz) to maintain visual fidelity. The sensor integration is similar; however, it may be possible to reduce the computation rate. The interfaces for weapon visual characteristics and weapon sensor cross sections are also identical.

Finally, in interfacing the EW environment with the other environment, the simulated wind must be provided for the computation of platform dynamic characteristics and weapon dynamic characteristics.

Air Vehicle/EW Environment Interfaces (I₂₅) and (I₅₂). In most WSTs currently in the field, the entire mission scenario can be processed as an IEWE.

Where specific limitations on the IEWE could be exceeded logic was built into the instructor console to prevent this situation. When larger IEWEs were necessary, e.g. the AN/ALQ-T4 and AN/ALQ-T5 simulators, the simulators were not WSTs. The pilot could not fly the simulator freely and thus, the flight path through the mission scenario could be identified prior to a training exercise. Since the flight path was fixed, the IEWE could be predicted prior to the training exercise. On WSTs, however, the pilot can control how the simulated air vehicle flies through the mission scenario. Thus, the IEWE cannot be predicted in advance. Since the mission scenario on new WSTs is large and the IEWE is a subset of it, it is necessary to provide an environment reduction program to convert the mission scenario to an IEWE in real time. The maximum IEWE may have limitations with respect to total JARMS, or JARM elements (e.g. JARM signals or platforms). Environment reduction programs are executed at low iteration rates (1 Hz or less) and map the mission scenario into the IEWE based on the element limits, radar horizon, and an arbitrary priority scheme. None of the functions of the environment reduction program except for the check of radar horizon correspond to the real world situation. Real world equipment will handle any environment although performance may be degraded. However, since computer resources and audio video generating equipment are required to process an IEWE, it must be limited. Thus, the WST interface, I₂₅, only partially corresponds to the real world.

The emitter also interfaces with the air vehicle to provide jamming of sensors as applicable (I₅₂).

The EW Equipment/Air Vehicle Interface (I₂₃₂)

This interface is very straightforward. The real world EW equipment is carried by the real world air vehicle. The interface is simulated largely within the WST computer program system. The major elements of this integration are:

a. EW equipment operates off aircraft power and must respond appropriately to all changes in state.

b. Different ECM pods added to different air vehicles produce unique weight, balance, and drag effects on the air vehicle. The significant effects should be simulated for each different pod. This requires the capability to vary the simulation of weight, balance, and aerodynamic coefficients as a function of pod configuration.

c. Expendables may affect weight and balance significantly.

d. Air vehicle attitude affects the signal power received and transmitted.

e. Jamming may affect sensors and communications on the air vehicle.

Integration of EW Equipment with Other Environment (I₃₄₃). When simulated flares are dropped there should be an appropriate flash on the visual system. This interface is easily accomplished

through the WST computer program system.

The thunderstorms which appear on the WST sensor or visual systems should also cause interference on panoramic receivers. This interface is accomplished by sending storm indications from the sensor simulation through the WST computer program system to the audio/video generators which produces the interference.

Simulation of War Gaming

Simulation of war gaming is the fourth major simulation trend; it is implemented on most new WSTs. In the context of Figure 1 it involves all subsystems and most interfaces, however I₂₅, I₅₂, and I₃₅, are especially important. The simulation is based on intelligence data or studies and engineering estimates where intelligence data is not available. It is accomplished largely within the computer program system. Low iteration rates, 1 Hz or less, can be used.

The problem begins with the operator, who using information obtained on receiving equipment takes action to counter enemy EW systems. This action may take the form of use of the countermeasures equipment or maneuver of the air vehicle. Transceiver systems may also take action independently of the operator.

In the real world, maneuvers, jamming and chaff are used to prevent ground based EW systems (S₅) from tracking the air vehicle (S₂) and launching weapons against it, ordnance is used by the air vehicle to destroy the enemy EW systems. When maneuvers (I₂₅), jamming (I₃₅), and chaff (I₃₅) are initiated in the WST, the JARMCE analyzes them to determine how well the simulated aircraft can be tracked. The derived information is sent to the JARM tactics element. If conditions are right, simulated weapons may be launched. If they are not right, the JARM tactics elements will adjust signal parameters to try to overcome the countermeasures. The signals parameters are transmitted to the EW equipment closing the loop. There may be iterative relooping. The JARM tactics element may be linked with other JARMS. Thus, where intelligence is good the JARM tactics element allows sophisticated simulation of real world air defense networks. Ordnance simulation will disable a JARM based on the simulated proximity of explosion.

When a simulated weapon is launched or fired (I₅₂), the JARMCE also evaluates the effectiveness of countermeasures against the simulated weapon. In the real world, the countermeasures include maneuver, release of flares to divert infrared missiles, the use of jamming and chaff. The JARMCE provides inputs to the JARM weapon dynamics characteristics to determine the simulated point of weapon impact or explosion. Based on this point of impact or explosion, the lethality algorithm introduces various malfunctions to simulate battle damage.

Figure 8 illustrates war gaming simulation. Since it is dependent on intelligence and enemy operators, results may not be absolute. Insertion of probability models into the various elements has been considered. The simulation must also be easily changed as a new intelligence becomes available.

11. SSP0-07878-4005A, Prime Item Development Specification for a Trainer, Flight Simulator, ASD/SD24, 1 Oct 1977.

12. Utilization Guide for Operating the B-52G Electronic Warfare Simulator Set, Defense Type AN/ALQ-14 (V-8), Reflectone Electronics Division, Universal Mutch Corporation, 1 Nov 1965.

13. Preliminary TO 43 E4-2-3-2, Technical Manual Maintenance Generator-Programming Group; Change 20, 15 May 1976 to 31 Oct 1962.

14. Malone, Daniel K., Col, USA, "Air Defense of Soviet Ground Forces", Air Force Magazine, March 1978, p. 78-83.

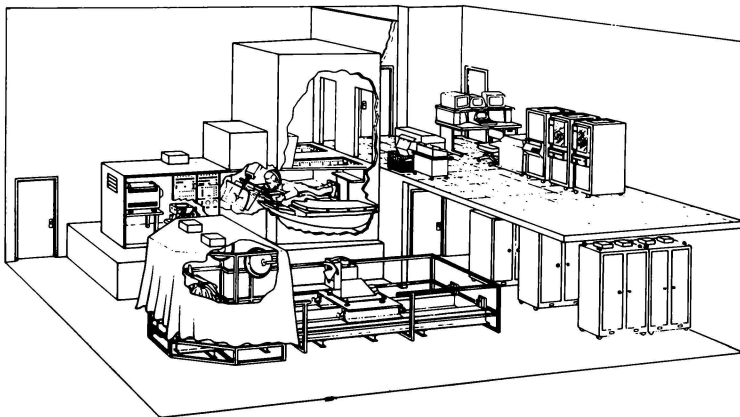
Joseph LaRussa
Farrand Optical Company, Inc
Valhalla NY 10595

F. Gerard Albers
University of Dayton
Dayton OH 45403

Samuel J. Rosengarten
Hybrid Division, Computer Center
Aeronautical Systems Division
Wright-Patterson AFB OH 45433

Aloysius J. Schneider, Captain, USAF
Simulator Division
Aeronautical Systems Division
Wright-Patterson AFB OH 45433

Richard J. Heintzman
Simulator Division
Aeronautical Systems Division
Wright-Patterson AFB OH 45433



Abstract

Training of boom operators for the KC-135 Refueling Tanker is currently limited to actual aircraft missions. Strategic Air Command documented, in recent years, a requirement for a high fidelity ground based simulator which could potentially drastically reduce the requirement for airborne training missions. Aeronautical Systems Division of the Air Force Systems Command recently completed, in house, the development of a highly unique and realistic KC-135 Boom Operator Part Task Trainer (BOPTT). The BOPTT includes many innovative simulation concepts. The key component of this trainer is an articulated model boom which is physically modeled within a virtual image optical system. This model boom was conceptualized by

Mr. LaRussa of Farrand. The primary advantage of the optically modeled boom is that it provides true parallax to the viewer as he moves within the viewing envelope. This paper describes the training requirement and system hardware and software design features. It discusses problems associated with operating an articulated three-dimensional model in optical space. Lessons learned associated with several design areas are covered. It describes the innovative use of a vendor supplied "Real-time Monitor" and FORTRAN compiler in a simulator environment. Along with the structure of the overall software system, various software models are discussed.

Introduction

The energy crisis of recent years has caused the USAF to re-evaluate its flight training program with a goal of reducing fuel consumption by reduced flight hours in aircraft. The obvious solution to meet this goal was to increase the use of training flight simulators. Increased usage involved not only more training hours in simulators, but broader application to include all flight tasks.

The Air Force in 1973 developed a five year master plan for simulators. This plan addressed training simulators for current and planned aircraft systems, research and development programs, and planned production programs.

In prioritizing simulator acquisition, particular importance was placed upon what was referred to as the large burners. High on this list were the B-52 and KC-135. For this reason, a large scale acquisition program was formulated for weapon system trainers (mission simulators) to support these aircraft. One highly critical training task involving these aircraft is aerial refueling. This task involves an unusually large amount of training time which would tie up the weapon systems trainers. For this reason, requirements for aerial refueling part task trainers to train B-52 pilots and aerial refueling trainers to train KC-135 boom operators were documented. Strategic Air Command (SAC) expressed the need for a KC-135 Boom Operator Part Task Trainer (KC-135 BOPTT) in SAC ROC 2-74, dated 25 Jan 74. The program for development was approved, however, funding limitation forced the program to be conducted in-house. Approval for in-house development by Aeronautical Systems Division (ASD) of Air Force Systems Command was granted in August of 1975.

Approach

A preliminary definition study was completed defining a hardware approach for the KC-135 BOPTT development. Several ground-rules were adhered to during this study. First of all, it was decided that the Farrand "True View" Display would form the basis for the visual system design. Secondly, emphasis was placed upon simplification of the visual system with maximum usage of existing designs in order to minimize non-recurring costs and insure reliability and low life cycle cost for the production systems. Dual approaches were recommended in several critical areas.

Initial software was to be completed on the ASD Computer Center XDS Sigma 7 and transferred to the SEL 32-55. All software was to be in FORTRAN. Tradeoffs investigated relative to the Farrand display included field of view, focal length of the display window, and methods of articulating the boom. Although it was agreed that the best method of generating the receiver aircraft image was a television camera/gimbaled model, many variations to the implementation of such an image generator were investigated. Included were types of camera tubes, methods of image articulation, types of gimbals, methods of closing the loop between a physically modeled boom and an imaged receiver aircraft, and many different types of special effects.

It was determined early in the program that instructor/operator features would make maximum use of computer software and display terminal features.

Figure 1 is a block diagram of the total KC-135 BOPTT system. The boom pod in this case was taken from a wrecked aircraft and refurbished. The infinity window is a Farrand "Pancake Window" and is located in front of the boom operator. It is mounted in the position of the actual aircraft window and presents the scene to the viewer at the correct position and distance. Servos for the boom are mounted above the pancake window. A high gain rear projection screen inputs the receiver aircraft image from a TV projector. The background scene is brought into the display with a beam-splitting mirror. The receiver aircraft image camera is mounted on a surplus NASA Apollo Simulator range bed and views the 3-axis gimbaled model. One unique feature of the KC-135 BOPTT is the servo control rack which allows substitution of synthetic drive signals for operating computer signals to check out hardware system problems. Interface or linkage of the computer to system hardware is accomplished with the commercial Real Time Peripheral Equipment (RTP).

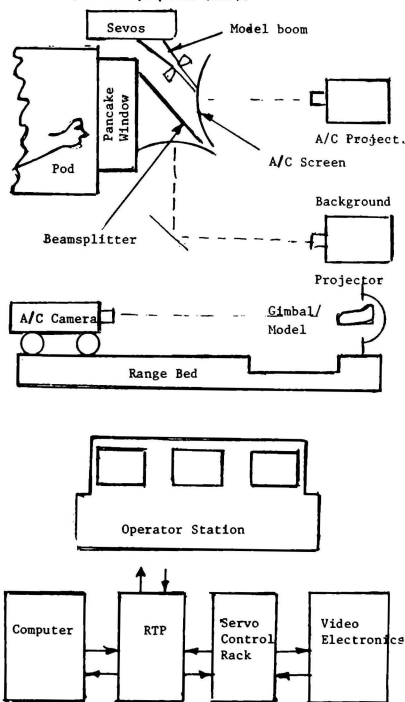


Figure 1

Display Design Criteria

The requirement was easily stated but the approach to the problem was unique in that the simulator would probably be much more demanding in terms of the visual cues that would have to be provided as compared to the typical aircraft simulator.

It is known that the training of a boom operator must, of necessity, require faithful visual cues since his task is one which depends upon coordinated responses to visual cues for its successful execution. As a matter of fact, the environment of the trainer should be made to duplicate the environment that exists in the actual refueling operation as closely as possible if the maximum training value is to be extracted from the Part Task Trainer. This approach becomes even more significant when we realize that we cannot differentiate which visual cues are most important, let alone the extent of their interdependence. It is, therefore, a good assumption that we will obtain the greatest return in training value by providing the maximum fidelity.

The question to be considered is what constitutes maximum fidelity for the Boom Operator's visual environment? From experience, the Farrand Optical Co, Inc, as the originator of large eye relief Infinity Displays, has determined that at the very least the following cues should be provided:

1. True angular sizes of receiver aircraft and boom must be subtended at the operator's eyes to provide true angular velocity cues.
2. True relative parallax between boom and receiver aircraft and between receiver aircraft and background should be duplicated.
3. Relative angular and relative translational rates must be reproduced in accordance with tanker, receiver and boom dynamics.
4. Boom dynamics and boom response, with respect to operator controls, must be faithfully reproduced.
5. As high a resolution image of the boom, boom nozzle extension and receiving portion of the B-52 as possible should be provided. Of lesser importance, but adding subjectively to the quality of the simulation are the following cues.

- a. Color cues, where possible.
- b. Motion effects within the Boom Operators environment.
- c. A field of view approximately equivalent to the real field of view available through the KC-135 window.
- d. As accurate a duplication of the KC-135 window as possible.

If we were able to experience an actual refueling mission we would understand why this is necessary. For example, Figure 2 illustrates a refueling operation in progress as seen out of the Boom Operator's window. Note that the upper end of the boom is close to the observer's eye while the nozzle end can be as far as 50 feet away.



Figure 2 - VIEW OF A REFUELING B-52 FROM OPERATOR'S WINDOW

The nose of the aircraft is noticeably much closer than the tail section by approximately 150 feet and the background is at infinity.

The focus of attention is obviously at the nozzle which is neither the closest nor the farthest image from the observer - quite unlike the typical aircraft visual simulator where all detail appears at infinity. The point of interest, the nozzle, will exhibit motion cues relative to the refueling aircraft which vary not only along the length of the boom but also with respect to aircraft depth and the cloud or terrain background.

To reproduce this scene on a one-to-one basis with the real world, relative distance cues must be accurate. We detect relative distance between objects using four predominant perceptual cues and these are relative size, occultation of one object by another, parallax and stereopsis. Figure 3 illustrates these four cues, three of which are immediately apparent but the fourth, or parallax, requires head motion to be seen. The parallax cue might be the most importance since it readily provides relative distance information between nozzle and receptacle. As an illustration of the usefulness of this cue we may observe the results of moving one's head from a central position in the boom operator's window to the extreme right in Figures 4, 5 and 6 respectively. The effect shown can only be achieved with a true three-dimensional view which supplies variable apparent distance of objects from the closest visible detail to objects at infinity.

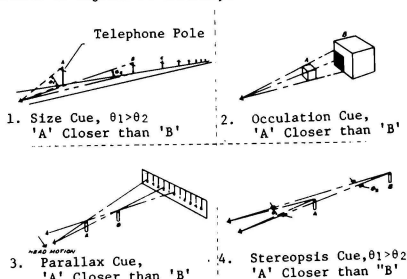


Figure 3 - RELATIVE DISTANCE CUES



Figure 4 - VIEW THROUGH PANCAKE WINDOW FROM CENTERED WINDOW POSITION



Figure 5 - VIEW THROUGH PANCAKE WINDOW FROM EXTREME LEFT WINDOW POSITION

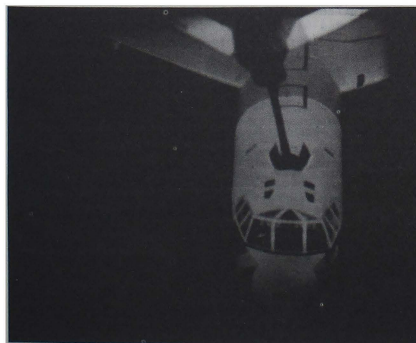


Figure 6 - VIEW THROUGH PANCAKE WINDOW FROM EXTREME RIGHT WINDOW POSITION

Farrand conceived of just such a system providing variable apparent distance, true parallax and stereopsis and called it the TRUE VIEW SYSTEM.* The device is shown schematically in Figure 7. Here we see the tilted birefringent PANCAKE WINDOW*** which eliminates all ghost images from the pupil, the fixed terrain input screen at infinity focus, the tilted, servo-driven receiver aircraft input screen and the servo-driven boom model. This relatively small image generation and display system provides a view which is exactly analogous to the real world view in terms of true apparent sizes of objects, true apparent variable distance of objects and true angular velocities in the field of view. Figure 8 illustrates what the true view system generates for the observer.

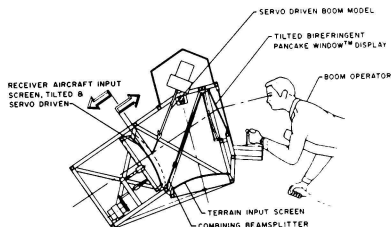


Figure 7 - FOCI TRUE VIEW SYSTEM

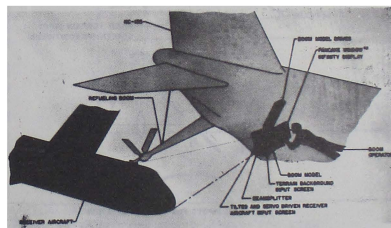


Figure 8 - FARRAND TRUE-VIEW BOOM OPERATOR PART TASK TRAINER VISUAL SYSTEM

How is this three-dimensional dynamic display achieved? When looking through an infinity display there is one position of the focal plane which projects all objects in that focal plane to apparent infinity (see Figure 9A). If the focal distance is shortened all objects in that plane will appear to be closer as for example, point B which we have elected to make appear at a distance of eight feet. The range between these two focal plane positions is called "foreshortened optical space" and by locating images anywhere between these two focal plane positions we can project objects from eight feet to infinity.

* Patent 40 933 47 (6 June 1978)
**Patent 27356 (9 May 1972)

Figure 9B shows how a boom model can be constructed in space to extend from eight feet to fifty feet. The boom model is viewed directly through the optical system which magnifies it and so the limit of resolution for this input is the human eye.

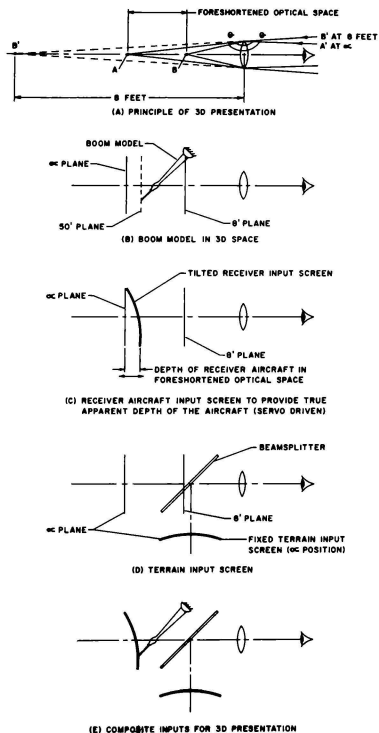


Figure 9

Similarly, Figure 9C illustrates the tilted receiver aircraft input screen which is servo-driven to bring the small image receiver aircraft from infinity to the magnified image refueling position. The tilted screen increases the apparent depth of the aircraft from nose to tail as the image grows on the screen providing a very important dynamic cue.

Figure 9D shows the terrain input screen which is fixed at the infinity position. The beamsplitter shown here combines and superimposes the terrain background on the receiver aircraft and boom inputs. The superposition of background on the aircraft and boom is not noticeable but the natural occultation of the aircraft image by the boom model provides

exceptional realism. Figure 9E illustrates the Farrand TRUE-VIEW SYSTEM in schematic form.

Optical System Modeling

General

The object space behind Farrand's pancake window produces a highly compressed infinity space in which to model the "real world." This object space is non-linear longitudinally and telecentric radially. Therefore objects in that space (e.g. the model boom) must be mathematically mapped into that space. In other words, the boom model must be distorted so that they will look correct through the window. Similarly, linear or angular motion in the real world must also be mapped into the object space so that it appears realistic to the boom operator. Furthermore, the rear-projected receiver aircraft image must be moved from infinity into the point of contact and, once contact is made by the boom operator, the model boom, aircraft projection screen and aircraft image must all move in very close harmony to provide the illusion of an actual refueling.

In order to model both the static boom and object movements within the object space a set of mapping equations was developed. The first equation

$$H = F\theta$$

describes the telecentricity of the "pancake window" (see Figure 10). That is, the distance H of the object space point of interest from the optical axis is equal to the focal length F times the solid angle θ subtended to the apparent real world point of interest. The rotational angle ROT is identical in the "real world" and the object space. The second equation,

$$RNGS = - \frac{F^2}{RNG + F}$$

describes the desired distance $RNGS$ of the object space point of interest from the infinity plane in terms of the apparent real world range RNG and the focal length F . However, the object space curves backward away from the eyepoint as the distance H increases from the optical axis due to the geometry of the "pancake window." Therefore, a plane surface perpendicular to the real world optical axis will actually have a radius of curvature R in the object space. In other words, if a rear projection screen with a spherical radius R is placed tangentially perpendicular to the simulator's optical axis, the image placed on the screen appears to be entirely in one vertical plane. (In actuality, the screen is tilted backward at the top so that the receiver aircraft's tail section appears farther from the eyepoint.)

As a consequence of the screen curvature, a point of interest moves back toward the "infinity plane" as the distance H increases. The amount of this movement (which must be compensated for by screen displacement) is the value of the screen's sagitta given by

$$SAG = R - R^2 - H^2$$

which is the third governing equation. The radius R for the BOPTT has been set at 80 inches.

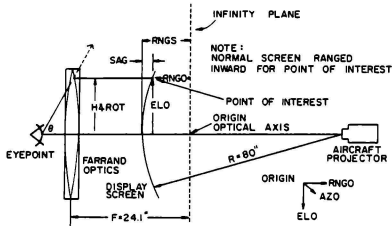


Figure 10 - OBJECT SPACE DESCRIPTION

The mapping operation consists of four distinct processes:

1. Determining the rectilinear coordinates (x,y,z) of a point-of-interest in the "real world" with respect to the optical axis.
2. Calculating its polar coordinates (RNG, ROT, θ).
3. Calculating the corresponding polar values (RNGS, H) values in the object space (ROT remains constant), and
4. Resolving the polar object space values into rectilinear object space values (RNGO, AZO, ELO).

The final RNGO, AZO and ELO values are then employed in the task at hand.

Model Boom Construction

The task of mapping the boom from the real world into the object space involved a concerted effort of obtaining thousands of coordinates of the real-world boom, computer programming, data entry, computer processing, and computer plotting. This series of procedures produced profile projection plots and section plots of the object space boom (see Figure 11). The computer software was designed so that the set of boom coordinates could be mapped into the object space for any valid azimuth or elevation angle of the real world boom (20° to 40° down elevation, 15° left to 15° right). As a result, profile projection plots were obtained for numerous positions of the boom throughout the envelope. It was discovered that a mathematically correct object space boom will change shape very noticeably from one position to another. For example, the boom centerline has a definite curvature and the ruddervators maintain almost a constant distance from the infinity plane as the boom is rotated in azimuth as shown in Figures 12A through

12D. Similarly, a very pronounced elongation can be seen in Figures 12E and 12F as a result of an elevation change. Obviously, only one boom position can be represented accurately by the rigid model boom and optical error will occur whenever the model boom is moved from that position. With this in mind, the mid-envelope position (30° elevation, 0° azimuth) was chosen for modeling the rigid part of the boom.

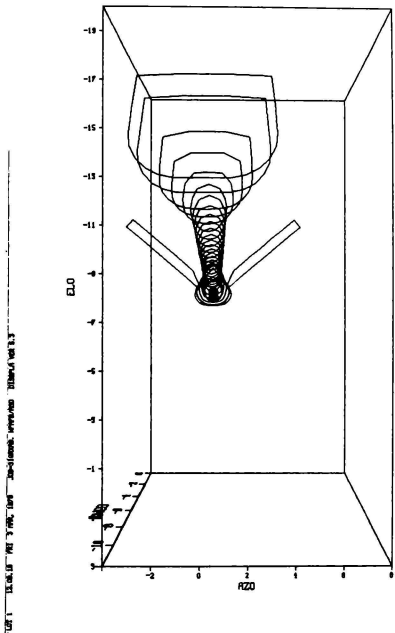


Figure 11 - SECTION PLOTS - BOOM POD VIEW

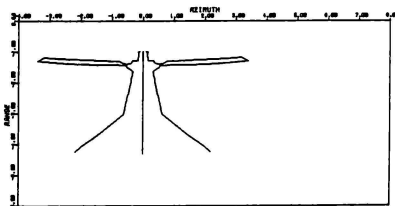


Figure 12A - KC-135 BOPTT MODEL BOOM OBJECT SPACE

TOP PROJECTION

Pitch = 30.0
Yaw = 0.0
RC = -2.7
RO = 0.0

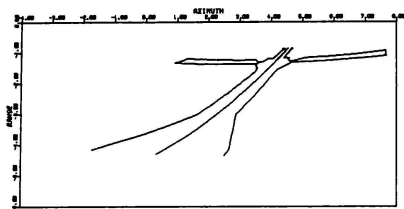


Figure 12B - KC-135 BOPTT MODEL BOOM OBJECT SPACE
TOP PROJECTION

Pitch = 30.0
Yaw = 16.0
RC = -4.8
RO = 16.0

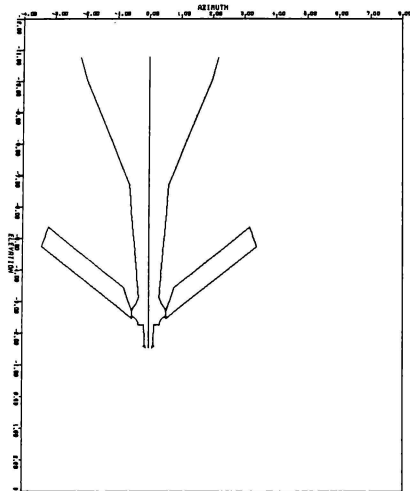


Figure 12C - KC-135 BOPTT MODEL BOOM OBJECT SPACE
REAR PROJECTION

Pitch = 30.0
Yaw = 0.0
RC = -2.7
RO = 0.0

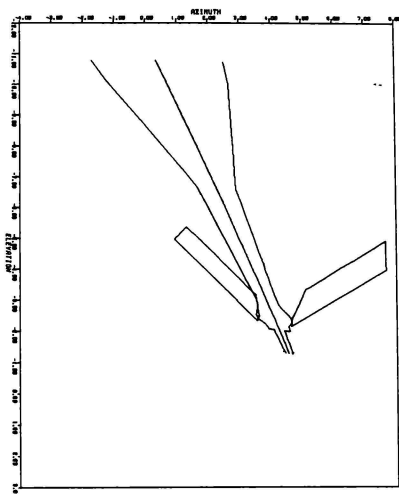
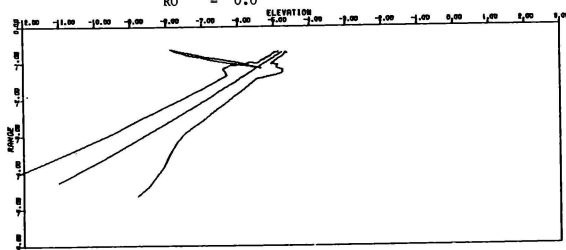


Figure 12D - KC-135 BOPTT MODEL BOOM OBJECT SPACE
REAR PROJECTION

Pitch = 30.0
Yaw = 16.0
RC = -4.8
RO = 16.0

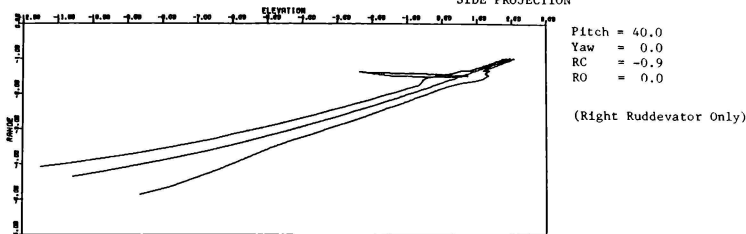
Figure 12E - KC-135 BOPTT MODEL BOOM OBJECT SPACE
SIDE PROJECTION



Pitch = 20.0
Yaw = 16.0
RC = 0.0
RO = 10.0

(Front Ruddevator Only)

Figure 12F - KC-135 BOPTT MODEL BOOM OBJECT SPACE
SIDE PROJECTION



Real-Time Boom Control

One of the big payoffs of the analytical study described thus far was the ability to predict the articulation which would be needed to construct a realistic enough display. The key word here is "enough" because an infinitely variable shape was the ideal. As a result of studying drawings of the type in Figure 11, ten servo drives were identified as being necessary to produce the required realism. Likewise, the travel limits were also determined and the servo systems were design accordingly.

The real-time processing in the BOPTT was carried out in such a manner that the equations of motion of the real-world boom were solved during each computer frame as shown in Figure 13. The boom orientation provided the location of specific points of interest on the real world boom so that the corresponding object space locations could be calculated as described above. This object space data was appropriately correlated to produce the values to drive the above mentioned servos. These servos are typical closed loop analog devices but one very noteworthy point must be mentioned. All ten servos were operated independently with no feedback into the processor drive equation! Linearity and dynamic response were excellent.

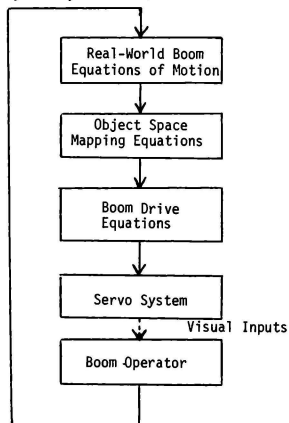


Figure 13 - MODEL BOOM CONTROL CONFIGURATION

Hardware Subsystems

Student Station

The student station consists of an actual rear section of a KC-135 tanker aircraft (the boom pod) including the student's controls, communication system and the pallets upon which the student, instructor and observer lie. Since the instructor and observer positions are the same as in the KC-135, this simulator can be used to train student instructors. The normal observation window has been replaced by the Farrand "Pancake Window" with a field of view of 30 high by 60 wide. TV cameras are placed so that the system operator can monitor the student's controls and the image the student is viewing through the window.

The boom pod is modeled in detail, as a boom operator must become intimately familiar with the operation of each control - and how to overcome any "malfunction." Some of the items that are modeled are the primary signal system; the normal/override mode; the automatic/manual telescope at disconnect switch; the hoist motor and latching levers, used for stowing the boom; the oxygen panel; the illumination starting switches; and the sighting door lever and its effect on a portion of the boom hydraulics.

Control loading is included on both the telescope and ruddervator controls to provide the normal feedback sensations. The control loading devices also introduce the symptoms of some of the malfunctions such as a locked ruddervator condition.

Speakers within the boom pod provide audio supplementation of the boom visual cues. In addition to the ambient boom pod noise, the student hears the sound of the boom extending/retracting, and of "clunks" in the boom system (the clunks are of varying intensity, depending on terminal boom rates). The sounds are generated by a micro-computer and are controlled by the main simulation program.

Control Station

The control station consists of the two TV screens for aid in monitoring the student station; a control panel with volume controls for the boom pod noises; audio controls for communication with the student and/or instructor; digital "stop-watches" hard-wired mission control switches; pilot-director lights for aiding the receiver pilot in flying to the ideal refueling position;

manual slew controls which allow the operator (instead of the student) to "fly" the boom or receiver; a computer terminal keyboard; and two terminal display screens.

Image Display

Display Inputs

The display system has three inputs: (1) the receiver aircraft image, (2) the background image, and (3) the model boom itself. The model boom will be discussed in detail in a later section. At this point, however, it is important to note that the model boom must be very accurately positioned in the object space of the Farrand "Pancake Window" so that its image will appear at the proper size and distance to the boom operator.

Receiver Aircraft Image

The receiver aircraft image is projected by a General Electric (GE) light valve onto the aircraft screen. The rear projection screen has a gain of eight. The high projector brightness and high screen gain provides a display brightness of six foot-lamberts in spite of the combined 0.6% transmissions of the beamsplitter and Farrand window. The telecentric geometry of the display provides even brightness across the field of view in spite of the high gain screen. Brightness does fall off rapidly, however, as the viewer moves away from the design eyepoint.

Since the boom operator uses both stereoscopic and parallax cues to judge distance to the receiver, the virtual image of the receiver must be dynamically shifted to appear anywhere from 30 feet to 7500 feet from the viewer. This shift is accomplished by servoing the aircraft screen to move it from the infinity focal plane forward as much as 1.5 inches. For proper visual cues, the nose of the receiver is made to appear closer than the tail by tilting the top of the screen back by six degrees. This tilt increases the required fore and aft screen range to about two inches.

Background Image

The background image is projected by a 16 mm motion picture projector onto the second (fixed) display screen. This screen is always at the infinity focal plane, and the ranging ability of the aircraft screen provides realistic depth perception between the aircraft image and the background. The background brightness is kept lower than the receiver brightness to avoid objectionable bleedthrough in the combined image.

The 16 mm projector uses a film loop that repeats every 10 or 15 minutes. It has five speeds from 18 to 45 frames per second, controlled by the computer as a function of tanker altitude and airspeed. The projector is mounted in a gimbal to roll the background image for simulation of tanker roll in a turn. Background brightness is reduced for dusk simulation by rotating a neutral density filter wedge in front of the projector lens.

Boom Mechanization

The Real World Boom

The actual KC-135 refueling boom has five axes of articulation; (1) elevation, (2) azimuth, (3) left rudderator, (4) right rudderator, and (5) nozzle telescope. When in contact, relative motion of the tanker and receiver causes the telescoping part of the boom to bend or flex. This flexure is equivalent to having two additional axes; magnitude and direction of flex.

The boom operator has direct control only over the rudderators and the nozzle telescope. When not in contact, he controls the angle of attack of the rudderators to fly the boom over a wide range of azimuth and elevation. For refueling, he aligns the boom nozzle with the receiver receptacle and extends the telescope to make contact. When in contact he uses his rudderator control to minimize the amount of flex.

The Model Boom

Optical Distortions

A true scale model of the KC-135 refueling boom could be mechanized by driving the seven axes mentioned above. (The two flex axes must be driven since there is no physical receiver model in the display to apply side forces as in the real world.) Unfortunately as was discussed earlier in the paper, the relationship between the optical space, in which the boom is modeled, and real world space, in which its virtual image must appear, is very nonlinear. The model boom azimuth drive must be capable of $\pm 50^\circ$ so that the virtual azimuth will appear to range between $\pm 15^\circ$. The model boom length must be varied so that the length of the virtual image will appear constant.

Moving the model boom azimuth to much larger angles than in the real world gave the boom operator unrealistic perspective views of the boom. The ice shield appeared twisted, one rudderator seemed to come back into the boom pod, and the other rudderator appeared very large and miles away. These distortions were compensated for by adding extra axes of articulation to the model boom. The need for such large azimuth angles was reduced by driving the entire model boom and its servo drive mechanisms laterally by ± 2 inches. This reduced the azimuth angles to $\pm 30^\circ$ but some perspective distortions remained. The twisted ice shield was compensated for by rotating the boom model around its longitudinal axis. The apparent distance to the rudderators was controlled by swinging each rudderator axis fore and aft to keep the rudderators in proper image planes. The final boom model has twelve axes of articulation. The first ten axes have independent servo drives as illustrated in Figure 14. The last two are driven through cams connected to boom length and boom rotation:

1. Azimuth
2. Elevation
3. Left Rudderator Angle of Attack
4. Right Rudderator Angle of Attack

5. Nozzle Telescope
6. Flex Direction
7. Flex Magnitude
8. Boom Length
9. Boom Rotation
10. Lateral Pivot Point Shift
11. Left Ruddevator Swing
12. Right Ruddevator Swing

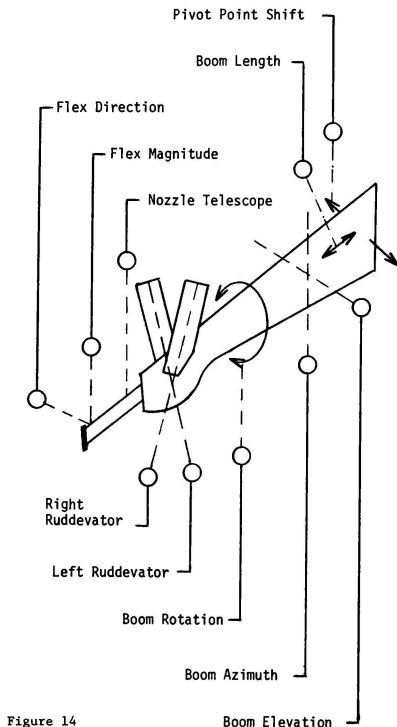


Figure 14

Servo Packaging

When one considers that the model boom is nominally twelve inches long and less than one inch thick, the complexity of the packaging problem becomes apparent.

The most difficult packaging problem was the combination of nozzle telescope with flex. The telescoping part of the model had to be less than 0.25 inch thick and had to vary in length from 0.5 to 2.5 inches. The flex mechanism could not be external to the telescoping hardware without being visible to the boom operator or interfering with the ruddevator drives. The

solution was to fabricate the telescoping nozzle from a tightly wound steel spring and insert the two-axis flex mechanism inside the spring. See Figure 15.

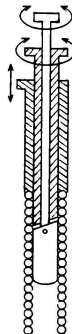


Figure 15 - NOZZLE TELESCOPE AND FLEX

The arrangement is three nested shafts. The figure is drawn out of scale for clarity; the inner shaft is actually about three feet long. The outer shaft slides over the inner pair to drive the spring in and out to simulate nozzle telescope. When the inner shaft rotates with respect to the middle shaft, the cam surfaces forces the tip of the device to bend, taking with it the spring. Rotating the inner and middle shafts together controls the direction of flex.

The entire assembly is inserted down the center of the model boom with the servo drives at the top of a tray which also holds the drives for three other axes. The model boom and the tray with its six servo drives is moved up and down over a ten-inch range by boom length drive. This combined seven-axis assembly is mounted inside a two-axis gimbal for boom azimuth and elevation. The outermost servo is the lateral pivot point shift.

Receiver Image Generation

Receiver Model

As viewed by the boom operator, the receiver aircraft image must have all six degrees of freedom. The three rotational degrees are obtained by mounting the receiver model on a three-axis gimbal. The model was fabricated from fiberglass rather than plastic to withstand the heat of two 1000-watt metal-arc lamps used for lighting.

All significant detail including lighting is included on the model. Since the detail had to change as a function of day, night, or dusk simulation, the model is painted in the primary colors, red, green, and blue. Subtractive dichroic filters are used selectively in front of the camera to create the impression of night or dusk conditions or to simulate failure of the lighting around the receiver receptacle. With this technique, the metal-arc lamps never need to be turned off, and the subsequent delay at turn-on is avoided.

Receiver Camera

The receiver camera operates at 1023 line, 30 frame with 2:1 interlace. The tube is a 1.25 inch plumbicon chosen for high resolution and low image retention.

The three translational degrees of freedom for the receiver image are obtained by a combination of electronic techniques and range bed motion. The 15-foot range bed permits a maximum simulated range of 1500 feet (on the 100:1 scale model). The remainder of the range out to 7500 feet is obtained by increasing the camera scan size for electronic zoom. Increased sensitivity which results from the scan size change is compensated for by a combination of automatic video gain adjustment and rotating a neutral density filter wedge in front of the camera tube. Vertical and horizontal translation is obtained by electronic beam shift in the camera.

Tracking

When simulating contact for refueling, it is important that the boom nozzle appear to be locked solid to the receiver receptacle. As the receiver moves around, it must appear to drag the boom with it, bending the telescoping portion in the process. Errors and non-linearities in the system, especially in the image generation, were such as to make it virtually impossible to drive both the image generator and the model boom open loop.

Most of the early effort at closing the loop involved tracking the receptacle location in the display and moving the boom to keep it over the receptacle. This was accomplished by placing a very small bright light in the receptacle on the receiver model. The location of this bright light was sensed in the video processing, and a special space and time varying pattern was inserted in the video in place of the light. Once the boom operator had flown the boom to contact, a photodiode in the nozzle sensed the special pattern. The output of the photodiode was processed to generate two error signals which were used to drive the boom to keep the nozzle at the receptacle.

This totally closed-loop tracker scheme proved to be very complex and troublesome, especially when playing back pre-recorded missions. Through some experimentation, we found that the positioning accuracy of the model boom and the linearity and stability of the light valve were such as to permit us to operate the system partially open loop. Both the photodiode and the special video pattern were eliminated. The location of the bright light in the video is sensed, but it is used to generate X and Y raster

position coordinates which are compared with the known, correct coordinates in the display image plane. The camera beam shift is then adjusted to place the receptacle at the correct coordinates.

Video Processing

Besides sensing the light defining the receptacle location, video processing is used to provide several special video effects. Normally, the video electronics senses the whitest white and the blackest black in the scene and sets these to preset levels. The remainder of the video information is then spread between the reference levels. The receptacle tracker light is ignored in this processing and is permitted to be compressed to the level of the reference white. For dusk simulation, the reference levels are moved closer together to reduce display contrast.

Scud and visibility effects are simulated by varying the black and white referenced levels. For reduced daytime visibility, the black reference level is brought up, brightening the black levels in the display. The effect is to reduce contrast and wash out the background image. In the limit, the receiver disappears, and the viewer sees flat white over the entire field of view. Reduced night-time visibility is accomplished similarly by lowering the white reference level. In the limit the receiver disappears, and the viewer sees total blackness over the entire field of view. No background imagery is presented for night simulation. Scud is handled the same as visibility except for being random momentary washouts.

Computer System

Hardware Components

The computer system includes a Systems Engineering Laboratory (SEL) mini-computer (SEL 32/55) with 64,000 (32-bit) words of core memory; two portable disk units, each with 10,000,000 bytes of storage, two cathode ray tube (CRT) terminal display screens; an input keyboard; a teletypewriter; a card reader; a line printer; standard, commercially available analog-to-digital and digital-to-analog converters; control lines; and sense lines.

Keyboard and Display Terminals

The operation of the KC-135 BOPTT has been designed around the operator control station and its alphanumeric keyboard and displays. The alphanumeric displays provide visibility for monitoring the activities of the student and the mission status. The alphanumeric keyboard permits convenient control of the training mission.

Together with the manual slew and the audio controls on the panel, the operator accomplishes his on-line tasks by use of the function keys, the number keys, the shift button, and the return key on the keyboard unit. Each function key activates a software process to establish or alter some condition or to effect some maneuver or procedure. There are forty such processes. For example, if the operator presses the fuel flow function key, the simulation equations will allow fluid to flow (if some other system conditions are present). For functions requiring data

entries (e.g., the percent of turbulence) it was decided to have a two-stage key system (function and return keys) so that the operator would have a chance to correct his mistakes or change his mind. The function key implementation allows for much more flexibility than hard-wired push buttons found on most simulators. Some other examples of the use of the functions keys are that they allow the operator to put the mission in a RUN, FREEZE, or RESET Mode; to change the mission from a day to a night or dusk mission; to change the visibility of the receiver; and to simulate a manual latching of the receiver's receptacle to the boom tip. During the pre-flight phase, the speed and altitude at which the refueling will take place is set, as well as the trajectory and time along that trajectory (the flight schedule) that the receiver will take in approaching the tanker from over a mile away. During the in-flight phase, the function keys are used to change such items as the pilot type (one to five proficiency levels), the strength of the wind gusts, and the amount of cloud scud (washout).

Through the control station, the operator can perform some of the duties that are normally performed by the various pilots. This was designed to aid the student's training because, in an actual mission, he must interact with these individuals. For example, he must learn the proper verbal communications, he must learn when to call for an emergency breakaway, and he must learn to discern small changes in receiver distances and be able to tell the pilot to move a few feet in a given direction in order to position the receiver in the boom's refueling envelope. (The latter is simply accomplished in the simulator by the operator's pressing the VERTICAL ADJUST function key and a number key. The receiver will then fly up by the amount keyed.)

The operator can call for one or more of 24 simulated malfunctions to occur either immediately or at a preset condition. The malfunctions are simulations of system failures that can occur during actual refueling missions. It is desired to train the student boom operators to handle such situations before they occur in the air and present an emergency. For example, one of the signal systems may fail, precluding normal refueling procedures, or a boom rudderator may lock up, or the boom may not extend on command.

The operator can monitor the student's performance by looking at the TV screens, or, more comprehensively, by looking at a terminal screen and watching one of the checklists that the student must go through before and after a refueling mission. All of the student's control switches and indicators are tied into the computer, and can be monitored and malfunctioned. The operator can call up some other pages on the screens and watch the mission progress - e.g., he can see the position of the receiver, of the boom, and of the receiver with respect to the ideal boom position. The latter can also be observed by monitoring the pilot director lights.

As an aid to hardware maintenance, the software has a calibrate mode used primarily to check the alignment of the visual system. The operator can monitor and set the states of the logical input and output signals and the numerical values of the analog input and output signals. The

operator can also call for diagnostics to be performed on any group of the interface equipment.

To obtain a history of the mission, the operator can print the terminal screen information onto the line printer. Or, more importantly, he can use the sophisticated record/playback capability for both the visual and audio aspects of the mission. Up to five segments totalling 20 minutes can be recorded. In playback, since positioning information has been stored, the model boom and the receiver image generation system are moved to duplicate their original motion. This playback capability also provides the means for performing demonstration and morning readiness checkout runs.

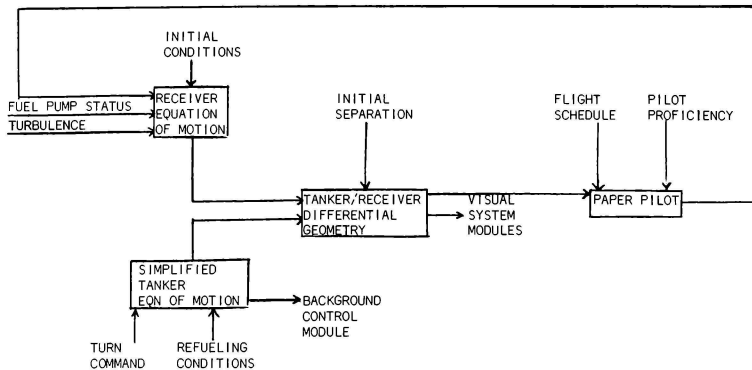
Computer Simulation Development

The BOPTT simulator can be viewed as a large real-time simulation program - but with many more interfaces. The student, operator, and visual systems can be looked at as devices to be sampled and controlled. There still are aerodynamic data that must be looked up and differential equations that must be solved.

Once the equations of motion were formulated, they were programmed in full-blown, six-degree-of-freedom simulations on the hybrid computer. This computer consists of a Sigma 7 digital computer and an Astrodata Comcor C15000/6 analog computer system. After each mathematical model was validated and its program verified - over the appropriate range of refueling altitudes and mach numbers - the model and program were simplified and made into all-digital programs. The stand-alone simulation was done in considerable detail in order to establish a baseline for checking the more simplified model. Rigorous streamlining was necessary to minimize digital execution times. The resulting programs were then transported to the BOPTT's SEL computer.

An example of a few of these all-digital real-time programs, and how they interact, can be seen in Figure 16. This diagram shows the flow of the basic tanker and receiver aerodynamics, excluding the boom aerodynamics and bow wave effects. The vertical arrows symbolize inputs from the operator station. These inputs include such initial conditions as the altitude and speed of each aircraft, the relative distance between them, the flight schedule, the proficiency of the receiver pilot, and the strength of the wind gusts. Although the receiver dynamics are modeled in detail, the tanker is viewed as a "stable platform" with everything else moving in relation to it. The distance and angles between the aircraft undergo a coordinate system transformation, the result of which goes into a mathematical model of a receiver pilot (paper pilot), and the resulting throttle and control surface commands are fed back into the receiver equations of motion.

This simulation required an all-digital approach for a multi-user environment. In most hybrid simulations where the design and capabilities of an aircraft are being checked out, higher order terms and very high frequency terms are important. In the BOPTT, on the other hand, any higher order terms and high frequencies



RECEIVER/TANKER DYNAMICS

Figure 16

not noticeable to the boom operator were eliminated in the simplification phase of the design. The programming design criterion of simplification also took on more importance in the BOPTT since there was a need to simulate many systems and not just one aircraft. The program is set up to be easily modified as new requirements become known for additional receivers. Furthermore, if and when the simulator will go into production, the manufacturer will need to understand and be able to modify the code. He may want to redesign a component of the system and/or he may want to use a different computer than the SEL.

It was criteria such as the above, and the overall complexity of the simulations, that led to the realization that a hierarchical structured approach was necessary. A top-down design was needed for the entire software package. Each module was designed for a specific purpose. For example, if the vendor wants to change the visual system, he only has to change the visual system module and not change the aerodynamic models, etc. To make the code easily understandable (in addition to a considerable amount of documentation), these specific modules were restricted to less than 120 lines wherever possible; their inputs and outputs were clearly stated - with the value of a variable assigned in only one real-time module; and as few "jump" statements as was possible were used. The code was also designed to be transportable between various computers - from Sigma to SEL, and possibly, to another computer chosen by the vendor. In fact, only a few minutes were required to transfer the simulation modules between the computers.

As a further aid in programming, understandability, and transportability, the code was written

almost exclusively in FORTRAN - as opposed to assembly language.

RTM provides various program services such as activating programs, checking their status, and performing input/output tasks. Furthermore, the vendor's Real-Time Monitor already provides the environment required to structure a computer program system as a number of independent programs. This programs can have different priorities and execution frequencies. The RTM timer service schedules their execution and activates them at the proper times. In the BOPTT system, alphanumeric display operator input translation occurs at relatively low frequency and low priority. In contrast, the computation of the equations of motion and communications with the hardware model occurs at relatively high frequency and high priority.

Computer Program Elements

The BOPTT computer program system can be thought of as being composed of the following elements:

RTM - The Real-Time Monitor supplied by the computer vendor - SEL.

TSS - The Terminal Support System, also supplied by SEL.

PO - The Initialization program. It is activated by Initial Program Load and is there-after active only when the RETURN key is hit after EXIT or when the use of TSS is terminated.

P1 - The keyboard input processing program. It has a relatively low priority and is executed approximately once per second. It interprets typed operator commands and initiates the required actions.

P2 - The clock receiver program. It has a high priority and is executed approximately 30 times per second. Through RTM, it monitors the activity and status of P3. The real-time module driver is initiated by a periodic clock interrupt. The clock is started when the operator types an appropriate command.

P3 - The true time-critical real-time modules program. It has a high priority and is executed approximately 30 times per second. One of its modules schedules when its other modules are called, as not all need to be executed at 30 times per second. This is the program which contains the simulation, integrations, table-look-ups....which were discussed above. During true real-time execution P1, P2, P4 and the resident RTM are also in core.

P4 - The alphanumeric display program. It has a low priority and is executed approximately once per second. Using RTM, it activates the desired programs, P5 or P6 or the programs necessary for real-time operation. As soon as real-time operation has been initiated, the display program will display the page requested on the selected terminal display screen. Thereafter, only changes to the requested page will be written as they occur.

P5 - The interface diagnostic program. It is active when it is invoked under control of P4.

P6 - The off-line execution program. It displays the panel referred to as the off-line menu. It is activated by either P0 or the off-line function key. The on-line functions are the states put into effect by the application of the function keys. The off-line functions are mainly auxiliary support activities like editing, testing and data-retrieval; these are initiated by using the standard keyboard to key in letter-number combinations from the menu.

Summary

The KC-135 BOPTT in-house program was from all aspects a highly successful development effort. It not only has provided SAC with a valuable training tool, but has demonstrated several technological milestones. The physical modeling within optical space of a portion of the visual scene to provide true parallax is probably the most significant contribution. The video system includes several innovative features, such as electronic articulation of the receiver aircraft and change of apparent time of day by camera filtering. The automated operator station is one of the most advanced. The computer system includes several noteworthy features such as the use of RTP equipment to provide linkage between system hardware and the computer. The present ease of implementing changes by individuals other than the original program designers is itself justification for the use of the vendor-supplied Real-Time Monitor and for the use of the hierarchical structured approach design of a highly complex program system. Mission record/playback on computer disc which includes voice is probably also a first.

The program has had many intangible effects on Air Force Engineering Personnel. It drew together many different organizations at Wright-Patterson AFB and the University of Dayton, and proved they could accomplish a highly difficult common goal. Probably of greatest importance to the Simulator Industry, it gave Air Force engineering a better understanding of many of the industry's problems.

by

Sheldon Baron, Ramal Muralidharan, David Kleinman
Bolt Beranek and Newman Inc., Cambridge, MA

ABSTRACT

The optimal control model (OCM) of the human operator is used to develop closed-loop models for analyzing the effects of (digital) simulator characteristics on predicted performance and/or workload. Two approaches are considered: the first utilizes a continuous approximation to the discrete simulation in conjunction with the standard optimal control model; the second involves a more exact discrete description of the simulator in a closed-loop multi-rate simulation in which the optimal control model "simulates" the pilot. Both models predict that simulator characteristics can have significant effects on performance and workload.

1. INTRODUCTION

The development of engineering requirements for man-in-the-loop digital simulation is a complex task involving numerous trade-offs between simulation fidelity and costs, accuracy and speed, etc. The principal issues confronting the developer of a simulation involve the design of the cue (motion and visual) environment so as to meet simulation objectives and the design of the digital simulation model to fulfill the real-time requirements with adequate accuracy.

The design of the simulation model has become increasingly important and difficult as digital computers play a more central role in the simulations. For real-time digital simulation with a pilot in the loop the design problem involves specification of conversion equipment (A-D and D-A) as well as of the discrete model of the system dynamics. The design of an adequate discrete simulation is also related closely to the cue generation problem inasmuch as the errors and, in particular, the delays introduced by the simulation will be present in the information cues utilized by the pilot. The significance of this problem has been amply demonstrated.^{1,2} Of course, human pilots can compensate for model shortcomings as well as for those of cue generation, with possible effects on the subjective evaluation of the simulation.

The objective of the work reported here was to develop a closed loop analytic model, incorporating a model for the human pilot (namely, the optimal control model), that would allow certain simulation design tradeoffs to be evaluated quantitatively and to apply this model to analyze a realistic flight control problem. The effort concentrated on the dynamic, closed loop aspects of the simulation. Problems associated with perceptual issues in cue generation were not considered. However, the limitations imposed by the dynamics of visual cue generation equipment are considered and the model

can be readily extended to incorporate the dynamics associated with motion simulation.

The optimal control model of the human operator^{3,4} is central to the closed loop analysis techniques that have been employed. This model has been validated and applied extensively and has a structure that is well-suited to analysis of the simulation problems of interest. The model can be used to generate predictions of attentional workload as well as of closed-loop performance. This is significant because, as noted earlier, pilots may compensate for simulation shortcomings but with a workload penalty; such simulation-induced operator tradeoffs need to be explored.

Two approaches to closed-loop modelling are considered. The first employs a continuous approximation to the open-loop dynamics of the digital simulation in conjunction with the standard OCM. The second model attempts to represent the discrete simulation dynamics more exactly. It utilizes a simulation version of the OCM. This latter model is referred to as the hybrid model.

In the remainder of this paper, the closed loop models are described and some results of applying the models are presented and discussed. More extensive discussion and additional results may be found in Reference 5.

2. CONTINUOUS CLOSED LOOP MODEL

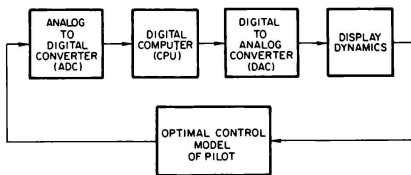


Figure 1. Simplified Model for Closed Loop Analysis of Digital Simulation

Figure 1 is a block diagram of a simplified closed-loop model for analyzing problems in digital, piloted simulation. The pilot model in Figure 1 is the OCM.^{3,4} The elements corresponding to the simulator are an analog-to-digital converter (ADC), a digital computer (CPU), a digital-to-analog converter (DAC) and a visual display system. Briefly, the ADC is a sampler

*The work described herein was performed under Contract No. NAS1-14449 for NASA - Langley Research Center. Mr. Russell Parrish was the Technical Monitor and contributed many helpful suggestions.

preceded by a low-pass filter included to minimize aliasing effects, the CPU implements difference equations so as to simulate the vehicle's response to the pilot's (sampled) input, the DAC is a data-hold (either zero-order or first-order), and the visual display system is a servo-driven projector that continuously displays target position (relative to the aircraft) to the pilot. These elements will be discussed in more detail below.

2.1 Optimal Control Model for Pilot

Some of the features of the OCM that are particularly relevant to subsequent discussions are reviewed briefly here. Figure 2 illustrates the structure of the OCM.

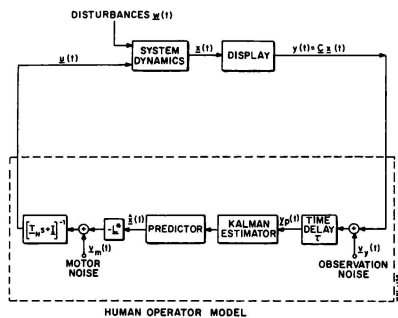


Figure 2. Structure of Optimal Control Model

The OCM as originally conceived and developed presupposes that the system dynamics, corresponding to the element to be controlled, may be expressed in state variable format

$$\dot{x}(t) = A_c x(t) + B_c u(t) + E_c w(t) \quad (1)$$

$$y(t) = C_c x(t) + D_c u(t)$$

where x is the n -dimensional state-vector, y is an m -dimensional vector of displayed outputs, u is the r -dimensional control input vector and w is a vector of disturbance and/or command inputs. The system matrices (A_c , B_c , C_c , D_c , E_c) are generally assumed to be time-invariant, although this restriction can be relaxed. The above system dynamics include the linearized dynamics of the aircraft (or other controlled element) and any dynamics associated with measurement, control and display systems. The subscript c on the system matrices is included to emphasize that the dynamics are assumed to represent a continuous system.

For purposes of discussion it is convenient to consider the model for the pilot as being comprised of the following: (i) an "equivalent" perceptual model that translates displayed variables into noisy, delayed perceived variables denoted by $y_p(t)$; (ii) an information processing model that

attempts to estimate the system state from the perceived data. The information processor consists of an optimal (Kalman) estimator and predictor and it generates the minimum-variance estimate $\hat{x}(t)$ of $x(t)$; (iii) a set of "optimal gains", L , chosen to minimize a quadratic cost functional that expresses task requirements; and (iv) an equivalent "motor" or output model that accounts for "bandwidth" limitations (frequently associated with neuromotor dynamics) of the human and an inability to generate noise-free control inputs.

The time delay or transport lag is intended to model delays associated with the human. All displayed variables are assumed to be delayed by the same amount, viz. τ seconds. However, delays introduced by the simulation can be added to the human's delay without any problem, so long as all outputs are delayed by the same amount. If such is not the case, then all outputs can be delayed by τ , where τ is now the sum of the minimal delay introduced by the simulation and the operator's delay, and additional delays for the outputs requiring them can be modeled via inclusion of Pade approximations in the output path.

The observation and motor noises model human controller remnant and involve injection of wide-band noise into the system. This noise is "filtered" by the other processes in the pilot model and by the system dynamics. It should be emphasized that the injected remnant is a legitimate (if unwanted) part of the pilot's input to the system and, therefore, significant amounts of remnant power should not be filtered out in the de-aliasing process of a valid simulation.

The neuro-motor lag matrix limits the bandwidth of the model response. Typically, for wide-band control tasks, involving a single control variable, a bandwidth limitation of about 10-12 rad/sec gives a good match to experimental results (i.e., a neuro-motor time constant of $T_N = .08 - .10$). For many aircraft control tasks there is no significant gain (i.e., reduction in error) to be obtained by operating at this bandwidth, and there can be some penalty in unnecessary control activity. For such tasks larger time constants (lower bandwidths) have been observed. In these cases, if the neuro-motor time constant is arbitrarily set at the human's limit (say $T_N = .1$) good predictions of tracking or regulation performance are usually obtained; but the control activity and pilot bandwidth tend to be overestimated. Inasmuch as it may be useful to have more accurate estimates of pilot bandwidth for making decisions concerning approximations to the discrete simulations, T_N was chosen in this study on the basis of a modal analysis of the tradeoff between error and control-rate scores. Essentially, this involves using the model to sweep out a curve of error-score versus control-rate score to find the value of T_N where marginal improvements in performance start to require substantial increases in rms control-rate (the "knee" of the curve). A value of approximately .15 sec (an operator bandwidth of about 1 Hz) was determined on the basis of this analysis.⁵

The optimal estimator, predictor and gain matrix represent the set of "adjustments" or "adaptations" by which the human attempts to optimize performance. The general expressions for these model elements depend on the system and task

and are determined by solving an appropriate optimization problem according to well-defined rules. Of special interest here is that, in the basic continuous OCM, the estimator and predictor contain "internal models" of the system to be controlled and the control gains are computed based on knowledge of system dynamics. The assumption is that the operator learns these dynamics during training. This is generally more convenient than assuming that the external model differs from the true model, and also leads to good performance prediction.⁶

The question arises as to the appropriate internal model when the human controls a discrete simulation of a nominally continuous system. It would appear that if the operator is trained on the simulation, then the appropriate model corresponds to the simulation model. If the simulation model is poor, a control strategy that is inappropriate for the actual system could be learned with negative results in, say, transfer of training. This issue can be addressed with the hybrid model described later. This will be the assumption employed with the continuous model.

Finally, it should be mentioned that the solution to the aforementioned optimization problem yields predictions of the complete closed-loop performance statistics of the system. Predictions of pilot describing functions and control and error spectra are also available. All statistical computations are performed using covariance propagation methods, thus avoiding costly Monte Carlo simulations.

2.2 Open-Loop Simulator Dynamics

The application of the standard OCM to closed-loop analysis requires a continuous state representation of the complete controlled element. Since the human pilot in closed loop control will operate on essentially continuous outputs to generate continuous control inputs even when digital computers are used in the aircraft simulation, it is meaningful to consider a continuous transfer function approximation to the open loop simulation dynamics. Such an approximation is developed here. It consists of a rational transfer function multiplied by a transportation lag. The rational transfer function approximates the amplitude distortions introduced by discrete integration of the flight dynamics. The delay accounts for all the phase lags introduced by the simulator components. These phase lags are the major source of degraded performance and increased workload in closed loop tasks. However, the amplitude distortions can be significant for open-loop responses.

Figure 3 is an elaborated diagram of the simulator portion of Figure 1. Note that the output of the visual servo, $y(t)$, is a continuous signal as is the input, $u(t)$, to the A-D dealiasing pre-filter.* For analysis purposes we use the notation implied in Figure 3. Variables or functions with argument s represent Laplace transforms and those with argument z correspond to z -transforms. The starred quantities correspond to

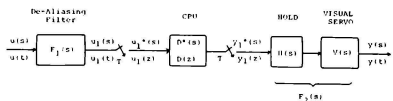


Figure 3. Open Loop Simulator Dynamics

Laplace transforms of impulse sampled signals or of functions of z and are defined, e.g., by⁷

$$u_1^*(s) = u_1(z) \Big|_{z=e^{sT}} = 1/T \sum_{n=-\infty}^{\infty} u_1(s+jn\Omega) \quad (2)$$

or

$$D^*(s) = D(z) \Big|_{z=e^{sT}} \quad (3)$$

where T is the sample period and

$$\Omega = 2\pi/T = \text{sampling frequency} \quad (4)$$

From Figure 3, we obtain

$$\begin{aligned} y(s) &= F_2(s) y_1^*(s) = F_2(s) D^*(s) u_1^*(s) \\ &= F_2(s) D^*(s) 1/T \sum_{n=-\infty}^{\infty} F_1(s+jn\Omega) u(s+jn\Omega) \end{aligned} \quad (5)$$

Equation (5) gives the exact transfer relation between $u(s)$ and $y(s)$. However, it is not a useful expression from the standpoint of closed-loop modeling because of the infinite summation.

The system function for a linear system (such as the simulation system under analysis) may be obtained by computing the steady-state response of the system to an input of the form $\exp(st)$. It is shown in Reference 5 that the system function from $u(s)$ to $y(s)$ (in steady-state) is periodic in time with a period equal to the sampling period. However, if the output $y(t)$ is considered only at sampling instants, which amounts to introducing a "fictitious" sampler at the output⁸ then the following time-independent transfer function is obtained.

$$G(s); \Big|_{\text{sample times}} = G(s) = F_2^*(s) D^*(s) F_1(s) \quad (6)$$

We shall consider $G(s)$ defined in (6) to be the "exact" transfer function for the simulation. Note that $F_2^*(s) = (VH_1)^*(s)$.

Equation (6) is intractable for use with the continuous OCM. Therefore, it will be necessary to approximate (6) for closed-loop analysis. A straightforward approximation is to ignore all but the $n=0$ term in the expression for F_2^* which results in

*For simplicity, we consider single-input, single-output systems. The results obtained here can be generalized to more complex situations.

$$G(s) = F_2(s)D^*(s)F_1(s)/T = V(s)H_1(s)D^*(s)F_1(s)/T \quad (7)$$

In utilizing (7) it will be necessary to approximate $D^*(s)$; the procedure for doing this will be discussed subsequently.

For the simulator of interest here,⁸ the transfer functions for the de-aliasing filter and servo are, respectively,

$$F_1(s) = \frac{\omega_c^3}{s^3 + 2\omega_c s^2 + 2\omega_c^2 s + \omega_c^3} \quad (8)$$

$$V(s) = \frac{\omega_n^2}{s^2 + 2\zeta\omega_n s + \omega_n^2} \quad (9)$$

The hold transfer function is either

$$H_0(s) = 1/s (1 - e^{-sT}) \quad (10)$$

or

$$H(s) = T(1+sT) \left[\frac{1 - e^{-sT}}{sT} \right]^2 \quad (11)$$

Sample periods, T , of $1/32$, $1/16$, $1/10$ will be considered as these cover the likely range of interest for piloted simulation. Therefore, if the cutoff of the de-aliasing filter is chosen on the basis of the sampling theorem, $\omega_c > 5\text{Hz}$. The visual servo dynamics of interest are characterized by $\omega_n \approx 25 \text{ rad/sec}$ and $\zeta = .707$.⁸ With these parameter values, each of the transfer functions of (8) - (11) may be approximated reasonably well by a pure transport lag in the frequency region of interest for manual control ($< 10 \text{ rad/sec}$). That is,

$$\begin{aligned} F_1(s) &\approx e^{-\tau_F s} \\ V(s) &\approx e^{-\tau_V s} \\ H_0(s) &\approx e^{-\tau_0 s} \\ H_1(s) &\approx e^{-\tau_1 s} \end{aligned} \quad (12)$$

where

$$\begin{aligned} \tau_F &\approx \frac{2}{\omega_c} = \frac{2T}{\pi} \\ \tau_V &= (\zeta\omega_n)^{-1} = .057 \text{ sec} \end{aligned} \quad (13)$$

$$\begin{aligned} \tau_0 &= T/2 \\ \tau_1 &= T \end{aligned}$$

Substitution of (12) into (7) yields

$$F_1(s) D^*(s) F_2(s) = D^*(s) \exp[-(\tau_F + \tau_V + \tau_1)s] \quad (14)$$

where $i = 0$ or 1 for the zero-order or first-order hold, respectively.

2.3 Effects of Discrete Integration

In the previous section the transfer function $D^*(s)$ was left unspecified as was the manner in which it was to be approximated for continuous closed-loop analysis with the OCM. In general, $D^*(s)$ will be a "distorted" version of the continuous system dynamics that are to be simulated. Some general features of the distortions introduced by various integration schemes are analyzed and presented in Reference 5 along with results pertinent to the F-8 dynamics that are to be analyzed later. Here, we present a brief discussion of the general effects of discrete integration followed by a description of the method that will be used to approximate $D^*(s)$ in the continuous closed-loop analysis.

Consider the continuous vehicle-dynamics as described in the state-variable form of Equation (1). For constant system matrices, the transfer matrix between system outputs and control inputs is given by

$$\begin{aligned} y(s) &= \phi_c(s) u(s) \\ \phi_c(s) &= C(sI - A_c)^{-1} B_c + D_c \end{aligned} \quad (15)$$

When equations (1) are "integrated" digitally, they lead to a discrete approximation with the following transfer matrix⁵

$$D^*(s) = [C_d(zI - A_d)^{-1} B_d + D_d] \Big|_{z=e^{sT}} \quad (16)$$

where the matrices in (16) depend on the particular integration scheme and sample period as well as on the corresponding continuous system matrices. Several points concerning Equation (16) are noteworthy. First, the elements of the discrete transfer matrix $D^*(s)$, cannot, in general, be expressed as the ratio of two polynomials in s of finite degree. Second, the Bode responses corresponding to (16) will differ from the continuous responses in both amplitude and phase; and, further, the responses for the discrete system are periodic in frequency with period equal to $2/T$. Third, the poles and zeros of Equation (16) are infinite in number and are given by, for example,

$$P_i = \sigma_1 + j(\omega_1 + 2\pi k) ; k = \dots, -2, -1, 0, 1, 2, \dots$$

Moreover, the principal values for the poles and zeros, i.e., those with $k = 0$, are not, in general, equal to the corresponding poles and zeros of the continuous system. Finally, simple integration schemes, such as Euler, will have the same number of principal poles as the continuous system, whereas multi-step integration schemes, like (Adams-Bashforth), will introduce principal roots that are spurious.

We now turn to the problem of approximating $D^*(s)$ so that the continuous representation of the simulator dynamics may be completed. Because of the restrictions imposed by the OCM, we restrict the possible approximations to the following form:

$$Y_i/U_j = D_{ij}^*(s) = \tilde{D}_{ij}(s) e^{-\tau_{cs}}$$

where $\tilde{D}(s)$ is a ratio of finite polynomials in s with numerator degree less than or equal to the degree of the denominator. Note that the same "computation" delay, τ_c is associated with each transfer function. This turns out to be a good approximation for the dynamics considered in Section 4. If different delays were needed, they would be included in \tilde{D} via a rational Padé approximation.⁹

The simplest approach to selecting \tilde{D} is to use (15) and let

$$\tilde{D}_{ij}(s) = \phi_{cij}(s) \quad (17)$$

From the standpoint of the OCM, this means that the state equations for the original dynamics are used and discrete integration is modeled by adding a delay determined from the phase distortion. As has been stated earlier, such an approximation probably accounts for the major source of difficulty of discrete integration in closed-loop control. However, to employ it exclusively is to leave us somewhat uncertain as to the closed-loop significance of the amplitude distortions.

It was found⁵ that very good approximations to discrete Bode responses could be obtained for the longitudinal control tasks that are to be analyzed later. These approximations involved perturbation of aircraft stability derivatives and CAS parameters to yield continuous modes that agreed with the discrete modes. In the case of A-B integration, it was also necessary to introduce a zero in the continuous vehicle transfer in order to reproduce the amplitude distortion introduced by this integration scheme.

When Equation (17) is substituted in (14), the basic result is that for the frequency range likely to be of interest in continuous aircraft control problems, the simulator transfer function can be modelled as

$$y(s)/u(s) = \tilde{D}(s) e^{-\tau_s s} \quad (18)$$

where $\tilde{D}(s)$ is an "approximation" to the Bode response for digital integration of the vehicle dynamics. The simulator delay, is given by

$$\tau_s = \tau_F + \tau_H + \tau_V + \tau_C \quad (19)$$

where τ_F , τ_H , τ_V and τ_C respectively, are the delays introduced by the de-aliasing filter, hold, visual servo and CPU (discrete integration).

The approximation of Equation (18) readily lends itself to efficient application of the OCM. The system matrices corresponding to a state representation of \tilde{D} and the values for τ_s are easily obtained for different sample periods, etc. For each condition, a single run of the OCM is sufficient to predict the corresponding performance. Adjustment of pilot parameters, specifically observation noise levels, allows the sensitivity to pilot attention to be examined.⁹

3. THE HYBRID MODEL

There are shortcomings in the continuous model. For example, the effects of aliasing are not considered. Thus, the degrading effects of the de-aliasing filter are included in the continuous model but not its benefits. This means that decreasing the bandwidth, ω_c , of that filter can only lead to negative results, a situation that is not obviously true, in general. Similarly, because only the delays inherent in the data holds are considered, zero-order holds will always show less degradation than first-order holds. But, in some instances, the first order hold may provide advantages that outweigh the additional delay penalty. This type of trade-off cannot be explored with the continuous OCM without more sophisticated approximation to the simulator dynamics. Because of these and other potential shortcomings, it was decided to develop a hybrid model.

The approach to developing the hybrid model is to "simulate" the closed-loop simulation. A discrete simulation version of the OCM¹⁰ was used in a closed-loop digital Monte Carlo type computation in which "continuous" elements of the loop are updated at a rate significantly greater than discrete elements. In other words, the hybrid model is a multi-rate sampling system, rather than a true hybrid system. (Informal experimentation indicates that a sample rate five times that of the discrete elements is adequate to simulate continuity for the cases considered here.) In addition, to different sample rates for continuous and discrete elements, the updating of the discrete equations of the hybrid model is different for the two kinds of elements. In particular, discrete elements are updated by means of the integration scheme and time-step specified for the "true" simulation. The equations for continuous elements are updated at the faster rate via transition matrix methods.

The equations describing the hybrid model are quite complex and are described in detail in Reference 5. Here, we simply note two features of the model that are interesting and useful in subsequent analyses. First, the hybrid model was implemented so that the prediction time in the predictor of the OCM (See Figure 2) could be selected arbitrarily. This contrasts with the standard OCM in which the prediction time is always equal to the time delay. This additional freedom allows us to "sweep out" curves of performance versus prediction time. Theoretically, best performance should be obtained when the prediction time is equal to the sum of the human's delay and the simulator's delay, i.e. when the operator compensates optimally for both delays. Since the human's delay is an assumed parameter, the compensation time for best performance yields an independent measure of the simulator delay.

A second feature of the hybrid model is that the internal model for the OCM need not be the same as the system model. This flexibility provides the hybrid model with a capability for examining transfer-of-training questions. In addition, since optimal performance should correspond to the operator's model being equivalent to the system model, the hybrid model can be used to evaluate different (internal) approximations to the discrete simulation.

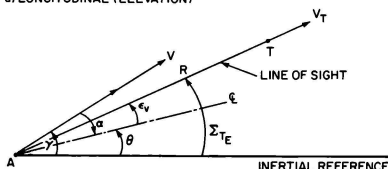
A final point concerning the hybrid model is worth noting. Because it is a Monte Carlo model, it normally will require many computer solutions to obtain meaningful statistics. In the analyses to be performed here, however, we are interested in the steady-state response of stationary systems. Rather than average over many Monte Carlo solutions, we have assumed ergodicity of the processes and utilized time-averaging of a single response. Even with this simplification, when compared to the continuous model, it is fairly expensive computationally to obtain valid statistical results with the hybrid model.⁵

4. AN EXAMPLE

The models for closed-loop analysis of simulator effects have been applied to an "example" simulation involving air-to-air target tracking. Results have been obtained for both longitudinal and lateral control tasks, for augmented and unaugmented dynamics and for different target motions. In addition, the effects of changes in design parameters of each simulation component have been explored. The full range of results may be found in Reference 5. Here, a sample of the results is presented to show the extent of the simulation effects and the capabilities of the closed-loop models.

Figure 4 shows the geometry of the air-to-air tracking in the longitudinal plane. The gunsight is assumed to be fixed and aligned with the aircraft body axis. For longitudinal tracking, we will assume that no information concerning the target's pitch angle, θ , nor the relative aspect angle is available. The pilot's task is assumed to be that of minimizing the mean-squared,

a) LONGITUDINAL (ELEVATION)



Σ_{TE} = INERTIAL LINE-OF-SIGHT ANGLE (ELEVATION)

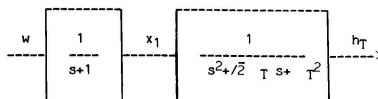
R = TARGET RANGE

ϵ_v = ELEVATION TRACKING ERROR = $\Sigma_{TE} - \theta$

Figure 4. Target Geometry

line-of-sight tracking error, ϵ_v .

The target is assumed to execute random vertical evasive maneuvers. In particular, target altitude variations are generated by passing white, gaussian noise through a third order filter as illustrated below.



By selecting the covariance of the white noise and the cutoff frequency of the Butterworth filter, rms altitude variations and normal accelerations may be specified. Here, a cutoff frequency of $\frac{1}{T} = .5$ rad/sec was used and the noise covariance was chosen to give an rms altitude variation of 267 ft. and an rms acceleration of 3.1 g. Of course, the linearity of the problem allows us to scale the results to correspond to higher or lower accelerations.

The longitudinal short-period dynamics of the F8 without augmentation will be the baseline dynamics. The relevant equations may be found in Reference 5. The short period dynamics have a natural frequency of 2.28 rad/sec and a damping coefficient of .29; this represents poor short period handling qualities.² Because of this, and because we are interested in the effects of simulation parameters as a function aircraft dynamics, a set of augmented longitudinal dynamics will also be considered. A pitch command augmentation system (CAS) is used to modify the base airframe characteristics. The CAS design is a modified version of the design proposed in Reference 11.

The equations for the augmented dynamics are given in Reference 5. The F8 with the pitch CAS has short period roots with a natural frequency of 2.78 rad/sec and a damping coefficient of .64; this constitutes a significant improvement in the short period handling qualities.²

5. MODEL RESULTS

5.1 Continuous Model

The continuous model was used to analyze the effects of both simulation parameters and problem variables. With respect to the simulation, the effects of sample period and integration scheme are presented for the longitudinal CAS-OFF dynamics. Problem dependent effects are illustrated by comparing CAS-OFF and CAS-ON results.

We define a basic simulation configuration, corresponding to Figure 3, in which the cutoff of the de-aliasing filter is set at half the sample frequency, the visual servo has the DMS characteristics ($\zeta = .707$, $\omega_n = 25$ rad/sec), and a zero-order hold is used in data reconstruction.

Figure 5 gives normalized performance for the basic configuration as a function of sample period and integration scheme. Normalized performance is defined as the tracking error obtained for the simulation configuration divided by the tracking error that would be obtained in a continuous simulation with no delays (or in flight).^a The

^aAs might be the case in an all analog simulation with analog displays providing undelayed visual information.

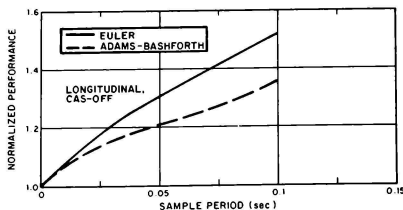


Figure 5. Effect of Discrete Simulation on Normalized Performance

normalization is determined by computing the performance utilizing the original, continuous state equations and assuming the only delay is that of the operator (.2 seconds).

Figure 5 shows substantial effects are introduced by the simulation, particularly at low sample rates. Even for the highest sample rate ($T = .03125$), there is a 16-20 percent performance degradation. A change of this magnitude exceeds the normal intra- and inter-subject variability in manual tracking tasks and would, therefore, be expected to be significant. For the lowest sample rates the performance degradation ranges from 35-50 percent, numbers that are clearly consequential. It is clear that, from a closed-loop tracking standpoint, A-B integration is superior to Euler integration.

The results in Figure 5 assume that the only adjustments in pilot strategy resulting from the simulation are an increase in prediction time to compensate for simulator delays and the adoption of an internal model that accounts for the amplitude distortions (and pole perturbations) introduced by the CPU. The results are based on the assumption of a fixed level of attention throughout. However, the pilot may choose to devote more attention to the task (work harder) and, thereby, reduce tracking error. A reasonable question to ask, then, is "How much more attention to the task would be required to achieve performance levels comparable to those that could be obtained in a continuous simulation?" This question can be addressed using the model for workload associated with the OCM.⁹ The result of this analysis is shown in Figure 6.

It can be seen from Figure 6 that to achieve the performance equivalent to that for continuous simulation, the pilot would have to increase his attentional workload by factors up to three for the conditions considered. There is a substantial workload penalty and it might be expected that a compromise between performance degradation and increased workload might evolve. This would be the case, especially if the pilot had not flown the vehicle or a continuous simulator in the same task so that there would be no basis for setting a criterion level of performance.

Before leaving the workload question, a further point is worth noting. In the describing function literature, it has been common practice to

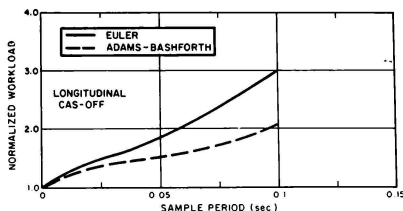


Figure 6. Simulation Workload Penalty

associate workload with the generation of lead. However, there has been no quantitative connection between the amount of lead and the increase in workload. In the present context, one can think of the increased prediction time necessary to compensate for simulator delays as imposing a (processing) workload analogous to that of lead generation. The measure of attentional workload given previously may then be thought of as an alternative means of quantifying the workload imposed by the requirement for additional prediction.

It was anticipated that there would be an interaction between the effects of simulation parameters and problem variables such as vehicle handling qualities. Thus, the above tracking task was analyzed for the CAS/ON configuration. Figure 7 compares normalized longitudinal CAS-ON and CAS-OFF performance for the basic simulation. It can be seen that the CAS-ON performance is degraded more by the discrete simulation than the CAS-OFF performance. These results are explained by the fact that the delays introduced by digital integration are larger for CAS-ON dynamics than they are for CAS-OFF dynamics. The effects of longitudinal dynamics when viewed in terms of absolute performance are interesting and are also shown in Figure 7. The absolute performance for continuous simulation is better for CAS-ON than CAS-OFF (by about 3.5 percent) and the sensitivity to incremental computation delay is about the same for the two configurations. Thus, for a given simulation configuration, absolute performance for CAS-ON and CAS-OFF configurations will be about the same if Euler integration is used and the CAS-OFF configuration can give better performance if A-B integration is used. In other words, the discrete simulation washes out any improvement due to the CAS!

5.2 Hybrid Model

The hybrid model was used to investigate several issues that could not be examined readily in the continuous model context. Results were limited to the longitudinal unaugmented dynamics because of cost and time considerations

Figure 8 shows the sensitivity of performance

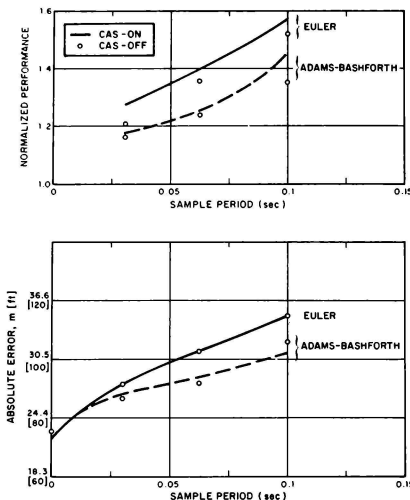


Figure 7. Effect of Vehicle Dynamics

to delay compensation time* for the basic simulation configurations with both Euler and A-B integration and for $T = .1$ and $T = .0625$. The "internal" models for the OCM in these cases are the continuous approximations to the discrete transfers that incorporate amplitude distortion effects; however, no delay is added to the human's delay of .2 seconds to account for the simulations delays. Thus, we expect the optimal prediction times to be approximately equal to the delay introduced by the simulation. This is indeed the case as can be seen in Figure 8. For Euler integration the minima occur at .26 sec and .2 sec. for $T = .1$ and .0625, respectively; the corresponding simulation delays are .27 and .19.

For A-B integration the minima are at larger compensation times than for Euler. This is a result of the method used to account for amplitude distortion. (Recall that a zero was introduced in the transfer function and this necessitated an increased transport delay to match the phase lag at mid-frequencies.) With $T = .1$, the optimal prediction time is around .3 seconds and the simulation delay is .32 seconds. For $T = .0625$, performance does not appear to be very sensitive to prediction time in the neighborhood of the optimum. The simulation delay is .21 seconds and performance for this prediction time is indistinguishable from optimal performance. Figure 8 also shows a curve for the case where the

*The prediction time in excess of that needed to compensate for the operator's intrinsic delay of .2 sec.

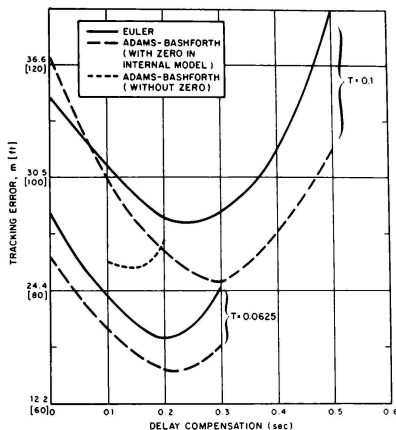


Figure 8. Effect of Operator Prediction Time

operator's internal model does not include a zero to match the amplitude distortion of A-B integration. It can be seen that for this case a delay compensation of only .17 seconds is required. This corresponds to the delays introduced by the servo, pre-filter and zero-order hold. The optimal performance is marginally poorer than for the case with amplitude distortion included in the internal model. These results suggest that although including the zero provides a better model of the effect of A-B integration, the increased delay compensation needed to offset the extra lead should not be viewed here as a workload penalty.

These results confirm the estimates of simulation delay used in the continuous model. They also demonstrate implicitly how operators may adapt their behavior to compensate for simulator inadequacy. The added prediction required may impose a workload penalty as noted earlier.

Another form of adaptation to the simulation involves the pilots internal model. Two questions are of interest: 1.) What model will the trained operator adopt when "flying" the simulator?; and 2.) What is the "transfer" effect of a wrong model when transitioning from discrete simulator to continuous simulator (flight)? At least partial answers to these questions for the longitudinal dynamics and Euler integration are provided by the results shown in Figure 9.

Figure 9 gives performance vs. delay compensation for $T = .1$ and two internal models. One internal model is that derived to match the corresponding discrete transfer function while the other is the basic continuous model. It can be

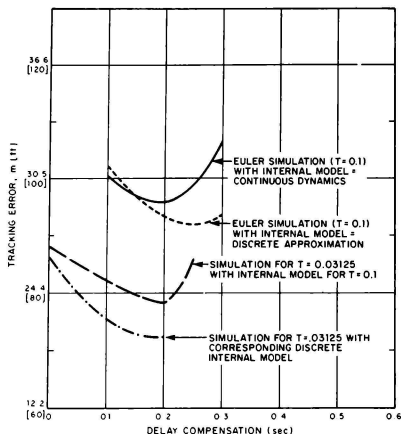


Figure 9. Effect of Internal Model

seen that better performance is obtained when the internal model corresponds to the approximate discrete model implying that this is a better model of the discrete simulation than is the original continuous model. Figure 9 also shows the effect of using the model corresponding to $T = .1$ seconds in a simulation where the actual sample period is .03125 seconds (i.e., nearly continuous) as compared to using the model for $T = .03125$ seconds (i.e., the correct one). If the operator optimizes delay compensation, performance will be degraded by about 10%. If, on the other hand, the delay compensation appropriate to $T = .1$ is used, a performance penalty of about 19% will be incurred. The effect is not substantial here but it might be in other tasks.

The effect of the cutoff frequency of the de-aliasing filter on performance is shown in Figure 10. Euler integration of the vehicle equations is used and other simulation parameters correspond to the basic configuration. The results are for a sample frequency of 10 Hz ($T = .1$) so a cutoff frequency of $\omega_c = 5$ Hz satisfies the Nyquist requirement. Results are obtained for $\omega_c = 1, 5$ and 20 Hz, respectively. The lowest value of $\omega_c = 20$ Hz is based on the assumption that there is not significant signal power beyond 5 Hz so there is no need to set the filter break-point at that frequency and incur the delay penalty. The results in Figure 10 favor using the higher cutoff frequency, $\omega_c = 20$ Hz, for this problem. Furthermore, there is a substantial penalty for using the low frequency cutoff. These two results imply that aliasing is not a problem here. We also note that the performance minima for $\omega_c = 20$ Hz and 5 Hz occur at about the correct value of prediction time; the optimum prediction time for

$\omega_c = 1$ Hz is much larger but not quite so large as the estimated total simulation delay of .53 seconds.

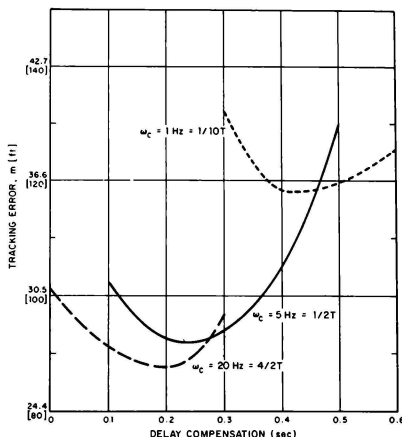


Figure 10. Effect of Dealiasing Filter Cutoff Frequency

The effects of using a first order hold instead of a zero order hold are shown in Figure 11 for both Euler and A-B integration at $T = .1$ and for Euler integration at $T = .0625$. The corresponding best zero order hold performance values are also shown for comparison purposes. At a sample period of .1 seconds, slightly lower tracking errors are obtained for Euler integration with a first order hold than with a zero order hold; in addition, the minimum performance is obtained with less delay compensation. The situation for A-B integration and a .1 second sample period is the reverse of that for Euler. That is, for A-B integration the first order hold degrades performance.

A possible explanation for these results is as follows. The first order hold uses intersample information which provides some lead. For long sample periods and Euler integration, the effective lead provided is apparently more beneficial than the lag penalty associated with the higher order hold. The beneficial effects of a first order hold should decrease as the sample period decreases. This is supported by the results for $T = .0625$ which show no difference between the two holds. In the case of A-B integration the added delay of the first order hold dominates. This may be due to A-B integration having an implicit first order hold at the input, thereby reducing any advantage in adding such a hold at the output.

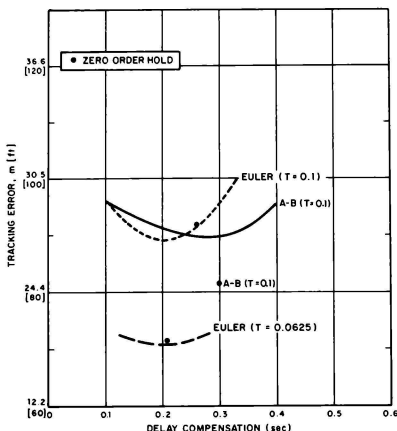


Figure 11. Effect of First Order Hold

6. SUMMARY AND CONCLUSIONS

In this paper we have examined the effects of simulation parameters and components on simulator fidelity, particularly with regard to predicting operator performance and workload. Our focus has been on the dynamical aspects of simulator primarily as they relate to closed loop control. We have generally ignored questions that would necessitate inclusion of detailed models for cue perception leaving these to future study.

An approximate continuous model of the discrete simulation was incorporated in the standard optimal control model for the human operator. The resulting continuous closed-loop model was used to analyze both overall simulation effects and the effects of individual elements. The results showed that, as compared to an ideal continuous simulation, the discrete simulation could result in significant performance and/or workload penalties. The magnitude of the effects depended strongly on sample period as expected. From a closed-loop standpoint it seemed clear that A-B integration was much to be preferred. With respect to the other simulation components it can be said that any reduction in delay is desirable. Such reductions inevitably involve increased costs (hardware or software) which must be balanced against the expected improvements.

In addition to the continuous model, a hybrid model was developed to allow investigation of situations that could not be treated adequately with the continuous model. Several interesting results were obtained with this model. It was shown that for this (fairly typical) aircraft control problem signal bandwidths were such that

the de-aliasing filter cutoff frequency could be set at a value greater than half the sample frequency. Also, there appeared to be a potential under certain conditions for improved simulator performance with a first order hold (rather than a zero order hold). The model was also used to show demonstrable effects for adopting the simulator dynamics as an internal model. The need to compensate for simulator delays via added prediction was also shown.

We believe the models developed here can be very useful in developing engineering requirements for flight simulators. These requirements will be problem dependent which is one reason why models are needed. As we see it now, the process for using the models would involve the following steps:

- i) Use standard OCM to analyze ideal continuous simulation to develop baseline performance and to determine expected signal bandwidths.
- ii) Analyze distortion introduced by discrete integration schemes and develop continuous models for discrete dynamics valid over the band of interest.
- iii) Analyze effects of integration, cue dynamics etc. using continuous model.
- iv) Use hybrid model to examine effects of data reconstruction, de-aliasing cutoff frequency etc.

Before this procedure could be used with complete confidence the models described herein need further validation and extension. It is especially important to collect data in a carefully controlled experiment to verify the individual simulation effects.

REFERENCES

1. Gum, D. R. and W. B. Albury, "Time-Delay Problems Encountered in Integrating the Advanced Simulator for Undergraduate Pilot Training," *Journal of Aircraft*, Vol. 14, No. 4, April 1977.
2. Queijo, M. J. and D. R. Riley, "Fixed-Base Simulator Study of the Effect of Time Delays in Visual Cues on Pilot Tracking Performance," NASA TN D-8001, October 1975.
3. Kleinman, D. L., S. Baron and W. H. Levison, "An Optimal Control Model of Human Response," *Automatica*, Vol. 6, No. 3, pp. 367-384, May 1970.
4. Baron, S., "A Model for Human control and Monitoring Based on Modern Control Theory", *Journal of Cybernetics and Information Science*, Vol. 1, No. 1, Spring 1976.
5. Baron, S., R. Muralidharan and D. L. Kleinman, "Closed Loop Models for Analyzing Engineering Requirements for Simulators", Bolt Beranek and Newman Inc., Report No. 3718, May 1978.
6. Baron, S. and J. Berliner, "The Effects of Deviate Internal Representations in the Optimal Model of the Human Operator," *Proceedings of Thirteenth Annual Conference on Manual Control*, M.I.T., Cambridge, Mass., June 1977.

7. Rosko, J.S., "Digital Simulation of Physical Systems" Addison-Wesley Publishing Co., Reading, Mass., 1972.
8. Ashworth, B.R. and W. M. Kahlbaum, Jr., "Description and Performance of the Langley Differential Maneuvering Simulator," NASA TN D-7304, NASA, Langley Research Center, June 1973.
9. Levison, W. H., J. I. Elkind and J. L. Ward, "Studies of Multi-Variable Manual Control Systems: A Model for Task Interference," NASA CR-1746, May 1971.
10. Kleinman, D. L., S. Baron and J. Berliner, "MCARLO: A Computer Program for Generating Monte-Carlo Trajectories in a Time-Varying Man-Machine Control Task," U.S. Army Missile Research and Development Command, Tech. Report TD-CR-77-2, Redstone Arsenal, Ala., June 1977.
11. Hartmann, G. L., J. A. Hauge and R. C. Hendrick, "F-8C Digital CCV Flight Control Laws," NASA CR-2629, February 1976.

William H. Levison
Bolt Beranek and Newman Inc.
Cambridge, Mass.

and Andrew M. Junker
Aerospace Medical Research Laboratory
Wright-Patterson AFB, Ohio

Abstract

An experimental and analytical study was performed to develop and test a model for the pilot's use of roll-axis motion cues. Principal experimental variables were the presence or absence of simulator motion, the nature of the external disturbance, simulated vehicle dynamics, and the nature of the motion cues provided during moving-base simulation. The effects of motion cues on closed-loop system performance and pilot response behavior were qualitatively and quantitatively dependent on the details of the tracking task.

The optimal-control model for pilot/vehicle analysis provided a relatively task-independent framework for accounting for the pilot's use of motion cues. The availability of motion cues was modeled by augmenting the set of assumed perceptual variables to include the position, velocity, acceleration, and acceleration rate of the roll-axis simulator with the exception that position information was omitted when the roll tilt cue was absent. Results were consistent with the hypothesis of attention-sharing between visual and motion variables.

Nomenclature

e tracking error, degrees
p plant position, degrees
u control force, pounds

Introduction

Increasing reliance on the use of ground-based simulation has caused the Air Force to take a critical look at the usefulness of moving base simulators. This interest has led to the requirement for a predictive pilot/vehicle model that is sensitive to complex motion environments. Such a model would have a number of important applications. For example, it could be used to (1) determine whether or not motion cues are used by the pilot in a particular control situation, (2) extrapolate the results of fixed-base simulation to a motion environment, (3) facilitate the design of ground-based simulators, and (4) identify situations in which misinterpretation of motion cues is likely to cause a pilot response that seriously degrades system performance.

A research program is being jointly pursued by the Aerospace Medical Research Laboratory and Bolt Beranek and Newman Inc.

©Copyright 1978 by William H. Levison and Andrew M. Junker with release to AIAA to publish in all forms.

in an attempt to satisfy this requirement. It has been directed towards developing a generalized description of the manner in which a pilot uses motion cues, with the ultimate goal of providing a model that can predict the effects of motion cues on system performance in a variety of control situations.

A series of studies conducted under this program relating to the pilot's use of roll-axis motion cues in steady-state tracking tasks are summarized. Major emphasis is given to the study that explored the interaction between the type of external input (target versus gust disturbance) and motion-cue effects. This study, documented by Levison and Junker^{1,2} illustrates both the task-dependent nature of motion-cue utilization and the ability of the pilot model to account for this dependency. Additional studies on the effects of vehicle dynamics^{3,4} and the pilot's use of the tilt cue^{5,6} are reviewed.

The modeling approach pursued in these studies departs from that generally used in previous studies of motion simulation.^{7,8} Earlier investigators tended to categorize motion-cue effects in terms of pilot response parameters (e.g., reduction in effective time delay, increase in gain), whereas our approach has been to model the presence or absence of motion in an informational context (e.g., by appropriate definition of the perceptual quantities available to the pilot). As we show in this paper, the latter approach appears to provide a firmer basis for developing a model with reliable predictive capabilities.

Methods

Experimental and analytical procedures described below were followed in the study of the interaction between the type of external input applied to the system and the pilot's use of motion cues. Procedures were similar for the other studies reviewed herein; deviations from the following description are noted in the discussion of results.

Description of Experiments

A flow diagram of the experimental configuration used in the study of disturbance type is shown in Figure 1. In this study, the subjects were required either to regulate against a simulated gust disturbance (the "disturbance condition") or to follow a commanded target (the "target condition") Target and disturbance inputs were not applied simultaneously.

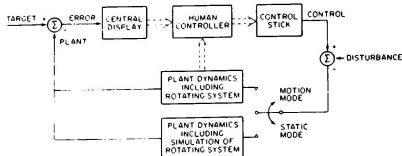


Figure 1
Block Diagram of the Tracking Task

In the target condition the task was to follow a target aircraft in the roll axis. The difference between the target roll angle and the controlled vehicle position was provided to the human operator on a 9-inch diagonal television monitor in the format sketched in Figure 2. For the disturbance condition, the displayed error equalled the bank angle of the controlled vehicle, and the task was to null out the bank angle by keeping the controlled vehicle upright.

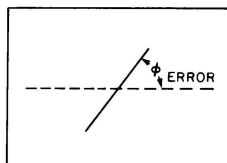


Figure 2
Sketch of the Central Display

Simulated plant dynamics were $K/s(s+5)$ to approximate roll-axis characteristics of high-performance fighter aircraft. These dynamics were modified by the high-frequency rolloff properties of the moving-base simulator and by delays of approximately 0.1 seconds introduced by recording and simulation procedures. The external forcing function was a sum of thirteen sinusoids constructed to simulate white noise shaped by a second-order filter with two identical real poles. Pole locations were 1.0 rad/sec for the target input and 2.0 rad/sec for the disturbance input.

Each input condition was tracked with and without the moving-base simulator operative, making a total of four experimental conditions. In all cases, the subject was presented with a compensatory display of roll error. Subjects were trained to asymptote on all conditions and were instructed to minimize a "cost" defined as

$$C = \sigma_e^2 + 0.1 \sigma_p^2$$

where σ_e^2 is the variance of the tracking error and σ_p^2 is the variance of the plant acceleration. The cost on acceleration was imposed partly to force the subjects (non-pilots) to track in a smooth manner, and partly to assure that roll rates and accelerations would be well within the physical limits of the moving-base simulator most of the time.*

Motion cues were provided by the Multi-Axis Tracking Simulator located at the AMRL facility; only the roll-axis capability was used in this experiment. The simulator consisted of a single-seat cockpit with a television monitor display and side mounted force stick for vehicle control. The vehicle cockpit was light-tight to eliminate external visual cues. The roll axis system dynamics were identified as approximately a first-order lag having a natural frequency of 20 rad/sec. These response characteristics were added to the analog simulation for the fixed-base conditions.

Analysis Procedures

Analysis of experimental data was performed in two steps. Data were first subjected to "primary data reduction" to obtain both amplitude- and frequency-domain statistics. Model analysis was then performed on the reduced data.

Primary Data Reduction

Variance scores were computed for each experimental trial for the tracking error, error rate, plant position (i.e., roll angle), plant rate, plant acceleration, control force, and control force rate. (For disturbance-regulation tasks, error and error rate were identical to plant position and plant rate.) Also computed was total "cost" as defined above. Square roots were taken of the measures to yield rms performance scores.

Performance scores were first averaged across replications of a given test subject for each experimental condition; the mean and standard deviation of the subject means pertaining to each experimental condition were then computed. In order to test for significant differences between motion and static conditions, paired differences were formed from corresponding subject means; these differences were subjected to a two-tailed t-test.

* Pre-experimental analysis was performed with the optimal-control pilot/vehicle model to select various experimental parameters (including the relative cost penalty on acceleration) to achieve certain experimental goals. This design procedure was very successful, and experimental results were close to those predicted *a priori* by the model. Use of the pilot model in the design of these experiments is described by Junker and Levinson ^{11,12}.

Frequency-response measures were also computed and subjected to statistical analysis. The pilot describing function (specified by amplitude ratio and phase shift as functions of frequency) was computed by dividing the Fourier transform of the pilot's control response by the transform of the tracking error. For situations in which the rotating simulator was operative, this transfer function reflects the combined effects of visual and motion cues on pilot response. In all cases, the measured phase shift was corrected to account for phase lags introduced by the simulation and data-recording procedures.¹

Estimates of "pilot remnant" were obtained by partitioning the spectrum of each control response into input-correlated and remnant-related (i.e., stochastic) components and, at each measurement frequency, obtaining the ratio of remnant-related to input-correlated power. As was done with other performance measures, these ratios were averaged across replications of a given subject and then across subjects. T-tests were performed on all frequency response measures in the manner described above.

Model Analysis

Model analysis of reduced data was performed with the so-called "optimal-control" model for pilot/vehicle systems. Readers unfamiliar with this model are directed to the literature for documentation of its theoretical development and validation.^{1,4,5}

The basic assumption underlying the model for the pilot is that the well-trained, well-motivated human controller will act in a near optimal manner subject to certain internal constraints that limit the range of his behavior and also subject to the extent to which he understands the objectives of the task. The model includes representations of system dynamics, environmental disturbances, commands, the display system, and the "optimal-control model" for the pilot. The system dynamics are comprised of the linearized dynamics of the aircraft and any dynamics associated with measurement, control, and display systems (also linearized). The equations for these dynamics are expressed in state-variable form, using vector-matrix notation. The quantities displayed to the human operator are assumed to be generated by linear operations on the state and control vectors. In general, both displacement and rate information are considered to be obtained from a symbolic display element.

For simple tracking tasks of the type explored in these studies, pilot limitations may generally be expressed in terms of an effective time delay associated with information processing, response bandwidth limitations, and "observation noise" to account for pilot remnant. The latter can

be related to a signal/noise limitation, which, through appropriate treatment, can account for the effects of attention-sharing.^{2,4,5}

An optimal predictor, optimal estimator, and optimal gain matrix represent the set of "adjustments" or "adaptations" by which the pilot tries to optimize his behavior. The general expressions for these model elements depend on system dynamics, task requirements, and pilot limitations according to well-defined mathematical rules.^{1,3,5}

The presence or absence of motion cues was treated in these studies primarily by an appropriate definition of the sensory variables assumed available to the pilot. A two-element "display vector" consisting of tracking error and tracking error rate was generally used to model fixed base tracking. To model pilot response in moving base tasks, this vector was augmented to include position, rate, acceleration, and acceleration rate of the moving simulator. Observation noise levels associated with these perceptual variables were adjusted in such a manner to reflect the assumption of attention-sharing between visual cues as a group and motion cues as a group. Application of the pilot model to the study of motion cues is documented in References 1-6.

The primary goal of model analysis was to determine a straightforward and reliable procedure for predicting the effects of motion cues in a variety of control tasks. To this end, we initially attempted to match data obtained from the various experimental configurations explored in a given study by varying only those pilot-related parameters that could reasonably be expected to relate to the kind and quality of information provided to the pilot.

Subsequent model analysis was usually performed to improve the match between model results and experimental data in order to gain further insights into the pilot's information-processing capabilities. A search procedure was performed on the pilot-related parameters as described by Levison, Baron and Junker.³

Principal Experimental Results

Effect of External Disturbance

Figure 3 shows that the influence of motion cues on rms performance was strongly dependent on the nature of the external disturbance. In the case of target tracking (Figure 3a), the availability of motion cues had little effect on rms performance measures for the target-tracking task. Plant position showed the greatest effect, decreasing by about 20% in the "motion" (moving-base) case. Smaller but statistically significant reductions were found

for total cost and for control-related scores. The fact that statistical significance (see Table 1) can be shown for these relatively small differences indicates that the influence of motion cues, however slight, was consistent across subjects.

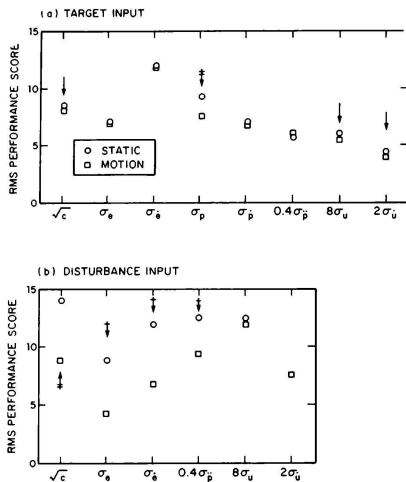


Figure 3

Effects of Motion Cues and Input Type on RMS Performance

Table 1

Coding for Significance Level

Symbol	Alpha Significance Level
†	0.05
‡	0.01
*	0.001

Differences between the "static" (fixed-base) and motion conditions were considerably greater for the disturbance-tracking task (figure 3b). Although no significant change was observed in the control related scores, total cost and error-related scores were reduced substantially; these differences were significant at the 0.01 level or lower.

The average frequency-response measures presented in Figure 4 show that motion-cue effects were qualitatively different for the two tasks. The three measures shown in the figure are, from top to bottom, amplitude ratio (i.e., pilot gain), pilot phase shift, and the ratio of remnant-related to input-correlated control power

(designed as the "remnant ratio")

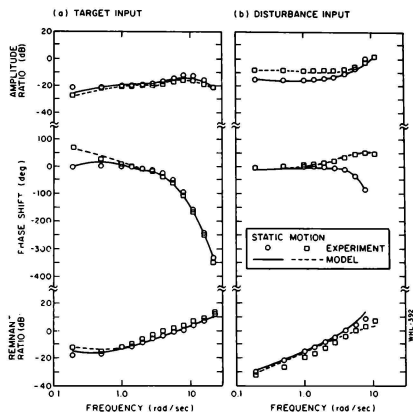


Figure 4

Effects of Motion Cues and Input Type on Frequency Response

Motion cue effects observed in the tasks with disturbance inputs agree with previous studies in which disturbance inputs were also used.^{7,10} Primarily, moving-base simulation allowed the pilot to generate more phase lead (or less lag) at high frequencies, thereby allowing the pilot to increase his amplitude ratio (i.e., "gain") at low and mid frequencies. Response bandwidth of the man-machine system was consequently increased and tracking error was reduced. These motion-static differences were statistically significant.

These effects were not observed for target-tracking. Rather, the primary effect of motion simulation was to allow a statistically significant increase in low-frequency phase shift. In this particular control task, no appreciable improvement in tracking performance resulted. (We show later in this paper that motion cues are helpful in reducing error in a target-following task if vehicle dynamics are sufficiently difficult.)

Model results (solid curves) shown in Figure 4 were obtained with a fixed set of parameter values for pilot-induced time delay, motor response bandwidth, and underlying signal/noise ratio for all four experimental conditions. The only change was to redefine the set of observation variables for static and motion conditions as described above and to adjust signal/noise ratios to reflect attention-sharing between motion and visual cues. Thus, we demonstrated in this study that what

appeared to be qualitatively different motion-cue effects in different task configurations could be accounted for by a consistent pilot model structure incorporating a straightforward informational analysis of available perceptual cues.

Figure 5 shows that this modeling philosophy accurately reflected the influence of both the nature of the external input and the presence or absence of motion cues on rms performance scores. Of the 28 scores predicted by the model, all but three were within 10 percent of corresponding experimental measures; and in only one of these cases did the model score fail to be within one standard deviation of the experimental mean.

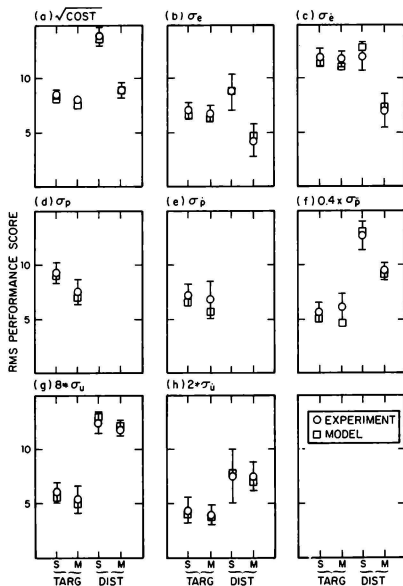


Figure 5

Comparison of Experimental and Model RMS Performance Scores

Effect of Plant Dynamics

Prior to the study described above, the effects of plant dynamics on motion-cue utilization were explored. The tracking configuration was as shown in Figure 1, but only the target input was used. Two simulated plants were studied, both of which were intrinsically more difficult to control than the one described above. "Task 1" used a plant that had approximate second-order

response characteristics over much of the measurement bandwidth, whereas "Task 2" employed dynamics that were approximately third-order. The properties of the sum-of-sines input signal were varied from one controlled plant to the next so that the subjects were always provided with a challenging tracking task, but one that did not severely restrict the bandwidth of the pilot's response.

Four experimental conditions were explored: each of the two sets of dynamics, fixed-base (the "static" mode) and moving-base ("motion" mode). In this study, subjects were instructed simply to minimize mean-squared error.

Results were qualitatively consistent with the target-tracking data described above. Figure 6 shows that motion cues allowed an increase in low-frequency phase shift (statistically significant) for both tasks. The effect was appreciably greater for the more difficult task, however. Furthermore, as shown in Figure 7, motion simulation allowed a substantial and statistically significant reduction in rms tracking error in Task 2, whereas there was no improvement in Task 1.

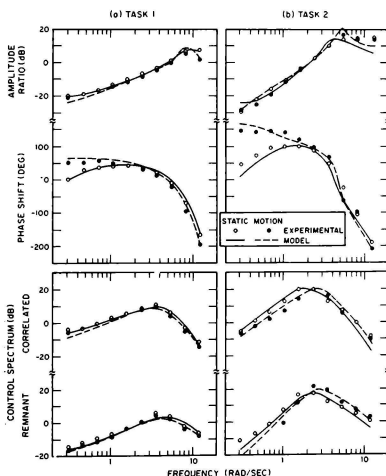


Figure 6

Effects of Motion Cues and Plant Dynamics on Frequency Response

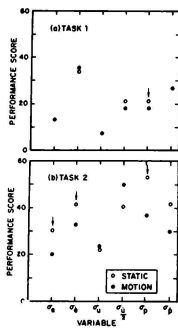


Figure 7

Effects of Motion Cues and Plant Dynamics on RMS Performance

The effects of motion cues were accounted for largely by the modeling philosophy described above. In addition, changes in other parameters (mainly pilot response bandwidth) were required to provide a good match to the data of Task 2. Important trends in both the frequency-response measures (Figure 6) and rms performance scores (model results not shown here) were mimicked by the model.

Additional analysis was conducted to determine the importance of motion sensor dynamics on predicting and replicating pilot response behavior. As described in Levison, Baron, and Junker, model analysis of Task 2 - the more difficult task - was repeated using models for vestibular sensing obtained from the literature. In keeping with the previous analysis, attention-sharing was assumed between visual cues and the cues provided by the motion sensors. Figure 8 shows that the model including motion sensor dynamics provided predictions nearly identical to those provided by the simple informational model that did not include such dynamics. We therefore conclude that, while models of vestibular dynamics are consistent with the results obtained experimentally, model accuracy is not enhanced by the consideration of such models. For the type of steady-state tasks explored in this series of studies, a simple informational analysis appears to be adequate.

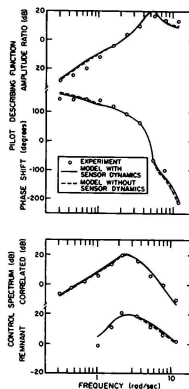


Figure 8

Effects of Sensor Dynamics on Predicted Frequency Response

Modeling the Use of the Tilt Cue

One of the problems associated with ground-based motion simulation is the introduction of unwanted or "false" cues that are not present in three dimensional flight. The particular set of such false cues present in a given simulation depends both on the nature of the flight task and the degrees of freedom of the moving-base simulator.

To explore the ability of the pilot model to account for the pilot's use of false cues, a study was performed in which the primary experimental variable was the presence or absence of the "tilt" cue (i.e., the deviation of the effective "gravity vector" from the usual head-to-seat orientation). Such a cue is "false", for example, if it is present in the simulation of a constant rate coordinated turn.

Preliminary model analysis was conducted using the optimal-control pilot/vehicle model to search for an experimental task for which performance would be sensitive to the presence or absence of the tilt cue. This analysis revealed that simple roll-axis tasks of the type explored previously would not be sufficiently sensitive. When the addition of another integration to the system dynamics was found to provide the desired predicted sensitivity, a simulated heading tracking task was adopted for this study. In all experimental trials the subject was provided with a visual display of heading error.

Motion about the roll axis was provided by the Dynamic Environmental Simulator (DES). When the roll axis of the simulator

was in the normal horizontal orientation, a roll displacement provided the subject with a tilt cue. The tilt cue was suppressed by rotating the DES 90 degrees so that the pilot was in the supine position. In this position gravity acted normally to the plane of rotation and could not provide the pilot with information related to the tracking task. Motion was provided only in the roll axis; yaw motion was absent.

Vehicle dynamics were of a higher order than those explored in the preceding study. The DES itself provided approximate dynamics of a single pole at 2 rad/sec and a complex pole pair having a natural frequency at about 10 rad/sec. "Target" motion was provided by a sum of sinusoids designed to approximate a second-order noise process.

Subjects were instructed to minimize a weighted sum of mean squared heading error and mean squared roll acceleration and were trained to near asymptotic performance on each of the four experimental conditions.

The informational analysis adopted in previous studies was used to account for the presence or absence of motion cues. For roll about the horizontal axis, moving-base simulation was assumed to provide the pilot with information related directly to vehicle roll angle, roll rate, roll acceleration, and roll acceleration rate. We further assumed that attention would be shared between visual cues as a group and motion cues as a group and that the pilot would allocate attention between these two sets of cues in a way that would minimize the objective performance cost. A similar treatment was adopted for roll about the vertical axis, only in this case the pilot assumed to obtain no cue related directly to plant position, and zero attention was ascribed to this variable. The model for static tracking was identical for the pilot in the upright and supine positions.

The comparison between predicted and measured rms performance scores presented in Figure 9 shows that the model predicted the major trend of the experiment: namely, that motion cues would benefit performance to a greater extent when the tile cue was present (i.e., horizontal roll axis). Except for changes appropriate to informational aspects, these model predictions were made with fixed values for pilot-related parameters for the four conditions explored in this study.

Although the model correctly predicted many of the changes in pilot frequency-response behavior (not shown) induced by the moving-base simulation, not all of the detailed motion/static differences were reproduced with the fixed-parameter model; other parameter changes were required to obtain an acceptable match between model and experimental results. Some of these variations could be ascribed to performance insensitivity. (e.g., the subjects appar-

ently "traded" error score for acceleration score without noticeably degrading the total performance score). Other changes, such as the increased observation noise required to match the fixed-base results, were indicative of degraded information-processing capabilities.

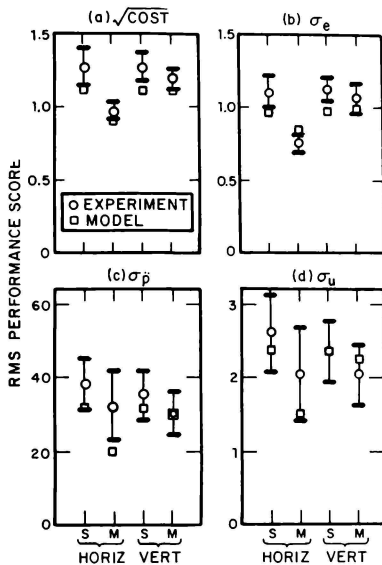


Figure 9
Effect of Motion Cues and Simulator Orientation on RMS Performance

Discussion

It is clear from the data presented here that the effects of motion cues on pilot response and system performance cannot be generalized in terms of classical response measures. We have shown that the effects of motion simulation on rms performance, pilot describing function, and pilot remnant can all differ qualitatively as well as quantitatively from one control situation to the next. Motion-cue utilization is influenced by factors other than type of input, vehicle dynamics, and orientation of the rotational axis with respect to earth-vertical as demonstrated here: pre-experimental model analysis indicated that input bandwidth and performance criterion would also influence motion/static differences in response behavior. Furthermore, the benefits of motion cues may be degraded or lost in simulation if excessive

delays are associated with generation of motion cues.²²

Different motion-derived cues appear to be used in different situations. For tasks involving only disturbance-type inputs (where motion and visual cues are, hopefully, synchronous), motion simulation provides the higher derivatives of tracking error that allow increases in the response bandwidth of the man-machine system.

Motion and visual cues provide different informational cues in target-following tasks. Where the visual display is one of compensatory tracking error (as was true in the studies reviewed in this paper), only the difference between target and vehicle motion is obtained visually. Motion cues, however, provide information directly related to the (simulated) vehicle; this information can help the pilot stabilize a vehicle having high-order dynamical response characteristics.

The effects of motion on target-following and disturbance-regulation that are observed when only one input is present are reproduced when both inputs are present simultaneously. In a recent study of simulator "washout" effects in which target and disturbance inputs were applied concurrently,^{5,24} motion cues allowed the pilot to track the disturbance input with higher gain and less high-frequency phase lag; at the same time, they allowed tracking of the target input with greater low-frequency phase lead.

The particular motion cue(s) used in a target-following task depends on the details of the task. Model analysis suggested that motion-derived vehicle-rate was of greatest importance in allowing the subject to reduce tracking error in the "Task 2" configuration described above. This hypothesis was supported by data from a companion study in which almost the same performance improvement was obtained in a fixed-base configuration using a peripheral visual display of (essentially) vehicle roll rate.²³ On the other hand, the tilt-cue experiment revealed a situation in which vehicle position, rather than rate, was the most useful motion-related cue; when that cue was suppressed, motion/static differences were largely insignificant.

The notion of modeling motion cues in terms of informational rather than response properties has been suggested previously.⁷ However, the study reviewed herein is the first to our knowledge to incorporate this notion into a model structure that allows reliable quantitative predictions of the effects of motion cues in a variety of tracking tasks. The generality of the model is largely due to the structure of the "optimal-control" pilot model which accounts for the interaction between pilot response behavior and task parameters.

Although a somewhat better match between model and data was generally obtained if attention-sharing was assumed, these studies did not allow us to determine conclusively whether or not attention was actually shared between motion and visual cues. If attention-sharing is assumed, however, tracking performance is consistent with the notion that attention is shared optimally. Thus, the hypothesis of optimal pilot response behavior can be applied to intermodal attention-sharing as well as control behavior.

One should be careful to avoid the general conclusion that motion sensor dynamics are unimportant. The experiments reviewed in this paper all employed steady-state tracking tasks for which response power was concentrated mainly in the band-pass region of the semicircular canals. For tasks (such as transient maneuvers) where very low frequency response characteristics are important, sensor dynamics may have to be considered.

The studies reviewed in this paper have concentrated on the use of motion cues in single-variable tracking tasks after thorough training of the subjects. Motion simulation may provide benefits in addition to performance benefits shown here. For example, motion cues may be helpful in learning the correct response behavior during the training phase, even if performance differences ultimately disappear. In addition, motion cues may alleviate attentional workload in multi-task situations.

The model appears to be more reliable as a predictive tool in tasks involving motion simulation than for fixed-base tasks. In particular, readjustment of certain pilot-related parameters from the "nominal" set of values is often required to match performance in static configurations employing relatively high-order vehicle dynamics. One explanation of this finding is that, in such situations, the human operator has difficulty constructing a good "internal model" of system dynamics with only a visual display of tracking error. Quite possibly, motion cues provide the additional information required for constructing such a model. (Alternatively, the enriched perceptual environment decreases the dependency of tracking performance on model-building). Improved modeling of pilot response behavior in situations involving high-order dynamics is a possible area for future research.

The design of experiments represents an important application of the pilot/vehicle model used in these studies. As noted above, pre-experimental model analysis was employed to design a tracking task for which the tilt cue would be important. In addition, similar analysis was performed prior to other studies summarized in this paper in order to specify input spectral characteristics, control gains, performance requirements, etc., that would provide tracking tasks having the desired degree

of difficulty, response bandwidth, and sensitivity to motion cues.

Summary

The principal results of the research program reviewed in this paper are summarized as follows:

1. Because of the strong interaction between motion-cue effects and task structure, a pilot/vehicle model is needed to generalize the effects of motion cues.
2. The qualitative effects of motion cues on response behavior are different for different external system inputs. The major effect of motion cues in target-following tasks is to allow the pilot to generate low-frequency phase lead. In disturbance-regulation tasks, motion cues allow more phase lead (or less lag) at high frequencies and an increase in man-machine system response bandwidth. Combined effects are likely to be present when both target and disturbance inputs are present.
3. For a given type of external input, the effect of motion cues on reducing tracking error will depend on a variety of task parameters.
4. The "optimal-control" model for pilot/vehicle systems provides a task-independent framework to account for the pilot's use of motion cues in tasks involving roll-axis motion. Specifically, the availability of motion cues is modeled by augmenting the set of assumed perceptual variables to include position, rate, acceleration, and acceleration rate of the moving vehicle. For situations in which the "tilt cue" is absent, vehicle bank angle is omitted from this list.
5. In general, good predictions of major trends are obtained using a single set of values for pilot-related model parameters. Greatest predictive accuracy is obtained for situations in which the pilot's information set is relatively complete (e.g., high-bandwidth system dynamics or low-bandwidth dynamics with combined visual and motion cues). Typically, model parameters have to be modified somewhat to obtain best correlation with experimental data when the pilot tracks a relatively low-bandwidth plant using only a visual display of tracking error.

6. Model results are consistent with the notion that the pilot shares attention between motion cues as a group and visual cues as a group. Further study will be required to test this hypothesis conclusively.
7. Consideration of the dynamic response characteristics of the human's motion sensors is not required for modeling the effects of roll-axis motion in tracking tasks involving zero-mean steady-state inputs.

Acknowledgement

This work was supported in part by the Air Force Office of Scientific Research under Contract No. F44620-75-C-0060.

References

1. Levison, W. H. and A. M. Junker, "A Model for the Pilot's Use of Motion Cues in Roll-Axis Tracking Tasks," AMRL-TR-77-40, Wright-Patterson Air Force Base, Ohio, June 1977.
2. Levison, W. H. and A. M. Junker, "Use of Motion Cues in Two Roll-Axis Tracking Tasks," presented at the Thirteenth Annual Conference on Manual Control, MIT, Cambridge, Mass., June 15-17, 1977
3. Levison, W. H., S. Baron and A. M. Junker, "Modeling the Effects of Environmental Factors on Human Control and Information Processing," AMRL-TR-76-74, Wright-Patterson Air Force Base, Ohio, August 1976.
4. Levison, W. H., "Use of Motion Cues in Steady-state Tracking," NASA TM X-73, 170, Twelfth Annual Conference on Manual Control, Urbana, Illinois, May 1976.
5. Levison, W. H., "A Model for the Pilot's Use of Roll-Axis Motion Cues in Steady-State Tracking Tasks", Report No. 3808, Bolt Beranek and Newman Inc., Cambridge, Mass., May 1978.
6. Levison, W. H., and A. M. Junker, "Use of a Tilt Cue in a Simulated Heading Tracking Task", Fourteenth Annual Conference on Manual Control, University of Southern California, Los Angeles, California, April 25-27, 1978.
7. Ringland, R. F., R. L. Stapleford, and R. E. Magdalenio, "Motion Effects on an IFR Hovering Task - Analytical Predictions and Experimental Results," NASA CR-1933, November 1971.
8. Stapleford, R. L., R. A. Peters, and F. Alex, "Experiments and a Model for Pilot Dynamics with Visual and Motion Inputs," NASA CR-1325, May 1969.
9. Shirley, R. S., "Motion Cues in Man-Vehicle Control," M.I.T., Cambridge, Mass., ScD Thesis, January 1968.
10. Ringland, R. F. and R. L. Stapleford, "Experimental Measurements of Motion Cue Effects on STOL Approach Tasks," NASA CR-114458, April 1972.
11. Junker, A. M. and W. H. Levison, "Use of the Optimal Control Model in the Design of Motion Cue Experiments," Proceedings of the Thirteenth Annual Conference on Manual Control, Massachusetts Institute of Technology, Cambridge, Mass., June 15-17, 1977.
12. Junker, A. and W. H. Levison, "Recent Advances in Modelling the Effects of Roll Motion on the Human Operator," Aviation, Space and Environmental Medicine, Vol. 49, pp. 328-334, January 1978.
13. Kleinman, D. L., S. Baron and W. H. Levison, "An Optimal-Control Model of Human Response, Part I: Theory and Validation," Automatica, Vol. 6, pp. 357-369, 1970.
14. Kleinman, D. L. and S. Baron, "Manned Vehicle Systems Analysis by Means of Modern Control Theory," NASA CR-1753, June 1971.
15. Kleinman, D. L., S. Baron and W. H. Levison, "A Control Theoretic Approach to Manned-Vehicle Systems Analysis," IEEE Trans. on Auto. Control, Vol. AC-16, No. 6, December 1971.
16. Baron, S. and D. L. Kleinman, et al., "An Optimal Control Model of Human Response - Part II: Prediction of Human Performance in a Complex Task," Automatica, Vol. 6, pp. 371-383, Pergamon Press, London, England, May 1970.
17. Levison, W. H., "The Effects of Display Gain and Signal Bandwidth on Human Controller Remnant," AMRL-TR-70-93, Wright-Patterson Air Force Base, Ohio, March 1971.
18. Baron, S. and W. H. Levison, "An Optimal Control Methodology for Analyzing the Effects of Display Parameters on Performance and Workload in Manual Flight Control," IEEE Trans. on Systems Man and Cybernetics, Vol. SMC-5, No. 4, July 1975.
19. Hess, R. A. and L. W. Wheat, "A Model-Based Analysis of a Display for Helicopter Landing Approach," IEEE Trans. on Systems, Man and Cybernetics, pp. 505-511, Vol. SMC-6, No. 7, July 1976.
20. Levison, W. H., J. I. Elkind and J. L. Ward, "Studies of Multivariable Manual Control Systems: A Model for Task Interference," NASA CR-1746, May 1971.
21. Levison, W. H., "A Model for Task Interference," Proc. of the Sixth Annual Conference on Manual Control, Wright-Patterson Air Force Base, Ohio, April 1970.
22. M. D. Fiore, A. M. Junker, and T. E. Cottenman, "Training and Performance Effects of Motion Delays on Compensatory Tracking," Proceedings of Fourteenth Annual NASA-University Conference on Manual Control, University of Southern California, April 25-27, 1978.

23. Junker, A. M., and D. Price, "Comparison Between and Peripheral Display and Motion Information on Human Tracking about the Roll Axis," Proceedings, AIAA Visual and Motion Simulation Conference, 26-28, 1978.
24. H. R. Jex, R. E. Magdaleno, and A. M. Junker, "Roll Tracking Effects of G-Vector Tilt and Various Types of Motion Washout," Proceedings of Fourteenth Annual Conference on Manual Control, University of Southern California, April 25-27, 1978.

PLANNING AND CONDUCTING SUBJECTIVE EVALUATIONS OF FLIGHT SIMULATORS

Fred A. Ragland*
The BDM Corporation
2600 Yale Blvd., S.E.
Albuquerque, New Mexico 87106

And

Major James A. Richmond
Simulator Systems Program Office ASD/SD 24T
Wright-Patterson Air Force Base,
Dayton, Ohio 45433

INTRODUCTION

When simulators were little more than procedural trainers, it was assumed that the trainer provided the expected training if the required gauges and switches worked and the trainer exhibited minimal flight characteristics. Now that simulators are designed to accurately simulate specific real-world aircraft, whether the simulator provides the training that is expected by the user in a given aircraft becomes a more complex problem. Simulators are expected to provide realistic training for many, if not most, of the specific tasks that a pilot or crew member performs in the aircraft.

PROBLEM

Will the simulator you are buying perform the training your organization expects? How can you determine if it will? That determination is difficult if you are to have confidence in the results. The basic Air Force approach is to first make an objective comparison of the simulator's performance to that of the aircraft by using flight test data as the criteria (Richmond, 1976). Although our primary interest is training effectiveness, objective measures inherently, although indirectly, address this issue and provide a useful first approximation to perceived fidelity. Perceived fidelity is a primary ingredient of training effectiveness, at least so far as the trainee is concerned.

The Air Force approach to determining training effectiveness is to obtain ratings of the simulator from pilots and crew members experienced in the aircraft. This subjective analysis could be conducted by one man - a senior, highly experienced pilot in the aircraft being simulated. But this is risky. Experts have been known to disagree, the voice of constructive dissent would not be heard and important issues would remain unresolved. Obtaining ratings from a sample of pilots who will be using the simulator minimizes this problem and allows differing opinions to be heard and resolved. The problem then is how to obtain a useful product from a group of evaluators. This paper will deal with conducting subjective analyses of simulators and will present both an ideal situation and some of the real-world problems that must be dealt with.

*Psychologist; BDM Test and Evaluation Section, Technical Applications Center.

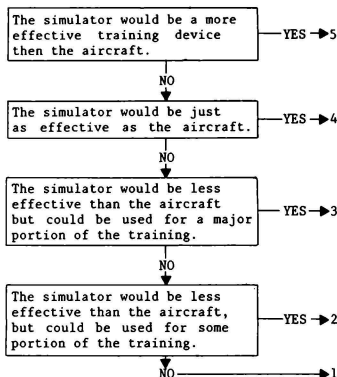
TEST DESIGN

Test planning and test design are the first steps in conducting a successful subjective evaluation. Test planning is the framework that describes how the testing will be conducted, who will conduct the testing, and what results are desired. Test design is implementation of the test plan including questionnaire development, selection of raters and data collection and analysis.

A questionnaire has proven to be a reliable method for systematically collecting subjective data. The use of a questionnaire to obtain the ratings assures that ratings are obtained in a consistent way across all raters, that the assessment systematically covers the required features, and that each rater receives the same information. Properly developed, it includes scenarios that step logically through training maneuvers, permitting the simulator to be evaluated in much the same manner as it will be used. The scenarios should contain all of the tasks that will be trained in the simulator. Other tasks should also be included to explore the boundaries of the training utility of the simulator. Tasks for which the simulator may conceivably be used and tasks for which it is not expected to be used should be included in the scenarios for this purpose.

The rating scale is a critical part of the questionnaire. A good rating scale should be easy to use, have equal and constant intervals between ratings, and be firmly anchored to criteria which has the same meaning for all evaluators. A scale with these qualities promotes accurate ratings, permits easy analysis of the data, and facilitates understanding of the results. A scale with all of these qualities, however, does not exist.

A recent study conducted by the Air Force (Miller, 1976) to devise a scale that could be used in the evaluation of simulator fidelity produced a five point dichotomous decision scale. This scale was adapted to rate the training utility of simulators (Figure 1). In the dichotomous decision scale, the rater enters the scale at the top and answers up to five questions with a "yes" or "no". When the rater first answers "yes", the decision tree leads to the selected rating. Although this type of scale does not have equal intervals, it is easily understood and used, and its flexibility permits wide application.



FIVE POINT RATING SCALE
Figure 1

With the test planned and the questionnaire written, raters must be selected for the task of rating the simulator. Each rater must be current and qualified for the crew position he is rating and it is preferable that the rater not have had previous experience in the simulator he is rating. There is less risk of contaminating expectations of the raters when their only basis for judging the simulator under test is comparison to the aircraft. A thorough briefing and an orientation flight prior to conducting the ratings provide any required familiarity with the task and the simulator.

When collecting data, each rater flies the maneuvers as many times as required to thoroughly evaluate and rate each maneuver before continuing to the next. Following each mission, the raters are debriefed to insure that the questionnaires are complete, that the ratings did not result from misinterpretation or error, and to discuss problems or questions that arose during the flight.

Following completion of the evaluation, the data collected from the questionnaires is tabulated and analyzed. During the data analysis, it is desirable to obtain measures of the reliability of the test procedures when used by a specific set of raters. Because of time constraints, there will be little, if any, time available to change the questionnaire or reevaluate the simulator, but validation of the test method can be of value in analysis and presentation of the test results.

VALIDITY

Although the questionnaire designer attempts to write concise, interpretable questions, the proof of success is not available until test results are evaluated. If the questionnaire design is then found to be less than desired, we are alerted to question the outcomes. When the test designer is successful, the raters will have understood the questions well enough to consistently evaluate the intended performance characteristics. The test in this case is said to be high in validity.

Validity problems occur when the test designer meant for raters to evaluate one aspect of performance and they chose something else. Although raters may agree on what the question required, they do not agree in the intended way. Validity of the questionnaire can often be statistically evaluated using techniques such as factor analysis (Thorndike, 1976). If test validity is inadequate, we have less confidence in test results.

If a question is not tightly focused, raters will consider different aspects of the object being evaluated. Consequently, their ratings will likely differ. Reliability analysis evaluates how well a question focuses on a specific and clearly understandable characteristic. Questions that are too general fail to identify which performance characteristic is to be evaluated from among the alternatives that apply. Error is admitted into test results as individuals responding to the same question choose differently from among the allowable alternatives. Test results can be analyzed using analysis of variance to determine whether reliability of the questionnaire was adequate (Winer, 1971).

Validity and reliability analysis, although after the fact, can provide important information on the type of question which is most useful. This knowledge can be used to shape future test design in the most effective direction.

EXPERIMENTAL CONTROL

Control of unwanted variance sources by test design is referred to as experimental control. A central concern during design of subjective simulator testing is selection and assignment of the raters. Experimental control requires that raters be selected and assigned randomly. When the sample of raters is random and of adequate size, the questionnaire samples from a broad enough variety of influences to expect offsetting biases to cancel each other out, leaving only the simulator performance to influence the rating.

Rater opinions can be expected to vary because of a wide variety of reasons. Among these are the type and amount of training or experience, age, attitude of associates toward simulators, proximity to events such as change

of duty or reassignment, the test environment, etc. It is, therefore, desirable that the rater sample be random and of adequate size to ensure offset among the unwanted influences.

Although it is rare that individuals meeting the experience requirements can be made available at random, the attempt should, nevertheless, be made. In the operational setting, opportunity to randomly sample from the overall population is rarely available. Sample size, however, can often be influenced, if not controlled. A major problem in test design is to predict the minimum sample size that will be adequate.

The research problem is to identify whether the pilot ratings significantly differed from an acceptable value. The question of sample size requires defining how big a difference is significant. If we wish to detect small differences between the ratings and an acceptable value, a larger sample is required than if we only wish to detect large differences.

For example, it is difficult to distinguish between the height of a large group of 15 year olds and another large group which are 16 year olds. A study of teen-age girls showed the differences in mean height to be about .5 inches with a standard deviation of about 2.1 inches within each group which makes distinguishing the groups difficult. With group differences this small, only 14.7 percent of the populations will not be overlapped. Stated alternately, only 57.9 percent of the 15 year old population is exceeded by the mean of the 16 year old population. Assume that we wish to use a group of raters to determine which is the 16 year old group. The difference between teen-age groups is so small that it cannot be easily determined by observation. As the rater sample decreases, their chance of making a wrong decision increases. Likewise, as we decrease the number of simulator evaluators, we decrease our chance of labeling the strengths and weaknesses in the simulator correctly.

When the size of the effect we are evaluating increases, fewer raters are required. For example, a large effect size can be illustrated with the height difference between 13 and 18 year olds. The two populations are so separated that 47.4 percent of the populations do not overlap. The mean of the 18 year olds exceeds 78.8 percent of the 13 year old group. These differences are easily perceived and the two groups could be accurately labeled by a small sample of raters. Similarly, in simulation, if the acceptable deviation from perceived fidelity is large, observer sample size can be reduced.

Research is being performed to address the question of rater sample size when evaluating simulators. The question of whether important differences from a standard will be detected with a given sample size will influence many of the test planning decisions. Cohen (1977) provides a discussion on estimation of sample size requirements.

The real world presents problems that make the desirable situation difficult to obtain. The test population may be small and a random selection of subjects may not be possible. In the case of simulators, test subjects (in fact, the entire test population) may become biased as a result of reports or rumors concerning the simulator. Conducting the test presents additional problems. Test time is limited, in turn limiting the number of evaluations and leaving little room for error or reevaluation; test subjects may affect each other's ratings; and test subjects may begin to lose their objectivity after the long hours required to accomplish a thorough evaluation. Interpretation of test results requires that real-world problems in the design and performance of the test be taken into account.

STATISTICAL CONTROL

When we cannot control the test to eliminate rater bias or other unwanted error sources, it is necessary to account for them statistically. Statistical control of unwanted error sources is performed on the data following the test. It may have been necessary, for example, to draw our sample of raters from among instructor pilots both with and without teaching experience in simulators. If we have observed that instructors with experience in simulators tend to be less doubtful of simulator instructional qualities than those without such experience, we can group the rater scores according to their experience with simulators. Differences between groups can then be statistically adjusted for, leaving only the desired performance characteristic to influence the outcome.

Statistical methods such as analysis of variance, analysis of covariance, and sensitivity analysis allow variance sources to be controlled, or adjusted for, while calculating the effect of the desired performance characteristic. The use of these advanced statistical techniques has allowed meaningful results to be obtained under difficult experimental design conditions.

ANALYSIS OF RESULTS

Analysis of the scores requires the analyst to take a position, perhaps unknowingly, on the issue of whether the scores will require the use of normal-theory or non-parametric techniques. These two fields of statistical analysis are based on different assumptions about the data being evaluated. Inferences drawn from the outcomes of the two techniques can be quite different.

Normal theory methods of analysis such as the traditional t-test assume an underlying normal distribution with uncorrelated error and units of measure which are constant and equal. If we agree that these assumptions hold, the normal theory techniques provide efficient, versatile, relatively easy to use methods of analysis.

If we assume the distribution of scores is not normal, that the score intervals are not equal or constant, then non-parametric techniques are required for analysis of the data. Non-parametric methods require more observations to reach the same level of confidence, are not available for all types of problems, and are tedious if not often difficult to use. Nevertheless, since outcomes of the normal-theory and non-parametric methods may differ, it is important to identify which set of techniques is appropriate.

Pilot ratings of simulators are normally obtained on a scale that is assumed for analysis to have equal and constant intervals. Preliminary analysis of simulator test data indicate that this assumption may not hold. If the analyst is to draw meaningful conclusions from the test data, he must carefully consider the choice of techniques used in the evaluation.

CONCLUSION

It was intended that this paper introduce organizations to methods of determining training effectiveness, or simulation fidelity, through subjective analysis. This was not, however, intended to be a step-by-step method of conducting a subjective analysis. Because there are unique problems that each organization must face, a discussion of the problems having the greatest bearing on conducting and analyzing subjective data has been presented. A structured statistical approach is a valuable tool when we must deal with subjective data. But the subjective analysis must also be carefully structured and planned well in advance if it is to be meaningful and beneficial in determining training utility.

BIBLIOGRAPHY

COHEN, Jacob. - Statistical Power Analysis for the Behavioral Sciences. New York: Academic Press, 1977.

MILLER, Ralph L. - Techniques for the Initial Evaluation of Flight Simulator Effectiveness. Thesis. Wright-Patterson Air Force Base, Ohio; Air Force Institute of Technology, December 1976.

RICHMOND, James A. - "Versimilitude Testing: A New Approach to the Flight Testing of Air Force Simulators". Proceedings, 9th NTEC/Industry Conference. Orlando, Florida: Naval Training Equipment Center, November 1976.

THRONDIKE, Robert L. - Educational Measurement. American Council on Education: Washington, 1976.

WINER, B. J. - Statistical Principles in Experimental Design. New York: McGraw-Hill, 1971.

William L. Curtice
U.S. Air Force, Aeronautical Systems Division
Wright-Patterson AFB, Ohio

Abstract

This paper discusses the ongoing development of a test instrumentation system designed to measure flight simulator handling characteristics. The need for such a system to support acceptance test activities for Air Force Simulator procurements is addressed, in conjunction with basic instrumentation performance requirements and capabilities. The technical approach selected and the potential application of this system are also discussed.

Introduction

Flight simulators have advanced rapidly in recent years, from devices which provide procedural and instrument flying training, to those providing tactical and visual mission training. Proper simulation of aerodynamic and flight control performance, especially in the area of flight handling qualities, is critical to the use of simulators for full mission training. Air Force procurement of full mission flight simulators for the A-10, F-16, F-15, and F-5 aircraft is now ongoing. Current simulator procurement acceptance test activities and projected certification processes for the future are now dependent on subjective pilot evaluations as the primary means of determining simulator acceptability in the handling characteristics domain. To date, no instrumentation system exists which is capable of comprehensive, quantitative, measurement of simulator flight handling characteristics. Although some degree of subjective evaluation will always be required, the total subjective approach to business has been shown to be highly inadequate. Recent simulator procurements have clearly shown the need for an instrumentation system to supplement and support existing simulator acceptance test activities. To that end, the Air Force is now developing the Simulator Data Test Instrumentation System (SDTIS) as an in-house project at the Aeronautical Systems Division. Air Force engineers started detail design tasks in June of 1978. Development completion is targeted for June of 1979.

The Problem

It Doesn't Feel Right

Simulator users, faced with the tradeoff of aircraft flying hours for simulator time, are now demanding far greater simulation fidelity than ever before. It is thus no surprise that handling qualities simulation has surfaced as a significant problem during most initial simulator acceptance tests in recent years. This is particularly true for tactical fighter type aircraft simulators. Air Force test pilots performing initial subjective evaluations of new simulators have concluded that the simulators "don't feel right". In effect, the integrated simulator performance does not exactly match the test pilot's memory of the aircraft. Such initial evaluations usually launch an extensive period of simulator "tweaking" in which the simulator design development is forced to continue

until the machine's performance meets the subjective expectations of the acceptance team pilots. Resultant hardware delivery delays have been extremely costly—both to contractors and the Air Force.

Numerous Causes

Numerous causes are responsible for poor simulation handling qualities fidelity. These include:

Use of Inaccurate Aero Data Bases. Simulator contractors tasked with data base development usually do the best they can in the limited time available. All too often, however, the aero data available is not representative of the aircraft to be simulated. Even when representative data is available, it is usually suitable for only airframe acceptance test purposes and lacks the fidelity and resolution required for good simulation. Data sources are often scattered, making it necessary to piece together available data and massage it into a model which is only loosely representative of the aircraft performance.

Model Shortcutting. Simulator system hardware designs often limit the size of the aero software such that some degree of "simplification" is usually required, which may degrade simulation quality.

Cue Phasing and Magnitude. Simulator pilots receive cues from numerous sources. These include aircraft instruments, simulator instruments, motion platforms, visual displays, g-seats, g-suits, and control stick feel feedback devices. The relative time relationship and magnitude of cues presented do not usually duplicate the aircraft. In many cases such time delays are caused by fundamental hardware limitations, such as computer cycle time or motion cylinder response times.

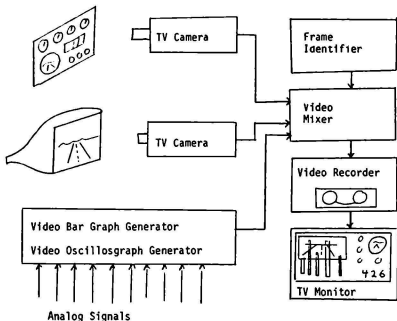
No Test Capability. Resolution of simulator cue fidelity problems has been impeded in the past due to lack of a comprehensive test and measurement capability.

Efforts are ongoing at ASD to remedy problems in each of the above areas. The SDTIS development is expected to directly impact the latter two listed.

Past Test Activities

Time Delay Measurements Performed

Four simulators have been instrumented by the ASD Simulator Engineering Division for cue time delay measurements over the past two years. The Undergraduate Pilot Training/Instrument Flight Simulator (UPT-IFS T-37), the Advanced Simulator for Pilot Training (ASPT T-37), the simulator for Air-to-Air Combat (SAAC F-4), and



ORIGINAL INSTRUMENTATION
(Figure 1)

the F-15 IFS were all instrumented using the system shown in Figure 1. A video recorder was used to record a composite video signal which included:

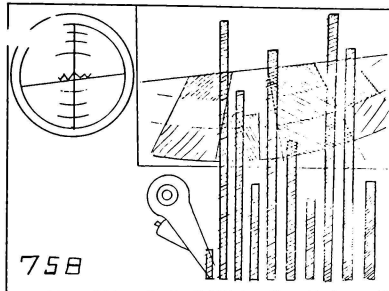
(a) Television Camera Video Images from cameras viewing the instrument panel, the motion platform, and the visual display.

(b) Video Bar Graphs representing simulator analog electrical command signal levels. Signals recorded included stick force and position, visual command (pitch, roll, and yaw) motion platform command, visual image generator servo follow-ups, instrument drives, and motion platform accelerometer signals.

Each successive video field recorded, in effect, a new snapshot of all measured parameters taken every 16 milliseconds. In addition, four signals were recorded such that they were sampled every 63 microseconds. The composite picture format is shown in Figure 2. Once recorded, all data had to be reduced from the video recording on a field by field basis. Such data reduction constituted a very slow and laborious procedure, as all cue time histories were reduced to conventional graphs.

Strengths and Weaknesses Identified

The technique used for past measurements offered several advantages over more conventional recording approaches. Primarily, it enabled the synchronous recording of both signal data and optically acquired (TV) data. Thus, movement of optical parameters (visual displays and instrument dial pointers) could be correlated exactly to movement of the simulator controls. Subjective evaluation of perceived cue onsets was also possible through review of the optical data recorded. Measurement fidelity was highly accurate. The system components were, in all cases, low cost devices; the commercial video recorder used represented an extremely wide band recording medium (3.5 mhz) at comparatively low cost. Thus, it was possible to record long periods of data with little of the inconvenience associated with other recording techniques.



ORIGINAL INSTRUMENTATION SYSTEM VIDEO FORMAT
(Figure 2)

Primary disadvantages of the approach used lie in the task of manual data reduction. Problems were also noted in determining onset thresholds of motion platform accelerometer signals obscured by hydraulic pump noise. A large variable in simulator response was also noted in that the simulator stick inputs used to initiate cue responses were performed by human operators; thus, the inputs were not standardized, and cue response data varied accordingly. Lastly, no basis or standard existed for evaluating the cue response times measured; truth was not defined by virtue of measured aircraft data.

New System Requirements/Capabilities

Evaluation of past recording efforts has resulted in the definition of performance requirements for a new system designed to meet the needs of future simulator acceptance tests. The system must:

(a) Quantitatively measure and record the magnitude, phase, and time relationship of simulator cues produced in response to standard control inputs. The recording capability must include simultaneous, synchronous acquisition of analog and digital signal data, optically acquired data such as dial pointer positions and visual display positions, g-seat and g-suit forces, motion platform position and acceleration, stick position, and stick force.

(b) Make measurements of cue time histories produced in response to control inputs produced by a mechanized, automated, simulator stick (and rudder) mover. The control mover must be programmable to produce standard reference inputs (step, ramp, and sine) as well as to duplicate aircraft control movements made by test pilots flying missions from which simulator reference data was taken.

(c) Automatically reduce data recorded into forms readily useable by simulator engineers. Data reduction is required on two levels; a limited, in-field, reduction capability is required to assist data collection and simulator performance diagnosis efforts, and a full scale reduction capability is required to properly

analyze the mass of data available. Both reduction systems shall produce finished graphics which co-plot stick position (or force) versus time and selected cues (magnitude or position) versus time.

(d) Automatically compare (graphically plot) data recorded against that obtained from flight-test and other data sources.

(e) Be electronically compatible with existing computer analysis and flight test instrumentation systems now in use.

(f) Self calibrate and automatically scale all data recording channels.

(g) Be field portable such that the system can be easily transported (as flight luggage) to contractor's facilities or USAF field sites.

System Design Approach

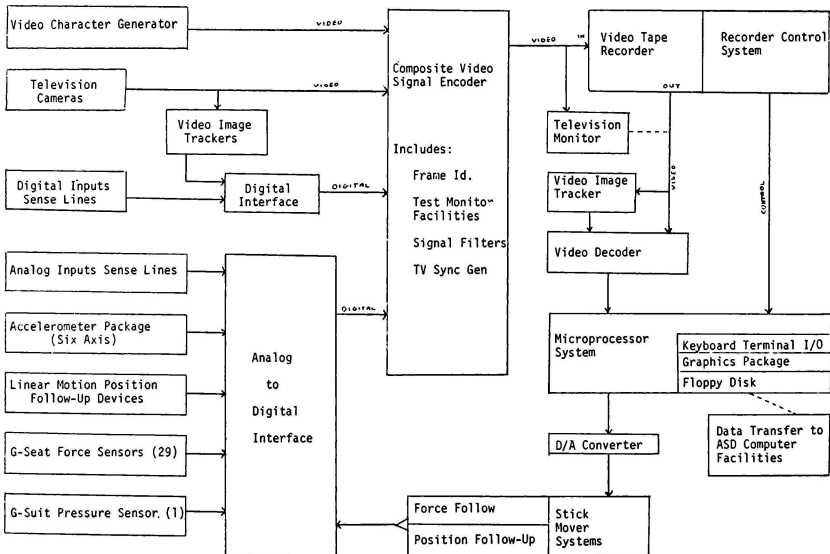
Figure 3 shows a simplified version of the system design. The system is comprised of sensors (or signal sense lines), signal encoding and recording hardware, playback signal decoding and analysis hardware, and a controls mover system. Basic features of each are discussed below.

Sensors

The SDTIS sensors must enable it to function in two ways. The first is to sense and record simulator cues as perceived by the pilot. In

essence, the simulator would be treated as a black box, with the instrumentation looking only at the input (stick movement) and output (perceived cues). Secondly, the instrumentation must perform as a diagnostic tool, capable of analyzing all signal processing performed by the simulator. The instrumentation thus must be capable of simultaneously recording numerous analog and digital signals acquired at various points throughout the simulator complex. The SDTIS will process and record 192 signals (either analog or digital - 16 bit) in addition to optically generated (TV) video. The majority of signals recorded will be acquired through sense lines (wires) running from the instrumentation equipment to the simulator. Signals recorded would typically include those available for control position follow-up, servo command, servo follow-up, and internal (inter-frame) computer data transfer. Sense line packaging, layout, and transportation represent a significant design challenge.

Other sensors planned include an accelerometer package for motion platform measurements. Signal filtering will be provided to suppress measured platform vibration caused by hydraulic pump noise. Use of long travel linear position and velocity transducers is also planned to enable independent measurement of controls positions and hydraulic cylinder extensions. An air pressure sensor will be provided to measure g-suit inflation levels. A g-seat force sensor system is also envisioned for use in both aircraft and simulator. This would take the form of a 3/8" thick cockpit seat liner sup-



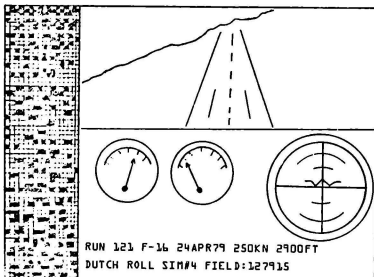
SIMULATOR DATA TEST INSTRUMENTATION SYSTEM
(Figure 3)

porting numerous force sensors (load cells) so located as required to measure force applied to the pilot's body by the g-seat. Current designs would use 29 sensors to cover the pilot's back, seat, and thighs.

Measurement of cues (as perceived by the pilot) through direct signal recording is not possible in some cases. Instrument dial pointer positions and visual display attitudes are both areas where reliance on command signal recording may be less than satisfactory due to unknown response characteristics of the display device. Television cameras will be used to acquire the optical image of such cue producers. Video/optical image position tracking electronics will then operate on the camera video signals as required to track the position of pointers, horizons, etc. The tracking electronics will provide digital (X and Y) position signals which may be recorded in the same manner as all other digital signals. The tracker may operate on camera video during recording, or on recorder playback video.

Encoding and Recording

All information to be recorded will be "packaged" or formatted into a standard 525 line television video signal which is acceptable to the video tape recorder. The video signal standard is structured such that all 525 lines constitute one frame (complete TV picture) which is written (refreshed) 30 times a second. Each frame is divided into two fields of 262 1/2 lines each (written as every other line within the frame). A new field is written (or recorded) every 1/60 of a second. Approximate 252 TV lines in each field are active, or useable for recording data. The SDTIS video signal will consist of two types of information formatted as shown in Figure 4. The first 1/8 of each TV line (appearing as the left 1/8 of the composite integrated picture) will be dedicated to recording digital data. One, 16 bit digital word will be placed at the beginning of each line. The remainder of each line (and hence of the total TV picture format) will be used for recording of conventional television video information. Video from each of three TV cameras, alphanumeric characters produced by a character generator, and bar graphs will be mixed (or switch segmented) to appear in the right seven eighths of the picture.



SDTIS VIDEO FORMAT
(Figure 4)

All electrical signal data (both analog and digital) must be encoded such that it can be recorded as 16 bit digital words appearing at the beginning of each TV line. The SDTIS system is structured such that each digital word (appearing on its respective TV line) is treated as one data channel; thus, the system will sample and record 262 "channels" of data every 1/60 of a second. Thus, we have a 262 channel data recording system with a 60 hz sampling rate. Present design utilizes only 240 of the 262 channels available. Of these, 48 channels will be used to record "overhead data" such as frame numbers, run modes, date, time, test title, etc. The remaining 192 channels will be used to actually record signal data. Previous test experience has shown that the 60 hz sampling rate is more than adequate for simulator instrumentation. However, if greater sample rates are required, the same data signal may be recorded on more than one channel within each field, thus increasing the sample rate at the expense of available channels.

The primary function of the interface and encoder modules shown in Figure 2 is to sample each analog or digital data signal, to convert the sample to a 16 bit digital word, and to place the word at the proper place in the video signal format. All analog data channels will be processed through a rotary analog to digital converter. All digital data signals will be buffered before insertion into the video signal format.

Video Recording/Reproduction

The composite video data signal will be recorded by a U-Matic Cassette Video Recorder. A commercially available U-Matic system designed for tape editing has been selected. The editing features includes tape handling capabilities considered essential to both automated and manual data reduction (still motion, fast motion, slow motion, play in reverse, etc.). The video recorder represents, in effect, a low cost wide band recording media which is well suited to the integrated recording of both signal data and optical data as required by the SDTIS.

Decoding and Processing

On-site data reduction will be accomplished using a portable microprocessor based computer system. The composite video signal will be processed through a decoder, wherein the digital information will be stripped from video and input to the computer. Optical/Video trackers will be locked on to camera acquired information of interest during tape playback. Tracker position information (in digital form) will be fed to the computer to be treated as any other digital signal. Playback signals for each run will be recorded on the floppy disk. Typical instrumentation recordings will last only a few seconds per run. The disk system will be capable of storing runs of up to 30 seconds in duration. Disk recording rates are slower than the real time tape playback data rate; thus the processing system will perform video tape to disk data transfer by making six tape passes. This process will be automatically controlled through integration of the microprocessor to the tape deck control system.

On-site automated data reduction may be performed after data is on disk. The portable system includes a graphic unit which will produce finished, labeled graphs plotting any data channel's time

history against any other channel or stored reference. Available aircraft performance data based on flight test will be prerecorded for use as a reference. The microprocessor system will also produce stick movement command signals required to excite the simulator.

Control Movers

The functional concept of the SDTIS is based on analysis of simulator cues produce in response to the simulator control movements (stick or rudder). Past simulator instrumentation efforts utilizing human pilot produced stick inputs have been devalued considerably due to the variability of stick movement rates from test to test. The SDTIS controls mover systems are intended to eliminate this problem.

The control movers now in design include a stick mover, a yoke/column mover, and a rudder mover. Each is a mechanical device which will clamp into the simulator cockpit and attach to the controls. Each will be driven by torque motors functioning as part of a closed loop servo system. The control movers will each include follow-up devices required to track stick position and applied force. Command signals will be generated by the SDTIS microprocessor system and applied to the servos in analog form. Command functions may be either force versus time, or position versus time. They may be of some "standard" nature (ramps, steps, sine wave) or may duplicate stick movement data taken from flight test. Current designs require use of two 350 in/oz torque motors for each mover. These would enable a stick to be moved 9 inches with 150 lbs force (maximum) in 600 ms., or with 250 lbs force in a one second period. Safety considerations for both the simulator and test personnel are a major factor in this design.

System Packaging

All SDTIS hardware must be sufficiently portable to enable its transportation as excess airline baggage. Use of fifteen environmentally insulated containers is planned to contain all portable instrumentation. Consolidated inter-cabinet cabling will enable field set up in a short period of time. The greatest time burden of test is therefore expected to rest in locating signals, attaching sense lines, and verifying connections.

System Impact

Properly applied, in conjunction with aircraft performance data from flight test and other sources, this instrumentation system should enable:

(a) The establishment of firm, quantitative simulator performance requirements in areas where current procurement specifications list only subjective criteria.

(b) Reduction of the costly contractor re-engineering efforts and program delays associated with simulator acceptance tests wherein the contractor is required to tweak his machine until it feels (subjectively) correct to the acceptance team pilots.

(c) The establishment of standard requirements specifications and acceptance procedures to be used by the industrial and government simulator engineering community.

(d) Development of a simulator certification program based on more than subjective evaluation in the flight handling characteristics area.

(e) Improvements in simulator handling fidelity achieved through use of more comprehensive test procedures.

Summary

Development of the Simulator Data Test Instrumentation System is now on-going. When complete, this system is expected to constitute a powerful tool to be used in support of flight simulator development.

G. L. Ricard and W. T. Harris*
Naval Training Equipment Center
Orlando, Florida 32813

Abstract

Problems of control produced by delays in simulations of flight are reviewed and data related to the problem that were available from an earlier experiment were analyzed. That study used a lead/lag transfer function to compensate for delays inserted into a closed-loop system, and pilot control performance was measured using various amounts of lag for a given setting of lead. These data indicated that an optimal ratio of lead to lag could be determined, and based upon the changes of phase and gain associated with subjects' best control performance, suggestions are made concerning compensation for delays.

Introduction

Some of the techniques used to create simulations of flight produce aspects of the resulting simulation that affect negatively the performance of pilots using a given device. A case in point is the production of time delays in flight simulation systems by the vast number of calculations needed to simulate the aerodynamic responses of an aircraft, to collect and display data for the control of flight instruction, and to provide computer-generated images for a visual display system. These are transport-type delays created by the simulation program's iterative calculations of aircraft parameters and then using that information for further calculations necessary to drive displays. As the requirements of training or research dictate an increase of the number of edges in a computer-generated image or the addition of computer-generated simulations of sensors like low-light level TV or forward looking infrared radar, the time between pilot control input and system response may increase, other things being equal, and the result would be poorer pilot control performance. Several papers exist that review the manual control of systems with delayed feedback^{1,2,3,4} and an indication of the importance of timing problems in flight simulators can be seen in Gum and Alberly.¹

Because the spatial orientation of the simulated aircraft must be known before a computer-produced visual image is recalculated, and because of the fact that for the most part those calculations are serial, there will always be time delays in digitally controlled simulations. Important questions for the simulation community are then: How much delay is tolerable for what kinds of flying tasks? Can a maximum tolerable delay be specified for a particular cue providing system, or axis of control and how would it relate to the type of aircraft being simulated?

When pilots attempt to maintain a constant method of control in the presence of delayed feedback, they will be forced to reduce their phase margins. For instance, in the 3 to 5 radians/second region of the spectrum where the gain-vs-frequency curve for the pilot-plus-system crosses over from greater-than to less-than unity gain,

pilots like to maintain a 25° to 45° phase margin. Computer image generation for visual displays presently takes about 100 milliseconds and this time would reduce the pilot's phase margin by 17° to 28°, depending on the location of the gain crossover point. Human controllers exposed to delayed feedback will attempt to generate more of a phase lead for their control inputs, and if they cannot, will then reduce their crossover frequency and possibly increase their low-frequency gain in order to minimize system error.⁵

How these tendencies relate to flying an aircraft is often not clear. Models of piloting control describe strategies of tracking behavior used by pilots when the display is a compensatory one. Usually a forcing function is used to create error to be nulled, no additional cues are provided, and the task is simply to control a single-loop system. When computer-generated visual displays are added to flight simulators, often no change is seen in the pilot's control of flying tasks such as free-flight. It is only when the task requires accurate control of the aircraft that pilot-induced oscillations are seen, usually along the lateral axis, but sometimes along the longitudinal axis as well. Traditionally it has been the requirement of maintaining an orientation or position relative to an external object close to the simulated aircraft that has caused pilots to produce oscillations when significant time delays were present. The pilot can clearly see how small responses of his aircraft shift him from an "ideal" position and the time delay prevents him from making the small quick control inputs that would correct the error. Pilot-induced oscillations have been seen during formation flight⁶ for instance, and we would expect that they would also be seen in tasks like air-to-air refueling as well.

Some work has related the amount of tolerable delay to the handling qualities of the aircraft being simulated. Queijo and Miller¹⁰ have shown, using the National Aeronautics and Space Administration Langley Research Center's Visual-Motion Simulator, that the delay that could be tolerated was related to the short-period frequency of the aircraft being simulated, and that the more complex the flying task, the shorter this tolerable delay was.

Their flight task was pursuit tracking of an aircraft image that underwent sinusoidal changes of altitude. To increase the complexity of their primary flying task, a side task was added or the frequency of oscillation of the lead aircraft was increased. Over the ranges of short-period frequencies and dampings used in their study, the maximum delay that seemed to be tolerable without affecting the subjects' flying performance or control style was about 141 milliseconds.

Evidence that additional cues can affect the magnitude of the delay that can be tolerated for a

*Member AIAA.

given task was presented by Miller and Riley^{7,8} who showed that when the motion platform of the Visual-Motion Simulator was activated, the tolerable delay for a simulation of a given aircraft was extended. Over ranges of short-period frequencies of 1.50 to 3.00 radians/second and damping ratios of 1.59 to 0.30, they found that best tracking was associated with a complete set of 4 degree-of-freedom motion cues (pitch, roll, heave and sway) and that when the set was reduced, tracking performance deteriorated and delays had more of an effect on control performance. This demonstration of the usefulness of motion cues is similar to that of Junker and Price⁹ who concluded that they provided additional cueing that enable pilots to generate low-frequency lead.

When a time delay in a simulation system causes problems of manual control, the usual engineering response is to adjust some of the values that are passed from one subsystem to another. The typical adjustment is to provide some "lead" by adding derivative information back onto a time series, in this case, the one passed from the flight dynamics processor to the computer image generation system. For a function $x=f(t)$, the form of this adjustment has been $x_{n+1}=x_n+h/2(f(Kx_n, \dot{x}_n-1, \text{etc.}))$ where h is the integration interval, \dot{x} is the first derivative of x , n denotes a point in time, and K and L are weighing coefficients. Such a rule provides a phase advance to counteract part of the time delay of a system, but it also amplifies the high frequency components of the signal being adjusted. For display systems that have wide bandwidths (like a visual display for computer-generated images), the result is an annoying jitter of the image when $f(t)$ contains high-frequency components. Usually such high-frequency excitation of simulation systems comes from pilots of the devices themselves.

Pilots are usually encouraged to control their craft using smooth movements of the controls, but it has been those flying tasks where accurate control and quick response to easily perceived error that have encouraged pilots to abandon this tactic for high-frequency "bumpy" movements of the control stick, and it has been these tasks where software delays and the adjustments for them have caused problems.

As a response to this situation, Ricard, Norman, and Collyer¹² added a low-pass filter $(1/(TS+1))$ to a first-order lead (KS) used to adjust the pitch and roll angles of a simulated aircraft over a prediction span - the time over which the variable is being adjusted - in this case K seconds. Their control system is depicted in Figure 1. They had subjects control an artificial horizon display where a delay could be inserted before the display, and several experiments were performed that either inserted a delay, and then a predictor and then the low-pass filter, or examined the acquisition of control skill under a variety of conditions of delay of visual feedback. In this report we will examine the data of their second experiment to make suggestions about the sort of compensation that may aid the manual control of systems containing delays.

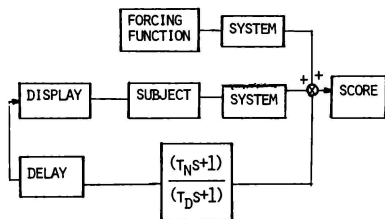


Figure 1. Schematic of the control system used in the Ricard, Norman, and Collyer (1976) experiment.

Description of the Experiment

In their experiment, Ricard, Norman, and Collyer had subjects use a two-axis, side-arm controller to provide inputs for a simulated artificial horizon display. The task was to maintain a straight and level attitude in the presence of mild turbulence. Wideband random numbers were filtered to approximate the spectrum of atmospheric turbulence and these were passed through the aerodynamic equations before the resulting errors of pitch and roll angle were displayed for the subject to null. An oscilloscope with a five-inch diameter CRT face was used for the display and subjects were seated so that this subtended a visual angle of 15° to 20°. Thus the task was compensatory tracking with a fairly narrow field of view display.

The dynamic responses of their system were those of a light, fixed-wing jet flying an altitude of 30,000 feet and an airspeed of 430 knots. They were simulated by an airspeed of 430 knots. They were simulated by the displayed pitch and roll angles produced by the following equations. The change of pitch angle (θ) per control stick deflection (δ) was given by:

$$\frac{\theta}{\delta_e} = 4.85 \frac{(102.04S+1)(.73S+1)}{\left(\frac{S^2}{.004} + \frac{.145}{.063} + 1\right)\left(\frac{S^2}{18.23} + \frac{.995}{4.27} + 1\right)}$$

and the change of roll angle (ϕ) per deflection of the control stick was produced as:

$$\frac{\phi}{\delta_a} = 49.25 \frac{\left(\frac{S^2}{3.46} + \frac{.48S}{1.86} + 1\right)}{S(.16S+1)\left(\frac{S^2}{3.53} + \frac{.48S}{1.88} + 1\right)}$$

A cross-coupling of the lateral axis of control to the longitudinal one was simulated by the addition of a downward "gust" of turbulence to the longitudinal axis according to the following:

$$G_{cc} = .73 \left(1 - \frac{1}{\cos \phi}\right)$$

To assess control performance, quantities that could be accumulated in real time and which were felt to reflect significant aspects of pilots'

control activities were measured. These were, for both axes of control, the system error, the size of the deflections of the control stick, and the relative spectral power within the band of 2 to 6 radians/second where pilots usually cause the gain curve of the system plus themselves to crossover. These were sampled at 20 Hz and then integrated and averaged over the length of each trial.

Transport delays were then inserted into the feedback loop, but before the values of pitch and roll angle were delayed, they were "adjusted" to compensate for the delay. This involved estimating a future value for each variable and then passing this predicted value through a first-order, low-pass filter. Thus the jitter produced by high-frequency control inputs could be attenuated by setting the filter appropriately, and pilots could take advantage of the phase lead being provided without the annoying noise.

Specifically the adjustment rule was a first-order lead/lag transfer function of the form $(T_N s + 1)/(T_D s + 1)$ where the ratio of T_N to T_D determined whether a phase lead or lag was formed. To show how such a transfer function can operate, in Figure 2 we have presented the gain and phase plots

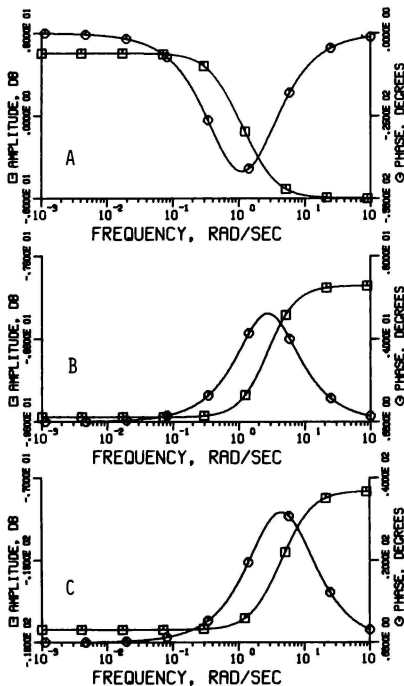


Figure 2. Bode plots of phase and amplitude changes

produced by various settings for the lead/lag transfer function. $T_N = .4$ seconds, and for (A), $T_D = 0.5$ rad/sec, for (B), $T_D = 3.0$ rad/sec, and for (C), $T_D = 8.0$ rad/sec. Note the changes of scaling.

for a constant delay (T_N) using various break points of the filter (T_D). For a low-frequency setting of the filter, the lead/lag function generates a phase lag of 51 degrees that is centered at 1.1 radians per second, and for a high-frequency setting, a phase lead of 60 degrees is produced that is located at 4.4 radians per second. At an intermediate setting of the filter, lead is balanced by lag, and close to a unitary transfer function results. The gain plots for these functions indicate the changes of output amplitude that accompany these changes of phase. To indicate the range of conditions of testing of the Ricard, Norman and Collyer study, Figure 3 presents the maximum change

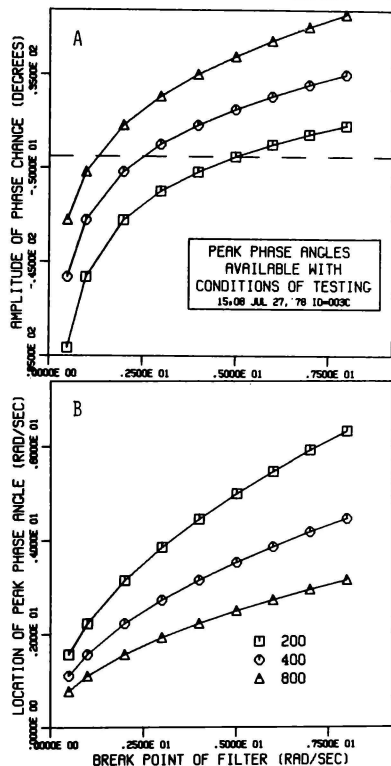


Figure 3. Maximum changes of phase and location of maxima produced by conditions of testing used by Ricard, Norman and Collyer (1976).

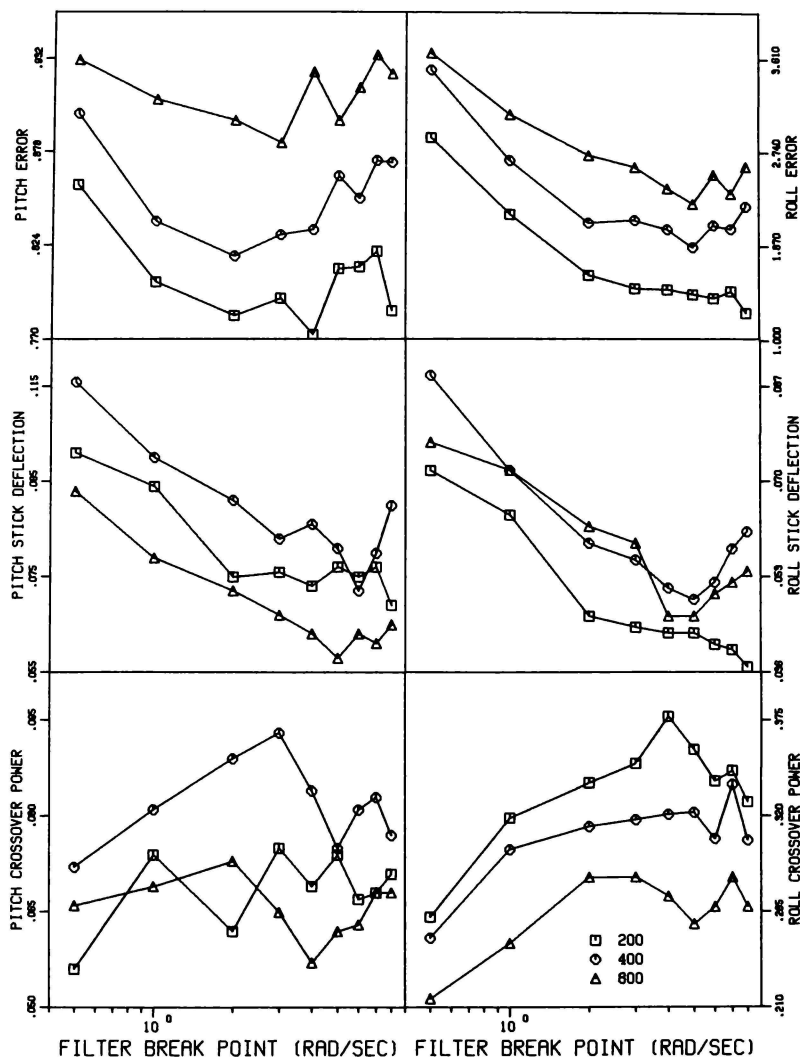


Figure 4. Mean control performance as a function of filter break points for delays of 0.2, 0.4, and 0.8 seconds. System error, control stick deflections, and relative power between 2 to 6 rad/sec for pitch angle control are presented in the left column, and those for the control of the roll angle are on the right.

of phase, either a lead or a lag, and the location of these maxima for the conditions of their experiment. For all of these conditions of delay, the lowest values of T_d produced a phase lag that quickly changed into a lead as higher and higher values of T_d were used. Both the magnitude of this lag and the point where it crossed over to a lead are dependent upon T_n , the display delay. T_n was always set to the delay of the visual feedback presented the subjects, and the experiment tested manual control for various settings of T_d . These were varied over a range where preliminary data had indicated best performance would be found.

Four subjects were asked to control the system for two-minute trials with inserted delays of 200, 400, and 800 milliseconds and break points for the low-pass filters of 1/2, 1, 2, 3, 4, 5, 6, 7, and 8 radians/second. A combination of these values was used to determine the testing conditions for a particular trial, and performance for a given combination was taken as the average of five such trials. The subjects were tested on all settings for a given delay before being switched to a new one; other than that, the order of testing was random. Usually they performed 18 trials per day.

Results

The results of that experiment, averaged across subjects, are presented in Figure 4. Analyses of variance revealed that there were significant differences of these measures due to subjects, but more importantly, for the control of both axes, there were effects due to both the presence of the transport delay and the various values of T_d . These are not particularly surprising, but it is the form of the functions relating the measures to break points of the filters that is important here. For the control of both the pitch and roll axis, the measures of the system error and the pilots' deflections of the control stick were reduced as higher and higher values of T_d are used, reasonably enough as controllers should not be expected to null error that they cannot see, but of considerable importance is the indication that there is an upward turn of these functions for high values of T_d . This seemed most pronounced for the measures of the deflection of the control stick, and some subjects seemed to display this trend more than others. While the downward trend of these measures clearly would be related to the removal of needed information from the display, the upward leg we feel reflects the degree to which an individual tried to null high-frequency error. Those who ignored high-frequency activity of the display tended to show this effect less. Correlated to these changes of system error and control stick deflection, the measure of relative power within the crossover band tended to increase and then decrease as the break point of the filters was raised.

These V- or U-shaped functions seem to reflect in a fairly straight forward manner the changes of control style necessary for these conditions of testing. In another experiment using these system dynamics, Ricard, Norman, and Collyer showed that controllers' responses to the insertion of a delay was to reduce their relative control power within the crossover region and make larger deflections of the control stick as the delay (and system error) increased. In these

data, the nonmonotonic functions are taken as reflecting the relative contributions of phase lag and phase lead as T_d is changed for a set value of T_n . For small values of T_d , the increased lag causes the control system to be sluggish and high-frequency errors are integrated and cannot be corrected. At large values of T_d , phase lead predominates and the increased responsiveness of the display encourages the controller to lower his gain crossover point and increase his low-frequency gain. Presumably intermediate values of T_d provide an appropriate ratio of lead to lag and this is reflected as better control performance. The extent to which human controllers respond to such manipulations of the signals that drive a visual display will determine the depth of these V- or U-shaped functions.

This analysis of the changes of control behavior seen in Figure 4 led us to measure an optimal T_n/T_d ratio by determining the minima (in the case of the error and stick deflection measures) and maxima (for the crossover power) of these functions. This we did by fitting to a least-squares criterion a quadratic equation to each function of Figure 4 and then solving for the inflection point of the fitted curve. This point was taken as the optimal T_d for the particular T_n , and these values were used to form a new transfer function that represented the phase and gain changes related to best control performance. By taking this value of T_d that represents "best" performance and solving for the maximum phase change produced by these new values of T_n and T_d , we can indicate the amount of phase lead or lag that human controllers seem to prefer or need for best control performance. For the three conditions of delay for which we had data, these maximum changes of phase produced by the fitted transfer function are presented in Figure 5. Each

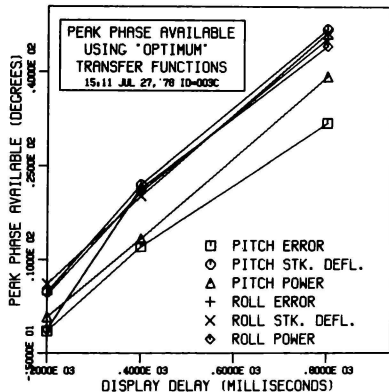


Figure 5. Maximum phase changes associated with conditions of best performance for the data of Figure 4.

function represents the estimates based on a given measure, and the striking feature of these data is the similarity of the estimates. All of them

indicate that human controllers prefer a phase lead that gets larger with longer delays, but all indicate that in the range of 150 to 200 milliseconds of delay that the amount of lead that produces best performance has reached zero! Above this point, lead is needed at a rate of about .07 to .08 degrees per millisecond of delay, so that for a 400 millisecond delay best control performance was produced by a phase advance of only 18 degrees. Not obvious from the figure are the changes of location of these maxima to lower and lower frequencies as the display delay is made longer. The peak of little over 29 of phase lead for a 200 millisecond delay was centered at .83 Hertz while the over 40° of lead for the 800 milliseconds delay was centered at about .4 Hertz. For these subjects then, the nature of the delay compensation that seemed to be preferred was one where a larger and larger phase lead was centered at a lower and lower frequency.

Should these data be extended to shorter delays, we might suggest that for systems with delays of less than 150 to 200 milliseconds a phase lag would be the preferred change of the display signals and that this should be centered at still higher frequencies. This seems reasonable enough as it is the presence of the delay that prevents controllers from effectively dealing with high-frequency error. By eliminating it from a visual display, better control behavior may be produced in certain situations. This may not always be the case though. The analysis we have presented here was based on data collected on a narrow field-of-view system, with fairly taxing forcing function producing error to be nulled, and with none of the auxiliary tasks characteristic of flying real aircraft.

As an example of a more realistic situation, Ricard, Cyrus, Cox, Templeton, and Thompson performed a similar experiment using the Advanced Simulator for Pilot Training at Williams AFB where performance of flying formation and opinions of the noisiness of the display were related to values of T_d . A summary of their data is presented in Figure 6 where a normalized control score (the average of pitch and roll errors) is presented along with the

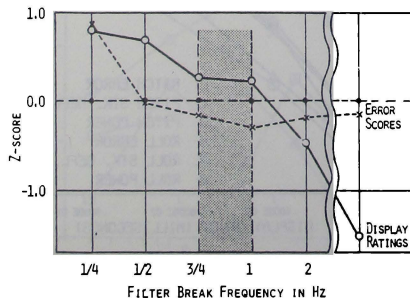


Figure 6. Control performance and pilot opinion as a function of filter break point (data collected in the ASPT simulator).

normalized pilots' ratings of the "noisiness" of the computer-generated display. The normal lead-generating software of the ASPT was used for this study, and break points for the low-pass filter were used that span the range discussed here, along with a no-filtering condition (the = break point). Clearly once a high enough break point was used so that control was not impaired, further reductions of T_d had no effect. Even when compared to no filtering, the higher values of $1/T_d$ did not affect control performance, but they did strongly affect pilots' opinions of the display. Filtering clearly produced a more acceptable image than no-filtering even though this was not reflected in measures of aircraft control.

Summary

We presented the analysis in this paper because we feel that a lead/lag form of delay compensation seems to be useful, even though it probably produced smaller amounts of phase lead than other methods of adjusting signals for visual displays. It seems that even for difficult tasks, only small peaks of phase change are needed to aid manual control and that in realistic simulations of flight, changes of piloting control may not be evident, but that some other change - probably of opinion or preference for a particular value of T_d - is quite likely to be seen.

References

1. Gum, D.R. and Albery, W.B. Time-delay problems encountered in integrating the advanced simulator for undergraduate pilot training. *Journal of Aircraft*, April 1977, 14, 327-332.
2. Junker, A.M. and Price, D. Comparison between a peripheral display and motion information on human tracking about the roll axis. *Proceedings of the AIAA Visual and Motion Simulation Conference*, Dayton, Ohio, April 1976.
3. Larson, D.F. and Terry C. ASUPT visual integration technical report. *Singer-Simulation Products Division Technical Report ASUPT-82*, Binghamton, March 1975.
4. McRuer, D.T., Graham, D., Krendel, E., and Reisner, Jr., W. Human pilot dynamics in compensatory systems. *Air Force Flight Dynamics Laboratory Technical Report AFFDL-TR-65-15*. Wright-Patterson Air Force Base, Ohio, July 1965.
5. McRuer, D.T. and Krendel, E.S. Mathematical models of human pilot behavior. *AGARDograph AG-188*, January 1974.
6. Muckler, F.A. and Obermayer, R.W. Control system lags and man-machine system performance. *NASA Contractor Report NASA CR-83*, July, 1964.
7. Miller, Jr., G.K. and Riley, D.R. The effect of visual-motion time delays on pilot performance in a pursuit tracking task. *Proceedings of the AIAA Visual and Motion Simulation Conference*, Dayton, Ohio, April 1976.

8. Miller, Jr., G.K. and Riley, D.R. Effect of visual motion time delay on pilot performance in a simulated pursuit tracking task. NASA Technical Note TN D-8364, Langley Research Center, January, 1977.
9. Poulton, E.C. Tracking Skill and Manual Control. New York: Academic Press, 1974.
10. Queijo, M.J. and Riley, D.R. Fixed-base simulator study of the effect of time delays in visual cues on pilot tracking. NASA Technical Note TN D-8001, Langley Research Center, October 1975.
11. Ricard, G. L., Cyrus, M.L., Cox, D.C., Templeton, T.K., and Thompson, L.C. Compensation for transport delays produced by computer image generation systems. Technical Report NAVTRAEQUIPCEN IH-297/AFHRL-TR-78-46, June 1978.
12. Ricard, G.L., Norman, D.A., and Collyer, S.C. Compensating for flight simulator CGI system delays. Proceedings of the 9th NTEC/Industry Conference, NAVTRAEQUIPCEN IH-276, November, 1976, 131-138.
13. Ricard, G.L. and Puig, J.A. Delay of visual feedback in aircraft simulators. Technical Note NAVTRAEQUIPCEN TN-56, March, 1977.

OPTICAL SIMULATOR WITH A HOLOGRAPHIC COMPONENT

Joseph A. LaRussa
Farrand Optical Co., Inc.
Valhalla, New York 10595

Arthur T. Gili
Human Resources Laboratory
WPAFB, Ohio 45433

Summary

The Farrand Optical Co., Inc. PANCAKE WINDOWTM optical simulator is a very fast, large aperture magnifier which can present to the observer a displayed image at optical infinity. The superb optical quality of this magnifier is due to the fact that reflective, and not refractive elements are used in this system. The unique configuration of this on-axis reflective system, and the optical properties of its elements are presented. Also, its latest improvement incorporating a spherical holographic beamsplitter mirror and a tilted birefringent package are discussed.

The PANCAKE WINDOWTM*, so called because of its minimal depth and, therefore, relatively flat appearance, has proven to be very successful as an infinity display system in many applications where performance and cost are important. For example, as far as performance is concerned, a typical PANCAKE WINDOWTM system can provide the following characteristics:

- 37 inches of eye relief for an 84° total field allowing 12 inches of head motion ("pupil" size) around the center of curvature of a 48" radius mirror.
- A typical focal length of 24 inches would result in an overall thickness under 12 inches.
- Maximum decollimation would be 9 arc minutes over any head motion and any field angle.
- No color or distortion over an 84° total field where the only significant aberration is the spherical aberration.

Considering this typical system as a large wide-angle eyepiece, we enjoy the remarkable combination of having an eye relief of 160% of the focal length.

In other words the total depth of this new type of infinity display system is scarcely greater than the depth of the sagitta of the spherical mirror employed.

This is evident in Figure 1 where the PANCAKE WINDOWTM is shown as both pupil-forming and a non-pupil-forming infinity display system.

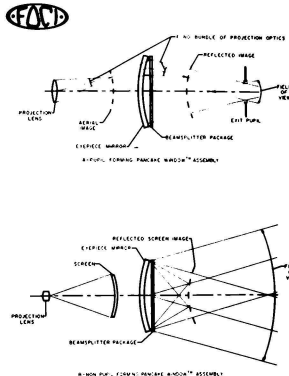


Fig. 1 Farrand PANCAKE WINDOWTM

It should be noted from the geometry that the input image source, whether of the screen type or the aerial image type, is substantially smaller in diameter than the PANCAKE WINDOWTM as well as being located behind the window and in-line with observer. These characteristics of minimal depth, in-line input behind the window and input size smaller than the window itself make the PANCAKE WINDOWTM ideally suited for mosaicking the displays in wide field of view systems such as the all-around visual system illustrated in Figure 2.

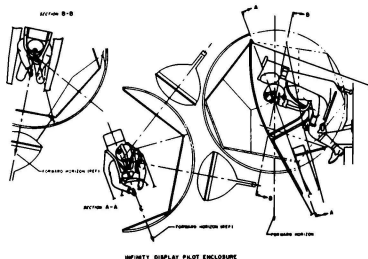


Fig. 2 PANCAKE WINDOWTM Sphere of Vision Infinity Display

* Patented - J. LaRussa, 3,443,858 RE27,356

It is this system in fact which was designed as a dodecahedron with pentagonally shaped PANCAKE WINDOWSTM for use in the air-to-air simulators known as the Simulator Air-To-Air-Combat (SAAC) and the Advanced Simulator Pilot Training (ASPT). These systems supply a partial sphere of vision exactly equal to the partial sphere of vision enjoyed by the actual aircraft they simulate. The fields of view are contiguous and even provide overlap fields between windows to allow for substantial head motion of the observer. Both systems are monochromatic because of monochromatic inputs but the classical PANCAKE WINDOWTM is capable of operation across the whole of the color spectrum.

How does the PANCAKE WINDOWTM function?

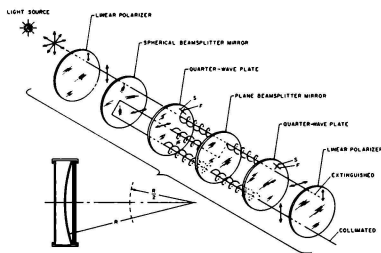


Fig. 3 Principle of Operation of the PANCAKE WINDOWTM

Referring to the above illustration (Figure 3) we see the elements of a PANCAKE WINDOWTM in an exploded view while in the lower left corner the elements are pictured as they are combined in an assembled window.

In the exploded view there is shown a source of unpolarized light which is usually an extended source.

A first polarizer imposes linear polarization on the light from the source which passes through it. The direction of polarization is identified by the vertical arrow although of course any arbitrary direction may be employed. The resultant polarization of the light passing through element is indicated by the vertical arrow on the flow line. From the polarizer a fraction of the linearly polarized light passes through a partially transparent spherical mirror convex toward the source. Beyond the mirror, i.e., to the right thereof, the linearly polarized light which passes through that mirror encounters a quarter wavelength plate. The plate has its mutually perpendicular fast and slow axes F and S oriented at 45° to the plane of polarization shown on the flow line. The linearly polarized light originating at the polarizer which emerges from the quarter wavelength plate is circularly polarized, either right or left according as the angle between the plane of polar-

ization and the fast axis F is 45° or -45° . Let it be assumed that the light emerging from the quarter wavelength plate is right circularly polarized, as indicated by the helical line. This right circularly polarized light next encounters a plane partially transmitting and partially reflecting mirror. The fraction of the right circularly polarized light which passes through the mirror encounters a second quarter wavelength plate whose fast and slow axes F' and S' are parallel respectively, to the corresponding axes of the prior quarter wavelength plate. Consequently, the light emerging from the second quarter wavelength plate along the direction of propagation has been reduced to linearly polarized light with a plane of polarization at 90° to that of the first polarizer. This is indicated in the illustration by means of the arrow on the flow line. This horizontally polarized light is blocked at a second plane polarizer whose plane of polarization is parallel to that of the first polarizer.

The fraction of the circularly polarized light from the first quarter wavelength plate which is reflected at the plane beamsplitting mirror is converted upon such reflection into circularly polarized light of the opposite rotation, i.e., into left hand circularly polarized light in the case assumed. This is indicated by means of the left hand helix. In its passage backward parallel to the direction of propagation but toward the source, this left circularly polarized light encounters again the first quarter wavelength plate from which it emerges as linearly polarized light with a plane of polarization at 90° to that of the light first polarized. This is indicated by means of the horizontal arrow on the flow line. This horizontally linearly polarized light is in part reflected at the concave beamsplitting mirror without change in the orientation of its plane of polarization. The light so reflected becomes left circularly polarized on passage through the quarter wavelength plate, as indicated by the left-hand helix. The fraction of this left circularly polarized light which gets through the plane beamsplitter is converted by the second quarter wavelength plate into linearly polarized light in a vertical plane of polarization, as indicated by the vertical arrow on the flow line. This light accordingly is permitted to pass through the second plane polarizer and constitutes the only fraction of the unpolarized light from the source which is visible to an observer located at the right of the elements shown in the structure.

This illumination is now collimated. Of course, it goes without saying that if the fast and slow axes of the two quarter wavelength plates are aligned perpendicular to each other, then the first and second polaroids must be aligned perpendicular to one another in order to achieve the same effect.

It soon became apparent that with the present state of holographic technology it might be possible to reduce the longitudinal thickness of the standard PANCAKE WINDOWTM by incorporating a holographic analog of the spherical beamsplitter mirror, thereby reducing size and weight and also the cost. Unfortunately however, we soon reasoned that reflection type holograms, typically produced

with monochromatic light, exhibit serious dispersion with broadband illumination when viewed in the transmission mode. This property of reflection-type holograms would apparently negate their usefulness in image-forming apparatus of the present type which are invariably used with broadband illumination since the light rays to be collimated by the holographic analog must first pass through the analog and be dispersed thereby. After having passed through the holographic analog this dispersed illumination is reflected by a plane beamsplitter back toward the collimating holographic mirror analog, and it was originally assumed that all the dispersed light rays reflected from the mirror analog would be collimated for viewing by the observer. This dispersion would completely destroy the usefulness of a system of this type.

However, in the course of experimenting with a holographic mirror analog in an in-line infinity display system we discovered unexpectedly that the dispersed illumination, after being reflected from the plane beamsplitter back to the analog, was effectively filtered by the holographic analog. The analog only reflected and collimated the narrow bandwidth of illumination preferential to the hologram, and the remaining illumination passed through the analog towards the source of illumination. As a result, the observer viewed a collimated dispersion-free version of the primary image, see Figure 4. The holographic mirror acted as a reflection filter, selecting and collimating a narrow band of illumination from the broadband illumination source.

As a result of this successful attempt of making a small holographic PANCAKE WINDOW™ the Air Force Human Resources Laboratory (AFHRL) at Wright Patterson Air Force Base awarded Farrand a contract to develop a 17" holographic PANCAKE WINDOW™ which was delivered and accepted. The window was a mere 5/8 inch thick! Farrand is now into the next phase of the development, i.e. where we are in the process of making three 21 x 24 inch holographic monochromatic PANCAKE WINDOW™ to be butted together for achieving a multiple input wide field of view. These windows will be a mere 7/8 inch thick!

Just recently, AFHRL recognizing the potential of the holographic PANCAKE WINDOW™, and again striving to advance the state-of-the-art in display technology awarded the Farrand Optical Co., Inc., a contract to develop a 17 inch full color trichromatic holographic PANCAKE WINDOW™. Thus far, Farrand has successfully put together a two-color holographic PANCAKE WINDOW™ of smaller size and is currently engaged in the larger 17 inch trichromatic endeavor.

The PANCAKE WINDOW™ as described so far, both classical and holographic, suffer imperfections such as ghosts and bleedthrough. These imperfections are not visible under projected daylight and dusk conditions; they are observable however, under nighttime projection conditions when a dark background with bright point light sources form part of the scene.

* Patented - J. LaRussa 3,940,203

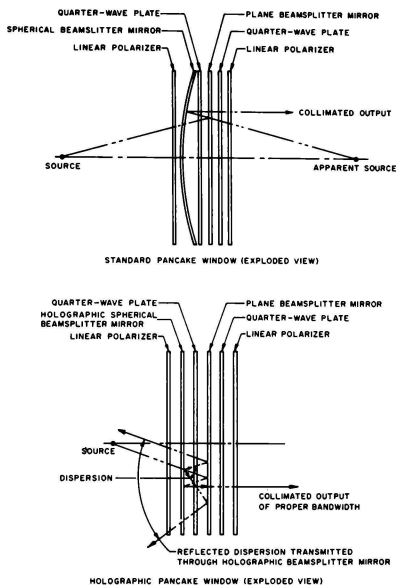


Fig. 4 Comparison of Standard and Holographic PANCAKE WINDOWS™

The ability to see the input image directly by looking through the PANCAKE WINDOW™ is called bleedthrough and is described in terms of the ratio of the unwanted image to the collimated or wanted image (see Figure 5). Current manufacturing techniques and materials result in a bleedthrough ratio of 1/75. Ghost images are formed by multiple reflections off of the plane and spherical beamsplitter mirrors as shown in Figure 5. Additional reflections forming ghost images beyond the R₃ ghost are too weak to be of any concern. In fact unless the observer is located at the proper distance as shown, the ghost images are invisible and manifest themselves only as very dim background noise.

A recent improvement in PANCAKE WINDOW™ design has succeeded in eliminating both bleedthrough and ghost images from the viewing volume. By tilting the birefringent package with respect to the viewing axis as shown in Figure 6, the multiple reflections off of the plane beamsplitter mirror in the birefringent package are directed away from the viewing volume. Since the screen must also be tilted at the same angle, the bleedthrough is also directed away from the viewing

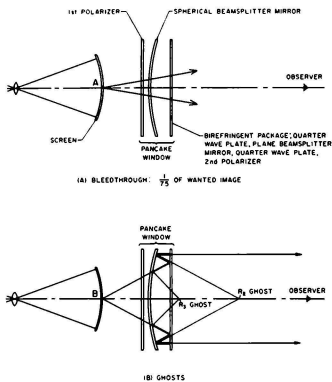


Fig. 5 PANCAKE WINDOW™ Imperfections

volume. It is expected that the Tilted Birefringent PANCAKE WINDOW™ * principle can be applied to making a holographic plane beamsplitter mirror in tilted form so that a Tilted Birefringent Holographic PANCAKE WINDOW™ can be manufactured. Such a system would preserve the minimal thickness of the Holographic PANCAKE WINDOW™ while eliminating all ghosts and bleedthrough effects.

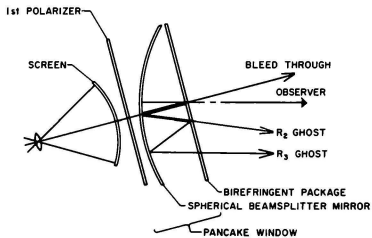


Fig. 6 Tilted Birefringent PANCAKE WINDOW™

* Patented - J. LaRussa RE27,356

